Developing an Oral-Insulin-Delivery System using GET-peptide-mediated transcytosis

Sahrish Rehmani

Pharm D., M.Phil. (Pharmaceutics)

Thesis submitted to the University of Nottingham for the degree of Doctor of Philosophy

May, 2021

Supervisor

Dr. James E Dixon, PhD

Associate Professor, School of Pharmacy,

The University of Nottingham

Co–supervisor

Prof. Dr. Kevin Shakesheff, PhD

Professor and Pro-vice Chancellor, School of Pharmacy, The University of Nottingham

Internal Assessor

Dr. Pavel Greshkovich, PhD

Associate Professor, School of Pharmacy,

The University of Nottingham

Thesis Declaration

I, Sahrish Rehmani D/O Muhammad Shafi Rehmani, hereby certify that I am the sole author of this thesis and neither any part of this thesis nor the whole of thesis has been submitted for a degree to any other University or Institution.

I state that this thesis is the result of my own independent work/investigation, except for otherwise stated.

I certify that, to the best of my knowledge, my thesis does not contain any material previously published or produced by another party in fulfilment, partial or otherwise, except for when due acknowledgment is made in the text. I understand the nature of plagiarism and that it is a serious academic offence. I confirm that no material in this thesis has been plagiarised and I consent to my work being run through a plagiarism checker.

Signature: ……Sahrish Rehmani……. **Date: ……01-05-2021…**

Contents

Acknowledgement

Firstly, I would like to express my most sincere gratitude to my main supervisor, Dr. James E Dixon, for always being there whenever I needed him, for his constant advice, for the provided freedom in the research, for the fruitful discussions, and for making me see this PhD topic was much more interesting than I originally thought. His wide knowledge and his logical way of thinking have been of great value for me. His understanding, encouraging and personal guidance have provided a good basis for the present thesis.

I would also like to thank my Co-supervisor Prof. Dr. Kevin Shakesheff for his trust in me, and for his constructive feedback and continuous support. His extensive discussions around my work and interesting explorations in operations have been very helpful for this study. Thank you both for your optimism, kindness and for believing in me.

I would like to acknowledge the funding sources of these studies: the Punjab Educational Endowment Fund, Pakistan for funding my Ph.D. at University of Nottingham, UK, as without them it wasn't possible to make this dream come true. I would extend my acknowledgement to the support of Medical Research Council and the Biotechnology and Biological Sciences Research Council UK Regenerative Medicine Platform Hub "Acellular Approaches for Therapeutic Delivery" (MR/K026682/1) for funding my supervisors Dixon and Shakesheff. The research has also received funding from the European Research Council under the European Community's Seventh Framework Programme (FP7/2007-2013)/ERC grant agreement 227845.

I would like to make a special mention to my lab mates who gave up their time to help and support my work. Thanks to Lia, and Hossam for initial training for cell culturing and *in-vitro* transfection assays, thanks to Aveen for her help with microparticulate preparation and for her support and guidance throughout Ph.D and for being nice friend, Jopeth, Mahetab, Inchirah, Aruna, Pritish, and Francesco for their help and guidance with various laboratory experiments and valuable suggestions, Gizem, and Syan for guiding on different transcytosis based assay, thanks to Trang and Amelie for supporting me in lab work and with their sincere

guidance and thanks to all other office and group members for making the office hours being much more bearable and entertaining. Moreover, I am thankful to my friends and colleagues who provided love and support during this journey specially Ammara, Ayesha, Amal, Mahmooda, Asiya, Roheena, Summiya, Sanjana, Aveen, Inchirah, Tauseef, Abu bakir, Jopeth, Francesco, Elisa, Hossam and Lia.

I would like to thank my internal assessor, Dr. Pavel Gershkovich for generously giving his time and expertise to evaluate my work. I appreciate his feedback to improve my work. Moreover, I would like to pay regards and thanks to my External Examiner Prof. Dr. Joan Taylor, as she provided her valuable feedback, and recommendations to improve the quality of thesis. She also raised some technical and important aspects which were worth discussion and were included in thesis as per her suggestions. I think I was lucky to have her as my external examiner.

I would like to express my gratitude as well to the staff and technicians at Boots Science Building and at the Centre for Biomolecular Sciences (School of Pharmacy), where the experimentation of this thesis was carried out. I would like to thank all technicians specially; Teresa Marshall, Ann Williams, Paul Cooling, Nicola Croxall, David Onion, Christopher Gell, Nicola Weston, and Jayson Bispham for their help with training on different laboratory instruments and software.

My parents have been a constant source of support – emotional, moral and of course financial – during my postgraduate years, and this thesis would certainly not have existed without them. And most importantly, thanks for their unconditional love which will carry me forever. I would like to dedicate this thesis to my **"Mother"** who passed away 3 years ago, I wish she would have been alive to cherish these moments with me. I am thankful to my Father for trusting in me for Education in Foreign Country, supporting me morally and emotionally, and praying for me and my success. and I feel my acknowledgement incomplete, if I do not extend my lots of thanks and heartiest compliments to my husband for his support & cooperation, and my daughter (5 months old) to cherish my life, and my brother and sister for their affection and prayers. I could not do anything without their help and support. Their prayers turned my dreams into reality. Almighty ALLAH enriches their grace and dignity always and their blessing should remain forever on us.

List of Publications

1) **Rehmani, S**., Shakesheff, K., & Dixon, J. E. (**2020**). GAG-binding enhanced transduction peptides as a novel tool for improved intracellular delivery of insulin (under preparation).

2) **Rehmani, S**., & Dixon, J. E. (**2018**). Oral delivery of anti-diabetes therapeutics using cell penetrating and transcytosing peptide strategies. Peptides, 100, 24-35.

List of Abbreviations and Symbols

AB/AM- Antibiotic/antimycotic

ATP- Adenosine-triphosphate

BA- Bioavailability

BM-BAPTA-AM (N,N'-[1,2-ethanediylbis(oxy-2,1-phenylene)]bis[N-[2-[(acetyloxy)methoxy]-2-oxoethyl]-1,1'-bis[(acetyloxy)methyl] ester-glycine)

BSA- Bovine serum albumin

Cat. No.- Catalogue number

CLSM- Confocal laser scanning microscopy

Conc.- Concentration

CPP/ CPPs- Cell penetrating peptide/peptides

CRP- Serum c-reactive protein

Da- Dalton

Del.- Delivery

Dex- Dextran

dH_20- Deionised water

DLS- Dynamic laser scattering

D-Mann- D-mannitol

DMEM- Dulbecco's Modified Eagle Medium

DPP-IV- dipeptidyl-peptidase-IV

Em- Emission wavelength

EthD-1- Ethidium homodimer

Eud- Eudragit

Eud-L100- Eudragit-L100 enteric polymer

Eud-S100- Eudragit-S100 enteric polymer

Eud-FS-30D- Eudragit-FS-30D enteric polymer

Eud-MPs- Eudragit-L100 microparticles

Ex- Excitation wavelength

FaSSGF- Fasted state simulated gastric fluid

FaSSIF- Fasted state simulated intestinal fluid

FBS- Foetal bovine serum

FCS- Flow cytometry software

FeSSIF- Fed state simulated intestinal fluid

FGF2- Fibroblast growth factor-2

F-GET- NHS-Fluorescein labelled insulin complexed with peptide forming nanocomplexes

FITC- Fluorescein isothiocyanate

FK- Forskolin

GAG- Glycosaminoglycan

GET - Glycosaminoglycan-binding enhanced transduction

GI- Gastrointestinal

GIP- Glucose dependent insulinotropic peptide

GIT- Gastrointestinal tract

GLP-1- Glucagon like peptide-1

GM- Growth media

HB-EGF- Heparin binding- epidermal growth factor

HBSS- Hanks balanced salt solution

HCl- Hydrochloric acid

hCT- Human calcitonin

HIV-1- Human immunodeficiency virus type 1

HP- Homing peptide

Hr- hours

HSV- Herpes simplex virus

HSPG- Heparan sulphate proteoglycans

Ins-F or F- Recombinant human insulin labelled with NHS-Fluorescein in lab

Ins-F*- FITC-insulin proprietary product purchased from Sigma Aldrich

Ins-T or T- Recombinant human insulin labelled with NHS-Rhodamine

Ins or N- Non-labelled insulin

I.V- Intravenous

L- LK15 is a synthetic amphipathic nucleic acid interacting peptide serving as linker molecule between GAG-binding domain and CPP

L-Glut- L-Glutamine

M- Molar solution

MCa- Maurocalcine

M-Caps- Minicapsules size-9 for *in-vivo* studies in rats/mice

Min- minutes

MTSs- Membrane translocation sequences

MW- Molecular weight

N- Normal solution

NA- Noradrenaline

NaOH- Sodium hydroxide

NAS- N-acetyl-sphingosine

NCs- Nanocomplexes

NHS- N-Hydroxysuccinimide

NLSs- Nuclear localisation sequences

NPs- Nanoparticles

OID- Oral insulin delivery

P- P21 is a 21 amino acid expressing sequence of putative heparin-binding domain of HB-EGF

P_{app}- Apparent Permeability co-efficient values

PBS- Phosphate buffer saline

Pen/ Strep- Penicillin/ Streptomycin

Pep- Pepsin

PLR- P21-LK15-8R

PTDs- Protein transduction domains

pVEC- Vascular endothelial cadherin

Prot. K- Proteinase K

PYY- Peptide-YY

R- 8R or octaarginine holds 8 arginine residues, most widely studied CPPs

RH-insulin- Recombinant human insulin

Rho- Rhodamine

R.T.- Room temperature

RUNX2- Runt related transcription factor-2

SEM- Scanning electron microscopy

S.D.- Standard deviation

SFM- Serum free media

SGF- Simulated gastric fluids

SIF- Simulated intestinal fluids

SPR- Surface-plasma-resonance

Tat- Transactivating transcriptional factor

TEER- Transepithelial electrical resistance

TEM- Transmission electron microscopy

T-GET- Ins-T-GET NCs

TRITC- Tetramethyl-rhodamine

TJ- Tight junctions

Tv- Total volume

Vol.- Volume

WR- Working reagent

YB- Yohimbine

λ- Wavelength

mM- Millimolar

µM- Micromolar

nm- Nanometer

mV- Millivolt

KDa- Kilo Dalton

List of Tables

List of Figures

Abstract

Insulin a peptide hormone regulates blood glucose levels and is considered a mainstay of treatment for diabetic patients. Oral insulin delivery still represents an overwhelming challenge due to its physio-chemical instability in gastro-intestinal tract (GIT) and poor intestinal permeability. A novel multidomain fusion-peptide system was employed to overcome these barriers termed Glycosaminoglycan (GAG)-binding enhanced transduction (GET) system, where GAG-binding motif promotes cell targeting and surface binding, whereas cell-penetrating-peptides (CPPs) region allows efficient cell entry. Here, potential of GET system in enhancing intestinal insulin permeation (transcytosis and translocation efficiency) was assessed across an *in-vitro* gut model system (Caco-2 cell monolayers). Insulin recycling was studied using different secretion regulators, moreover functional activity (by employing insulin-reporter cells) and stability of insulin-GET nanocomplexes (NCs) was also determined. In-house synthesised NHS-Fluorescein labelled insulin (Ins-F, non-quenchable) was used for studying internalisation, and transcytosis. Different stability assays were developed for GET system and insulin-GET NCs using quenchable proprietary FITC-insulin (Ins-F*). The difference in fluorescent behaviour of both insulins was studied using quenching and dequenching assays. pH-sensitive micro-particulates (MPs) based on Eudragit-L100 served as an enteric carrier system for insulin-GET NCs. These Eudragit-L100-MPs were characterised for their size, charge, morphology, drug release as a function of pH, and cellular uptake efficiency of released NCs across Caco-2 monolayers. Furthermore, enteric coated minicapsules were developed as an alternative to MPs for oral insulin delivery.

GET-peptide generates NCs with insulin and efficiently enhances its transport across differentiated model of intestinal epithelium (>8.7-fold greater translocation efficiency over un-modified insulin). Both the GET-system and insulin-GET NCs were resistant to proteolytic degradation, and NCs were stable and stayed intact even after being translocated inside cells. GET-peptide quenched the fluorescence of Ins-F*, which was successfully reversed using different proteolytic enzymes. Various studied inhibitors had insignificant effect on transcytosis and

cellular uptake of NCs. Functional assessment using transcription reporter assays activated by insulin signalling (iLite-cells) revealed that NCs retain biological activity and may induce pharmacological response. Spherical Eudragit-L100-MPs (diameter 1250 nm & surface potential -8.3mV) displayed an entrapment efficiency of 77%. These MPs prevented insulin release at pH 1.2, with maximum release observed at pH 7.4. Likewise, enteric-coated minicapsules exhibited pH-dependent release in biorelevant media providing complete release in FaSSIF. The ability of this multidomain peptide sequence (GET) in promoting insulin permeation, transcytosis and intracellular uptake across *in-vitro* intestinal model while retaining insulin's functional activity might provide a step forward towards development of on oral insulin delivery system. Overall, this work underlines the application of non-viral vectors to overcome gastrointestinal barriers associated to oral insulin delivery. Current focus is to improve insulin bioavailability by formulating novel carrier system, which may possibly allow GET peptides to be an alternative approach in establishing effective oral peptide therapeutics for diabetes.

Chapter 1. Introduction

1.1. Background

The content of this Chapter of thesis is modified from the publication (review article) by Sahrish *et al*., 2018 [1] in which I was the leading author.

Advances in biotechnology and molecular biology has led to introduction of an increased number of new therapeutic proteins/peptides into market which are extensively employed for therapeutic applications in medical and biomedical sciences. Due to their exquisite specificity, selectivity, and bioactivity; therapeutic proteins are regarded as drugs of choice for treatment of an assortment of diseases. Formidable obstacles in effective oral delivery of proteinaceous molecules that must be overcome include; low stability, poor absorption, lack of lipophilicity resulting in lower permeation, and rapid inactivation/degradation by the gastrointestinal enzymes thereby compromising the bioavailability and therapeutic efficacy [2-4]. Protein drugs have been in use since 1920, when bovine and porcine insulins were introduced for treatment of diabetes. According to a recent estimate, protein and peptide drugs share greater than US$40 billion/year and 10% of the pharmaceutical market [5]. A recent review has revealed that so far at present there are approximately 140 peptide molecules in phase of clinical trials with 500 peptides in the phase of advanced preclinical testing and more than 60 US FDA approved therapeutic proteins are in the market [6]. In recent years several novel peptide delivery strategies have emerged for overcoming the problems of biopharmaceutical instability associated with proteins, thereby improving productivity. These alternative routes of administration for peptide-based drugs include oral route (penetration enhancers, protease inhibitors, polymeric or mucoadhesive carriers, and chemical modification), mucosal route (nasal spray, sublingual or pulmonary delivery), transdermal route, and improved controlled release parenteral routes [7-9].

During the past two decades, cell penetrating peptides (CPPs) or protein transduction domains (PTD) have emerged as powerful trans-epithelial vectors for the efficient intracellular delivery of large variety of cargoes through the biological

membranes [10-12]. CPPs are relatively small functional carrier peptides, typically cationic or amphipathic with 5-30 amino acids, water soluble, and can be isolated from naturally existing proteins, modified or designed *de-novo* [13, 14]. They can enter cells in a non-invasive manner without disrupting cell membrane integrity. CPPs have successfully delivered a large variety of drugs inside cells, such as proteins, nucleic acids, phospho-peptides, contrast agents, radiotherapeutic agents and drug carrier systems including liposomes, quantum dots, micelles and nanoparticles (NPs) [15-17].

Derivatives of CPP i.e. CPHP that combine features of both translocation and cell specificity of CPP and homing peptides (HP) were designed successfully, which imparted cell specificity to CPPs by targeting specific markers on the cell surface [18]. These CPPs are capable of penetrating biological cell membranes at low micromolar concentrations, through adsorption to cell-surface GAGs and subsequently are processed by endocytic pathway without significantly affecting the membranes [19, 20]. The use of transactivating transcriptional factor (Tat) as first CPP vector for enhancing the *in-vitro* insulin absorption efficiency across the intestinal epithelium was reported in 2005 [21]. Several types of CPPs (arginine rich and amphipathic peptides) have been studied for enhancing insulin absorption through rat ileal segments, showing that co-administration of insulin with CPPs can significantly increase ileal insulin absorption [22]. Numerous attempts have been made previously to optimise the potential of CPPs to function as efficient transepithelial/transmucosal vectors for delivery of therapeutic peptides such as interchanging amino acid position within peptide sequence, and altering amino acid stereochemistry from L to D. Several studies highlight the importance of utilising protease-resistant D-peptides as a predominant strategy to overcome proteolytic sensitivity. One of the common concerns for therapeutic applications is to optimise CPPs-based delivery using various strategies to prevent premature degradation of CPPs before they reach their target site *in-vivo*. This issue could be combated by employing CPPs consisting of D-amino acids (D-CPPs). This is particularly because D-CPPs containing D-amino acids are much more resistant to protease degradation compared to L-amino acids counterparts due to altered stereochemistry. This increased serum stability is not only limited to peptides

entirely containing D-amino acids, however it was also seen for small peptides with partial D-amino acid substitution at termini, and for CPPs linked to morpholino-nucleotide oligomers [23].

Recently, our group has constructed novel fusion protein that couples GAG-binding motifs and PTDs also termed as CPPs for efficient intracellular delivery of functional cargoes. Dixon *et al*., fused "P21" a heparin binding domain with "8R" a CPP widely studied for enhancing intestinal delivery of therapeutic peptides [24]. This inclusion of both P21 and 8R synergises to enhance the uptake of cargoes in different cell lines such as mouse embryonic stem cells (mESCs), human ESCs, and induced pluripotent stem cells (hiPSCs). Different therapeutic moieties; enzymes (neomycin phosphotransferases), nucleic acids, native proteins (cytochrome C), transcription factor (NANOG), and magnetic nanoparticles have been delivered successfully at two folds greater magnitude compared to previously reported studies [24].

This Ph.D. is aimed at modulating insulin using GET system in order to promote intracellular transduction of insulin across the *in-vitro* intestinal Caco-2 cells. Various experiments were performed using two different fluorescently-labelled insulins i.e. Sigma-FITC abbreviated as Ins-F* (proprietary product) and NHS-Fluorescein labelled insulin or Ins-F (in-house labelled insulin). The FITC binds with primary amines (glycine, lysine, or phenylalanine) on insulin molecule at position A1, B1 or B29 to yield mono-, di or tri-substituted FITC-insulin conjugate. The structural conformation of insulin could be affected by degree and position of FITC substitution which would ultimately influence the biological activity of a FITC-labelled insulin [25]. The difference in the type of fluorescent probe i.e FITC and NHS-Fluorescein (NHS-ester derivative of Fluorescein), labelling protocol, site of labelling and the mole of fluorescent probe per mole of insulin, altogether contributed to the differences in their fluorescent behavior on complexing with GET. This difference in fluorescent behavior of these two Fluorescently -labelled insulins upon complexation with GET was exploited successfully to develop various assays for studying the insulin transcytosis, recycling, and stability of GET system and insulin-GET NCs.

1.2. Diabetes Mellitus

Diabetes is a group of metabolic disorders caused by autoimmunological destruction of β-islet cells of pancreas, characterised by hyperglycaemia due to defects in insulin action, and/ or its secretion (Figure 1.2) [26, 27]. It is regarded as genetically heterogeneous group of disorders sharing glucose intolerance in common, being one of the leading causes for morbidity and mortality worldwide. The secretory product of pancreatic β-cells themselves are central to diabetes pathophysiology [28, 29]. In normal individuals, glucose levels in blood are maintained by balance of hormones particularly insulin and glucagon which are produced by specific type of pancreatic cells i.e. α-cells producing glucagon and β-cells producing insulin. The classic trio of symptoms associated with onset of diabetes are designated as diagnostic hallmarks which include polyphagia, polydipsia and polyuria [30, 31].

The long-term diabetic complications lead to various pathological conditions, including neuropathy with either peripheral effects such as risk of foot ulcers, or autonomic neuropathy associated with genitourinary, GI symptoms and sexual function impairment, retinopathy with potential for visual loss and blindness, and nephropathy leading to renal failure. Diabetic patients have higher incidence of peripheral vascular, cerebrovascular, and cardiovascular disorders [32].

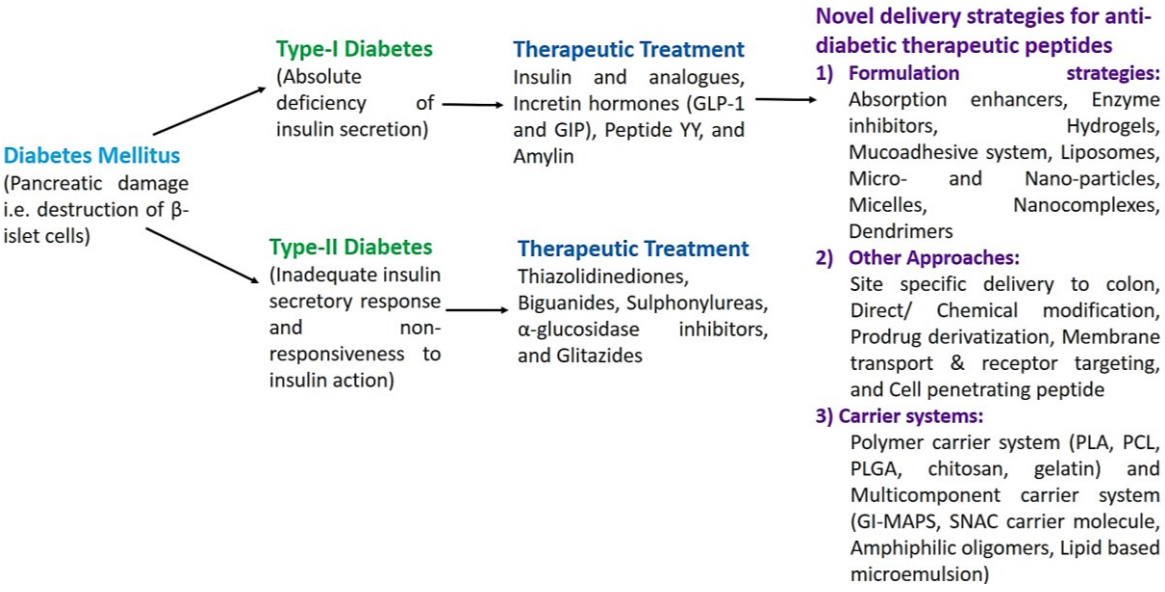

Figure 1. 1 Schematic illustration of Diabetes, its types, therapeutic management, and various novel strategies for delivery of anti-diabetic therapeutic peptides taken from review article published by Rehmani *et al*., [1].

A feedback control system regulates insulin concentration in body in response to plasma glucose levels. Additionally, insulin is also produced in response to fatty acids and amino acids and the magnitude of this response is regulated by various hormonal agents (somatostatin, glucagon-like-peptide, and glucagon), and neural factors (parasympathetic and sympathetic autonomic systems). Some of the preliminary manifestations of disordered β-cell function are following; temporal irregularities in insulin secretory oscillations and pulses, blunted and delayed response to glucose in body, and loss of tight coupling between pulses in glucose and insulin [31, 33, 34]. Moreover, diabetes could be associated with impaired conversion of proinsulin form to active insulin, resulting in greater circulating proinsulin compared to total immunoreactive insulin in diabetic patients than in healthy individuals [32].

Diabetes is characterised by chronic rise in prandial glucose levels as well as real-time calorie turnover, therefore diabetic control requires a basal and boost doses of insulin, thus delivery systems must be efficient enough to cope with the variation of boost and basal doses and also to achieve the real-time response. For facilitating development of optimal basal-bolus approaches in order to improve insulin therapy; substantial efforts have been made by altering the physicochemical and pharmacological properties of insulin [35]. Now-a-days, basal-bolus regimen is commonly used for type-I diabetic patients. Key-approach in battle against insulin comprises of once daily dosing of Long-acting insulin (insulin- glargine or -detemir) at bedtime or, two-times a day to meet basal needs alongwith bolus dose using rapid acting insulin at either premeal or meal time in accordance with the specific meal content [36]. Type-I diabetic patients on average require an insulin dosage of 0.5 - 1.0 insulin units/ kg per day, but patients newly diagnosed with diabetes may need reduced amounts due to production of some endogenous insulin. The intake of carbohydrate intake and self-monitoring of blood glucose levels are key features for establishing flexible insulin regimens [37]. It is well-established fact that *in-vivo* pancreatic insulin release occurs in a biphasic manner; where initial burst of insulin secretion occurs rapidly at 2-4 min, which lasts for 10 min, followed by gradual progressive increase to a pseudo-steady state, whereas the 2nd phase of insulin

release occurs in 2-3 hours as observed in humans [38, 39]. The endogenously produced insulin has a half-life of only 4 to 6 min [40].

In current world the insulin replacement strategies consist of administration of basal doses of insulin (small doses) during the entire day and bolus doses (appropriate insulin doses) pro-re-nata such as subtracting for exercise or supplementation in-case of additional carbohydrate intake in order to maintain near-normal glycaemia in majority of patients. In a non-diabetic patient; the real-time basal insulin level is ~10 mU/L [41] which is equal to a concentration of 6.01 x 10^{-8} mmol/L, as the assumed distribution volume of body is 19.6L, which accounts for 1.18 x 10^{-6} mmol as the total insulin mass present in circulation, whereas a bolus insulin concentration of ~70 mU/L which is equivalent to 8.25 x 10^{-6} mmol. The recommended insulin dosage for most Type-I diabetic patients is 0.5- 1.0 IU per kg/ day (Hirsch, 1999). Based on average adult body weight as 72 kg, per day insulin requirement for a diabetic patient with type-I diabetes would be 2.14 x 10^{-4} to 4.25 x 10^{-4} mmol per day.

Its recommended to take 30-50% of the total daily insulin requirements either as a long or intermediate acting insulin at bedtime, while rest of insulin dose being given as rapid/ short acting before each meal (i.e. breakfast, lunch and evening) based on the individual needs.

As Daily Insulin requirements = 0.5-1 units / kg

Normally body weight is approximately 72kg e.g. 0.5 x 72kg = 36 units or

1 x 72kg = 72 units

Thus, taking e.g. 60% 'for safety' 36- 72 units x 60% = 22- 44 units

For commencing a basal-bolus regimen consisting of 3 pre-prandial doses of rapid/ short acting insulin (to be taken prior to breakfast, lunch and evening meal) and long/ intermediate -acting insulin analogue at time for bed, the daily insulin dose is calculated as following; 22-44 units as above.

Here, Basal dose is 50% of the total daily dose which is 11-22 units, which upon rounding off for ease of administration would be 10-20 units. Bolus dose of rapid/ short acting insulin would be; 22 -10 (basal dose) = 12 units or 44- 20 = 24 (basal dose), which is divided into 3 doses of 4 units (0.5 IU) or 8 units (1 IU) per meal, and 10 units (0.5 IU dose) or 20 units (1 IU) of intermediate/long-acting insulin as basal

dose is given at bedtime. Insulin dosage can be tailored according to the individual requirement.

The International Diabetic Federation has predicted global projection in number of diabetic patients from 463 million people in 2019 to 700 million people in 2045, accounting for 51% rise in global burden of diabetes having an annual growth rate of 1.97% with the greatest increases in the developing countries of Africa, Asia, and South America [42]. The burden of diabetes is enormous in terms of both humans and financial resources, causing 4.2 million deaths and incurring global health expenditure of USD 760.3 billion dollars representing a 4.5% increase in expenditure on the 2017 estimate and accounts for 21.3% of total global spending [42]. There is a global rise in prevalence of diabetes, health expenditures associated with diabetes and deaths attributable to diabetes, alongwith social, developmental and financial implications. Diabetes in all forms is imposing an unacceptable high social, human and economic cost globally on all countries at all levels of income.

1.2.1. Types of diabetes

The development of diabetes involves several pathological processes ranging from autoimmune destruction of pancreatic β-islet cells leading to consequent insulin deficiency to abnormalities causing diminished tissue response to insulin due to insulin resistance. The classification and diagnosis of diabetes is complex and assigning individual with the type of diabetes often depends on circumstances present at diagnosis time. The American Diabetes association has recommended two broad etiopathogenetic categories for diabetes; Type-I and Type-II diabetes [26, 28, 43]. These two forms of diabetes differ from each other on basis of different genetics (i.e. non-HLA-related in type-II diabetes vs HLA-related in type-I diabetes), different natural history for both forms, and putative environment triggers (e.g. obesity in type-II and viral infection in type-I diabetes) [44]. Additionally, there are some other less common types of diabetes including secondary and monogenic diabetes. Monogenic diabetes results from the mutation in a single gene i.e. in an autosomal dominant gene, while type-I and -II diabetes results from multiple genetic mutation in different genes and environmental factors. Monogenic diabetes accounts for 1-5% of total diabetes cases and typical

examples of monogenic diabetes include maturity-onset diabetes of the young (MODY) and neonatal diabetes mellitus. Whereas, secondary diabetes arises as a result of complication of other diseases such as pancreatic diseases (e.g. pancreatitis), hormonal disturbances (e.g. acromegaly or Cushing syndrome), or as a result of using drugs (e.g corticosteroid, thiazides) [45].

1.2.1.1. Type-I diabetes

It is an absolute deficiency of insulin secretion, due to precipitation by an immune associated, if not directly immune mediated destruction of pancreatic β-cells. On the basis of immunological involvement in disease pathogenesis, type-I diabetes is further classified into; type-IA (autoimmune) diabetes associated with immunological, self-reactive autoantibodies which accounts for 70-90% of type-I disease [46], and type-IB or idiopathic diabetes which lacks evidence of autoimmune aetiology of insulin secretory defect [31, 47]. This form accounts for 5-10% of those with diabetes, occurring commonly in children or young adults, therefore it was formerly termed as juvenile-onset diabetes. It is clinically characterised by sudden onset of symptoms, particularly insulinopenia, proneness to diabetic keto-acidosis and dependence on insulin injection [29]. Biological markers for immunological destruction of pancreatic β-islet cells include insulin autoantibodies, autoantibodies to the islet cells, GAD65, and tyrosine phosphatases IA-2 and IA-2β. This disease is linked to multiple genetic predispositions such as; strong association to HLA with linkage to DQA, DQB, and DRB genes and is related to environmental factors (gestational infections, β cell toxins and other infections) as well [26, 34].

At time of diagnosis, the β-cell mass is reduced by 70-80%, which is attributable to variable degree of insulitis and lack of detectable β-cell necrosis, this β-cell loss takes place progressively over years. This β-cell death during insulitis is caused due to direct contact with T-cells and activated macrophages and their secretory products such as nitric oxide (NO), cytokines such as IL-1β, interferon (IFN)-γ, and tumour-necrosis factor (TNF)-α, and oxygen free radicals. IL-1β and/or TNF-α + interferon (IFN)-γ are known to induce apoptosis of pancreatic β-cell by the activation of β-cell gene networks. Apoptosis, the major cause of death of

pancreatic β-cells at onset of type-I diabetes is extremely regulated process, being modulated by intracellular ATP, cascades of phosphorylation, extracellular signals, and expression of pro- and anti-apoptotic genes [44].

Prevention of diabetes could be done at three possible stages, primary prevention (pre-autoimmunity) [48], secondary (post-autoimmunity, pre-diabetes) [49, 50] or tertiary (post-diabetes) [51]. Diabetes can be possibly prevented before the developmental signs of autoimmunity through; **i)** removal of early childhood diabetogenic exposure, **ii)** in high risk individuals at pre-autoimmune state via use of non-biologically active insulin analogues/ peptides, and **iii)** administering insulin chain 9-23 peptide before the progression of autoimmune assault into diabetes [31, 43]. For type-I diabetes, the primary mode of treatment and management is the exogenous insulin administration via parenteral route. Depending on the intended duration of action, insulin is formulated as lente long acting, isophane intermediate acting and soluble short acting and is largely manufactured through recombinant DNA technology [43, 52]. Different alternative administration pathways of insulin are being explored by researchers for its oral, buccal, nasal, pulmonary, ocular, rectal, and transdermal delivery [53-55].

1.2.1.2. Type-II diabetes

This form of diabetes is characterised by combination of inadequate compensatory insulin secretory response and resistance/non-responsiveness to insulin action, which altogether leads to hyperglycaemia. At each end of this spectrum are several mechanisms responsible for development of insulin resistance, and β-cell dysfunction including increased inflammatory cytokines, adipokines, mitochondrial dysfunction, amyloid formation, glucotoxicity and lipotoxicity [28, 56, 57]. This disorder accounts for 90-95% of diabetic cases and is also referred to as non-insulin dependent diabetes mellitus (NIDDM) or “adult” onset of diabetes, but it may be seen in children and young adults [26, 45, 57, 58]. Obesity is regarded major risk factor for NIDDM and most patients with this form of diabetes are obese [59].

A progressive decline in function of pancreatic β-cell function leads to glucose intolerance, which subsequently results in type-II diabetes. In humans with type-II diabetes changes in glucose-induced insulin secretion are theoretically caused by changes in function of β -cells**,** their mass or both. Patients with type-II diabetes are

at increased risk of developing microvascular and macrovascular complications because of accelerated atherogenesis. Management of NIDDM not only involves exercise and dietary control but also requires the use of combination of anti-diabetes agents (thiazolidinediones, biguanides, sulphonylureas, α-glucosidase inhibitors, glitazides, glucagon like peptides, and finally employing insulin) with antihypertensives, lipid lowering and anti-platelet drugs [26, 57].

1.2.2. Insulin and analogues

Insulin a polypeptide hormone (Molecular weight (MW) 5800 Da) was first isolated from pancreas by Banting and Best in 1922. It was one of the exciting discoveries in medical field as it revolutionised the diabetes treatment [60]. Insulin is the first protein having its chemical synthesis and primary structure being established. Elucidation of its 3-D structure, crystallisation in various forms and explication of the biosynthetic pathway in pancreas, all contributed to great scientific achievements and milestones for developing understanding of protein function and structure [61]. Insulin is an anabolic hormone having a significant role in maintenance of glucose homeostasis (Figure 1.3). Therefore, insulin is regarded as an important regulator of metabolism (carbohydrates, proteins, and fats), it facilitates glucose uptake by cells and increases the synthesis of glycogen and triacylglycerols, and stimulates DNA and RNA synthesis by modification of activity of different enzymes and transport processes [62].

The human insulin is composed of 51 amino acids, having two polypeptide chains A and B with 21 and 30 amino acids, respectively, which are linked together by disulphide bonds. The two disulphide bridges are inter-chain cysteine linkages at A7-B7 and A20-B19, and the third forms intra-chain cysteine linkage at A6-A11 [43, 63, 64]. Thus, the compact 3-D- conformation of insulin is comprised of 3-disulphide bridges and 3- α-helices (residues A1-A8, A12-18, and B9-19) and a β-strand (B21-B30). Insulin core contains hydrophobic amino-acid residues i.e. nonpolar residues (A6-A11) and aliphatic side chains of residues A2, A16, B11 and B15, with two extensive non-polar surfaces surrounding the core which are also used for insulin binding to its receptors. One of these surfaces is flat and aromatic

being responsible for forming dimer structure, while the other extensive one is involved in hexamer formation. Commercially available insulin preparations usually

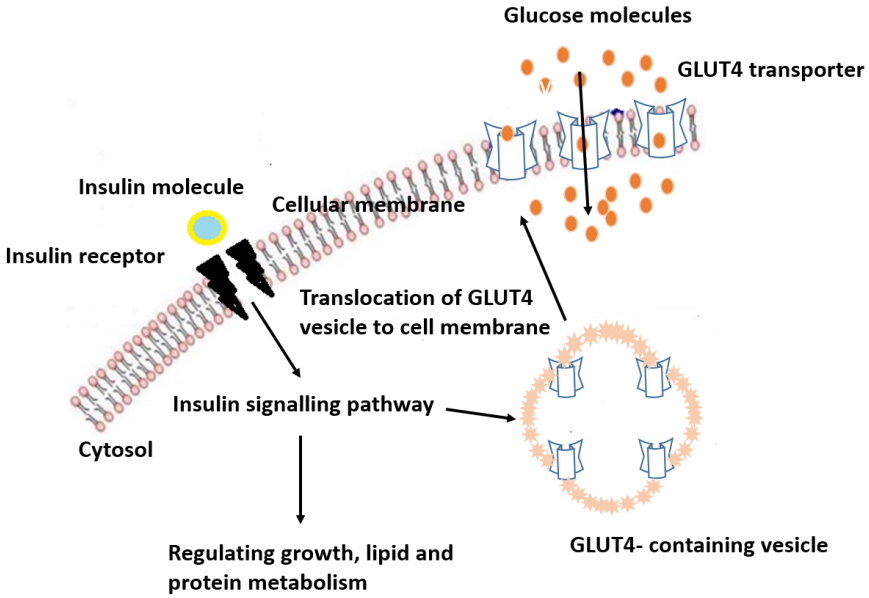

Figure 1. 2 Schematic illustration of insulin interaction with its receptors and activation of molecular mechanisms and glucose uptake, taken from review article published by Rehmani et al., [1].

contain phenol or *m*-cresol as a preservative, which promote α-helical conformation of the B-chain (B1-B8). The insulin crystals can exist in monomer, dimer and hexamer state. All pharmaceutical formulations share insulin hexamer as a common structural unit which also represents its storage form in body in the presence of zinc ions, whereas biologically active insulin is monomeric, and it dimerises at micromolar level. The zinc ions are in polar region in the centre of the hexamer linked to B10 His. The hexamer insulin form can exist in two different states i.e. T- and R- state which corresponds to an extended or α-helical conformation, respectively of the N-terminal of B-chain [65, 66]. The R-state of hexamer is induced by phenol in the presence of zinc ions, which has lesser tendency to dissociate and is more stable [61]. Insulin is broadly categorised based on its intended duration of action as soluble short/rapid acting insulin, isophane intermediate acting and long acting lente insulin [61, 64, 67].

Insulin actions at cellular level are instigated by binding of insulin to its plasma membrane receptors. These receptors are virtually located in variable concentration on all mammalian tissues, such as few as 40 receptors on circulating

RBCs to greater than 200,000 receptors on hepatocytes and adipocytes [68]. Insulin molecule recognition by its receptor is a complex molecular event and is linked intimately to transmission of signal. The insulin molecule's binding domain is composed of distant regions of chain A and B, which due to 3D-folding of molecule come together on one surface to form the receptor binding region [69, 70].

The insulin receptor is a heterotetrametric glycoprotein, consisting of two α-subunits (MW= 135,000) and two β-subunits (MW= 95,000) which are linked together through disulphide linkage to give β- α – α- β structure. Action of insulin is initiated by binding and activating its cell-surface receptor, composed of two α- and two β- subunits which form α2-β2 heterotetrametric complex via disulphide linkage. This α- subunit is positioned entirely extracellular and therefore contains insulin binding site, it transmits signal across the cell membrane and activates the tyrosine kinase domain of the β-subunits. As these β-subunits are transmembrane proteins thus these are involved in intracellular signalling. Following receptor activation, a series of intracellular transphosphorylation reactions takes place where one of the β-subunit phosphorylates its nearby partner at tyrosine residues. Evidence from studies has suggested that different tyrosine residues account for different functions, e.g. phosphorylation of terminal COOH- tyrosine activates mitogenic action of insulin, while tyrosine phosphorylation in juxtamembrane domain may play role in substrate binding, whereas the one located in kinase domain regulates catalytic activity of β-subunit of insulin receptor [71, 72]. Based on chemical aspects the insulin history can be divided into three phases, the first phase lasting over 30 years which culminated with the determination of primary sequence of insulin. The second phase lasted until the first successful development of method for the biosynthesis, chemical and semisynthetic synthesis of native human insulin, which is now largely manufactured through rDNA technology. Depending upon this foundation, the last and current investigation period is now focused on the structural optimisation and investigating various alternatives to conventional injectable administration.

1.3. Barriers/limitations in oral protein and peptide delivery

The epithelium of human GIT tends to act both as a biochemical and physical barrier for the absorption of orally delivered therapeutic proteins and peptides (Figure 1.4) [7, 73]. The impermeable intestinal epithelium is primarily attributable to cellular membranes, tight epithelial intercellular junctions, mucin lining, and drug efflux systems thereby acting as physical barrier or gatekeeper which selectively restricts

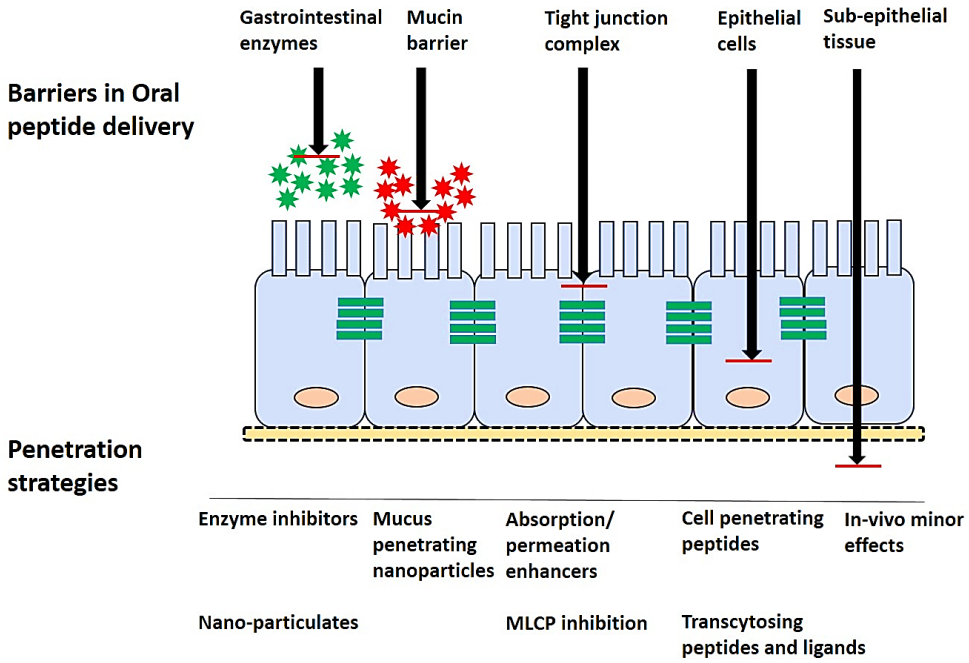

Figure 1. 3 Gastrointestinal (GI) barriers in oral delivery of peptides include; GI enzymes, mucin barrier, Tight junction (TJ) complexes and intestinal tissue barriers particularly by epithelial and sub-epithelial tissues. For overcoming these various physiological barriers different strategies could be employed, as shown in figure taken from review article published by Rehmani *et al*., [1] including; the use of enzyme inhibitors, nanoparticles, absorption/permeation enhancers, Myosin light chain phosphatase (MLCP) inhibition, cell penetrating peptides (CPPs) and transcytosing peptides.

transportation of large therapeutic moieties into the systemic circulation. Acidic denaturation/ degradation of protein drugs into non-essential amino-acids or small oligopeptides by proteolytic enzymes or luminal micro-organisms represents the biochemical barrier thus making oral protein delivery tremendously challenging [7, 73-75]. Oral bioavailability (BA) of therapeutic proteins is also limited by other factors such as; acidic microenvironment and proteolytic enzymes present in stomach, at brush border membranes of GIT (endopeptidases), in intestinal lumen

(trypsin, pepsin, chymotrypsin), in blood plasma and intracellular enzymes such as cathepsins [7].

Some other factors that severely hamper and limit the intestinal BA and absorption of orally administered proteins include; ineffective cellular uptake at target sites, uptake into non-target tissues, and possibility of inducing an immune response [76]. A number of factors are responsible for regional differences in site specific absorption of therapeutic drugs across the GIT based on; the drug nature and regional differences in composition, pH, thickness of mucosal membranes, available surface area, residence time, and enzymatic activity [77].

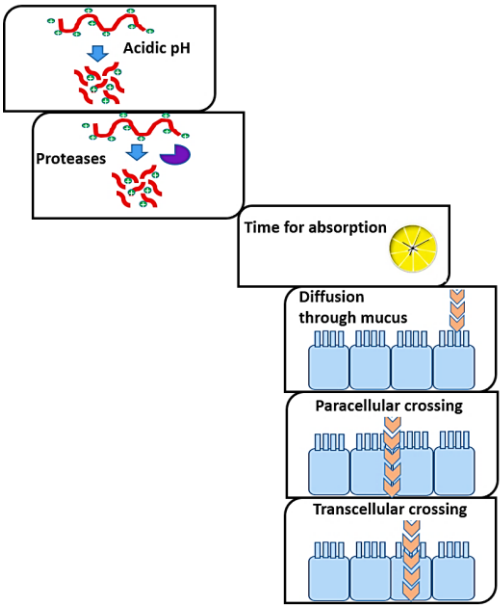

	Steps
Transit through GI tract (degradation and residence time)	
1.	Transit in stomach Degradation in acidic environment of stomach
2.	Transit in GI fluids Degradation catalysed by proteolytic enzymes
3.	Residence time of drug in the absorption window
Crossing gastrointestinal mucosal barriers	
4.	Promoting diffusion through mucosal layer by association with nanoparticles (<200nm)
5a.	Promoting <<paracellular transport>> by tight junction openers
5b.	Promoting <<transcellular transport>> by ligand receptor recognition, permeation enhancer, cell penetrating and transcytosing peptides
Routing	
6.	Portal route-> liver
7.	Systemic exposure -> peripheral tissues

Technology

Targeted tissue

Figure 1. 4 Consecutive steps confronted in oral absorption of therapeuti**c** peptides can be categorised as; 1) Transit through gastrointestinal (GI) tract (stomach, GI fluids, residence time in absorbance window), 2) Crossing GI mucosal barriers through diffusion, paracellular or transcellular transport using NPs, tight junction openers, permeation enhancers, Cell penetrating peptides, and 3) Routing either through portal route or systemic exposure (figure taken from review article published by Rehmani et al., [1].

The prerequisite steps for oral absorption of therapeutic peptides can be classified into; transit (through stomach, GI fluids, and time of residence in absorption window), passage across intestinal biological barriers (by simple diffusion, transcellular or paracellular transport), and finally the routing (Figure 1.5). Specific type of barrier (biochemical, chemical or physical) is associated with each of these steps which limits the entry of peptide drugs into the systemic circulation.

A review has been recently published by our group in which detailed application of CPPs and transcytosing peptides in oral delivery of anti-diabetic therapeutics has been discussed. This review focuses on CPPs origin, their classification, various CPPs which have been used to-date for oral and nasal delivery of insulin and other anti-diabetic peptides, their cellular uptake mechanism, and relative efficacies [1]. In recent years, various oral protein delivery strategies have been explored in order to overcome the traditional problems encountered with oral delivery of therapeutic proteins such as; use of enzyme inhibitors, membrane transporters, cell penetrating peptides, physicochemical modifications, mucoadhesive systems, stimuli responsive polymer systems, and site specific targeting or delivery [3, 8, 9].

1.4. Drug transport mechanism in Gastrointestinal tract (GIT)

A number of drug transport mechanisms are responsible for absorption of therapeutic drug molecules across GIT and can be broadly categorised into; simple diffusion (either paracellular or transcellular pathway), carrier mediated transport, active drug transport, and endocytosis or pinocytosis [7, 8, 78]. Physicochemical properties of therapeutic moieties which define drug transport mechanism through intestine include; molecular size and charge of drug, H-bonding potential, lipophilicity, and conformation in solution for transversing the apical and basolateral membrane [75, 79, 80]. Most of the orally administered clinical drugs are absorbed via transcellular passive diffusion, being adopted by drugs having high permeability and a steeper concentration gradient across cellular membranes [81]. Intestinal permeability of drugs is inversely proportional to their MW but increases proportionally with increasing lipophilicity. The phospholipid bilayers of cell membranes favour absorption of drugs which is limited to lipophilic drugs of MW below 700Da, while most of the therapeutic proteins are hydrophilic with MW greater than 3000Da thereby making it challenging for them to be transported through the cellular membranes. The presence of tight junctions (TJs) between adjacent cells tends to limit the transport of drugs across the intestinal epithelium via the paracellular route, thereby allowing only small hydrophilic drugs (MW <200Da) to pass through. Consequently, even with the availability of number of

different transport mechanisms, the oral absorption and BA of most proteins is limited following oral administration [82, 83].

1.4.1. Transcellular pathway

The transcellular pathway involves passive diffusion, receptor mediated endocytosis or facilitated transcellular transport of drugs through the intestinal epithelial cells and M cells of Peyer's patches which could be passive or active [7, 84]. Passive diffusion takes place through nonspecific permeability pathways across the intestine, in comparison facilitated transcellular transport involves specific membrane-associated transporters or channels, however studies have shown that the receptor mediated endocytosis is more efficient than pinocytosis [78]. Transcellular route for drug absorption also operates through the use of specific carriers such as amino acid and peptide transporters which transport drugs molecules from the lumen of intestine into the cells [85]. In addition to typical amino acid transporters, some specific carrier systems are used for active transportation and absorption of intact di- and tripeptides in small intestine [86].

The efficient transport of peptide and peptide-like drugs across the intestinal membrane is dependent on intestinal peptide system which has an unrecognised role in drug transport and therefore needs greater understanding of its molecular specificity for the preparation of orally active peptides [7, 87]. Transcellular passive diffusion of drugs is dependent on various physio-chemical properties of drug molecules including charge, size, and lipophilic character to ease the passive drug flux across the lipophilic intestinal membranes [88]. Transcellular route offers extensive surface area for the drug absorption and is regarded as ideal for absorption of lipophilic drugs, however the drugs absorbed through this route are often substrate for the p-glycoprotein mediated efflux system [85, 89].

1.4.2. Paracellular pathway

This route involves transport of molecules through aqueous filled pores between the cells which comprise approximately 0.01-0.1% of total intestinal surface area and is most preferred route of transport for hydrophilic drugs. Drug transport through paracellular pathway relies on molecular dimension and overall ionic charge. The drug entry through this route is regulated by tight epithelial junctional

proteins and this route only allows small solutes, water, and ions to pass through. The intestinal junctional complex exists between the adjacent intestinal epithelial cells and is composed of three parts including, zonula occludens (tight junctions), zonula adherens and macula adherens. The presence of tight junctions (TJ) complex at the apical neck constitutes the major rate limiting barrier in paracellular transport and the narrow spaces between adjacent enterocytes tends to restrict the absorption via the paracellular route. Protein and peptide drugs are hydrophilic with logP value <0, enabling them to be transported majorly through paracellular route, but the presence of TJ and zonula occludens between epithelial cells of intestine severely hamper the penetration of these polar macromolecules [90, 91]. These tight junctions contain fenestrae having average diameter of 3-10A^{o}, functioning as a gate by controlling drugs diffusion and are selectively permeable to small hydrophilic molecules <100-200 Da (ions, drugs and nutrients). However, polypeptides exhibit higher conformational flexibility thus it is likely that even bigger drug molecules can diffuse across the tight junctions [92]. Paracellular transport can be increased through modulation of tight junctions associated with this pathway or by modification of drug molecules. Paracellular transport plays important role in absorption of peptides such as salmon calcitonin, throptropin-releasing hormone (TRH), octreotide, and peptidomimetic renin inhibitors [73].

1.5. Cell penetrating peptides (CPPs)

Over the last two decades, CPPs also termed as PTDs have emerged as powerful trans-epithelial vector for the efficient intracellular delivery of large assortment of drug cargoes across the biological membrane. Alternatively, CPPs are also termed as Trojan peptides or membrane translocation sequences [10-12]. CPPs are small functional carrier peptides (5-30 amino acids), typically cationic or amphipathic, water soluble, and can be isolated from naturally existing proteins, modified or designed *de-novo* [13, 14]. These peptides offer advantages in terms of biocompatibility and as their peptide sequence can be modified thus providing highly tuneable features i.e. stability, hydrophobicity, charge, affinity and solubility. CPPs have provided new insights for research and application in biomedical sciences due to their versatile functionality and ability to undergo structural

modification for enhancing intracellular delivery of macromolecular complexes. More than 100 CPPs consisting of variable amino acids sequence (5-40) have been identified over the last 20 years, which can proficiently internalise into mammalian, bacterial, and plant cell membranes, thus facilitating the intracellular transport of a great number of biologically active drug molecules, cargoes, and drug delivery vectors [15]. In year 1988, first CPP was discovered from the retrovirus human immunodeficiency virus type 1 (HIV-1) termed as trans-activator of transcription (Tat_{48-60}), which readily entered and translocated the nuclei of cultured HeLa cells *in-vitro* and achieved intra-cellular access [93, 94]. Penetratin, a 16 amino acid transcription factor of Drosophilia melanogaster was isolated in 1991, it exhibited receptor independent penetration ability, enabling it to efficiently enter the nerve cells, thus regulating the neural morphogenesis [95]. The vehicular potential of CPPs was found in year 1995, as some studies provided evidence that pAntp peptide could be linked to bioactive drug molecule to form a conjugate complex for intracellular delivery [96].

Following this, preliminary *in-vivo* experiment using Tat covalently linked to β-galactosidase provided insight into CPPs potential to act as transepithelial vectors [97]. This impermeable macromolecule was successfully delivered in a cell type independent manner to cytoplasm of several tissues. Later on, large number of novel natural and synthetic CPPs have been discovered or designed rationally and have been studied for their translocation efficiency such as, VP22 derived from herpes simplex virus (HSV), synB vectors, maurocalcine (MCa), vascular endothelial cadherin (pVEC), transportan, and human calcitonin (hCT) [10]. Another important breakthrough was made by Wender and Fukati in year 2000, when they demonstrated that 8R alone is sufficient for enhancing *in-vivo* uptake of peptides [98, 99].

1.5.1. Cellular uptake mechanism of CPPs

A variety of cellular uptake mechanisms for CPPs appear to be operative in different systems, which are influenced by physicochemical parameters of CPPs such as; concentration, charge delocalisation, hydrophobicity, molecule length and secondary structure as well as by specific cargo of interest (nature, type and active concentration), mode of interaction with the cell surface components, formulation

approach, cell type, membrane composition, and incubation time [100-103]. Direct translocation was evoked as first mechanism for CPPs internalisation, which was then refuted as an artefact of fixation, but later on mechanism of direct translocation for cellular uptake of CPPs was confirmed through fluorescence in living cells, quantification of uptake in the absence of endocytosis (depleted ATP) and at 4^{o}C and via different biophysical approaches in model system [104]. Since then cellular uptake mechanism of many CPPs has been re-evaluated and it was reported that not only direct membrane translocation, but also endosomal pathways are commonly exploited by CPPs. But all these mechanisms for cellular uptake are somehow interconnected and can occur simultaneously, as up-regulation of one pathway may lead to down-regulation of other.

Broadly there are two distinctive mechanisms through which CPPs can translocate the cellular membrane; firstly, the energy-dependent vesicular transport which is also termed as endocytosis and secondly via energy-independent i.e. direct translocation across membrane lipid bilayer (Figure 1.6). The former CPP-mediated transport has been reported to take place through various endocytosis routes such as; macropinocytosis via caveolae- or lipid-raft mediated, through cholesterol-dependent clathrin-mediated pathway or clathrin-dependent pathway [105]. For cationic carrier peptides, positively charged groups allow them to adhere to cells via electrostatic interaction by coupling with anionic moieties present on cell surface. This carrier peptide-drug complex is then internalised by permeation through membrane by remodelling of the actin networks accompanied with selective activation of small GTPase Rho A or Rac1, leading to gradual release in cytoplasm [106, 107].

Macropinocytosis is regarded as one of the specialised forms of endocytosis which could be caveolae-, clathrin-, and lipid-raft-mediated independent endocytic process. This process of macropinocytosis involves a range of events initiated by massive restructuring or ruffling of plasma membrane to form specialised structures called macro-pinosomes which are subsequently enclosed and then internalised [108]. One of the first and best characterised endocytic pathway is clathrin-mediated endocytosis, this process starts at the surface of cell membrane, followed by the formation of clathrin-coated invaginations which gets ultimately

pinched off to form clathrin-coated-vesicles [109]. It is known that direct translocation of CPPs across the cellular membranes takes place in an energy-, receptor-, and temperature-independent manner, additionally it may also be accomplished through changes in transmembrane potential and via inverted micelles formation.

Various hypothesis have been reported for demonstrating direct translocation as cellular uptake mechanism for CPPs across the lipid bilayer including inverted micelle formation, adaptive translocation, pore formation model, carpet model,

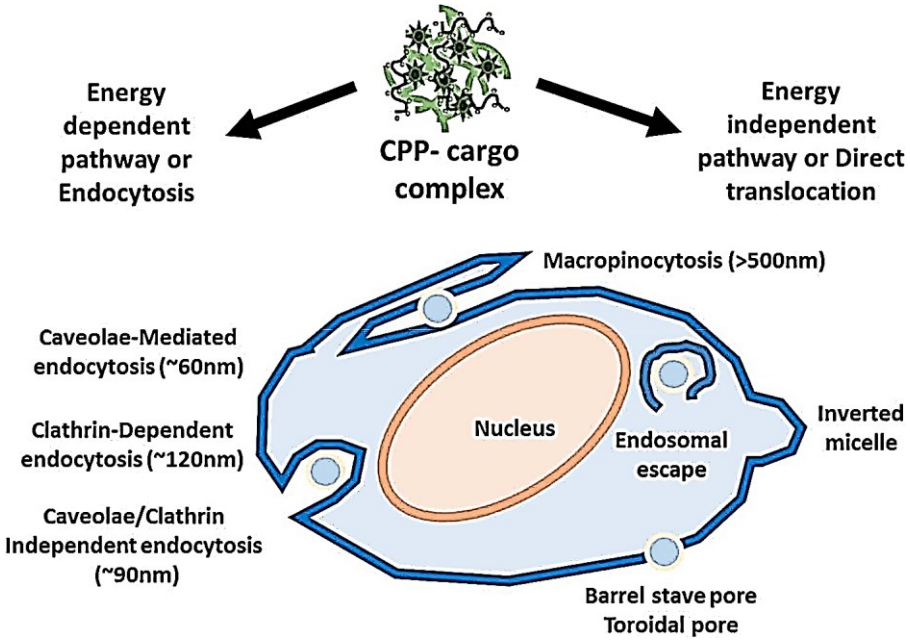

Figure 1. 5 Mechanism for uptake of cell-penetrating-peptide-cargo complexes across the cellular membrane; and is taken from review article published by Rehmani et al., [1].

and membrane thinning model [100, 104]. Inverted micelle formation was the first proposed model involving the interaction of basic residues with negatively charged phospholipids in cell membrane followed by subsequent interaction of hydrophobic residues with the membrane core. This altogether led to destabiliisation of lipid bilayer forming a negative curvature by invagination of membrane and simultaneous reorganisation of neighbouring lipids induced the formation of inverted micelle encapsulating the CPP in its interior [110, 111]. Adaptive translocation/ diffusion is driven by plasma membrane potential and is dependent on the capacity of guanidinium head groups to form bidentate H-bonds

and thereby enables oligoarginines to reveal either hydrophobic or hydrophilic character based on the associated counter anion. This interaction between phospholipid head groups and guanidinium-rich peptides tends to attenuate the polarity of CPP by masking its charge and thus facilitates the adaptive diffusion of peptide into and across the membrane [112, 113].

1.5.2. CPP-mediated cargo delivery of insulin

With the advent of CPPs it is now possible to achieve efficient intracellular trafficking of drug-cargoes or payloads. Development of delivery systems based on CPPs as cargo carriers have emerged as an attractive strategy for addressing and overcoming the current limitations in oral insulin delivery. Conjugation of antidiabetic therapeutics with CPPs tends to provide a potentially effective approach for enhancing the intracellular delivery of drugs and protecting them from degradation by the harsh GI environment. The potential of Tat to act as a transepithelial vector for the therapeutic proteins was determined both *in-vivo* and *in-vitro,* where Tat-p27 proteins efficiently and rapidly transduced 100% cells in concentration dependent manner, which was refolded *in-vivo* while retaining their biochemical and biological properties [114]. Additionally, intraperitoneal injection of Tat fused to β-galactosidase protein resulted in efficient delivery to all tissues of mice including brain [115]. These promising results opened new possibilities for direct delivery of therapeutic proteins. Since then, numerous CPPs have been employed as transmucosal delivery vectors for therapeutic peptides/ proteins, and recently several more advanced CPP- based oral drug delivery systems have been reported in literature.

1.5.2.1. CPP-mediated delivery of insulin for enhancing intestinal absorption

Tat-peptide was reported as first CPP vector for enhancing the absorption efficiency of insulin by Liang and co-workers in 2005. This insulin-Tat conjugate enhanced the insulin permeability by 6-8 fold in comparison to normal insulin as tested on Caco-2 monolayer [21]. Kamei *et al*., reported the use of diverse types of CPPs particularly amphipathic- and arginine rich- peptides for improving absorption of insulin through ileal segments of rats. Co-administration of insulin with R8, penetratin, RRL helix, and pVEC peptides showed significant improvement of insulin ileal absorption [22].

It is an established fact that D-amino acids based CPPs are protease resistant and less prone to proteolytic degradation which renders them more stable than their co-responding L-isomers. CPPs undergo rapid degradation when exposed to serum or cells, which in turn can render these carrier/ delivery molecules ineffective both *in-vitro* and *in-vivo* [116, 117]. One of the common strategies employed to protect CPPs from degradation is to use D-CPPs instead of their counter-part L-amino acid based CPPs, this approach has been applied to various CPPs including R9, Tat, penetratin, pVEC, hLF, and sweet arrow peptide [118, 119]. Simple co-administration of R6 and R8 with insulin caused an increased insulin absorption, this effect was dependent on length of peptide sequence, however increasing the chain length to R10 resulted in reduced insulin absorption. Among studied polyarginines, the D-R8 had the greatest effect on enhancing insulin absorption across the intestine and therefore induced stronger hypoglycaemic effect in a dose dependent manner [120]. D-amino acid-based arginine-rich CPPs are reported to be less susceptible to proteolytic degradation with high affinity for serum proteins and provide greater internalisation and intercellular delivery compared to its counterpart L-form. Few arginine residues are required to efficiently interact with tumour cells, resulting in prolonged retention and accumulation in tumours [121].

Further studies were performed by Kamei and co-workers in order to verify the validity of their hypothesis regarding the involvement of electrostatic interaction between carrier peptide and drug molecule. Selected 16-peptide drugs with different isoelectric values were co-administered with D-R8 peptide, followed by analysis of intermolecular binding using surface-plasma-resonance (SPR)-binding assay and *in-situ* absorption study in intestinal loop of rats. The results indicated that D-R8 was capable of enhancing intestinal absorption of only three drugs namely insulin, GLP-1, and gastrin [122]. These findings provided an insight that strategies involving use of polyarginines as CPPs for enhancement of intestinal permeability of drugs often require involvement of intermolecular binding forces (electrostatic interaction) between drug cargo and the carrier peptide.

Kamei *et al*., explored key factors essential for optimising the *in-vivo* insulin delivery using non-covalent approaches. They reported D-form of penetratin and PenetraMax to be highly effective in enhancing oral insulin absorption, where D-

PenetraMax was most efficient in terms of providing a much rapid onset of insulin absorption enhancement effect [123]. Another study attempted to identify the sequence of peptide which could provide optimal intestinal insulin absorption. For this purpose, 26 penetratin analogues were developed by varying; length of chain, basicity, hydrophobicity, and amphipathicity. Modifying penetratin peptide by; alteration of chain length by shortening the peptide sequence, varying hydrophobic units, altering arginine or lysine residues to leucine units, and addition of tetra arginine (R4) residues to N- or C- terminus of penetratin, resulted in abolishment or weakening of absorption-enhancement effect of insulin. Additionally, shuffling all amino acids in peptide sequence resulted in complete abolishment of absorption enhancement effect of penetratin, but the shuffled RK-fixed analogue [(shuffle (RK-fix)-2] boosted the intestinal insulin absorption more efficiently compared to parent penetratin [124]. Single amino acid modification of R8 at position 7 (R → glutamic acid (E)) and 8 (R → W) together with N-terminal conjugation with stearic acid (SA-R6EW) exhibited considerably more effective insulin permeation enhancement effect than R8 and R6EW both in *in-vitro* and *in-vivo* models*,* this SAR6EW-insulin complex also provided protection to insulin against proteolytic degradation [125]. Table 1 enlists different CPP for promoting the insulin delivery both *in-vitro* and *in-vivo*.

1.5.2.2. Advanced formulations exploiting CPPs for enhancing insulin delivery

In recent years, various novel and advanced approaches have been adopted for improving the therapeutic and functional potential of CPP-drug cargo formulation. As evident from studies, these promising results of CPPs in enhancing transmucosal delivery of therapeutic proteins needs further improvement in terms of designing formulation using functional excipients and/or employing recent advanced technologies for developing a suitable final dosage form. Some of the CPP-drug cargo formulation are listed in Table 2.

R8 conjugated hydroxypropyl-β-cyclodextrin (HP-β-CD) formulations exhibited variable transportation efficiency in the following order: insulin-HP-β-CD-CPP> insulin-CPP> insulin-HP-β-CD> insulin with 8-10, 5-7- and 2-times greater transportation efficiency, respectively across Caco-2 cells compared to normal insulin. Both formulations, insulin-HP-β-CD-CPP and insulin-CPP significantly

decreased glycaemia in diabetic rats while maintaining blood glucose levels at low level for upto 4 hours (hr) [126]. Similarly, CPP-conjugated carboxymethyl-β-cyclodextrin inclusion complexes showed significantly higher insulin internalisation (3-fold) across Caco-2 monolayers compared to insulin/CM-β-CD. Moreover, *in-vivo* studies in rats showed best biological response in terms of significant hypoglycaemic response, with highest increase in insulin permeability, and no toxicity [127]. Penetratin based NCs were developed by modifying bis-β-CD through conjugation. These P-bis-CD NCs were reported to be significantly more effective than PEN-NC in enhancing insulin transport and permeation across Caco-2 cell monolayers and provided a prominent hypoglycaemic effect which lasted for 6 hr in diabetic rats [128].

1.5.2.3. CPP-mediated delivery of insulin for enhancing nasal absorption

Administration of drugs through nasal route is another non-invasive approach which keeps a great promise for the absorption of therapeutic proteins/peptides due to efficient permeation and lower degradation offered by nasal mucosa. Similarly, to the intestinal mucosa, the nasal mucosal epithelium also holds numerous microvilli which offer relatively larger surface area for absorption of drugs and additionally this route also circumvents the hepatic first-pass metabolism. The potential application of CPPs for delivery of drugs via nasal route was demonstrated by a group of researchers using Tat-peptide for the efficient delivery of genes through the nasal respiratory epithelium [129]. The first time use of CPPs for enhancing nasal insulin delivery was reported by Khafagy *et al.* The L- and D-isoforms of penetratin were more efficient in enhancing the nasal absorption of insulin in comparison to L- and D- octa-arginine. L-penetratin was most efficient among the studied CPPs in promoting the nasal absorption of insulin showing a significant dose-dependent relationship of insulin bioavailability [130].

L-penetratin and its twenty analogues synthesised by amino acid shuffling were studied for enhancing the nasal insulin absorption in rats, where only shuffle-2 analogue (Arg, Lys fix) significantly increased the nasal insulin absorption, and had negligible LDH release in nasal lavage fluid without compromising the nasal epithelium integrity [131]. A series of cationic CPPs (Tat, oligoarginine (R9), and oligo-lysine (K9)) were employed for improving nasal absorption of insulin across

the alveolar epithelial barrier. Among studied CPPs variants, the R9 was most efficient CPP in enhancing and improving the alveolar insulin absorption. Additionally, a steady decline in blood glucose levels was observed in diabetic rats which sustained over time following intratracheal instillation of INS-cR9 [132]. Recently, intranasal route has been reported as one of the alternative routes for the effective drug delivery to brain by circumventing the blood brain barrier (BBB). Here intranasal administration of CPPs with model peptide resulted in accumulation of insulin-CPP complex in the olfactory bulb and other areas of brain, these complexes also reached various distal brain regions such as, cerebellum, cerebral cortex, and brain stem. This is a pioneer study which has reported improved insulin brain delivery following intranasal administration [133].

1.6. Glycosaminoglycan (GAG)-binding Enhanced Transduction (GET) system

GET peptide technology can be regarded as a series of novel fusion proteins which tends to couple CPP with a membrane docking peptide to heparan sulphate GAGs. The cell penetrating component in this system is octa-arginine (8R), while P21 derived from heparin-binding epidermal growth factors (HB-EGF) is the heparin binding domain having high affinity for heparin, and LK15 a nucleic acid interacting sequence acts as a linker molecule between CPP and GAG-binding motif, this composite peptide was termed as GET (Figure 1.7). This multi-domain sequence comprising of CPP fused to a heparan sulfate (HS) cell targeting sequence results in improved association to cellular membrane and synergistically improves the intracellular delivery of variety of therapeutic moieties. The GET peptide used in this study displayed basic charge attribute, containing 44 amino acid residues with an average MW of 5538.04 g/mol. This peptide has an iso-electric point at pH 12.39, having net charge of 23.9 at pH 7, and extinction co-efficient of 1280 $M^{-1}cm^{-1}$. The percentage charge-based composition of this peptide sequence is as follows; basic 56.82%, acidic 2.27%, neutral 9.09%, and hydrophobic 31.82%. This multi-domain peptide has following sequence and structure as shown in Figure 1.6.

Eltaher *et al*., demonstrated the use of GET system in a 3D-hydrogel matrix system to generate gradients for intracellular transduction in mammalian cells. GET system efficiently delivered molecules (myogenic master regulator (MyoD) and mRFP-1 reporter protein) spatio-temporally into cells, this in turn enabled development of

gradients of hydrogel cell programming [134]. To overcome the conventional challenges associated with differentiation of MSCs, non-virally derived transcription factors with GET delivery system (P21 & 8R peptides) were employed

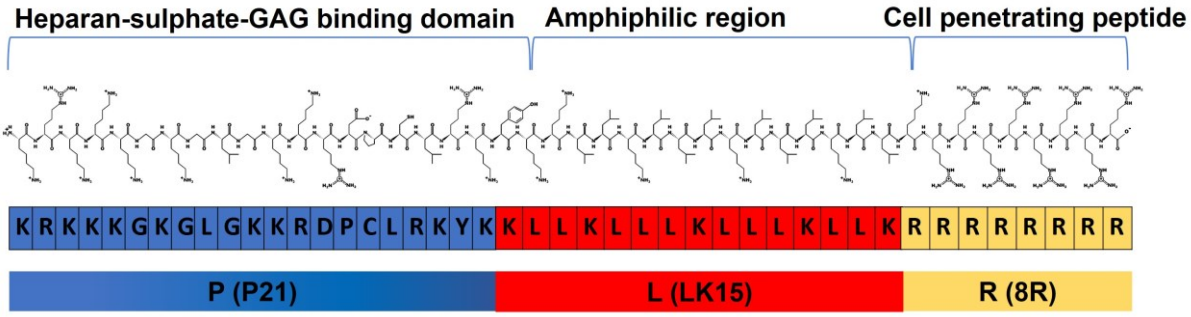

Figure 1. 6 Glycosaminoglycan (GAG)-binding Enhanced Transduction peptide system

while using osteogenic master regulator (Runt related transcription factor-2, RUNX2). Results indicated that GET-RUNX2 can efficiently transduce MSCs and can directly enhance targeted gene expression by triggering osteogenesis, as depicted by loss of stem-cell surface markers, matrix mineralisation and up-regulation of osteogenic genes [135]. GET-mRFP protein loaded MPs had high encapsulation efficiency (~65%) and efficiently tailored the release of protein, but post-release there was significant inhibition of intracellular transduction. Therefore, for retaining the activity of GET-peptide, a strategy was adopted by co-encapsulating L-histidine, which formed complex with degradation products of PLGA, and thus enhanced the release of protein [136].

The initially generated transfection peptide (PLR) by our group is the prototypical example which has been efficiently used for transfection of nucleotides [24]. When this multi-domain sequence was tested against commercial transfection reagent termed "Lipofectamine 2000", it was found that PLR has comparable transfection efficiency though requiring a higher dose of DNA to produce similar effect. Moreover, other derivatives of this novel fusion peptide containing different HS-binding sequences were also analysed, one of which is FGF2B derived from fibroblast-growth-factor-2 (FGF2) [137]. FGF2B is a short peptide (16-residues) which lacks inherent cell penetrating properties, but upon coupling with CPPs there was 100-fold greater delivery of recombinant proteins compared to unchanged CPP. Recently use of FGF2B-based GET-peptide transfection (FGF2B-

LK15-8R, FLR) has been reported for superior complexation of DNA for enhanced gene delivery to lungs and to attain highly efficient transfection. The incorporation of controlled PEG density on the particle surface imparted stabilisation in biological fluids while retaining improved transfection activity and ability to penetrate human CF sputum swiftly [138].

GET-labelled Nanomag (250nm SPION) have been employed for *ex-vivo* MRI tracking of autologous MSCs in ovine osteochondral defect model. The results indicated significant enhancement in MRI contrast due to GET-Nanomag labelling, with no obvious increase in serum c-reactive protein levels (CRP) as determined by ELISA [139]. GET was able to deliver pDNA efficiently (62%; compared to Lipofectamine® 3000) and safely to 'difficult-to-transfect' MSCs. Additionally, when combined with biomaterial scaffolds localised transfection with host cell infiltration was attained with short-term but sustained changes in gene expression. *In-vivo* application of this system resulted in single-treatment therapeutic factory which caused induction of host cells for producing angiogenic and osteogenic proteins [140].

Table 1. 1 CPP-mediated delivery of Insulin

CPP	Class	Amino acid sequence	Purpose of study	Outcome/ Result	References
GET-peptide (P21-LK15-8R, PLR)	Cationic	KRKKKGKGLGKKRDPCLRKYK KLLKLLLKLLLKLLKRRRRRRRR	Promoting intestinal permeability and intracellular uptake of insulin	GET-peptide significantly enhanced insulin transport across Caco-2 monolayers by greater than 8.7-fold compared to unmodified insulin without damaging the integrity of monolayers, the insulin-GET NCs provided superior protection to insulin and retained insulin biological/ functional activity.	Results of this study, yet to be published.
FGF2B-LK15-8R, FLR	Cationic	TYRSRKYTSWYVALKRKLLKLL LKLLLKLLKRRRRRRRR	Enhanced gene delivery to lungs	FLR provided superior complexation of DNA leading to highly efficient transfection of cells in-vitro and enhanced gene delivery to lungs, while PEG coating imparted stabilisation to this complex in biological fluid	[138]
Tat	Cationic	CGGGYGRKKRRQRRR	Improving intestinal permeability of insulin *In-vitro*	Increased insulin transport across Caco-2 cells and preventing intracellular degradation.	[115]

Tat	Cationic	CGGGYGRKKRRQRRR	Increasing insulin intestinal permeability *In-vitro* (Caco-2)	Insulin-CPP hybrid 6-8 fold increase in intestinal absorption efficiency.	[21]
Arginine rich peptides (R6, R8 and R10)	Cationic	RRRRRR RRRRRRRR RRRRRRRRRR	Enteric delivery of insulin *In-vivo*	Co-administration of insulin with oligoarginine markedly increased intestinal insulin absorption without damaging cellular integrity.	[120]
Arginine octamer (R8) Arginine dodecamer (R12) HIV-1 Tat (48–60) HIV-1 Rev (34–50) Penetratin pVEC Erns RRL helix	Arginine rich peptides Amphipat--hic peptides	RRRRRRRR RRRRRRRRRRRR GRKKRRQRRRPPQ TRQARRNRRRRWRERQR RQIKIWFQNRRMKWKK LLIILRRRIRKQAHAHSK RQGAARVTSWLGLQLRIK RRLRRLLRRLRRLLRRLR PRLPRLPRLPRL GLSASPNLQFRTV	Promoting intestinal insulin absorption *In-vivo* (rat ileal segments)	L-forms of these peptides exhibited superior intestinal absorption of insulin except for R8, where the D-form of R8 showed stronger insulin enhancing ability than L-form.	[22]

PRL4 Random peptide					
D-R8	Cationic	D-RRRRRRRR	*In-vitro* (in-situ absorption study in isolated rat ileal segment	Determined the importance of presence of electrostatic interaction between CPP and the macromolecules on the enhancement of intestinal drug absorption	[122]
Tat Oligoarginine (R9) Oligolysine (K9)	Cationic	PGRKKRRQRRPPQ RRRRRRRRR KKKKKKKKK	Pulmonary delivery of insulin *In-vitro* (RAECM & HepG2 cell lines) and *in-vivo* (rats)	Oligoarginine enhanced the absorption rate of insulin across the alveolar epithelial barrier.	[132]
L-and D-Penetratin L-and D-octaarginine	Cationic	RQIKIWFQNRRMKWKK RRRRRRRR	Nasal insulin delivery *In-vivo* (rats)	L-penetratin was the most effective promoter of nasal insulin absorption with 76.7% bioavailability	[130]
L-penetratin and its shuffled 20 analogues	Cationic	RQIKIWFQNRRMKWKK	Nasal insulin delivery *In-vivo* (rats)	A shuffle (R, K fix) analogues most effective penetratin analogue for improving non-invasive insulin delivery through nasal route compare to parent L-penetratin and other analogues.	[131]

L-penetratin and it 26 analogues	Cationic	RQIKIWFQNRRMKWKK	Intestinal insulin delivery *In-situ* loop absorption study	Shuffle (R,K fix)-2 analogue showed strongest insulin absorption-enhancement effect in intestine as compared to original penetratin and other structural analogues	[124]
L- and D-Penetratin	Cationic	RQIKIWFQNRRMKWKK	Oral insulin delivery *In-vivo* proof (mice)	D-penetratin increased the stability of insulin in intestinal fluids and is promising candidate for development as an oral absorption enhancer for insulin delivery.	[141]
R8 and its structurally modified derivatives (R6EW SAR6EW)	Single amino-acid modification and N-terminally stearylated cationic peptide		Oral insulin delivery *In-vitro* (Caco-2 cells) *In-vivo* (diabetic rats)	Amphiphilic-lipopeptide-insulin (SAR6EW-insulin) complex exhibited superior performance in enhancing the insulin permeability both *in-vitro* and *in-vivo*. Provided sustained control of blood glucose levels for upto 6 hours.	[125]
Penetratin and its analogues (PenShuf, PenArg, and PenLys)	Cationic	RQIKIWFQNRRMKWKK RWFKIQMQIRRWKNKK RQIRIWFQNRRMRWRR KQIKIWFQNKKMKWKK	Importance of cationic residues and pH for complexation with insulin and for enhancing insulin permeation	Pre-complexation of insulin with penetratin and its analogues at pH 5 resulted in greater insulin permeation as compared to that observed at pH 7.4.	[142]

Penetratin	Cationic	RQIKIWFQNRRMKWKK	Carrier morphology influencing intestinal insulin absorption *In-vivo* (mice and rats)	CPP grafted polymeric carrier effectively enhanced the intestinal absorption profile of insulin. *In-vivo* studies in mice showed effective suppression of glucose levels	[143]

Table 1. 2 Formulations exploiting CPPs for improving insulin delivery

CPP	Class	Amino acid sequence	Type of Nano-carrier	Purpose of study	Outcome/ Result	References
R8	Cationic	RRRRRRRR	Hydroxypropyl-β-CD complex	Oral insulin delivery *In-vitro* study (Caco-2 cells) *In-vivo* (diabetic rats)	Insulin–HP- β -CD–CPP significantly enhanced insulin transport across Caco-2 cell, protected insulin from degradation by intestinal proteases and provided best biological response and glycaemia control in diabetic rats.	[126]
Penetratin	Amphiphilic and cationic	CRQIKIWFQNRRMKWKK	Bis-cyclodextrin nanocomplexes	*In-vitro* cellular studies (Caco-2) In-situ intestinal loop studies *In-vivo* (diabetic rats)	P-bis-CD nanocomplexes significantly enhanced the insulin permeation with better glycaemic control and BA compared to PEN-NC.	[128]
Penetratin	Cationic	CRQIKIWFQNRRMKWKK	pHPMA-coated penetratin-insulin nanoparticles	Oral insulin delivery *In-vitro* (HT29-MTX-E12)	Self-assembled pHPMA-coated penetratin-insulin NPs can effectively overcome the mucus and epithelial barriers. Additionally, oral administration in diabetic	[144]

				In-vivo (diabetic rats)	rats produced prominent hypoglycaemic response.	
STR-R8 STR-Tat STR-Pen STR-Sec	N-terminally stearylated cationic peptides	Stearyl-RRRRRRRR Stearyl-GRKKRRQRRRP Stearyl-RQIKIWFQNRRMKWKK Stearyl-QSLAQELGLNERQIKI	PLGA nanoparticle	Oral delivery of insulin *In-vitro* (Caco-2 cell line) and in-vivo (rats)	CPP modified PLGA nanoparticles significantly enhanced the oral bioavailability of insulin in rats with stronger hypoglycaemic control	[145]
Penetratin	Cationic	CRQIKIWFQNRRMKWKK	β-cyclodextrin-graft chitosan (BCC) polymeric carriers (molecular carrier and NPs)	Permeation-enhancement effect *In-vivo* (intestinal absorption study in rats and oral administration study in mice)	CPP grafted polymeric carrier effectively enhanced the intestinal absorption profile of insulin. *In-vivo* studies in mice showed effective suppression of glucose levels	[143]

1.7. Research aims and objectives

This study aims at modulating insulin through the use of multifunctional GET-peptide, P21-LK15-8R (PLR), which is composed of GAG-binding motifs, an amphipathic sequence, and protein transduction domain exhibiting both membrane activity and cell penetrating ability, which might altogether contribute towards enhancement of intracellular trafficking of insulin.

1.7.1. Study objectives

A four-pronged approach was designed as shown in Figure 1.1; to indicate the objectives of the present PhD thesis and are briefly listed below,

- Firstly, exploiting the efficiency of GET system in enhancing the trans-epithelial transport of insulin *in-vitro* across Caco-2 cells alongwith GET-peptide mediated transcytosis and recycling. In addition to this, insulin was also labelled differently with dyes i.e. NHS-Rhodamine dye (Ins-T or T) in order to visualise and distinguish between the incoming and outgoing insulin during the recycling process. Different cell secretion modulators were also employed to study insulin recycling across Caco-2 cells.

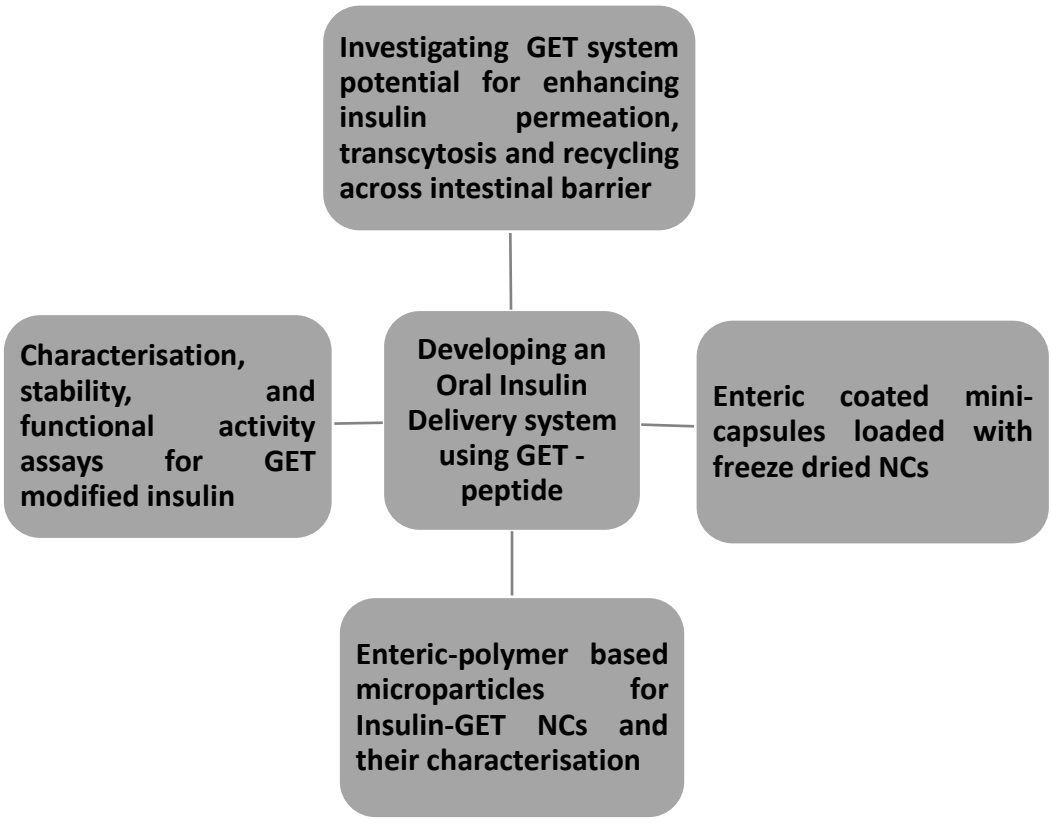

Figure 1. 7 Summary of the Project.

- The second aim was to characterise these GET-based insulin nanocomplexes and to assess the stability and functional activity for GET-peptide modified insulin. Insulin-reporter-iLite cells were employed to assess the functional activity of NCs and to determine the concentration of GET-peptide that causes maximal activation of these cells while preserving the biological activity of insulin (Chapter 4).
- The third aim was to develop an efficient carrier system (enteric microparticles) for these insulin-GET NCs in order to prevent drug release and protect drug from degradation in early GIT and testing it in *in-vitro* Caco-2 model for cellular uptake (Chapter 5).
- Furthermore, enteric coated mini-capsules (M-Caps) were developed to achieve goal of development of an efficient oral insulin delivery system by encapsulating these NCs in M-Caps (Chapter 6).

Chapter 2. Materials and Methods

2.1. Materials

Recombinant human insulin (Cat. No. 91077C), FITC-insulin (Ins-F*, Cat. No. I3661), Hoechst 33258 (Cat. No. 94403), pepsin from porcine gastric mucosa (Pep, Cat. No. P7012), pancreatin from porcine pancreas (Pan, Cat. No. P3292), trypsin (Cat. No. 59418C), D(+)-trehalose dihydrate (Cat. No. T4167) D-mannitol (D-Mann, Cat. No. M4125), sucrose (Cat. No. S-7903), glycine (Cat. No. G5417), L-histidine (Cat. No. H6034), Poly-L-lysine 4KDa (PLL, Cat. No. P0879), PLL 0.01% solution (P4707), PLL 70-150KDa (Cat. No. P6282), ATP (Cat. No. A6419), yohimbine HCl (YB, Cat. No. Y3125), N-acetyl-D-sphingosine (NAS, Cat. No. A7191), nor-adrenaline salt (NA, Cat. No. A0937), 4.4KDa (Cat. No. T1037) and 70KDa (Cat. No. T1162) tetramethyl-rhodamine isothiocyanate-dextran (TRITC-Dex) were obtained from Sigma Aldrich (UK). NHS-Fluorescein (Cat. No. 46410), NHS-Rhodamine or NHS-tetramethyl-rhodamine (Cat. No. 46406), forskolin (FK, Cat. No. BP25201), LIVE/DEAD™ viability/cytotoxicity Kit for mammalian cells (Cat. No. L3224), Alexa fluor-647 phalloidin (Cat. No. A22287), micro-BCA protein assay kit (Cat. No. P123235) were purchased from Thermo Fischer Scientific (UK). BAPTA-AM was supplied by Calbiochem (BM, Cat. No. 196419). Corning Transwell polyester cell culture inserts (Cat. No. 3460) 12mm diameter transwell inserts with 0.4µm pore size were purchased from Corning life sciences, UK.

GET peptide system (PLR) was kindly provided by Dr. James E Dixon (University of Nottingham), this peptide was prepared using solid phase tert-butyloxycarbonyl (t-Boc) chemistry by Novabiochem (Beeston, Nottinghamshire, UK). The procedure consisted of cloning peptides as cDNAs into vector (pGEX6-PI), which were expressed in BL21 pLysS E.coli and purified. The Dual-Glo® Luciferase assay kit (Cat. No. E2940) was purchased from Promega (UK). Proteinase K (Prot. K, Cat. No. 1014023) was obtained from Qiagen (UK). Eudragit (Eud)-L100, Eud-S100, and Eud-FS-30D was received as a kind gift from Evonik, Germany. FaSSIF/FeSSIF/FaSSGF biorelevant powder (Cat. No. FFF01) was purchased from the Biorelevant company. For cell culture, Dulbecco's modified eagle's medium (DMEM) (Cat. No. 42430-025), DMEM phenol red free (Cat. No. 21063-029) and Roswell Park Memorial

Institute Medium (RPMI) 1640 phenol red free (Cat. No, 32404014) and all other standard cell culture reagents were purchased from Life Technologies, UK. All other chemicals and reagents were of analytical grade.

2.2. Fluorescent labelling of insulin

NHS-Fluorescein is regarded as a fluorophore of choice and has been widely employed to label proteins fluorescently via amine group, this could be attributed to its property of quantum yield and high molar absorptivity. The insulin permeation and internalisation by cell monolayers, transcytosis and release was studied using different fluorescently labelled insulins i.e. NHS-Fluorescein and NHS-Rhodamine. The recombinant human (RH)- insulin (Cat. No. 91077C) was labelled with NHS-Fluorescein (Cat No. 46410) or NHS-Rhodamine (Cat No. 46406) using standard protocol as described below.

Insulin was labelled with green (NHS-Fluorescein) or red (NHS-Rhodamine) fluorescent dyes separately, to obtain a stock concentration (2mg/ml) of labelled insulin (Ins-F and Ins-T, respectively). Briefly 2mg of RH- insulin was dissolved in 100 µl of 0.01M HCl, followed by addition of 100 µl of 0.01N NaOH (the solution turns cloudy), and then adding 300 µl of PBS (with no Ca^{+2} containing 200 µM EDTA) until a clear solution was obtained. Insulin solution equivalent to 10mg RH- insulin was labelled with NHS-Fluorescein or NHS-Rhodamine using 3 mol to 1 mol (Insulin: Dye) ratio. The calculated quantities of respective fluorescent dyes were added to the pre-formed insulin solution separately and the pH was adjusted to 7.0. The solution was protected from light using aluminium foil and allowed to mix at room temperature using digital tube roller for required reaction time. Finally, buffer exchange was carried out on Tris-Bio-6 spin columns by applying samples to the centre of columns and centrifuging columns for 4 minutes (min) at 1000 ×g.

For studying permeation and internalisation by cell monolayers, transcytosis, recycling and release (during and post-delivery), the NHS-Fluorescein-insulin (Ins-F, non-quenchable), NHS-Rhodamine -insulin (Ins-T), and non-labelled insulin (Ins) were used. For studying different stability assays for GET- peptide and insulin-GET NCs, the Sigma-FITC-Insulin (Ins-F*, quenchable) was used.

2.3. MicroBCA assay for insulin quantification in the labelled insulin

2.3.1. Preparation of Standard i.e. Diluted Bovine Serum Albumin (BSA)

A series of BSA protein standards solutions (0-200 µg/ml) were prepared. The BSA standard 2 mg/ml ampule given with the kit was diluted to prepare a set of solutions using a diluent similar to the sample buffer. These samples were prepared in triplicates.

2.3.2. Preparation of the Working reagent (WR) for the micro-BCA

Working reagent was prepared by mixing micro-BCA reagents in following proportion: 25 parts of micro-BCA Reagent MA, 24 parts Reagent MB, and 1 part of Reagent MC (25:24:1, Reagent MA: MB:MC).

2.3.3. Procedure for MicroBCA using microplate

The procedure consisted of pipetting 150 µl of each standard or the unknown sample replicates into a white microplate well. This was followed by addition of 150µl WR to each of the well and plate was mixed gently using a plate shaker for 30 seconds. The plate was covered with the sealing tape and incubated at 37 °C for a period of 2 hr. After this, plate was removed from incubator and cooled down to room temperature. The absorbance of plate was measured at 562nm using the TECAN microplate reader. Average absorbance values of blank replicates was subtracted from the absorbance reading of all other individual standard and unknown sample replicates. A standard curve was plotted using the average Blank-corrected reading for each of the BSA standard vs. its concentration in µg/ml. This standard curve was used to determine the concentration of protein for each unknown sample.

2.4. Calibration curve for labelled insulin

A number of serial dilutions of NHS-Fluorescein-labelled insulin (0- 40 µg/ml) were made in media. The samples were prepared in triplicates, and 100 µl of samples were added to 96 -black well microplates. Fluorescence was measured using the TECAN microplate reader. The average value of blank replicates was subtracted from each of the individual sample values. The standard curve was constructed using average blank corrected fluorescence for each of the insulin sample vs its respective concentration (µg/ml).

2.5. Preparation of drug-GET carrier peptide NCs

Specific amount of insulin (Ins-F, Ins-T, or Ins-F*) was mixed separately with specified volume of GET-peptide system (PLR; 1mM) in polypropylene tubes. Following addition of labelled insulin to GET-peptide, the mixture was incubated at room temperature for 15 min to form insulin-GET NCs. Final concentrations of insulin and GET-peptide in solution were 20 µg/ml and 10 µM, respectively.

2.6. Cell lines and cell culture

Human colorectal adenocarcinoma Caco-2 cell line (HTB-37) was obtained from ATCC for all experiments. The cells were cultured and maintained in DMEM growth media (GM) supplemented with 10% v/v foetal bovine serum (FBS), 100 µg/ml streptomycin, 100U/L penicillin, antibiotic/antimycotic (AB/AM), and 2mM L-glutamine. Cell cultures were cultivated in an incubator at 37 ^{o}C in a humidity-controlled 5% CO_2 environment. The cell flasks were passaged once they reached 80% confluency. For all experimental assays serum free media (SFM) was used, which consisted of DMEM phenol red free media supplemented with standard additives except the FBS.

For cellular permeation studies, 48-well plates were initially seeded with cells at a concentration of 50,000 cells/well (5 × 10^4 cells/ well) in 0.5ml of DMEM GM (DMEM +FBS +Phenol red) with added supplements. The cells were placed in an incubator (37 ^{o}C, 5% CO_2), allowed to grow and form well-differentiated monolayers for 7-8 days. For Transwell® based assays, Caco-2 cells were seeded onto the filter supports or Transwell® inserts at a concentration of 200K cells/insert (2 × 10^5 cells/ well in 0.5ml media/ well) using DMEM GM, and incubated in cell culture incubator (37 ^{o}C, 5% CO_2). Cells were fed from both sides and were used only once they formed monolayers with tight junctions (7-10 days old).

The insulin reporter or iLite insulin ready assay cells is an avian DT-40 cell line (Product code BM3060) purchased from Svar Life Sciences (formerly operational as Euro Diagnostica AB). These cells have been engineered genetically to render them responsive to insulin by displaying a specific expression of Firefly luciferase. Moreover, a second reported gene i.e. Renilla Luciferase reporter gene construct is used to normalise serum matrix effects and cell counts under the influence of a

constitutive promotor. These cells were employed for assessing the functional activity of insulin-GET NCs, as the reporter genes in these cells are turned "ON" following exposure to insulin and thus responding to luciferase reagent.

iLite cells were thawed and assayed in RPMI 1640 medium supplemented with 10% FBS, 100 µM β-mercaptoethanol, 1% chicken serum, 100U\L penicillin and L-glutamine. This cell line was also maintained at 37 ^{o}C under 5% CO_2. The cell concentration was kept constant at one million/ml in flasks for all the assays.

2.7. Cellular uptake/ internalisation experiment set-up in Growth media (GM) and Serum-free media (SFM)

A generalised method for all cell-based assays (delivery, translocation, cellular uptake in presence of different cell secretion regulators, and etc) using Caco-2 monolayer is described in this section (Chapter 3). The 48-well plates were initially seeded with cells at a concentration of 5×10^4 cells/ well in 0.5ml of growth media (DMEM +FBS +Phenol red + additives) with added supplements. The cells were placed in an incubator (37 ^{o}C, 5% CO_2) where the media was changed every other day and cells were allowed to grow and form a well-differentiated monolayer for 7-8 days. Insulin-peptide solution (Ins-F-GET NCs) was prepared by complexing insulin with GET-peptide in SFM and mixing for 15 min. Prior to assay, growth media was aspirated from the surface of plated cells, followed by washing with phosphate buffer saline (PBS) three times, and then replacing with SFM (DMEM + additives, no phenol red and no FBS). The sample media containing fluorescently labelled-insulin (Ins-F or Ins-T, stock solution 2 µg/µl) with and without GET-peptide i.e. 25 µl of Ins-F [2.5 µl Ins-F (2 µg/µl) + 22.5 µl SFM or Insulin- GET NCs [2.5 µl PLR (1mM) +10 µl SFM and 2.5 µl Ins-F + 10 µl SFM] was added to appropriate wells containing 225 µl SFM and left overnight (O/N) in an incubator under standard conditions. Each variable group was repeated in triplicate. After O/N, the media was collected from each well and added to 96-black well plate for analysis on the Tecan infinite 200-PRO microplate reader (For Ins-F, Fluorescein channel; Ex/Em = 490/ 520 nm, For Ins-T, TRITC channel; Ex/ Em= 550/ 580nm). Following media collection, the cells were washed twice with PBS, treated with 25% (w/v) trypsin (250 µl) for 12 min, and next 300 µl GM was added. The cells were then centrifuged at 200 ×g

(1650 rpm) for 5 min, followed by aspiration of media. The cells were fixed using 400 µl paraformaldehyde (PFA, 3.7%) and analysed using MoFlo, Astrios cell sorter (Beckman coulter) flow cytometer using blue diode/ argon laser (495nm) and Hg/Arc lamp or green laser (561 nm) to detect staining for green and red fluorescent proteins, respectively (20,000 events per sample). Flow cytometry results were analysed using WEASEL software and mean fluorescence intensity was used for statistical analysis, where background from non-treated/transfected cells was subtracted and values were expressed as percentage comparative to un-modified insulin.

2.8. *In-vitro* transepithelial insulin permeation assay using Caco-2 cultured Transwells®

For carrying out permeability studies (Chapter 3) with well-differentiated Caco-2 cells monolayer, Caco-2 cells were seeded onto the filter supports at a concentration of 2×10^5 cells/ insert in 0.5ml growth media, and incubated in a cell culture incubator (37 ^oC, 5% CO_2). Cells were fed from both sides and were used only once they formed monolayer with tight junctions (7-10 days old). Culture media was aspirated, cells were washed with PBS thrice, followed by addition of sample mixes i.e. insulin (Ins-F or Ins-T) and insulin-GET NCs (Ins-F-GET NCs or Ins-T-GET NCs) in SFM (500 µl). Moreover, 1000 µl GM was added to the basal chamber (Figure 2.1). TEER values were measured and samples collected from basolateral chamber at various time intervals (0hr, 1hr, 2hr, 4hr, 6hr and 24hr) were analysed using Tecan fluorescent microplate reader (For Ins-F use of Fluorescein channel; Ex/ Em= 490/ 520 nm, For Ins-T use of TRITC channel; Ex/Em= 550/ 580nm) to determine percent drug transport/ transcytosis. Caco-2 cells were harvested from the Transwell® after O/N and analysed for determination of cellular internalisation of Ins-F or Ins-T and Ins-F-GET- or Ins-T-GET- NCs using a MoFlo Astrios cell sorter (Beckman coulter) flow Cytometer using blue diode/ argon laser (495nm) and Hg/Arc lamp or green laser (555 nm) to detect staining for green and red fluorescent proteins, respectively (20,000 events per sample). Apparent permeability co-efficient (P_{app}) was also determined for delivery molecules. For this purpose, a calibration curve was constructed using a range of insulin

concentrations based on the initial insulin concentration (the one added to apical chamber of Transwell®) used for the experiment to determine the flux of insulin transport with and without GET-peptide. The P_{app} was calculated the using the formula given below.

$$P_{app} = \frac{dQ}{dt} \times \frac{1}{A \times Co}$$

Where, dQ/dt is the flux of NCs from donor to the acceptor compartment, C_o is the initial concentration of NCs in the donor compartment, and A is surface area of membrane (cm^2).

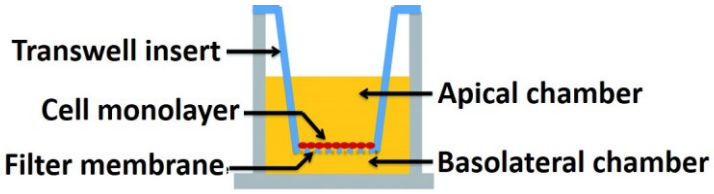

Figure 2. 1 Corning® Transwell® well plate insert showing the apical and basolateral layers of the well. The cell monolayer develops on a filter which allows exchange from apical to basal layers to study delivery, transcytosis and recycling through this monolayer.

2.9. Transepithelial electrical resistance (TEER) measurements

TEER was measured in Transwell inserts with Millicell ERS-2 Voltohmmeter (MERS00002) equipped with chopstick Silver/Silver-Chloride (Ag/AgCl) electrodes (Millipore, USA), these electrodes were dipped in media contained in transwell inserts. Following seeding of Caco-2 cells on Transwell®, TEER values were measured every day in order to confirm the growth of cells and their differentiation on the Transwell® inserts (Chapter 3). For calculating the intrinsic TEER of monolayer, electrical resistance of filter inserts in medium before seeding cells was measured and subtracted from the total measured electrical resistance. During Transwell permeation experiment, TEER of the Caco-2 monolayer was measured over defined time points (0hr, 1hr, 2hr, 4hr, & 6hr) and at the end of 24 hr incubation for detecting any damaging effects of applied molecules on the monolayer integrity (intercellular tight junctions). TEER measurements were expressed as percentage values calculated by dividing the TEER value (Ω cm^2) at each time point with the initial value.

$$R_{cell\ layer} = R_{sample} - R_{blank}$$

Where, $R_{cell\ layer}$, R_{sample}, and R_{blank} is resistance measured for cell layer, sample, and blank, respectively.

TEER (Ω^* cm^2) = $R_{cell\ layer}(\Omega)$ × area of transwell insert (cm^2)

Percent TEER= $\frac{TEER_t}{TEER_i} * 100$

2.10. Cell viability assay

AlamarBlue is regarded as a proven track indicator of cell viability / health, it works through use of natural reducing ability of living cells in converting resazurin (blue, non-fluorescent, non-toxic and cell permeable) to the resorufin a red fluorescent molecule (Chapter 3). Briefly, Caco-2 cell were grown on Transwells® at a density of 200K cells/ well in 0.5ml media and cultured for 7 days to form monolayer. Prior to the assay, culture medium was removed, and cells were incubated with Ins-F or Ins-F-GET NCs for a period of 24 hr. Following specified time, samples were aspirated, and cells were washed thrice with PBS. The AlamarBlue (10X) solution was diluted with Hank's balanced salt solution (HBSS), and 150 µl of 1X AlamarBlue solution was added onto the cells, followed by incubation at 37 ^oC for 30-60 min. Following specified time, the samples were collected, added to 96- black well plate and fluorescence was measured using the TECAN microplate reader at the absorbance of 560/590 nm (Ex/Em). The 1X AlamarBlue in HBSS media was used as a positive control for 100% cell viability.

2.11. Effect of buffer nature on cellular uptake of Ins-F and Ins-F-GET NCs

2.11.1. Cellular uptake in different buffers

This assay was performed to investigate the influence of different buffers on cellular uptake of Ins-F and Ins-F-GET NCs, to figure out the best transfection media (Chapter 3). Additionally, effect of these solvents on cellular viability and maintenance of monolayer integrity was also taken into consideration. For this assay, insulin complexes were prepared in different buffers i.e. Ins-F was reacted with GET-peptide in SFM, PBS, and direct complexation with no solvent. Following complexation, NCs were incubated with Caco-2 monolayers in respective media under standard conditions (as Section 2.7), for directly formed complexes SFM was used as a solvent. Ins-F with no modification was incubated with Caco-2

monolayers separately in same buffers (SFM, and PBS) to serve as respective control. The cellular uptake in different buffers was determined using flow cytometer, results were expressed as a percentage of fluorescence per Caco-2 cell normalised to insulin; and transportation efficiency was compared in these buffers.

2.11.2. Cellular uptake in commercial Biorelevant media

In order to simulate the GI conditions, cellular permeation and internalisation studies were carried out in commercial biorelevant media (Chapter 3) i.e. Fasted state simulated gastric fluid (FaSSGF, pH 1.6) with/ without pepsin (Pep) enzyme, Fasted state simulated intestinal fluid (FaSSIF, pH 6.5) with/ without pancreatin (Pan) enzyme, and Fed state simulated intestinal fluid (FeSSIF, pH 5). The purpose of this assay was to determine whether GET-peptide can retain its property of enhanced cellular uptake and internalisation of insulin under physiological GI conditions, stability of Ins-F-GET NCs in GIT fluids, and type of GIT fluid (pH, composition and enzyme) which might interfere with GET-mediated insulin transport. The pH of biorelevant media was determined using ThermoFisher pH strips both before and after executing the experiment, to confirm whether the pH is maintained throughout the procedure. Additionally, a viability assay was also performed in each of the biorelevant media using the standard procedure as described in section 2.10. This assay was performed according to the procedure mentioned in section 2.7, where Ins-F and Ins-F-GET NCs in different biorelevant fluids (FaSSGF ± Pep, FaSSIF ± Pan, or FeSSIF) were incubated with Caco-2 cells seeded on 48 well plates for O/N under standard conditions. The results of each cell viability assay were expressed as percentage viability, while insulin absorption and internalisation were determined using flow cytometer and expressed as a percentage.

2.12. Cellular internalisation with GET-peptide derivatives

In order to determine the potential and relative efficiencies of different CPPs i.e. GET-peptide and derivatives in promoting the cellular uptake of insulin (Chapter 3). insulin with GET-peptide and its derivatives in SFM were incubated with Caco-2 monolayers under standard conditions (37 ^{o}C, and 5% CO_2), as described in section 2.7. Accordingly, the cellular permeation and internalisation was assessed using

flow cytometry and microplate reader was used for finding relative uptake by measuring depletion of media fluorescence.

2.13. Cellular internalisation of freeze dried nanocomplexes

This assay was carried out to determine the effect of freeze drying on GET-peptide mediated cellular transport of insulin, and whether freeze drying can preserve the enhanced cellular uptake imparted by insulin complexation with GET-peptide (Chapter 3). The procedure consisted of preparing fresh NCs using protocol (Section 2.5), and freeze drying in a freeze dryer for 3 days. The freeze-dried samples i.e. insulin with and without GET-peptide in SFM were incubated with Caco-2 monolayers under standard conditions (37 ^{o}C, and 5% CO_2), as described in section 2.7. Accordingly, cellular permeation and internalisation was assessed using flow cytometry.

2.14. Dextran (Dex)-based assay for measurement of permeability and integrity of Caco-2 monolayer

This assay was used to determine the apical to basal flux of 4.4 KDa TRITC-Dex (0.5mg/ml) or 70 KDa TRITC-Dex (0.5mg/ml) to assess the impact of GET-peptide on paracellular permeability and integrity of monolayers (Chapter 3). This assay was performed by replacing culture media with SFM in both apical (500 µl) and basal (1000 µl) compartment, allowed to equilibrate for 30 min, followed by measurement of TEER (section 2.9) prior to use to confirm monolayer integrity. Following the application of different MW Dex and insulin with or without GET-peptide (Ins-F or Ins-F-GET NCs) to the apical compartment of transwell, defined volumes were collected from basal compartment at set times (0, 1, 2, 4, 6, and 24 hr) and replaced with the fresh SFM. Fluorescence of collected basal samples was determined using the TECAN microplate reader to determine the percentage transport of Dex and NCs as a measure of monolayer permeability. After 24 h, the apical compartment Dex and sample solution (Ins-F or Ins-F-GET NCs) were removed and replaced with fresh PBS and TEER values were documented to assess the monolayer recovery and integrity for further 30 min. For calculating the TEER values blank filter readings were subtracted from all readings, normalised and expressed as a percentage of initial TEER value (Section 2.9). Cellular internalisation

of Dex (TRITC channel) and NCs (Fluorescein channel) was also quantified using MoFlo Astrios flow cytometer to determine the relative uptake of different MW Dex as a measure of monolayer viability and integrity. Apparent permeability co-efficient for different MW Dex (4.4KDa and 70KDa), and Ins-F ± GET-peptide both on empty transwell and transwell seeded with Caco-2 monolayers was determined (Section 2.8). Appropriate positive and negative controls were also established and treated under similar condition to make appropriate calculation.

2.15. Study of cellular uptake and recycling mechanism

2.15.1. Transcytosis inhibition by Nor-adrenaline (NA)

The extent of the inhibitory effect of nor-adrenaline (potent inhibitor of insulin endocytosis and secretion) on the insulin recycling (cellular uptake and release) was assessed using Caco-2 cells seeded on Transwell® inserts (Chapter 3). Caco-2 cells were cultured and maintained to form monolayers as described in section 2.6 and 2.7. In this specific inhibition study, the cells were incubated with Ins-F and Ins-F-GET NCs both in the presence and absence of 100 µM NA. The first part of the experiment consisted of incubating Caco-2 cells with 50 µl of Ins-F ± GET in SFM (450 µl) with and without NA, while the second part consisted of normal O/N incubation with Ins-F or Ins-F-GET (with no added NA). After O/N, the post-transfection media was replaced with SFM or SFM containing NA i.e. (450 µl SFM+ 5 µl NA). Samples were collected from basolateral chamber at defined time-points (0hr, 1hr, 2hr, 4hr, 6hr, and 24hr) and analysed using Tecan plate reader. The cellular uptake of Ins-F and Ins-F-GET NCs was determined using MoFlo Astrios flow cytometer.

2.15.2. Studying cellular uptake and recycling using cell secretion regulators

For inhibition of cellular internalisation and studying recycling mechanism (Chapter 3), the transcytosis/ transport efficiencies of Ins-F and Ins-F-GET NCs were modified using specific cell secretion regulators i.e. forskolin (FK; activates adenylyl cyclase increasing intracellular levels of cAMP), BAPTA-AM (BM, cell-permeant chelator), ATP (responsible for active transport of molecules and ions), N-acetyl-D-sphingosine (NAS), and yohimbine (YB, insulin secretion stimulator through blockade of central α_2-adrenoceptors). Cells were pre-transfected with Ins-F and

Ins-F-GET NCs and left O/N (24hr) in SFM, after which cells were washed thrice with PBS. Later the cells were incubated with one of the endocytosis or secretion inhibitor at a chosen concentration. The amount of Ins-F and Ins-F-GET NCs exocytosed out of the cells in the presence of specific endocytosis inhibitor was calculated using fluorometric analysis via TECAN microplate reader at specific time points (0 hr, 1 hr, 2 hr, 4 hr, 6 hr, and 24hr). The amount of intracellular fluorescence was also determined using MoFlo Astrios flow cytometer.

2.16. Multifection (multiple incubation) for studying insulin recycling across Caco-2 monolayers

2.16.1. Recycling assay with double delivery of NCs to Caco-2 monolayers

This assay was conducted to determine the effect of sequential delivery on insulin uptake, release, recycling and transcytosis using differently labelled insulins (Chapter 3). Caco-2 cells were cultured and maintained on Corning Transwell® plates as described in section 2.6 and 2.7. The Caco-2 monolayers were incubated with Ins-F with and without GET-peptide in SFM at 37 ^{o}C for 2 hr. Following 2 hr, sample was removed, cells were washed three times with PBS, then the 2nd delivery was added to cells; Ins-T with or without GET-peptide system, or no delivery (SFM). The post-incubation release was analysed in Ins-T with ± GET or SFM by collecting samples (50µl) from bottom well at specified time intervals i.e. 1, 2 and 4 hr. These collected samples were subsequently analysed on a microplate reader for both green (Ex/ Em= 490/ 520 nm) and red fluorescence (Ex/ Em = 550/ 580nm) to assess the percent drug release of Ins-F/ Ins-F-GET NCs from Caco-2 cells in the presence and absence of 2nd delivery with Ins-T. The Caco-2 cells harvested from Transwell® were analysed on flow cytometer for measuring insulin deposited inside cells, alongwith its relative internalisation.

2.16.2. Recycling assay with triple delivery of NCs to Caco-2 monolayers

This assay was performed to study the post-transfection release after two successive deliveries with the non-labelled-(N) and NHS-Fluorescein-labelled insulin (F) onto Caco-2 cells seeded transwell inserts (Chapter 3), to explore whether the pre- (1st delivery with N) or post- (2nd delivery with F) delivered insulin comes out first, by observing post-incubation release from cells in the presence and

absence of NHS-Rhodamine-labelled insulin (3rd delivery with T). Caco-2 cells cultured on transwell inserts were transfected for 2 hr with "N" (2 µg/µl) with and without GET system in SFM, after which cells were washed thrice with PBS. Then, the 2nd delivery was with "F" free or complexed with GET system, or no delivery (SFM) for a 2-hr period. Following this, the cells were again washed with PBS, and cells were lastly incubated with "T" free or complexed with GET. Post-transfection release was analysed in "T" with ± GET or SFM by collecting samples from the basolateral chamber after 1, 2 and 4hr. Collected samples were subsequently analysed on a microplate reader for both green (Fluorescein channel i.e. Ex/ Em= 490/ 520 nm) and red fluorescence (TRITC channel i.e. Ex/ Em = 550/ 580 nm). Finally, the harvested Caco-2 cells from the transwell were analysed on MoFlo Astrios flow cytometer.

2.16.3. Recycling assay with continuous and alternative phases of delivery (On), or no delivery (Off) with Insulin-GET NCs

The purpose of this assay was to assess whether continuous and alternative phase of delivery, or no delivery influences the cellular uptake and to what extent, and which may be the best way to achieve maximum internalisation of insulin (Chapter 3). Caco-2 cells were seeded onto Corning Transwell® plates and maintained as discussed above in section 2.6. The experimental set-up consisted of incubating Caco-2 cells with Ins-F, alone or complexed with GET-peptide in SFM for 8 hr, 4 hr of delivery and 4 hr of no delivery (4 hr On/Off), 2 hr of delivery with 2 hr of no delivery and repeating this cycle until 8 hr (2hr On/Off), and 1hr of delivery with 1hr of no delivery and repeating this cycle until 8 hr or 3 times (1 hr On/Off). The media samples were collected for analysis at 1hr interval from the basal chamber and analysed using a Tecan microplate reader. Cell samples were harvested after 8 hr for determination of cellular contents.

2.17. Fluorescence quenching of Fluorescent-insulin (Ins-F or Ins-F*)

This assay was developed to depict the difference in fluorescence behaviour of different insulins (in-house synthesised i.e., Ins-F and proprietary Sigma-FITC-insulin i.e., Ins-F*) after complexing with GET-peptide, and to further establish various assays for the GET system (Chapter 3). Different samples were prepared (as

described in Section 2.5) with correspondingly increasing concentrations (0 -16 µM) of GET-peptide and its derivatives (L-PLR, D-PLR, PR, PL, PL, FLR), alongwith this the individual components that constitute the GET-peptide were also tested i.e. P (P21), L (LK15), and R (8R). Samples were then analysed for measuring green-fluorescent signals at excitation wavelength (λ) of 420 nm and over a range of emission λ i.e. 500-580 nm with 5 nm interval using the Tecan microplate reader.

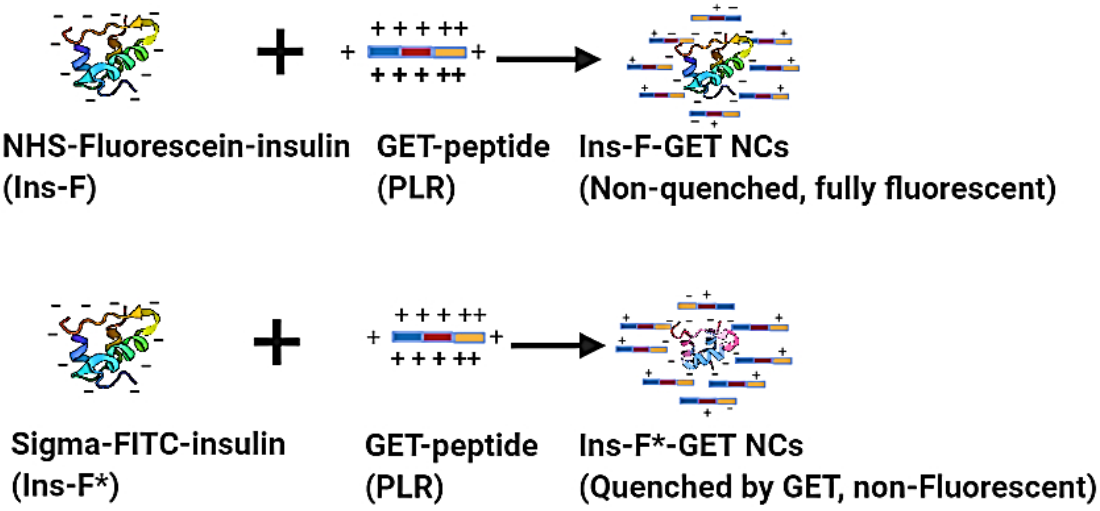

Figure 2. 2 Schematic presentation of fluorescent behaviour of Ins-F and proprietary Ins-F* upon complexation with GET-peptide.

2.18. Fluorescence dequenching of Ins-F*

In order to prevent this interaction as a function of quenching, and for recovering the fluorescence of Ins-F*-GET NCs, an alternative assay was developed to show that quenching is reversible (Chapter 3). This assay was used as an indicator of stability of insulin-GET NCs, as fluorescence quenching reflected that the complex is intact, on contrary fully fluorescent samples reflected decoupling of GET from insulin. For recovering the fluorescence quenching of Ins-F*-GET NCs, this assay was developed employing the use of various proteolytic enzymes (Prot. K, pepsin, and trypsin) in different working concentrations i.e. Prot. K (0 -0.2 µg/µl), Trypsin (0 -20 µg/µl) and Pepsin (0 -1 µg/µl). Free Ins-F* and Ins-F* complexed with GET-peptide were incubated with defined concentrations of different reagents separately in SFM for 2 hr at 37^{o}C. As a control, Ins-F* and Ins-F*-GET-NCs were incubated in SFM at 37 ^{o}C in the absence of these reagents. Emission of samples was measured at different time points (0, 10, 20, 40, 60, 120, 180 min) using the Tecan microplate reader.

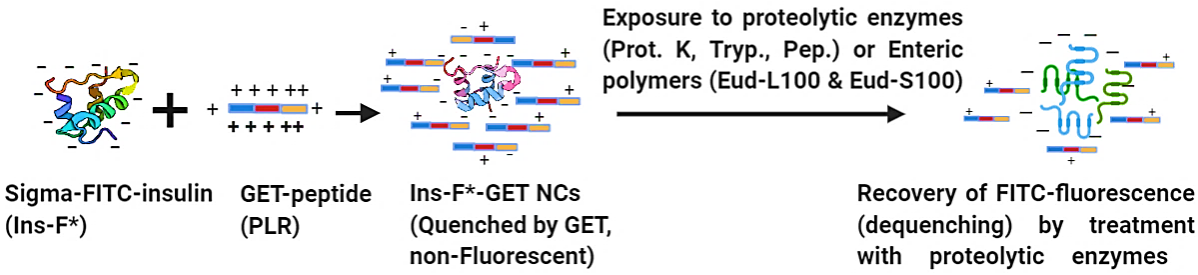

Figure 2. 3 Schematic illustration of fluorescence quenching of Sigma-FITC-insulin with GET system and subsequent recovery of fluorescence upon treatment with proteolytic enzymes or another reagent such as polymer.

2.19. Zeta sizing and zeta potential

The Z-average diameter and PDI for insulin (non-labelled) and insulin-GET NCs were measured (Chapter 4) using Dynamic light scattering (DLS), through the Zetasizer Nano ZS (Malvern instrument, UK) equipped with 633 nm laser and 173^{O} detection optics. With the same instrument laser, Doppler electrophoresis was used to determine the zeta potential of both samples. Insulin complexation was carried out with the GET-peptide system in dH_2O (neutral pH) at 37 °C to get an appropriate concentration. All measurements were performed in triplicate.

2.20. Transmission electron microscopy (TEM)

The morphology and particle size of insulin-GET NCs was further confirmed through TEM (FEI, Tecnai™ G2 12, USA) with an accelerating voltage of 100kV (Chapter 4). Briefly, 10-15 µl of samples (Ins-F and Ins-F-GET NCs) were applied on a 300-mesh carbon coated copper grid for 5 min, and excess of the solution was blotted before the grid was air dried for 15 min. Uranyl acetate alternative or heavy metal stain (TAAB EM-336) was then added dropwise and left for 1 min to negatively stain the sample, followed by washing with 20µl dH_2O and drying grids completely before analysis. Images were acquired using a FEI Tecnai G2 12 Biotwin transmission electron microscope at several different magnifications.

2.21. Confocal laser scanning microscopy (CLSM)

The localisation of Ins-F and Ins-F-GET NCs within the subcellular compartments was studied using CLSM (Chapter 4). Briefly, Caco-2 cells were cultured for one week on a 24-well CultureWell™ chambered cover-glass (MatTek Corporation, US) at a density of 50K cells/well to form a monolayer with tight junctions. Cells were

treated with the Ins-F in the presence and absence of GET-peptide for 5 hr, after which samples were removed. Cells were washed with heparin followed by rinsing thrice with PBS, fixed using PFA for 30 min and immunostained. Ten microliters of Alexa Fluor -647 Phalloidin was added to stain the cytoskeleton of cells for 30 min, followed by three times washing with PBS. Subsequently, the Hoechst reagent (2µg/µl) was used for staining the cells nuclei for 15 min. These stained samples were mounted and visualised using CLSM (Zeiss LSM 880) using a 40x 1.2 NA water immersion lens. Alexa-fluor-647 phalloidin, Fluorescein, and Hoechst were imaged using 633 nm, 488 nm and 405 nm laser lines, respectively. Emission was recorded between 648-690 nm, 506-551 nm and 426-491 nm. The frame size was set to 952x952 giving a pixel size of 0.09 µm. Images were acquired sequentially and as z-stacks with a spacing of 0.45 µm. Laser power and detector gain were adjusted to give good exposures and was kept constant throughout the imaging of all samples.

2.22. ImageStream analysis OR Imaging flow cytometry

This analysis was done to determine the relative cellular uptake and internalisation of Ins-F with and without GET-peptide, to assess the ratio of surface bound insulin to that which is internalised, and the effect of time as a variable in influencing cellular uptake of insulin (Chapter 4). Caco-2 cells were seeded on 48-well plates (5×10^4 cells/ well) to grow and form monolayers under standard conditions. These monolayers were incubated with Ins-F and Ins-F-GET NCs suspended in SFM for different time intervals (1 and 24 hr), after which they were washed with PBS thrice, harvested, centrifuged (200 ×g for 5 min) and resuspended in 40 µl PFA. The cell samples images were acquired using the ImageStreamX MKII imaging flow cytometer (Amnis, USA), 5000 events were collected per sample at magnification of 40× giving a 10 µM optical slice image, thus allowing internalisation studies to be undertaken using this approach. A 488 nm wavelength laser was used to excite the Ins-F both free and complexed with GET. Fluorescence images of sample were acquired using different spectral detection channels (Ch) including; Ch01 (brightfield camera1), Ch02 (488nm laser power: 10mW), and Ch06 (side scatter 785nm laser power: 10mW).

IDEAS image analysis software was used for analysing and interpreting the sample images acquired through the ImageStreamX MKII. Firstly, the population of single cells was isolated using gating on a bivariate plot of aspect ratio vs. cell. Further a 2-dimensional plot of image contrast vs. root mean squared (rms) gradient was used for selecting cells within the focal plane. IDEAS software was used to compare the probe location (Ins-F) with the location of nucleus for each of the acquired cell by using a probe similarity algorithm. Calculations were performed to determine the proportion of subpopulation of cells in which translocation occurred and expressing it as a percentage, additionally the samples were also compared to control without any Fluorescein-labelled insulin delivery.

2.23. Live/Dead viability/ cytotoxicity assay

This is a two-colour based fluorescence cell viability assay that enables simultaneous determination of both live and dead cells using two different probes (Chapter 4). It measures the established parameters of cellular viability i.e. plasma membrane integrity and ubiquitous intracellular esterase activity. The Live/Dead viability/ cytotoxicity Kit for mammalian cells (Cat. No. L3224) from Thermo Fisher scientific (UK) was used according to the manufacturer's protocol with the Time-lapse fluorescence microscope. In this fluorescence-activation assay, cultured cells were exposed to ethidium homodimer (EthD-1) and Calcein AM. Caco-2 cells (50,000 cell/well) were seeded on 48-well plates and incubated under standard conditions to from monolayer for 7 days. Caco-2 cell monolayers were incubated with Ins-F-GET NCs with progressively increasing concentrations of GET-peptide (0 -40 µM) with constant increments for a specified time period (24 hr). After which the cells were washed twice with PBS, and then 100 µl of solution containing 2 µM Calcein AM and 4 µM EthD-1 was added to each of the well and further incubated for 45 min. Cells were washed with PBS before acquiring images on a Time-lapse fluorescent microscope (Leica, Germany).

2.24. Proteolytic Stability of isoforms of GET- system

To determine the stability of GET-peptide system (L-PLR and D-PLR), an assay was developed (Chapter 4) based on the quenching behaviour of Ins-F*, where peptides were treated with Prot. K (0.2 µg/µl) and heat inactivated Prot. K (as a control). The

procedure consisted of mixing defined volume of GET-peptide with SFM, these samples were then subsequently treated with specific volume (2.5µl) of Prot. K (samples) or just blank media (no added Prot. K, control), and incubated at 37 ^{o}C for 1 hr. The samples treated with Prot. K and control were read at different time points (0, 10, 30, and 60 min) using a microplate reader. Following 1 hr, Prot. K was inactivated by incubating samples at 95 ^{o}C in incubator for 10 min. Sigma-FITC-insulin or Ins-F* (2.5µl) was then added to these samples and samples fluorescence was measured at 0 and 15 min to determine whether the GET-peptides are still intact to quench fluorescence of Ins-F*. The negative control consisted of just Prot. K (with and without heat inactivation) in media, the controls were exposed to similar experimental conditions.

2.25. Stability of Insulin-GET-peptide NCs

2.25.1. Stability assay by exposure to different pH conditions

To assess the Sigma-FITC-insulin fluorescence behaviour and its stability (Chapter 4) in the form of Ins-F*-GET-NCs, complexes and free insulin were exposed to different pH conditions in the presence of Pep (1 µg/µl) (to simulate the GIT environment). The samples were exposed to three distinct conditions in an incubator for 3 hr at 37 ^{o}C i.e. neutral with no HCl (with Pep), acidic (0.01M HCl containing Pep), and neutralised using NaOH (0.01M HCl containing Pep neutralised with 0.01N NaOH). As a control, free Ins-F* and Ins-F*-GET-NCs were exposed to similar types of media supplements (no added HCl, acidic, and neutral with NaOH addition) in the absence of Pep. Emission of the samples was analysed at different time points (0, 10, 30, 60, 120, 180, 260 min) at excitation and emission wavelength of 490 nm and 520 nm, respectively using a microplate reader.

2.25.2. Stability assay in commercial Biorelevant media

To further evaluate stability of Ins-F-GET NCs in media simulating GI microenvironment, commercially available biorelevant media (with and without enzymes) were employed (Chapter 4). These biorelevant media consisted of FaSSGF ± Pep (pH 1.6), FaSSIF ± Pan (pH 6.5), and FeSSIF (pH 5). This assay was based on fluorescence quenching and dequenching of Sigma-FITC-insulin complexed with GET via electrostatic interactions, where changes in fluorescent

intensity signals (increase and decrease) following exposure to different buffer systems was measured using a microplate reader. The procedure consisted of complexing Ins-F* with specified volume of GET-peptide and incubating for 15 mins, followed by dilution in biorelevant media. 25µl of samples (Ins-F* or Ins-F*-GET NCs) were added to 225µl of biorelevant media, followed by homogenous mixing of samples. As FITC-fluorescence is affected by changes in pH, 40 µl of each sample was diluted in 360 µl PBS (Total volume 400µl, 10x dilution) to neutralise the pH, and fluorescent signals of samples were measured at the same pH, to avoid false interpretation of results. This was followed by addition of 100 µl diluted samples to 96-black well plate and samples were read at defined time points (0, 30, 60, 120, 180, 240, and 1440 min). Results were expressed as a percent fluorescence recovery values normalised to insulin.

2.25.3. Stability assay using differently labelled insulins

This assay was carried out to assess the stability of insulin-peptide complex, by adding an excess of un-complexed insulin in different amounts (Ins-F* or Ins-T) to the NCs, to see whether or not the GET-peptide detaches from the insulin-peptide complex and gets bound to the available free added insulin (Chapter 4). Therefore, to measure stability of NCs, differently labelled insulins (Ins-F* and Ins-T) were used, so that the change in degree of fluorescence of these complexes on exposure to excess free insulin could be detected by measuring respective fluorescence of two insulins.

The procedure consisted of preparing samples of both insulins (Ins-F* and Ins-T) separately with varying concentrations of GET-peptide (0 -10 µM), mixing them together in SFM, and allowing to react for 15 min. Then each of these samples was divided into 5 portions by adding 50 µl in 96-well black plate. The un-complexed free insulin solution (Ins-F* or Ins-T, stock solution 2µg/µl) was added in excess in different volumes (0 -20 µl, corresponding to concentration of 0- 40µg/ml) to the samples in a black well plate (Ins-F* was added to Ins-T-GET-NCs and Ins-T to Ins-F*-GET-NCs). These samples were analysed for both NHS-Rhodamine (TRITC channel: Ex/ Em= 550/ 580nm) and NHS-Fluorescein fluorescence (FIuorescein channel: Ex/ Em= 490/ 520nm) using a microplate reader.

2.25.4. Assay for determining stability following cellular uptake based on fluorescence dequenching

In order to assess the stability of insulin-GET complexes uptaken by the cells and to determine whether the GET-peptide gets detached from insulin after being translocated into Caco-2 cells (Chapter 4), a fluorescence recovery assay was developed using a potent cell lysate (Prot. K). The sample mix (Ins-F* ± GET-peptide in SFM) was delivered to cell monolayers (7-10 days old, seeded with 50K cells/well) for overnight. After O/N incubation, the cells were trypsinised, counted and re-suspended in SFM to make a total volume of 250µl. Then, 100 µl of each sample and control (SFM) was pipetted out thrice into a black assay plate and read for absorbance. The cell samples were put into polypropylene tubes (making sure cells have NOT settled), and then 25 µl of Prot. K (reagent sample) or distilled water (control) was added to each of the cell sample, mixed and incubated at 37 ^{o}C for 2 hr. Sample fluorescence was measured at different time points (0, 5, 10, 30, 60, 120, and 180 min) using a microplate reader. Following 180 min, samples were incubated at 56 ^{o}C (optimum temperature for maximum activity of Prot. K) for 10 min. Transfection media samples collected following O/N from the basal chamber of each Transwell® were treated in similar way to cell samples as described above, except for the volume of Prot. K (5µl) used.

2.26. Functional activity assay using insulin-reporter cells (iLite cells)

The biological/functional activity of insulin after modification with GET-peptide (NCs) was evaluated using iLite™ insulin-assay ready cells, expressing receptors for insulin and related reporter gene, using the manufacturer's protocol (Chapter 4). The concentration of Insulin reporter cells was maintained at one million/ml for the assay. For this assay, non-fluorescent insulin was used, and a series of Ins and Ins-GET peptide dilutions were made and tested for their functional activity. For Ins and Ins-GET samples, the tested final insulin concentrations ranged from 0 -200 µg/ml. Additionally, for the Ins-GET-NCs, the concentration of GET-peptide was also varied over a range of 0- 50 µM to determine the extent to which this peptide system can disrupt the insulin's biological activity and to determine the peptide concentration which could cause reduction of activity. A Luciferase assay was

performed in triplicate with 2×10^3 live cells (2 µl of 1M cells/ml) in a total volume of 42 µl. Samples (40 µl) were added to 96-well white plate and stimulated for 5 hr in an incubator at 37 ^oC with a 1:20 dilution of iLite cells. 40 µl of Dual-glo luciferase was added, mixed and luminescence signals (Firefly values) were recorded. This was followed by addition of Stop and Glow reagent (40 µl), mixing and quantification of luminescence intensity (Renilla values) using the Tecan plate reader. All result values were normalised as fold over non-stimulated control.

2.27. Functional activity assay for post-transcytosis released insulin from transwells

This assay was performed to assess the functional activity of insulin-GET complexes following their delivery, transcytosis and release from Caco-2 cells seeded onto Transwell® inserts (Chapter 4). Caco-2 cells were cultured and maintained under standard conditions (Section 2.6) on transwell inserts, for 7-10 days until they formed monolayer with tight junctions. For maintaining insulin concentration at 20 µg/ml post-transcytosis in the basolateral chamber, the media volume in apical and basolateral chamber of the Transwell® was tailored by adding 100 µl of sample mix to 100 µl SFM (20 µg/ 200 µl) and reducing volume in receiving chamber to 500 µl. The cells were incubated O/N with NCs (Ins, Ins-GET NCs, Ins-F, and Ins-F-GET NCs), samples were collected from the basal chamber and analysed for their functional activity using insulin-reporter cells (maintained at 1M/ml), by measuring their luminescence activity using luciferase reagent.

2.28. Preparation of Eudragit (Eud)-L100 microparticles (Eud-L100 MPs)

2.28.1. Bulk nanoprecipitation method for Eud-L100 MPs preparation

Insulin loaded Eud-L-100 MPs were prepared by a method reported by Zhang *et al*. (Chapter 5), with slight modification [146]. Eud (4mg) was dissolved in defined volume of deionised water, after adjusting pH to 11.0 using 1 N NaOH. The system was subjected to sonication for 3 min to form a homogenous suspension. The labelled insulin solution (500 µl of Ins-F, 1 mg/ml) was added to Eud solution dropwise under gentle magnetic stirring. Subsequently, the pH of this reaction mixture was adjusted to pH 3 using 0.01 M HCl, unless an opalescent dispersion was obtained. This microsuspension was mixed using magnetic stirrer (100 rpm) for

15 min at room temperature. In order to prevent particle aggregation, this microsuspension was mixed with equal volume of 2% D(+)-trehalose dihydrate (cryoprotectant). The resulting MPs were collected by three times centrifugation at 12000 rpm (30000 ×g) for 30 min. Finally, the collected MPs were re-dispersed in 2% trehalose solution, the pH of microsuspension was adjusted to pH 3 and lyophilised. The MPs were stored at 4 ^{o}C unless used and were resuspended before using for further studies. Additionally, insulin-GET NCs loaded Eud-MPs were prepared similarly, except that insulin in specified amount was mixed with quantified volume of GET-peptide and allowed to react for 15 min at room temperature. The insulin-GET NCs solution was then added to polymer solution, and the remaining steps were similar to those described above.

2.28.2. Microfluidic method for Eud-L100 MPs preparation

Eud-L100 MPs were also prepared using the micro-assembler benchtop device, the process was optimised to get MPs of defined size range with reproducibility (Chapter 5). The aqueous alkaline polymer solution (0.2% w/v) was mixed with 0.01M HCl at a flow rate ratio of 1:2 (polymer solution: HCl buffer). The flow rate optimised for polymer solution was 30 ml/hr (0.5 ml/min), while for HCl buffer it was adjusted to 2 ml/min. For the drug loaded MPs, the Ins-F or Ins-F-GET NCs were premixed with polymer solution as mentioned in section 2.28.1, followed by use of microfluidic system to get MPs. As described above, MPs were mixed with equal volume of 2% trehalose, collected by centrifugation, adjusting pH to 3 and finally lyophilised to get solid MPs which were stored at 4 ^{o}C unless used.

2.29. Characterisation of MPs

2.29.1. Size and Zeta potential

The mean diameter of unloaded and drug loaded MPs, their size distribution and zeta potential were determined using the Zetasizer Nano ZS (Chapter 5), applying the principle of DLS. Measurements were done on MPs dispersion in dH_2O adjusted to pH 3 at 37 °C. All measurements were made in triplicate.

2.29.2. Morphology

A uniform thin layer of MPs was placed onto an adhesive stub and coated with platinum using a POLARON SC7640 sputter coater (Balzers Union Ltd., Lichtenstein)

for 90 seconds at 15-20 mA. The morphology of these MPs was determined using scanning electron microscopy (XL30, SEM), using a JEOL 6060L imaging system (JEOL Ltd., Hertfordshire, UK) with an accelerating voltage set to 10 kV (Chapter 5).

2.29.3. Entrapment efficiency, Drug loading contents and dosage calculation

The insulin entrapment efficiency of MPs was assessed by determining the amount of free fluorescent insulin in the supernatants (indirect method) and also by dissolving prepared MPs in PBS for measuring released contents directly (direct method) using a microplate reader (Chapter 5). The drug entrapment efficiency was determined indirectly using Equation as described below:

$$\text{Entrapment efficiency (EE, \%)} = \frac{\text{total amount of drug} - \text{amount of drug in supernatent}}{\text{total amount of drug}} * 100\%$$

$$\text{Loading content efficiency (LC, \%)} = \frac{amount\ of\ drug\ in\ microparticles}{weight\ of\ microparticles} * 100\%$$

2.29.4. *In-vitro* release of insulin

The *in-vitro* release profile of insulin from fabricated Eudragit MPs was studied using HCl (pH 1.2) and PBS (pH6.8 and pH7.4) buffers simulating the GI conditions as discussed previously with slight modification (Chapter 5). Briefly, 5 mg of drug-loaded Eud-L100 MPs were dispersed in 1.5 ml HCl solution (pH 1.2) and placed in incubator at 37 ^{o}C under constant shaking (100 rpm) for a period of 2 hr. At pre-defined time intervals (0, 0.5, 1 and 2 hr) Eud-L100 MPs were centrifuged at 13000 rpm for 30 min, and 0.5 ml sample aliquots were withdrawn for insulin quantification. To maintain sink condition, volume removed was replaced by an equal volume of respective dissolution medium. For simulating the progression of MPs moving from stomach into small intestine, after 2 hr the HCl buffer was replaced with PBS buffer pH 6.8 and samples were withdrawn at 2.5, 3, and 4 hr (starting from initial time). After which MPs were centrifuged and buffer (pH 6.8) was replaced with PBS buffer pH 7.4, and samples were withdrawn at defined time intervals starting from the initial test (5, 6, 8 and 24 hr). Collected samples were analysed for fluorescence values for insulin quantification as percent cumulative drug release.

2.29.5. Insulin transport across Caco-2 cell monolayers

In parallel with *in-vitro* release measurements, cellular internalisation of released Ins-F and Ins-F-GET NCs from formulated MPs was determined in respect of transportation efficiency across the Caco-2 cell monolayers seeded onto the Transwell® (Chapter 5). The MPs were placed onto the apical chamber of Transwell®, after 6 hr incubation media was aspirated. The insulin concentration and internalisation (total delivered protein) was determined using MoFlo Astrios flow cytometer.

2.30. Investigating interaction between Polymer and GET-peptide

2.30.1. Insulin internalisation assay in presence of Eud-L100

To investigate the possible interaction between GET-peptide and Eud-L100 (Chapter 5), progressively increasing concentrations of polymer solution (0.8% w/v) were added directly onto the cells with simultaneous addition of sample mixes (Ins-F or Ins-F-GET NCs). The polymer concentration was varied from 0 -1mg/ml. Cells were seeded onto 48-well plates at a density of 50K cells/well to form monolayers under standard conditions. Culture media was removed from cells, washed with PBS, and SFM containing different polymer concentration was added to each well. The sample mix (Ins-F or Ins-F-GET NCs) was then added to wells containing different polymer concentrations and incubated for 24 hr. Media samples were removed, cells were washed with PBS, trypsinised, centrifuged at 200 ×g for 5 min, and fixed using PFA. The cellular uptake in the presence of polymer was quantified using MoFlo, Astrios flow cytometer.

2.30.2. Insulin internalisation assay in presence of other enteric Eudragit polymers

This assay was conducted to study the influence of Eud-S100 and Eud-FS-30D on cellular uptake of Ins-F and Ins-F-GET complexes, and to identify the polymer which least interferes and de-complexes GET-peptide from insulin (Chapter 5). The procedure adopted for this assay was similar to one as described previously in Section 2.30.1. Different polymer concentrations (0 -1mg/ml) were used for this assay. Caco-2 cell monolayers on 48 well-plates were washed with PBS, media containing different polymer concentrations was added onto each well, followed

by addition of prepared sample mixes (Ins-F or Ins-F-GET NCs), and incubated for 24 hr. After specified time, cells were trypsinised and cellular content (for internalisation) of Ins-F and Ins-F-GET NCs was determined using MoFlo Astrios flow cytometer.

2.30.3. Dequenching assay using Eudragit polymers

The destabilisation and decoupling of Ins-F*-GET NCs was further studied through dequenching assay utilising proprietary FITC-insulin (Chapter 5). Here, the fluorescence of Ins-F*-GET NCs was recovered using various Eudragit based enteric polymers (Eud-L100, Eud-S100, and Eud-FS-30D) in different working concentrations (0 -1mg/ml), same as used in section 2.30.1. The procedure used for this assay was same as previously mentioned in section 2.18. Free Ins-F* and Ins-F* complexed with GET-peptide were incubated with defined concentrations of Eudragit polymers separately in SFM for 2 hr at 37 ^{o}C. As a control, Ins-F* and Ins-F*-GET-NCs were incubated in SFM at 37^{o}C in the absence of polymers. The fluorescent signals of samples were measured at different time points (0, 10, 20, 40, 60, 120, 180 min) using microplate reader.

2.31. Strategies for overcoming interaction between polymer and GET in Enteric MPs

2.31.1. Using different poly-cations

The use of poly-cationic moieties may reduce the anionicity (negative charge) of polymers imparting overall neutral charge to the drug-peptide conjugate, prevent the disruption of electrostatic interactions between GET-peptide and insulin in the presence of polymer, and stabilise complex by interacting and complexing with the anionic groups to retain the enhanced intestinal permeability imparted by the peptide (Chapter 5). Basic or poly-cationic amino acids such as L-histidine, and Poly-L-lysine (PLL) were employed as charge neutraliser agents in this assay due to their inherent basic nature. The concentration used for the L-histidine was varied from 0 -80 mM, while for PLL the tested concentration ranged from 0 -0.04 mg/ml. The procedure used was same as mentioned in section 2.18. Free Ins-F* and Ins-F*-GET-NCs were incubated with defined concentrations of poly-cationic agents separately in SFM for 24 hr at 37 ^{o}C. As a control, Ins-F* and Ins-F*-GET-NCs were

incubated in SFM at 37 ^{o}C in the absence of polymer and cationic species. The emission of samples was measured at different time points (0, 10, 20, 40, 60, 120, 180 min) using the Tecan microplate reader.

2.31.2. Saturation with GET-peptide

This assay was developed to assess whether the addition of excessive amounts of GET-peptide quenches back the Ins-F* fluorescence in the presence of an enteric polymer, as an indicator of coupling/ association or re-building of electrostatic interaction between insulin and GET-peptide (Chapter 5). High degree of anionic groups in enteric polymer display strong affinity for GET-peptide bonded electrostatically to insulin in the Ins-F-GET NCs. This competition between negatively charged insulin and polymer leads to decoupling of positively charged GET from insulin which in turn binds to strongly anionic polymer. The procedure consisted of mixing specified volumes of GET in polypropylene tubes with insulin, followed by incubation at room temperature for 15 min. The sample mix was diluted in SFM after adjusting for the volume of polymer solution (31.25 µl) to be added and incubated for 60 min, which allowed time for polymer to dequench the Ins-F*-GET fluorescence. The above sample mixtures were then added to a 96-black well plate, and fluorescence values were measured using microplate reader to get control value (0 time point). Following this, additional GET was added to samples in well plate in small and progressively increasing increments with gentle mixing until maximum concentration (54x dilution) was attained. At each sequential addition, the fluorescence intensity of samples was determined.

2.31.3. Order of addition testing for formulation variables

Another approach employed to overcome this polymer mediated decoupling of GET-peptide from insulin was to alter the order of mixing for reagents used during the MPs preparation (Chapter 5). In this assay, polymer was mixed directly with insulin, followed by addition of GET to interact and from complexes with insulin. As a control, insulin samples with no peptide, and insulin with no polymer and peptide were used. The polymer concentration was varied from 0 -0.2mg/ml to analyse and compare the impact of polymer addition on cellular uptake, by modifying the order of mixing. Next, samples were incubated with Caco-2 cell monolayers (cultured

according to the standard protocol as mentioned in section 2.6) for 24 hr. After this samples were aspirated, cells were washed with PBS, followed by trypsinisation and centrifugation at 200 ×g for 5 min, and were fixed using PFA. The cellular internalisation by Caco-2 cell monolayers was determined using the MoFLo Astrios flow cytometer.

2.32. Preparation of enteric coated mini-capsules

2.32.1. Cellular uptake studies in presence of different bulking agents

In an attempt to freeze-dry NCs for future *in-vivo* studies, the concept of using bulking agents was taken into consideration. As the normal sample mixes of NCs were minute in volume, freeze drying of samples would have resulted in very little powdered material probably an amount that would be hard to handle practically, especially during manual capsule filling. Therefore, previously reported bulking agents were selected for freeze drying of sample mixes (Ins-F and Ins-F-GET-NCs). These bulking agents were selected based on their property to form crystalline or amorphous structures upon freeze drying. The procedure consisted of preparing stock solutions of bulking agents based on the previously reported concentrations used in the literature, stock solutions of 10% D-mannitol (D-Mann), and sucrose, while 1% solution of glycine was prepared (Chapter 6). The concentration of bulking agents was varied as follows, for D-Mann from 0 -40 mg/ml, for sucrose from 0 -20 mg/ml, for glycine; 0 -2mg/ml, for combination of D-mannitol and sucrose (D-Mann: sucrose); 20mg/ml: 5mg/ml, and 40mg/ml: 10mg/ml, and for D-mannitol plus glycine (D-Mann: Glycine); 40mg/ml: 1mg/ml, and 40mg/ml: 2mg/ml. The procedure consisted of removal of culture media from Caco-2 monolayers, SFM containing defined concentrations of bulking reagents was added to well, followed by addition of sample mixture, and incubated for 24 hr. Effect of bulking agents on cellular uptake of Ins-F and Ins-F-GET NCs was determined using MoFlo Astrios flow cytometer.

2.32.2. Freeze drying with different bulking agents

NCs were prepared according to the standard protocol as depicted in section 2.5, followed by addition of defined volumes of bulking agent solutions (containing defined concentration as mentioned below), and making up total volume to 250 µl

with SFM to maintain constant insulin and GET concentration. The bulking agent concentrations used for freeze drying of NCs were; D-Mann; 40 and 20mg/ml, for sucrose; 10 and 5mg/ml, for glycine; 1 and 2mg/ml, for combination of D-Mann and sucrose; 40mg/ml D-Mann with 10mg/ml sucrose and 20mg/ml D-Mann with 5mg/ml sucrose, and for D-Mann and glycine; 40mg/ml with 1- and 2-mg/ml glycine (Chapter 6). Samples were added to polypropylene tubes, and holes were pierced in top caps to allow liquid evaporation from samples. The samples were placed in a vacuum freeze dryer for 3 days, to get dried powdered mixes of Ins-F or Ins-F-GET NCs with bulking agents. These freeze-dried powders were reconstituted in a mixture of SFM and deionised water for later use.

2.32.3. Cellular uptake studies using NCs freeze dried with different bulking agents

The cellular internalisation of insulin with and without GET-peptide freeze-dried with different bulking agents was carried out to provide proof of concept that freeze dried NCs in the presence of bulking agent does not interferes with the cellular uptake (Chapter 6). This would provide a step forward towards capsule filling with freeze dried NCs for future *in-vivo* studies. The procedure consisted of preparing stock solutions of various bulking agents, and freeze drying at a specific concentration with the sample mixes. Freeze-dried sample mixes were reconstituted in a mixture of SFM and dH_2O prior to addition onto Caco-2 cell monolayers. Positive control consisted of freshly prepared mixes of Ins-F with specified volume of SFM or GET-peptide for 15 min. Media was aspirated from monolayers, reconstituted powdered mix solutions were added to the cells, and incubated for 24 hr. Following this samples were aspirated, cell were washed thrice with PBS, trypsinised, and fixed with PFA. The collected cell samples were analysed for cellular uptake using MoFlo Astrios flow cytometer.

2.32.4. Preparing enteric coated mini-capsules by manual dipping

The plain fill mini-capsule size 9 (M-Caps for rats) were purchased (Torpac, USA), moreover a kit (funnel and stand) provided with these capsules was used for capsule filling. M-Caps were manually filled with NCs freeze dried with bulking agents i.e. D-mannitol and glycine (Chapter 6). For precise handling of powdered

material, stainless steel capsule funnel was used. Empty capsule body was placed in capsule holder, funnel was placed over the capsule body, and a pre-measured amount of powdered material (freeze-dried mix) was dosed in these capsules. If necessary, tampering was used to compress powdered material, followed by removal of funnel, and locking the capsule with the cap by pressing firmly. The control consisted of empty capsules just filled with the bulking agents. M-Caps were coated with aqueous solution of enteric polymer (Eud-L100) 10% (w/v) in 1:1 mixture of solvents acetone and isopropanol. Manual dipping method was employed for coating these filled capsules. The M-Caps were coated by dipping three times in an Eud-L100 solution (10%), with intermittent drying between each coat to obtain uniform coating.

2.32.5. *In-vitro* dissolution testing in commercial Bio-relevant media

The *in-vitro* dissolution testing of these enteric coated M-Caps was performed using commercially available biorelevant media (FaSSIF/ FeSSIF/ FaSSGF) in the presence and absence of enzymes (Chapter 6). Enteric coated M-Caps filled with NCs (Ins-F or Ins-F-GET NCs) freeze dried with bulking agents were initially placed in 1 ml FaSSGF pH 1.6 or FaSSGF containing Pep (pH 1.6) and incubated at 37 ^{o}C under constant shaking (100 rpm) for a period of 2 hr. At pre-defined time intervals (0 and 2 hr), 200 µl sample aliquots were withdrawn for insulin quantification. To maintain sink condition, the volume removed was replaced with an equal volume of respective dissolution medium. Further simulating the progression of M-Caps through the GIT moving from stomach into small intestine, after 2 hr the M-Caps were removed and washed twice with PBS, and media (FaSSGF or FaSSGF with Pep) was replaced with FeSSIF buffer pH 5. The M-Caps were exposed to this slightly alkaline pH 5 for 2 hr, after this an aliquot of sample was collected, followed by washing of M-Caps with PBS, and replacing it with FaSSIF media (with or without Pan). The samples (200 µl) were withdrawn at defined time intervals starting from the initial test (5, 7, 9 and 24 h), and tested for fluorometric analysis using a microplate reader. All experiments were carried out in triplicate and the cumulative insulin release was calculated.

2.33. Statistical analysis

All experiments were done in triplicate and quintuplicate (5 times in most assays). Results were expressed as mean values and standard deviation (mean ± SD). Significance differences were determined using ANOVA (one way- and two-way ANOVA with Bonferroni and Tukey's test, along with determination of normality and distribution of data, and identifying outliers) between the treatments and the respective controls and *p*-value of <0.05 was considered to be significant.

Chapter 3. GET-peptide mediated intracellular insulin delivery, transcytosis and recycling

3.1. Introduction

Numerous clinical studies have demonstrated that its possible to achieve subsequent absorption of macromolecular drugs following oral administration, but yet the bioavailability remains variable and low [147]. The cell membranes are constituted of a mosaic of proteins and lipids enabling them to act as stringent gatekeeper which hampers the entry of extracellular chemicals, except some ions and a handful of biomolecules essential for cell function [148]. Therefore, the cell membrane displays distinctive feature of a double-edged sword, limits the permeability to ensure steady cytoplasmic conditions and shows hindered intracellular access to potentially useful hydrophilic therapeutic drugs.

Various earlier studies have investigated the potential of a variety of CPPs in improving poor insulin permeability across the mucosal membrane of intestinal epithelium. Recent discoveries in exploration of this novel class of CPPs and related peptides depicts that low insulin permeability across cellular membranes may be improved either by conjugation of specific CPP with membrane impermeable macromolecule or through electrostatic coupling of negatively charged insulin with positively charged CPP to form a stable physical mixture. Additionally, CPPs could be grafted onto the cargoes. Oligoarginine is the most widely studied chimeric CPP so far, consisting of 6-12 arginine units and passes across the cellular membrane by endocytosis or direct penetration [15]. P21 is a heparin binding domain (HBD) which specifically binds to cell surface heparan sulphate proteoglycans (HSPG) [24]. HB-EGF contains 86 amino acid, shares similarity with EGF and TGF-α, binds to the same receptors as them and displays strong affinity for heparin. The interaction of HB-EGF with cell surface HSPG is regarded essential for its optimal attachment to EGFR and thus promotes the growth/migratory activity of this molecule [149, 150]. CPPs can deliver number of drug cargoes to cells, yet the nature of the specific type of membrane interactions and mechanism of cellular transport remains disputed. Therefore, an improved understanding of these mechanisms and interactions may result in further refinement of existing CPPs and thus extension of their therapeutic

applications. Our group has previously demonstrated that this multi-function domain sequence i.e. GET peptide (particularly PLR, and FLR) is efficient in delivering and enhancing intracellular transfection of DNA, small inhibitory RNAs, for RUNX2 delivery to MScs, for spatio-temporal cell programming in hydrogel systems, and for enhanced gene delivery to lungs. This in turn prompted the question of identifying the application of GET-peptide system in enhancing the cellular uptake/ permeation and internalisation of insulin across model intestinal Caco-2 cells, identifying the type of interaction and cellular mechanism involved in the cellular uptake of insulin. Accordingly, the key objectives of this chapter could be categorised as;

1. Exploring the potential of GET-peptide in promoting cellular uptake and internalisation of insulin, its intracellular localisation, and transcytosis efficiency across the cultured Caco-2 monolayers.
2. Examining and characterising the mechanism of cellular uptake by employing different cell secretion regulators.
3. Analysing the recycling of GET-conjugated insulin and its potential to act as depot for sustained insulin release over time.
4. Determining GET-peptides cytotoxicity and viability using different assays.

3.2. Experimental design

Based on objectives stated above, this chapter will focus on different assays to check and establish ability of GET peptide in enhancing insulin permeability across *in-vitro* Caco-2 model cells, detailed description of processes adopted for these assays is mentioned in Chapter 2. Reference to each performed assay and respective detailed procedures can be located by referring to respective Sections as stated below. Initially GM and SFM media were used to evaluate and compare cellular uptake of in-housed synthesised NHS-Fluorescein labelled insulin and proprietary-Sigma-FITC both as un-complexed and complexed with GET-peptide (Section 2.7). One of the most applied and famous amine-specific functional groups which are incorporated into reagents for protein labelling and cross-linking are NHS-esters and imidoesters NHS-Fluorescein is basically amine-reactive derivative of renowned fluorescein dye and it has been widely used for labelling of proteins, antibodies and other probes for various biomedical and molecular applications.

The N-hydroxy-succinimidyl-ester (NHS-ester) is the functional group responsible for activation of NHS-Fluorescein. In comparison to FITC, this NHS-ester derivative exhibits more specificity toward primary amines such as lysine side chains in the presence of other nucleophiles thus resulting in a more stablilised linkage after labelling. While the proprietary fluorescently labelled insulin was labelled with FITC, which is unstable compared to NHS-Fluorescein labelled insulin. This was followed by analysing transcytosis (transport efficiency), apparent permeability co-efficient, and cellular uptake of insulin and NCs across Transwell® cultured with Caco-2 monolayers (Section 2.8), moreover changes in TEER values (section 2.9), and effect on cellular viability was also monitored (Section 2.10). Moreover, effect of different buffers (Section 2.11.1) and biorelevant media (Section 2.11.2) on cellular uptake of NCs was also determined. Cellular internalisation of NCs formulated with different GET-derivatives was also performed to see which GET variant works well to enhance insulin permeability (Section 2.12), moreover freeze dried NCs were also tested to check whether freeze-drying alters permeation capability of GET-based insulin NCs. This was followed by use of high and low molecular weight TRITC- Dextran to further study influence of GET peptide on extent of cellular permeation and to verify cellular mechanism which operates for the transport (trans- or para-cellular) of these NCs (Section 2.14). In order to further study cellular uptake mechanism of NCs; different cell secretion regulators were employed (Section 2.15). Various recycling assays were established and performed using differently labelled insulin by using concept of multifection (repeated transfection), to understand uptake and recycling process sequentially (Section 2.16). Lastly, both Ins-F and Ins-F* were complexed with different GET- derivative and changes in fluorescence values were monitored as quenching (Section 2.17) and dequenching (Section 2.18), which formed bases of different stability assays as described in Chapter 4.

3.3. Result and Discussion

3.3.1. Cellular uptake of Insulin-GET NCs in Growth- and Serum free media

As mentioned earlier, CPPs act as potential transepithelial vectors for enhancing the intracellular permeation and internalisation of a variety of therapeutic drugs,

including macromolecules. Cellular internalisation of Ins-F and Ins-F-GET NCs in SFM compared to control was also determined through Flow cytometry software (FCS) express 7 software (Figure 3.1a). The results showed that Ins-F complexed to GET is uptaken more readily by Caco-2 cell monolayers, compared to unmodified insulin as evident from mean relative fluorescence values (Figure 3.1b), where decreased media fluorescence values were observed for Ins-F-GET NCs. Fluorescence depletion was more apparent in SFM in comparison to GM. Flow cytometric analysis was used to quantify the cellular uptake of GET-peptide bonded Ins-F (NCs) at 37 ^{o}C in both SFM and GM for a period of 24 hr, as shown in Figure 3.1c. The result values were expressed as percent of mean fluorescence in Caco-2 cells noramilsed to insulin (Ins-F) with no modification i.e. percent relative fluorescence of GET-modified insulin to un-complexed/ free insulin. A significantly increased fluorescence intensity was observed when Ins-F-GET NCs were incubated with Caco-2 monolayers compared to Ins-F. GET-bond insulin showed approximately 4-fold greater cellular permeation and internalisation relative to free insulin.

Enhanced gene delivery across HEK 293 cells in the presence of serum and at lower pH has been reported using low MW chitosan/DNA complexes[151]. DNA/PLL complexes have shown significantly reduced transfection efficiency in presence of 10% FBS compared to without FBS (or serum), which could be attributed to serum proteins adsorption onto the surface of complexes, thus hampering adsorptive endocytosis of NCs into the cells. In contrast, KALA/DNA/GEG-g-PLL NCs exhibited greater transfection efficiency in the presence of 10% FBS compared to positively charged DNA/PLL NCs [152]. The results of our study revealed that presence of serum provided statistically insignificant difference in internalisation compared to in its absence. As serum proteins tend to adsorb on surface and interfere with the cellular uptake, and interstitial lumen lacks blood/ serum, therefore SFM media was employed as solvent for all experiments.

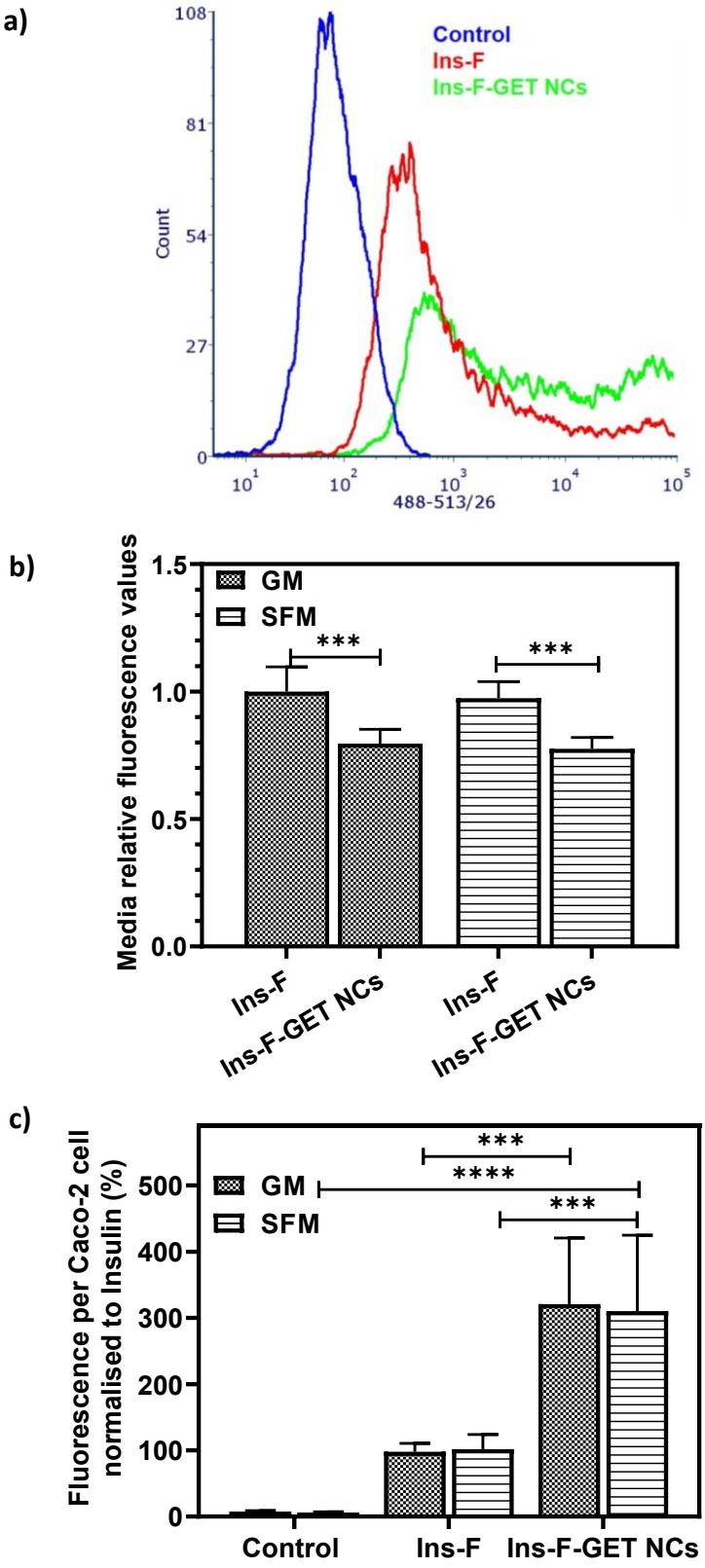

Figure 3. 1 GET-peptide mediated intracellular delivery of NHS-Fluorescein-insulin. Graphs comparing fluorescence depletion and cellular uptake of Ins-F ± GET-peptide on Caco-2 monolayers cultured on 48 well plates; a) FCS graph showing relative cellular uptake of Ins-F and Ins-F-GET NCs in SFM compared to control, b)

Relative media fluorescence values in GM and SFM for Ins-F and Ins-F-GET NCS, c) Flow cytometric analysis showed greater cellular permeation and internalisation of insulin in presence of GET in GM and SFM, thus revealing potential of GET-peptide in enhancing intracellular delivery of insulin, negative control consisted of cells with no transfection. All results were statistically significant obtained through Ordinary one-way ANOVA with Tukey's test, n=6, mean ± S.D., *= *p-value* <0.05, **= *p-value* <0.005, ***=*p-value* <0.0005, ****= *p-value* <0.0001, *ns*= not significant.

3.3.2. Comparison of cellular uptake of Ins-F-GET NCs and Ins-F*-GET NCs in different media

The uptake of proprietary Ins-F* was compared with that of Ins-F both as free molecule and bonded to GET-peptide using Caco-2 cell monolayers. Surprisingly, the results from microplate reader showed maximum (statistically significant) fluorescence depletion (90%) for Ins-F*-GET NCs in both SFM and GM, depicting that almost all of the nanocomplexes have been uptaken and internalised by cells, indicating maximum transfection efficiency of insulin in combination with GET (Figure 3.2a). The flow cytometer results were opposing to those observed with the microplate reader, where there was statistically insignificant increase in cellular uptake of GET-peptide bonded insulin compared to un-modified insulin as shown in Figure 3.2b. This figure also showed that GM provided better cellular uptake for Ins-F*-GET NCs compared to SFM. The GI lumen is composed of heterogenous environments, where each segment reflects its specific function such as different pH, GI fluid composition, spatial heterogeneity of microbiota, and enzymes. The luminal contents on intestine are separated from the epithelial compartment by mucus layer, thus no blood/ serum is present in the surrounding. Therefore, ideally SFM mimics *in-vivo* conditions, so all experiments were performed in SFM, unless otherwise stated.

Furthermore, a comparative study was executed for studying the differences in the depletion of media fluorescence and cellular uptake of these two different types of fluorescently labelled insulins i.e. proprietary Sigma-FITC (Ins-F*) and in-house synthesised NHS-Fluorescein-insulin (Ins-F) both as free and coupled with GET-peptide. The results displayed greater depletion of media fluorescence for Ins-F*-GET NCs compared to Ins-F-GET NCs both in SFM and GM, as shown in Figure 3.2c and 3.2d, respectively. These results suggested that Ins-F*-GET-NCs had greater

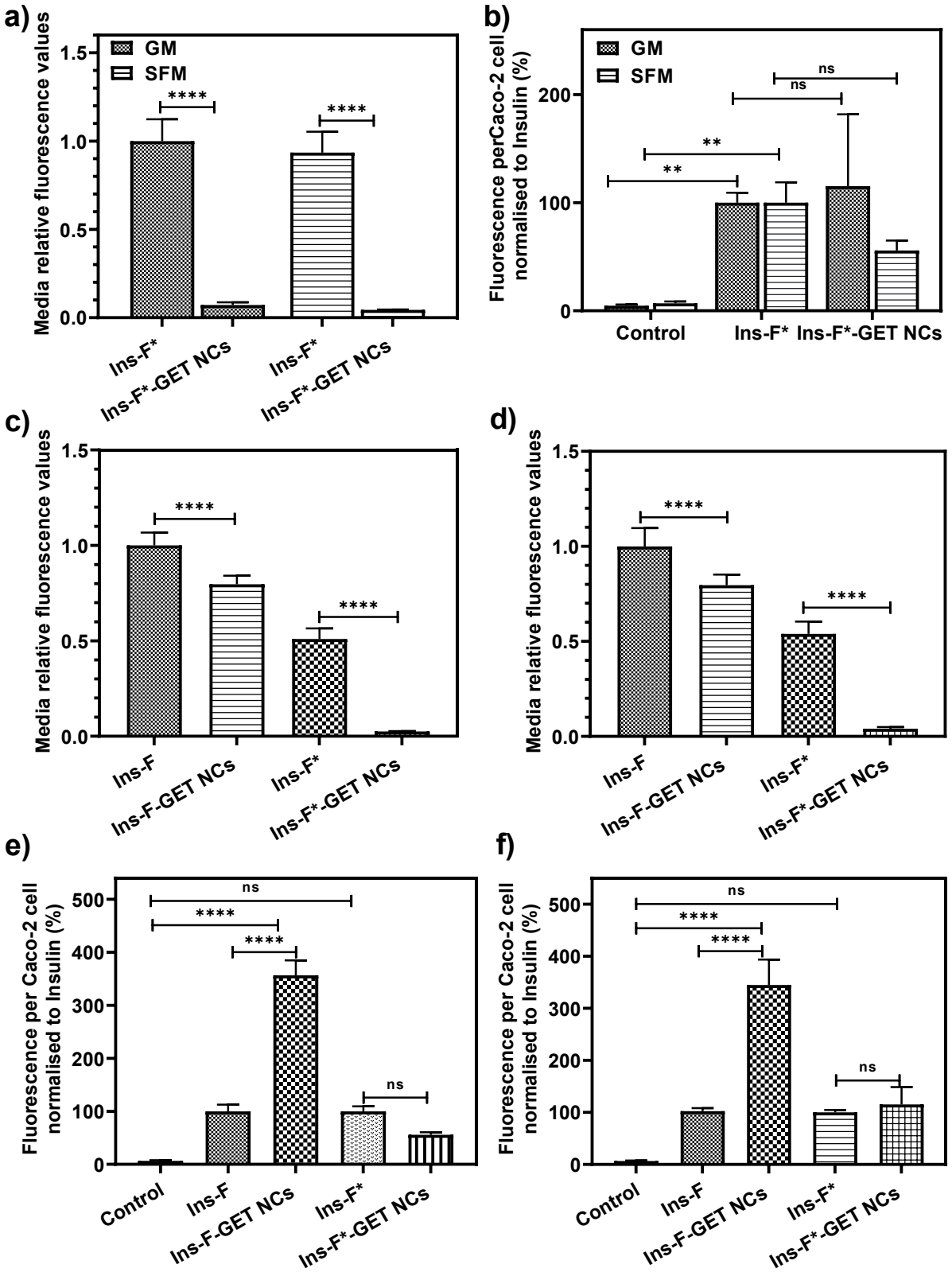

Figure 3. 2 Comparison of in-house labelled NHS-fluorescein labelled insulin (Ins-F) and proprietary FITC-insulin (Ins-F*) in the presence and absence of GET-peptide for depletion of media fluorescence and cellular uptake by Caco-2 monolayers cultured on 48 well plates. a) Relative media fluorescence values for Ins-F*± GET

peptide in GM and SFM, b) Flow cytometric analysis showing statistically insignificant increase in cellular uptake of Ins-F* in presence of GET-peptide both in GM and SFM. Comparative depletion of media fluorescence for Ins-F and Ins-F* with and without GET-peptide in c) SFM and d) GM, results indicated highest fluorescence depletion for Ins-F*-GET NCs. Percentage fluorescence values per Caco-2 cells normalised to respective insulin showing cellular uptake for Ins-F and Ins-F*± GET-peptide in e) SFM and f) GM, showing contradicting results to one obtained via plate reader, where Ins-F*-GET NCs exhibited lowest cellular uptake compared to Ins-F-GET NCs, and Ins-F* in SFM. All results were statistically significant obtained through Ordinary one-way ANOVA with Tukey's test, n=5, mean ± S.D., *= *p-value* <0.05, **= *p-value* <0.005, ***=*p-value* <0.0005, ****= *p-value* <0.0001, and *ns*= not significant.

transfection efficiency compared to Ins-F-GET NCs in both types of media. Figure 3.2e and 3.2f show cellular uptake of Ins-F and Ins-F* with and without GET-peptide in SFM and GM, respectively. Interestingly, only Ins-F-GET NCs exhibited improved cellular uptake showing 4-fold greater internalisation compared to Ins-F, while Ins-F*-GET NCs had poor uptake and internalisation efficiency even less than Ins-F* and Ins-F. All results were statistically significant. These results were in contradiction with microplate reader results showing complete fluorescence depletion.

The fluorescence of fluorescent species is reduced when several molecules are in close proximity or due to self-aggregation or oligomerisation, a phenomenon termed fluorescence quenching [153]. The phenomenon of quenching may involve formation of dimers between proximate fluorophores, collisional quenching, energy transfer, transient excited state interaction, or involving formation of non-fluorescent ground state species [154]. The FITC-fluorescence is sensitive to the polarity of its environment and thus can be studied in solution form. This was related to the lower fluorescent signals detected for Ins-F*, where the complexation of Ins-F* with GET resulted in fluorescence quenching and low/weak fluorescent signals were detected both by microplate reader and flow cytometer. Fluorescence quenching is a reversible phenomenon which could be overcome by dilution of samples, or thorough the use of proteolytic enzymes. In later sections (3.3.10 and 3.3.11) this quenching and dequenching phenomenon are studied in detail using GET-peptide and its constituent species to gain better understanding of this phenomenon.

3.3.3. *In-vitro* transcytosis assay using GET-peptide across Caco-2 cultured transwells

Caco-2 cells are human colorectal carcinoma cells which are widely employed as an *in-vitro* model for intestinal permeation study. Caco-2 cells form monolayers on Transwell® inserts, these monolayers are highly polarised and show close morphological and functional resemblance to the intestinal barriers. The intestinal permeation and transport properties of Ins-F and Ins-F-GET NCs was compared *in-vitro* on Transwell® grown Caco-2 cell monolayers, for investigating the effect of GET system on the transport properties of insulin. The insulin was poorly transported across the Caco-2 cell monolayers as shown in Figure 3.3, with the GET-peptide system significantly (statistically significant) enhancing transport of insulin (n=6). The transcytosis efficiency of Ins-F-GET NCs across the Caco-2 cell monolayer was 8.7-fold greater than insulin alone (Figure 3.3a). There was an increased amount of transmembrane transportation for insulin complexed with GET system (Ins-F-GET NCs) from the apical layer of the transwell, either into the cells or into the basal layer of the wells. This enhanced transcytosis efficiency was attributed to the CPP segment in the multi-domain sequence of GET, leading to significantly higher insulin transport across cultured monolayers. Cellular internalisation of insulin was significantly promoted when coupled with GET-peptide, compared to free insulin and control, thus Ins-F-GET NCs were found to be localised more in cells with this novel fusion peptide (Figure 3.3b). Thus, the results indicated that GET system (P21-LK15-8R) can sufficiently enhance the insulin delivery, transport (both apical to basal and basal to apical), transcytosis, and release through the Caco-2 monolayers. Additionally, Ins-F-GET NCs continued to release from cell monolayers post-transfection, giving insight into insulin recycling with cells acting as an insulin depot for sustained release.

These results are in concordance with previous studies, where CPPs have increased the intestinal absorption of insulin. Absorption of insulin was increased dramatically following co-administration with oligoarginines (L- and D-forms of R6, R8, and R10) in a dose dependent manner, leading to increased intestinal insulin absorption without damaging cellular integrity [12, 21, 120]. Similarly, potential of different CPPs such as R8, R12, HIV-1 Tat (48–60), HIV-1 Rev (34–50), Penetratin,

pVEC, Erns, RRL helix, PRL4 and random peptides was analysed for enhanced intestinal insulin absorption, with results indicating that L-forms of these peptides exhibited superior intestinal insulin absorption (except for R8), where the D-R8 showed stronger insulin enhancing ability than the co-responding L-form [22]. D-R8 was found to be most efficient in promoting insulin permeation and cellular internalisation, and this oligoarginine based enhanced intestinal transport of protein drugs takes place through unsaturable energy independent internalisation [155]. Another study reported the use of amphiphilic lipopeptide (SAR6EW), which was superior compared to R8 and R6EW in enhancing insulin permeation both *in-vitro* and *in-vivo.* These improved results with amphiphilic lipopeptide could be attributed to strong intermolecular interactions, superior enzymatic stability, and different internalisation pathways [125]. These results indicate that lipophilic modification of GET-peptide may provide greater transcytosis and cellular uptake, leading to significantly enhanced transepithelial permeability.

The TEER values were measured at each of the defined time points to check whether the monolayer integrity was maintained, and whether GET-peptide has destructive effects on monolayer integrity. At the start of permeation experiment, the mean TEER value was 960 ± 50 Ωcm^2, showing the Caco-2 monolayers junctional integrity. In comparison with controls (untreated cell monolayers), a statistical insignificant decrease was observed in TEER values upon incubation with either Ins-F or Ins-F-GET NCs (Figure 3.3c). When samples were added to apical chamber of the transwell, TEER values immediately dropped to 70% and 90% of the initial values within 30 min, for both Ins-F-GET NCs and Ins-F in comparison with the control, respectively. This drop in TEER values with Ins-F-GET NCs was transient, as over time the TEER values increased progressively and recovered to baseline control values, indicating that the cellular barrier potential had recovered fully. Thus, GET system modulates the membrane permeability temporarily for potentially promoting the momentarily insulin transcytosis. Meanwhile, results showed that the GET-peptide compromises the integrity of monolayers temporarily, which might result in absorption of other molecules present in GI lumen, which in turn may led to toxicity. As GI epithelial barrier are inhabited by various bacteria, viruses and lipopolysaccharides so there is likelihood of

absorption of these unwanted/ foreign agents specially in patients with inflammatory bowel disease, which may contribute towards further toxicity in these individuals.

Similar results were observed in studies analysing the effect of CPP mediated insulin transcytosis on cellular integrity, in the form of TEER measurements. Insignificant change was observed in TEER values even after incubation with highest concentration of CPPs; oligoarginine (15-120µM) and penetratin (10-100µM) in the absence of insulin, but TEER values were decreased only when 15µM insulin was incubated with the 120µM Fl-D-R8 [155]. Slow decline in TEER over a 4 hr period by 19% was reported on incubating insulin-cR9 (covalent conjugation by substitution) with RAECM monolayers, while there was no change in TEER on incubation with insulin alone or 1:1 mixture of Insulin and oligoarginine (cR9). This could be attributed to fact that conjugates interact indirectly or directly with the intracellular or extracellular components, which might result in modulation of tight junction properties [132]. Complexes of insulin and penetratin, PenLys, or PenArg displayed no significant decrease in TEER values at all studied pH values (pH 5, 6.5 and 7.4) and all tested concentrations in permeation study, on contrary incubation of 5 µM insulin with 20 and 30 µM PenShuff caused a significant reduction in TEER values at pH 5 [142].

The P_{app} values for Ins-F and Ins-F-GET NCs were calculated across empty (control) and seeded Transwell® inserts for comparison, as inserts with no cells would provide more transport due to absence of any barrier for transport. P_{app} values for both Ins-F and Ins-F-GET NCs through cells was much lower than on empty Transwell® inserts at 6 and 24 hr time point, indicating that monolayers provide barrier function to transport of these molecules (Figure 3.3d & 3.3e). The P_{app} values of Ins-F-GET NCs (9.35×10^{-6} cm/sec) were significantly superior to Ins-F (1.98×10^{-6} cm/sec) across Caco-2 monolayers after 6 hr (Figure 3.3d). P_{app} values were slightly reduced following time, but still P_{app} values for Ins-F-GET NCs (5.14×10^{-6} cm/sec) were significantly higher than Ins-F (1.05×10^{-6} cm/sec) at 24 hr time point. These results suggest that GET promotes cellular permeation/ intracellular insulin delivery, and thereby enables greater transcytosis across the Caco-2 monolayers. GET-based decrease in TEER profile could be attributed to capability

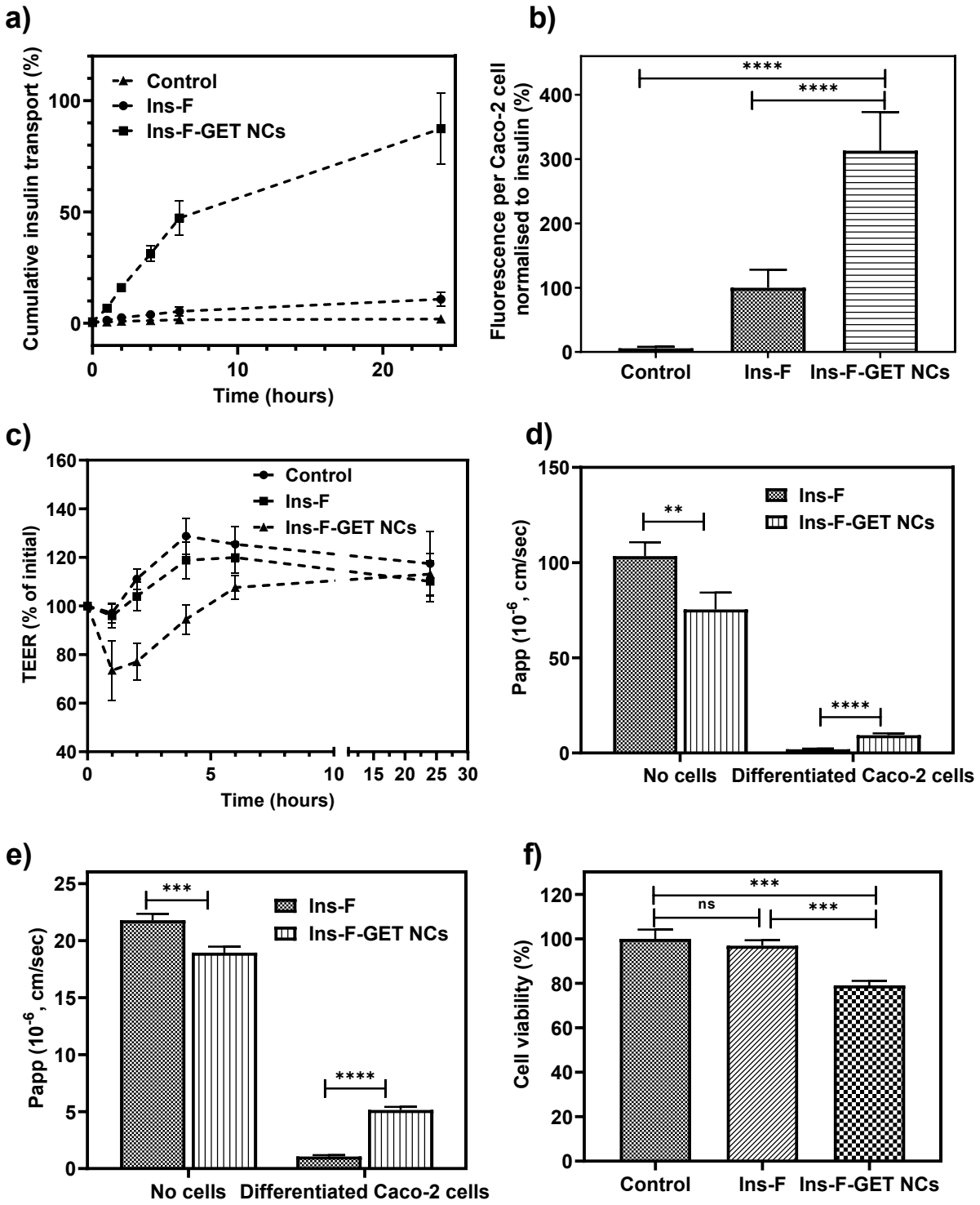

Figure 3. 3 GET-peptide mediated insulin (Ins-F) transport across Transwell® grown Caco-2 monolayer after incubation with 10μM GET for 24 hr. Samples were collected at indicated time points for determination of transcytosis, TEER, P_{app} values, and cellular contents were measured. a) GET system enhanced the insulin transcytosis efficiency by greater than 8.7-fold, leading to more apical-basal and basal-apical transport, b) Flow cytometric analysis showing greater fluorescence per Caco-2 cells for Ins-F-GET NCs compared to Ins-F, indicating that this novel

multidomain peptide domain sequence can significantly improve cellular permeation and internalisation of insulin, c) TEER values depicting cell monolayer integrity is affected/ compromised temporarily upon incubation with Ins-F-GET NCs, d) P_{app} values at 6 hr showed increased permeation for insulin complexed with GET peptide, and e) P_{app} values at 24hr, and f) Cytotoxicity assay using AlamarBlue revealed significant reduction in cell viability is caused by Ins-F-GET NCs compared to Ins-F and control (just SFM). The values represent the mean ± S.D., n=6, *= *p-value* <0.05, **= *p-value* <0.005, ***=*p-value* <0.0005, ****= *p-value* <0.0001, and *ns*= not significant. 2-Way ANOVA with Tukey's test.

of this multi-domain peptide sequence to modulate and widen the paracellular route through interaction and interference with TJ proteins which ultimately results in increased flux of Ins-F-GET NCs across Caco-2 monolayers. These TEER results indicate that GET-peptide promotes paracellular transport of insulin, in addition to the transcellular transport. Thus, GET-peptide increases the transepithelial permeation of insulin by approximately 6-fold compared to un-complexed insulin, but permeation was slightly reduced following 6 hr possibly due to recovery of monolayer integrity over time and partially could be due to saturation of cells with complexes. This decline in apparent permeability values over time co-relates with recovery of TEER measurements with time. These results indicate ability of GET system in promoting cellular uptake and permeation of insulin across the biological intestinal barriers.

pH-dependent increase in insulin permeation was seen upon co-administration with CPPs (penetratin, PenArg, or PenShuf), where increasing the ratio of carrier peptide-insulin from 4:1 to 6:1 resulted in an increase in insulin permeation by a factor of 1.4 for PenShuf and 1.7 for PenArg [142]. Increasing the number of hydrophobic Trp residues in CPPs backbone tends to augment cell penetration ability by promoting the affinity of interaction with the cell surface GAGs [156]. Tat-peptide (CPP) enhanced the transportation efficiency of insulin by 5–8 times (Insulin/Tat conjugate) higher than that for free insulin as shown by P_{eff} values [21]. Similarly, N-terminal R9-PTH (parathyroid hormone) conjugates provided highest increase in PTH permeation and superior transepithelial delivery with approximately 2-3 fold increased permeation compared to C-terminal conjugated R9,Tat or VP22 with PTH [157].

Vital parameters in evaluating the cellular health are, firstly the analysis of cellular proliferation and secondly the cytotoxicity. The metabolic activity of cells and number of live cells is proportional to the amount of absorbance/ fluorescence of AlamarBlue dye, while non-viable or damaged cells display lower fluorescent signal values due to their innate lower metabolic activity. Cell viability assay was carried out using AlamarBlue to determine the cytotoxic effect of Ins-F and Ins-F-GET NCs on Caco-2 monolayers as given in Figure 3.3f. Results indicated that Ins-F has insignificant effect on cellular viability compared to control, where the monolayers maintained their integrity and were viable with no substantial cytotoxic effects. In contrast, co-administration of insulin with GET-peptide (NCs) caused a statistically significant decrease in cell viability in comparison to both Ins-F and control. This observation indicated a tendency that Ins-F-GET NCs were more toxic to Caco-2 cell monolayers than the Ins-F. However, despite the reduced cellular viability upon exposure to Ins-F-GET NCs, only a transient effect on the epithelial integrity of Caco-2 monolayer was observed, as indicated by TEER values which dropped upon initial incubation with these drug-carrier complexes. This observation implies that lowering of TEER values during initial hours is an indicator of compromised integrity of tight junctions (TJs) leading to opening of paracellular route. TJs are dynamic structures which are responsible for regulating trafficking of compounds, fluids and nutrients between the submucosal layer and intestinal lumen. Impaired intestinal permeability due to TJs downregulation may contribute towards increased transport of pathogens and xenobiotics through the epithelial barrier, which might induce risk of infections in immunocompromised individuals. Therefore, it is necessary that sufficient barrier function is retained by controlled and reversible opening of the TJs.

D-isoforms of both R8 and penetratin had no significant effect on cellular viability at the tested concentration, additionally there was no difference in LDH release from Caco-2 cells at 37^{o}C and 4^{o}C [155]. Pen NCs and Pen-bis-CD NCs at 1-2mg/ml concentration had no significant effect on cellular viability compared to control, but at 5mg/ml the Pen NCs showed a significant reduction in cellular viability [128]. PLGA NPs co-modified with various CPPs (Tat, R8, Pen, and stearyl derivatives of these CPPs) developed for oral insulin delivery, displayed no apparent cytotoxicity

at the tested concentration for these CPPs compared to control, except Tat-NPs and Sec-Tat NPs which had slightly more toxic effects than other NPs [145].

3.3.4. Cellular uptake of Ins-F and Ins-F-GET NCs in different medias

3.3.4.1. Comparative cellular uptake in various buffers (PBS, SFM, & direct)

In the previous sections (Section 3.3.1 and 3.3.2), substantial permeability enhancement and cellular internalisation were observed across Caco-2 cell monolayers for insulin co-modified with GET-peptide system in both SFM and GM. The following experiment was aimed at assessing the cellular uptake of Ins-F-GET NCs in different available buffers. The concept behind examining the effect of PBS on uptake efficiency was to demonstrate that in the absence of essential nutrients (required for cell growth) the internalisation is reduced, which could be attributed to cellular death. PBS lacks essential nutrients of cellular growth, but contains some electrolytes which might contribute to survival of cells. Direct complexation of insulin with GET in absence of any solvent was also carried out to detect the influence of absence of solvent on degree of complexation which in turn may affect the cellular uptake.

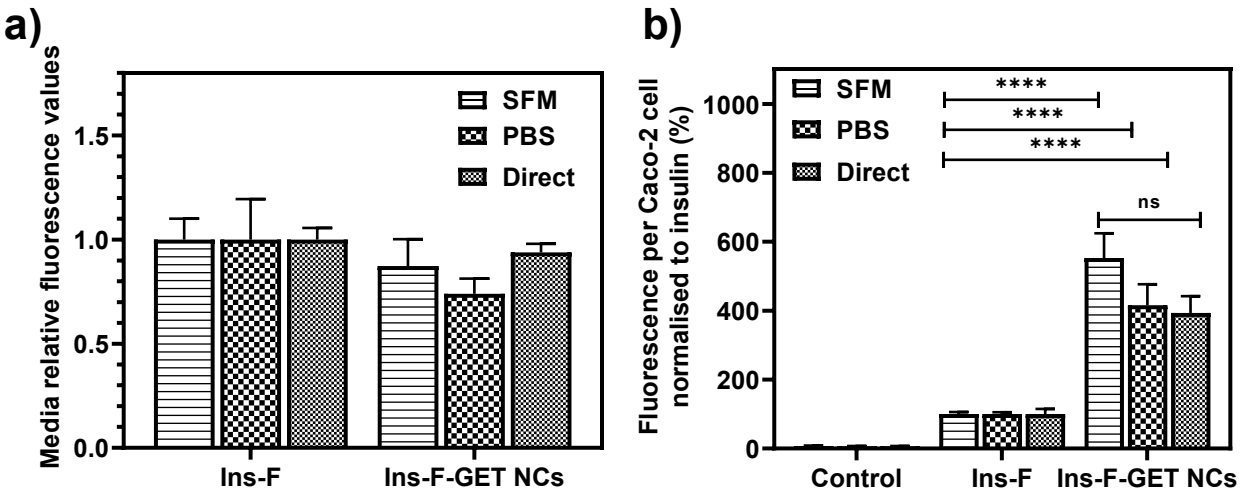

Figure 3. 4 Influence of nature of growth media on media fluorescence depletion & cellular uptake of NHS-fluorescein insulin (Ins-F) alone or coupled with GET across Caco-2 monolayers; a) greatest media fluorescence depletion for Ins-F-GET NCs was observed in PBS, indicating higher relative cellular uptake compared to SFM, or Direct, b) cellular uptake study showing highest cellular absorption and intracellular delivery in SFM compared to other medias. All values are presented as mean ± S.D, n=5, *= *p-value* <0.05, **= *p-value* <0.005, ***=*p-value* <0.0005, ****= *p-value* <0.0001 and *ns*= not significant. One-way ANOVA with Tukey test.

Figure 3.4a and 3.4b present graphs for relative media fluorescence depletion and cellular uptake of Ins-F and Ins-F-GET NCs by Caco-2 monolayers in SFM, PBS, and direct complexation mixes. The permeability and intracellular delivery of Ins-F-GET NCs was significantly superior in SFM compared to other buffers in the following order; SFM > PBS > Direct. In contrast, the Ins-F cellular uptake and internalisation was comparable in these solvents with no significant differences. As SFM more closely mimics physiological environment of intestinal lumen *in-vivo*, therefore SFM would be most useful media in enhancing the GET-peptide mediated permeation and intracellular delivery as compared to other solvents/ media.

3.3.4.2. Cellular uptake in commercially marketed Biorelevant media

Here, we assessed the possible influence of biorelevant media on cellular viability, and enhancement of permeability and cellular internalisation of insulin complexed with GET peptide (Ins-F-GET NCs). The commercially marketed bio-relevant media were used in an attempt to simulate the GI environment, to identify the effect of GI conditions on NCs stability, their effect on cell viability, and ultimately the intracellular delivery of NCs in biorelevant media. The significantly enhanced uptake of NCs in FaSSGF compared to SFM and control (Ins-F) was surprisingly remarkably high and gave an insight for evaluation of cellular viability using AlamarBlue. Figure 3.5a presents the effect of biorelevant media (FaSSGF ± Pep, FaSSIF ± Pan, and FeSSIF) in the absence and presence of SFM on the cellular viability/ metabolic activity as determined by AlamarBlue assay. All values were normalised to control, SFM was used as a standard media (control) for comparison of cellular uptake with different biorelevant media, while negative control consisted of HBSS on empty wells. Viability assay showed that cells exposed to SFM exhibited highest viability, while FaSSGF with/ without Pep enzyme, FeSSIF, and FaSSIF with/ without Pan with no added portion of SFM showed significant reduction in cellular viability. While buffer media containing combination of SFM with these biorelevant medias as a solvent mix, the cellular viability was significantly improved for FaSSIF, which displayed insignificant difference from SFM in terms of cellular viability, but there was only slight improvement in cellular viability on mixing SFM with FaSSGF or FeSSIF. These results indicated that FaSSGF

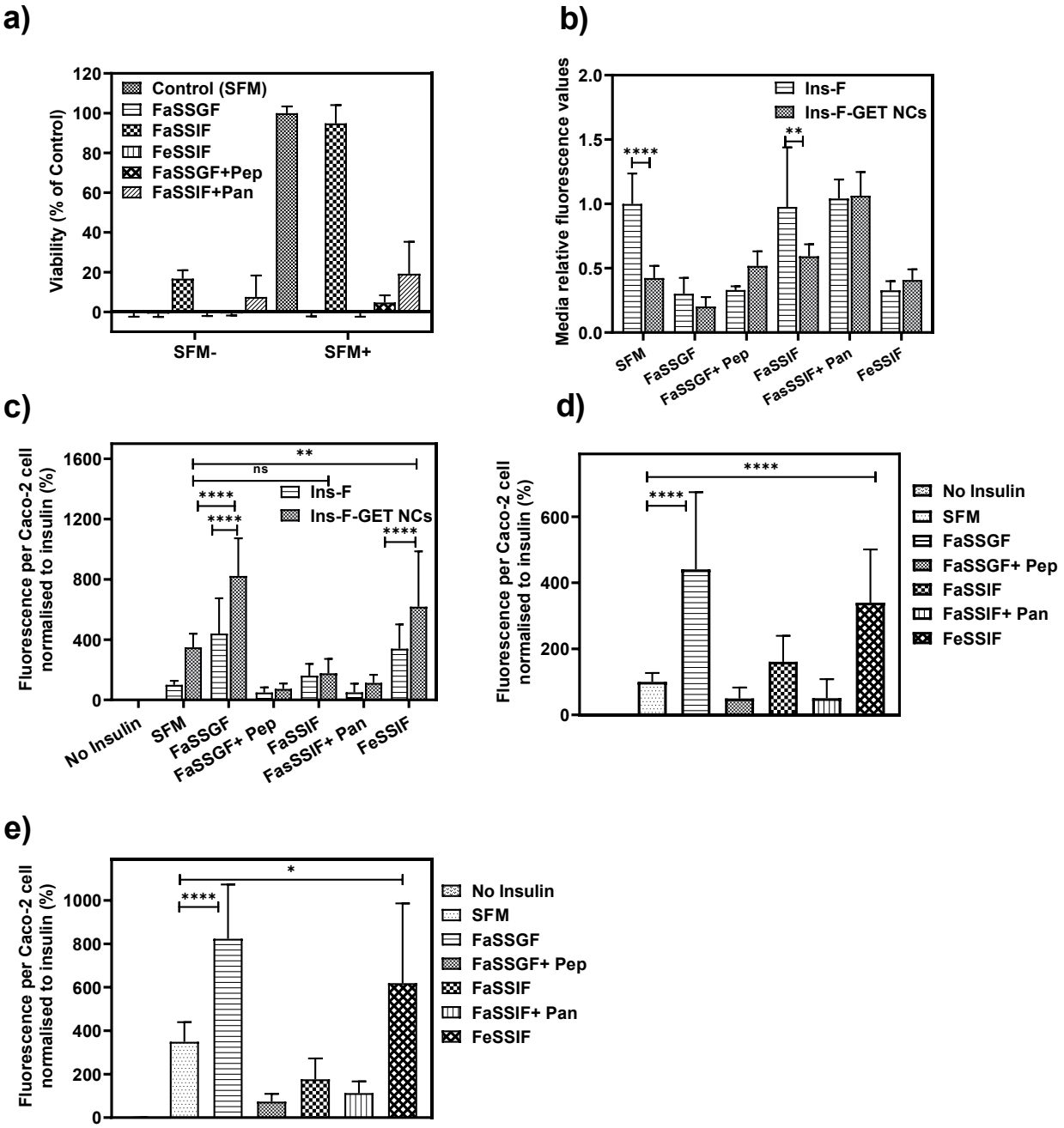

Figure 3. 5 Low pH induced cellular death and thereby showed false increased cellular uptake of NHS-Fluorescein-insulin in commercially available biorelevant media. a) Cell death observed in all types of biorelevant media with no added SFM as indicated by Cellular viability assay, while in presence of SFM the cellular viability was significantly improved for FaSSIF , b) Fluorometric analysis showing depletion in media fluorescence indirectly reflected more cellular uptake for Ins-F-GET NCs, c) flow cytometric analysis for cellular uptake revealed highest permeation and intracellular delivery for Ins-F-GET NCs in FaSSGF vs control (SFM) which could be attributed to cell death in acidic media, d) Ins-F cellular uptake in various biorelevant media with no added portion of SFM, and e) Ins-GET-NCs cellular uptake in different media with no added portion of SFM. All values are presented

as mean ± S.D., n=5, *= *p-value* <0.05, **= *p-value* <0.005, ***=*p-value* <0.0005, ****= *p-value* <0.0001, and *ns*= not significant. Two-way ANOVA with Tukey's test.

(+/- Pep) and FeSSIF had the strongest cytotoxic effect on Caco-2 cell monolayers, both in presence and absence of added portions of SFM. The mix of FaSSIF and SFM showed no cytotoxic effect on monolayers, thus displaying significant improvement of cellular viability from less than 5% viability with FaSSIF (no SFM) to 95% viability with mix of FaSSIF with SFM. Toxicity of biorelevant media to Caco-2 cell monolayers is a well-known phenomenon and it is mostly because of the absence of protective mucus layer, as they lack mucus secreting property. Therefore, it is recommended to test relative permeability studies in standard serum free media (SFM) to compare formulations/approaches, and then further assessment should be done *in-vivo* to reach to conclusion.

Media fluorescence depletion, cellular uptake and internalisation was also studied using biorelevant media with no added SFM, results obtained for these samples are presented in Figures 3.5b-3.5e. The fluorescent values for Ins-F were different in various media although the pH of acidic media was neutralised using PBS, prior to analysis on plate reader. These differences could be attributed to different composition of media due to presence of different salt and ionic contents (Figure 3.5b). Incubating cells with Ins-F-GET NCs in different biorelevant media resulted in variable cellular internalisation, where incubation in FaSSGF resulted in greatest intracellular delivery which was 8-fold higher than Ins-F (SFM, control). There was increased intracellular uptake for both Ins-F and Ins-F-GET NCs in FaSSGF & FeSSIF, which was due to cells being no longer viable (Figure 3.5a), reflecting false/ pseudo enhanced uptake/delivery of NCs. Thus, results from the transfection assay correlate well with the viability assay, as dead cells were no longer able to offer any barrier for permeation leading to maximum internalisation of NCs giving insight into false uptake of NCs. In contrast, FaSSGF with Pep and FaSSIF with Pan showed least cellular uptake and internalisation, possibly due to breakdown of drug-carrier complex and cellular death. All results were statistically significant compared to the control (SFM).

Biorelevant media have been employed for examining the stability of PEG-PGA enveloped hydrophobically-modified-R8 NCs, with results indicating adequate

colloidal stability for ENCP enveloped either with branched or diblock PGA-PEG in simulated intestinal fluid (SIF) for 4 hr. In commercially available complex intestinal medium (FaSSIF-V2), ENCP enveloped with branched PGA-PEG were significantly aggregated but diblock based ENCP were stable upto 6 hr. Additionally, ENCP efficiently protected insulin, where significant amount of insulin was still active after incubation in proteolytic medium (SIF containing 1% Pan) for 2 hr, with free insulin undergoing complete degradation within 15 min [158].

3.3.5. Uptake and intracellular delivery with different GET-peptides

Figure 3.6 presents the uptake properties as measured by fluorescence intensity profiles of different GET-peptides as percentage normalised to insulin. Ins-F with no modification showed least cellular internalisation, while complexation of insulin with GET-peptide and derivatives i.e. L-PLR, D-PLR, or FLR led to an enhanced cellular internalisation. Both L- and D-PLR caused significant increase in cell permeation and internalisation of insulin, but D-PLR was superior to L-PLR in enhancing the intracellular insulin delivery. Insulin uptake was also improved slightly by FLR, but this increase in cellular uptake was insignificant compared to other GET-peptides vs control (no peptide). Overall, the level of cellular fluorescence and uptake observed for Ins-F-GET NCs in the presence of different GET-peptide derivatives was greater than the insulin alone.

Dixon *et al.,* have reported the application of GET system in efficiently enhancing transfection of nucleotides, mediating the delivery of RNA (mRNA, siRNA,) and DNA- (plasmids) based macromolecules into cells [24]. Self-reporting cargo protein coupled with GET (GET-mRFP proteins) were successfully encapsulated in PLGA MPs for controlled release and sustained delivery to the cells for extended time period while retaining the functional activity [136]. FGF2B-based GET transfection was employed for superior complexation of DNA for enhanced gene delivery to lungs, where incorporation of PEG density on particle surface imparted stabilisation in biological fluids, while retaining the improved transfection activity [138]. CPPs composed of D-amino acids are less prone to proteolysis than their co-responding L-isomers. D-amino acid-based arginine-rich CPPs were reported to be less susceptible to proteolytic degradation and provided greater internalisation and

intercellular delivery compared to its counterpart L-form, and revealed that fewer arginine residues are required to efficiently interact with tumour cells. Hence, the improved stability of D-isoform of CPPs in blood, and its high affinity for serum proteins and tumour tissues may attribute to its higher accumulation in tumour tissues [121].

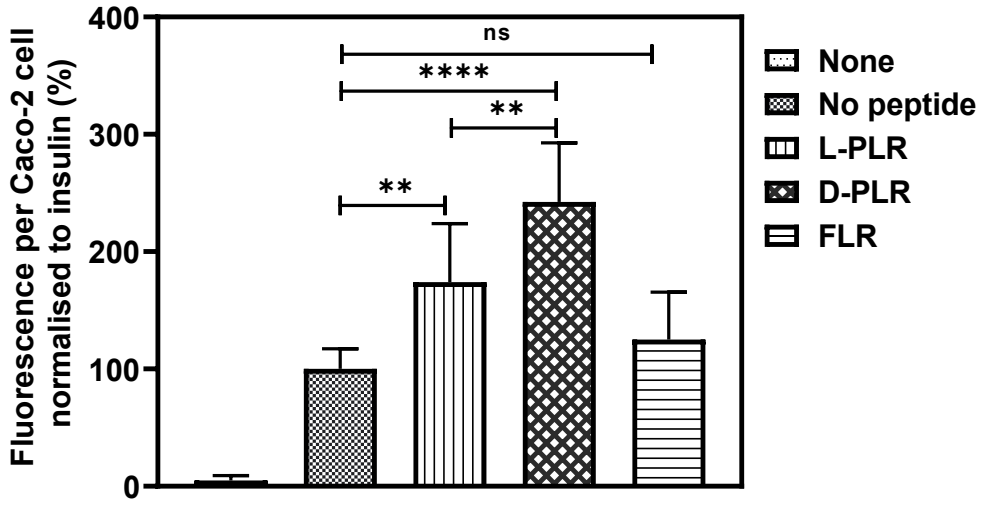

Figure 3. 6 Intracellular trafficking of NHS-fluorescein-insulin coupled with different GET- peptide derivative across Caco-2 cell monolayers, showing that D-PLR is most efficient in enhancing the cellular uptake of insulin compared to other derivatives, control consisted of untreated cells with exposure to just SFM. All values are presented as mean ± S.D, n=5, *= *p-value* <0.05, **= *p-value* <0.005, ***=*p-value* <0.0005, ****= *p-value* <0.0001, and *ns*= not significant. One-way ANOVA with Tukey test.

3.3.6. Cellular internalisation with freeze dried nanocomplexes

Figure 3.7 illustrates the depletion of relative media fluorescence (3.7a and 3.7c) and cellular uptake and internalisation for freshly prepared and freeze-dried Ins-F and Ins-F-GET NCs in SFM, PBS and dH_2O (3.7b and 3.7d), respectively by Caco-2 monolayers at 37 °C. As a control, freshly prepared NCs and Ins-F in similar media (SFM, PBS and dH_2O) were incubated with Caco-2 monolayers under standard conditions. Microplate reader results showed more media fluorescence depletion for both fresh and freeze-dried Ins-F-GET NCs (Figure 3.7c) compared to Ins-F (Figure 3.7a), thereby indirectly reflecting greater cellular uptake of NCs. These results were further supported by flow cytometry, where both freeze dried and freshly prepared NCs (Figure 3.7d) exhibited greater cellular uptake and internali-

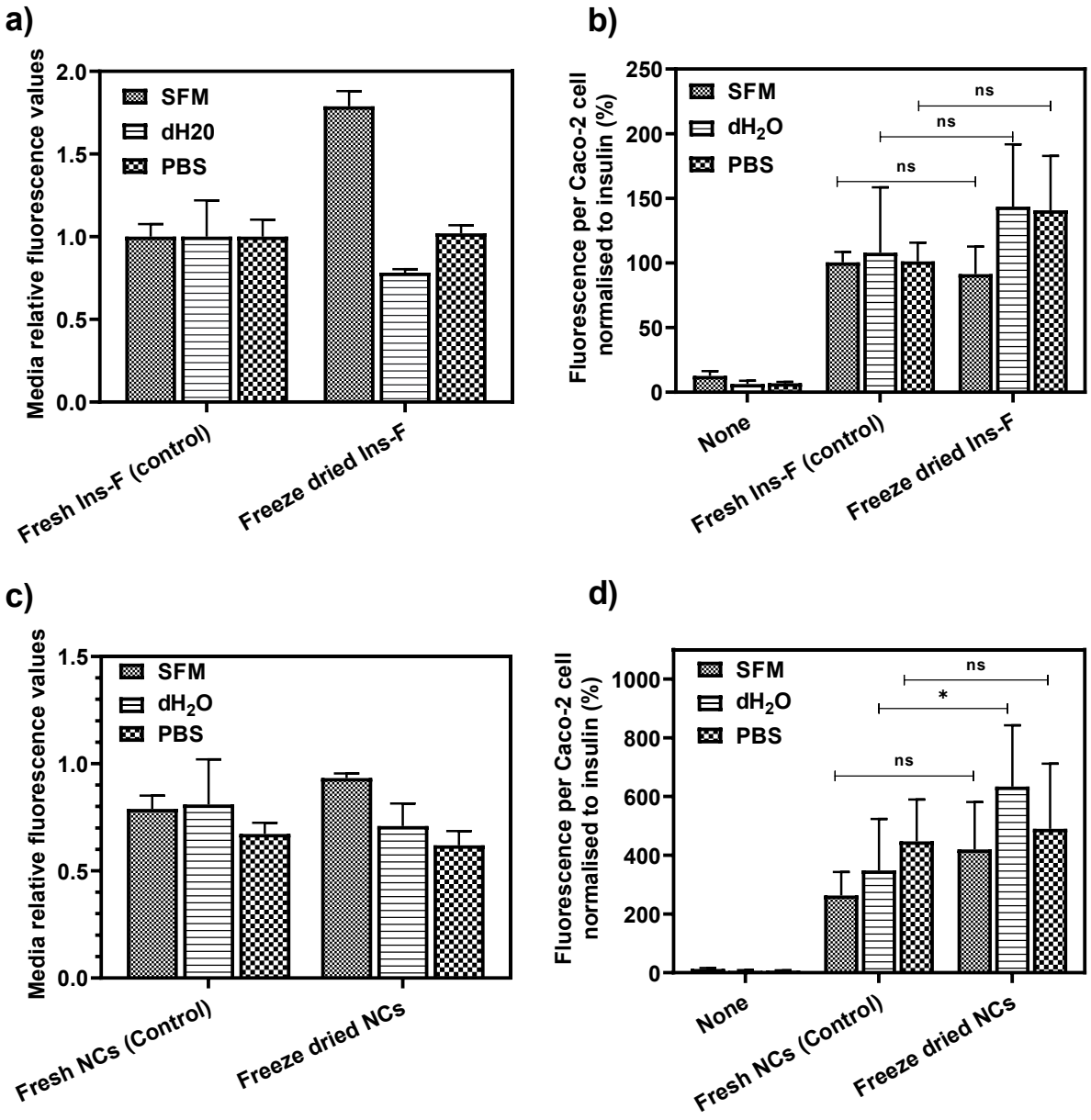

Figure 3. 7 Cellular uptake of freeze dried and freshly prepared Ins-F-GET NCs in SFM, PBS and dH_2O was comparable and freeze dried NCs were more efficient than fresh NCs in promoting insulin permeation and delivery. Comparison of fresh and freeze-dried Ins-F in various media a) fluorometric assay showing depletion of media fluorescence, and b) cellular uptake of Ins-F. Ins-F-GET NCs comparison in fresh and freeze-dried state for c) media fluorescence depletion and d) flow analysis showing greater insulin permeation and internalisation with GET-peptide in freeze dried form compared to fresh samples. All values are presented as mean ± S.D, n=5, = *p-value* <0.05, **= *p-value* <0.005, ***=*p-value* <0.0005, ****= *p-value* <0.0001, and *ns*= not significant. Two-way ANOVA with Tukey test.

-sation compared to Ins-F (Figure 3.7b) in all tested mediums (SFM, PBS and dH_2O). Overall, freeze dried NCs in all studied medias were superior to freshly prepared

NCs and provided significantly higher permeation and internalisation of insulin vs control (fresh nanocomplexes). Thus, these results revealed we can achieve better insulin delivery and intracellular accumulation by freeze drying NCs.This study provided positive insights in term of storage of drug-carrier complexes as freeze-dried powders while retaining their activity, which could further be aerosolised, compressed in form of small pills or filled in capsules as a forward step towards oral delivery of insulin.

There have been numerous studies where CPPs based nanoparticles, nanohybrids or polymer conjugates have been freeze-dried for efficient processing of nanocomplexes and to ensure their stability. Pappalarado *et al*., conjugated Tatp-to pNP-$PEG_{3.4K}$-DOPE, followed by dialysis, freeze drying and storage at -80^{o}C until used for preparation of liposomes. Incubating pEGFP-loaded TaTp-liposomes with APC cultures for 48 hr showed a significant rate of transfection i.e. 60 ± 10% compared to plain-L-based lipoplexes where the transfection yield was only 15 ± 4% [159]. Octa-arginine conjugated alpha-cyclodextrin (CDR) complexes prepared by thiol-ene coupling reaction, followed by dialysis and freeze drying CPP-polymer conjugates, were later on mixed with DNA solution and dextran to form polyplexes. Improved physiological stability was imparted by dextran shell of CDR/Az-I-Dex/DNA polyplexes with 6-300 times greater transfection efficiency than CDR/DNA polyplexes [160]. All of these studies reflect application of freeze drying in preserving the discrete features of NCs and NPs, and imparted enhanced stability to NCs which is in accordance with the results of our study.

3.3.7. Dextran based assay for measuring Caco-2 monolayer permeability and integrity in presence of Ins-F-GET NCs

In order to adequately determine the effect of GET-peptide on monolayer integrity and the cellular uptake mechanism (paracellular or transcellular pathway), transport of hydrophilic tracers was studied i.e. low and high MW TRITC-Dex (4.4KDa- and 70KDa-Dex) across monolayers together with measurement of response changes in TEER. The transport of Ins-F or Ins-F-GET NCs, and different MW Dex was maximum across the transwell inserts with no grown cell monolayers, these inserts served as a positive control (Figure 3.8a and 3.8b).

Apical application of Ins-F or Ins-F-GET NCs with different MW Dex didn't show any significant difference in cumulative insulin transport compared to samples having no added dextran. Moreover, damaging monolayers by treatment with 5N NaOH caused increased flux of both Ins-F and Ins-F-GET NCs owing to disruption of the cellular barrier. GET-peptide enhanced the intracellular permeation of insulin by 4-fold compared to un-modified insulin. The co-application of insulin with different MW Dex caused no significant changes in cellular uptake of both Ins-F and NCs as shown in Figure 3.8e. These results are consistent with those obtained in Section 3.2.3.

In the presence of Caco-2 monolayers on Transwell® inserts, the cumulative transport and transcytosis of Dex was remarkably reduced compared to controls i.e. 3.4% and 0.65% for 4.4KDa- and 70KDa-Dex, respectively owing to the intact membrane which provided a physiological barrier to transport. Apical application of different MW Dex with Ins-F or Ins-F-GET NCs to Transwell® inserts showed that in the absence of GET-peptide the transports of different dextrans was comparable to apical application of only Dex, but in the presence of GET-bond insulin the apical transport of both 4.4KDa- and 70KDa- Dex was increased to 10.2% (3.2 fold) and 1.5% (1.6 fold), respectively (Figure 3.8 c and 3.8 d). These results provided insight that in the presence of GET-peptide, membrane integrity was affected as evident through lowered TEER values (Figure 3.8f and 3.8g) which might contribute to indirect toxicity *in-vivo*; however, TEER values were fully recovered in 24 hr. Additionally, destroying grown monolayers by pre-treatment with 5N NaOH, revealed that cumulative transport for different MW Dex was increased dramatically to 90% and 16% for 4.4KDa- and 70KDa- Dex, respectively, showing that monolayers offer a barrier to the transport of molecules. Flow cytometric analysis showed considerably higher cellular uptake for both Dex in the absence of NCs, while in the presence of Ins-F or Ins-F-GET-NCs the cellular uptake of both 4.4KDa- and 70KDa- Dex was remarkably reduced, possibly due to competition between the nanocomplexes and dextran (Figure 3.8e).

The apical application of GET-peptide complexed to insulin with 0.5mg/ml 4.4KDa- or 70KDa Dex resulted in comparable responses as evident by changes in TEER values (Figure 3.8f and 3.8g). The TEER values were reduced abruptly during the

first few hours, but with time, reversal of TEER depression was observed. Under all conditions, TEER values were recovered to 75-85% of initial values within 24 hr. Apical application of GET-bonded insulin increased the rate of 4.4KDa-Dex transport by approximately 3.5 fold, which could be attributed to the impact of the combination of GET-peptide and macromolecule (4.4KDa-Dex) on TEER value which was abruptly dropped initially but was recovered to 70-75%% of initial TEER value by 24 hr. GET-peptide caused approximately 1.6 fold increase in permeability of 70KDa-Dex, despite displaying nearly identical changes in TEER profile compared to in presence of 4.4KDa-Dex with NCs mix. As discussed earlier in Section 3.2.3., this lowering of TEER values due to opening of TJs may lead to absorption of unwanted molecules even pathogens thus reflecting potential for toxicity *in-vivo*. The linearity of flux enhancement of 4.4KDa- and 70KDa-Dex together with Ins-F and Ins-F-GET NCs suggests that permeability changes induced by GET system were quite rapid, despite the time required to achieve the plateau phase of TEER response. These results suggest that the GET may induce more rapid onset but less durable and robust opening of the paracellular pathway for drug transport.

The P_{app} values for both 4.4KDa and 70KDa-Dex and insulin in the absence and presence of GET-peptide were also determined as shown in Figure 3.8h and 3.8i. Results indicated that in the absence of monolayers, the permeability of 70KDa-Dex (19.5×10^{-6} cm/sec) was half of the one for 4.4KDa-Dex (9×10^{-6} cm/sec). On the other hand, the permeability for both MW Dex and Ins-F with and without GET-peptide was significantly reduced across Caco-2 monolayers grown on filter inserts compared to empty inserts. Here, GET-peptide enhanced the permeability of insulin across monolayers by 5 -fold (9.5×10^{-6} cm/sec) compared to free insulin (1.9×10^{-6} cm/sec), thus indicating the potential of GET-peptide in improving insulin transport, delivery, transcytosis, and cellular internalisation. The P_{app} values for 4.4KDa-Dex across the monolayer was 1.27×10^{-6} cm/sec which was approximately 19-fold greater than for 70KDa-Dex having P_{app} value of only 0.066×10^{-6} cm/sec (Figure 3.8i). The presence of GET-peptide significantly enhanced the transport and flux of 4.4KDa-Dex across monolayers, but there was insignificant effect on the transport of 70KDa-Dex. Results from this study suggest that the apical application of GET temporarily disrupts the Caco-2 monolayers integrity, resulting in enhanced

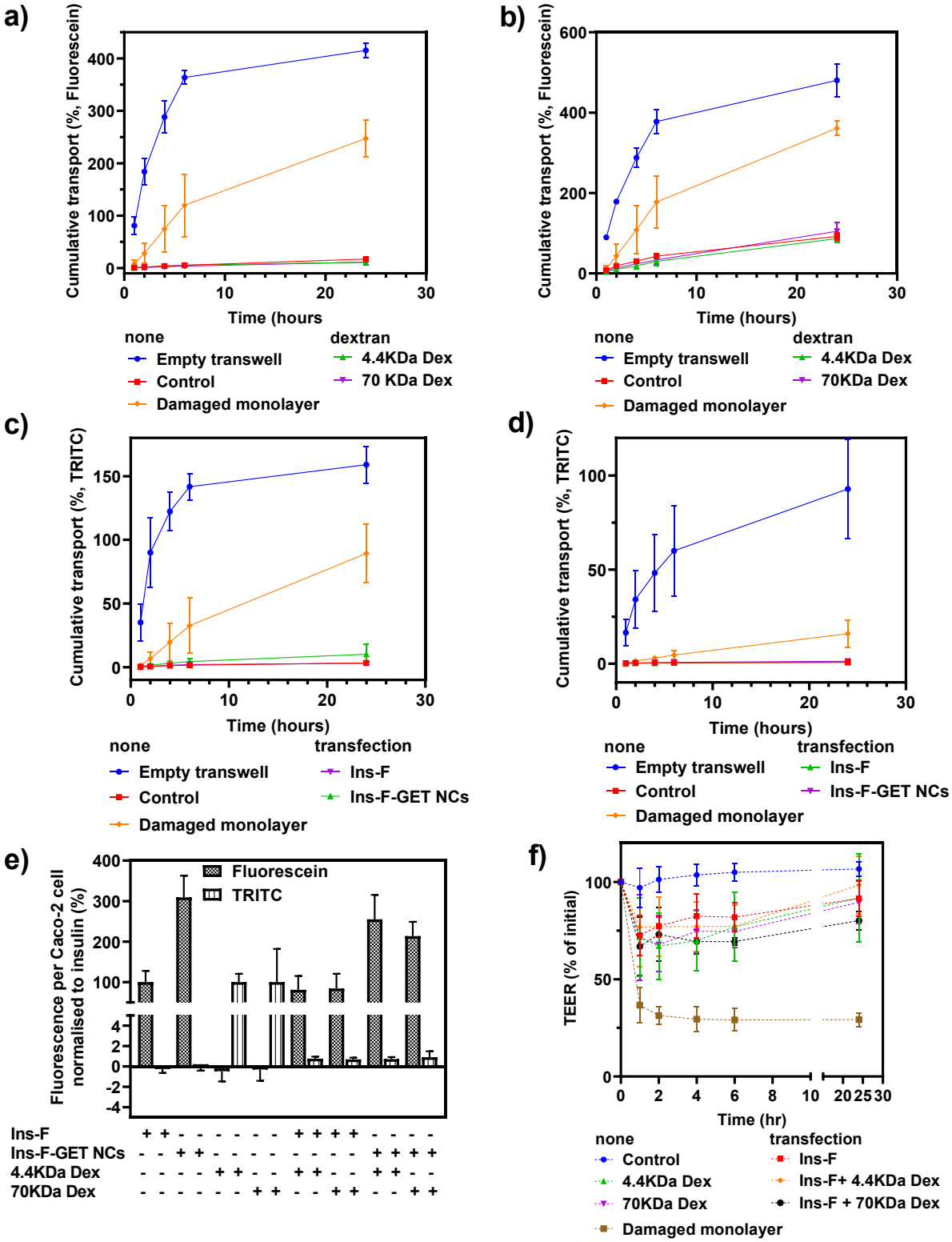

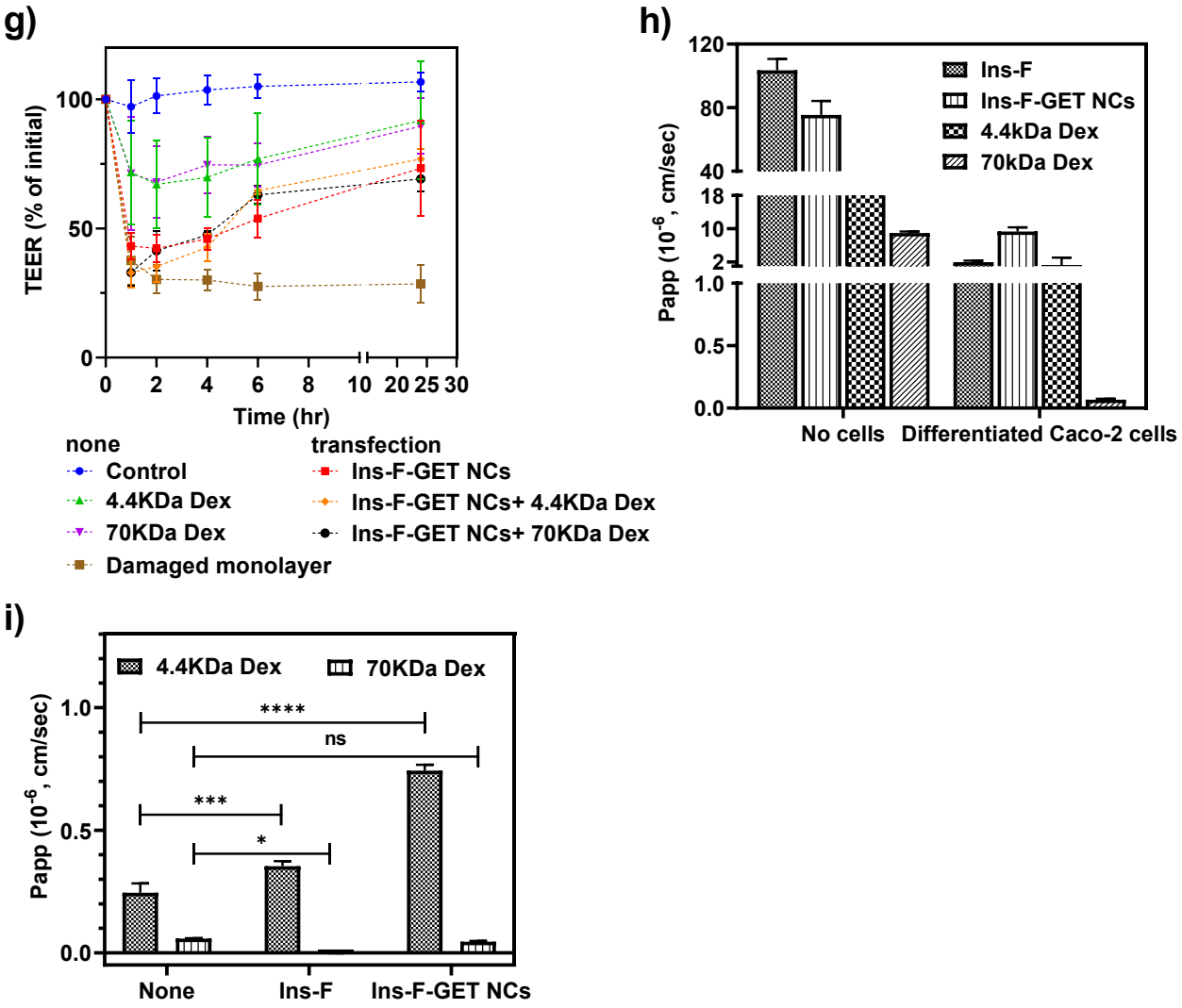

Figure 3. 8 Integrity of Caco-2 cell monolayers grown on Transwell® inserts during transcytosis in presence of GET-peptide was maintained as determined using different MW Dex; a) percent cumulative Ins-F transport (Fluorescein channel) in the presence of different MW Dex, control consisted of cells treated with only Ins-F, b) percent cumulative Ins-F-GET NCs transport (Fluorescein channel) in presence of different MW Dex, control consisted of cells treated with only Ins-F-GET NCs c) percent cumulative 4.4KDa-Dex transport (TRITC channel) in presence of Ins-F or NCs, control consisted of cells exposed only to 4.4KDa-Dex, d) percent cumulative 70KDa-Dex transport (TRITC channel) in presence of either Ins-F or NCs, control consisted of cells exposed only to high MW Dex , e) flow analysis for cellular uptake of Ins-F and Ins-F-GET NCs (Fluorescein & TRITC channel), f) TEER measurement with Ins-F, g) TEER measurement with Ins-F-GET NCs, h) Apparent permeability with no cells and differentiated Caco-2 monolayers at 6 hr, and i) P_{app} values for different MW Dex across differentiated Caco-2 monolayers in presence of Ins-F and NCs. All values are presented as mean ± S.D, n=5, * = *p-value* <0.05, **= *p-value* <0.005, ***=*p-value* <0.0005, ****= *p-value* <0.0001, and *ns*= not significant. Mixed effect analysis and One-way ANOVA with Tukey ‘s test.

flux and paracellular transport. This transient loss of membrane integrity during initial hours, as indicated by lowering of TEER depicted that barrier function of membrane is affected by GET-peptide, which was further confirmed through use of different MW Dex, where the permeability and transport of both Dex was increased, thus suggesting that barrier function of membrane is no longer preserved. This loss of barrier function may limit the application of GET-peptide due to potential of toxicity, specially in in immunocompromised patients and those with GIT infections. Thus, results from the cumulative transport, TEER, and P_{app} all are well co-related and indicated that transient initial loss of integrity promotes paracellular transport of molecules in addition to transcellular route.

Apical application of PIP peptides 640 and 250 caused transient, reversible and non-toxic reduction of Caco-2 monolayer TEER values and thus leads to opening of paracellular route (by induction of myosin light chain phosphorylation) for both 4- and 70-KDa-Dex by PIP 250, while PIP 640 opened paracellular route only for 4KDa-Dex. These results are in accordance with our results, where GET-peptide also induced reversible and transient lowering of TEER [161]. Similarly, high MW Dex was used to determine whether the co-incubation of CPP (angiopep-2) with spheroids disrupts the surface barrier or not. Results indicated higher influx for angiopep-2, where the spheroid surface stayed impermeable to Dex, thereby demonstrating that angiopep-2 is transported across the intact surface of spheroid [162]. L-tryptophan has been used as an effective absorption enhancer for oral delivery of insulin, GLP-1, and Exendin-4. The co-administration of L-tryptophan (32mM) with different MW Dex effectively improved the intestinal absorption of all Dex (4.4-, 20- and 70KDa-Dex), but this effectiveness of enhancement was reduced with increased MW of drug-cargoes [163].

3.3.8. Studying cellular uptake and recycling mechanism using cell secretion regulators

3.3.8.1. Noradrenaline based assay

For studying the insulin recycling and investigating uptake mechanism through Caco-2 cells, specific insulin secretion regulators were used. The effect of NA was tested on the delivery and transcytosis of Ins-F and Ins-F-GET NCs, to determine

whether endocytosis is the mechanism for intracellular uptake of insulin across Caco-2 monolayers. As described earlier in Section 2.15, two separate assays were performed for analysing the effect of NA. For the first assay, the results showed that NA had a variable effect on cumulative transport of Ins-F and Ins-F-GET NCs (Figure 3.9a). The NA significantly increased Ins-F cumulative transport, resulting in greater insulin exocytosis. Whereas cumulative transport of Ins-F-GET NCs was not affected insignificantly. The cellular uptake of Ins-F and Ins-F-GET NCs was quantified using flow cytometer (Figure 3.9b), NA had insignificant effect on cellular contents of Ins-F, but the cellular contents of Ins-F-GET NCs was significantly decreased compared to control (no added NA).

Thus, to further test this hypothesis, another study protocol was designed where cells were incubated with NCs followed by post-incubation release in media containing NA. The results obtained were similar to one obtained earlier (Figure 3.9c and 3.9d), where NA had insignificant effect on cumulative transport of both Ins-F and Ins-F-GET NCs. Flow cytometric results were consistent with earlier results and revealed that NA have not reduced the cellular uptake of Ins-F, while for Ins-F-GET NCs there was significant decrease in cellular uptake compared to control (Ins-F-GET NCs with no added NA). These results indicated that NA inhibits GET-peptide mediated insulin transport, transcytosis and most importantly the cellular uptake of insulin. Thus, it can be concluded that nor-adrenaline can significantly decrease the cellular uptake and transcytosis of insulin formulations with GET-peptide, suggesting that one of the possible mechanisms for the cellular uptake of these NCs is endocytosis.

GET-peptide mediated cellular uptake of insulin was reduced in presence of NA, which is in agreement with previously reported studies where NA has known to be a powerful inhibitor of insulin secretion and endocytosis. NA exerts its action through activation of K^+ channels to repolarise or hyperpolarise cell or via coupling to α2- adrenergic receptors and leads to subsequent activation of G_1/G_o proteins, and it is also known to inhibit endocytosis. NA can reduce the number of exocytotic events without affecting vesicle size and inhibits Ca^{+2}-evoked exocytosis. NA inhibits both early and late phases of endocytosis, additionally it also lowers initial rate of slow endocytosis and it's amplitude [164, 165].

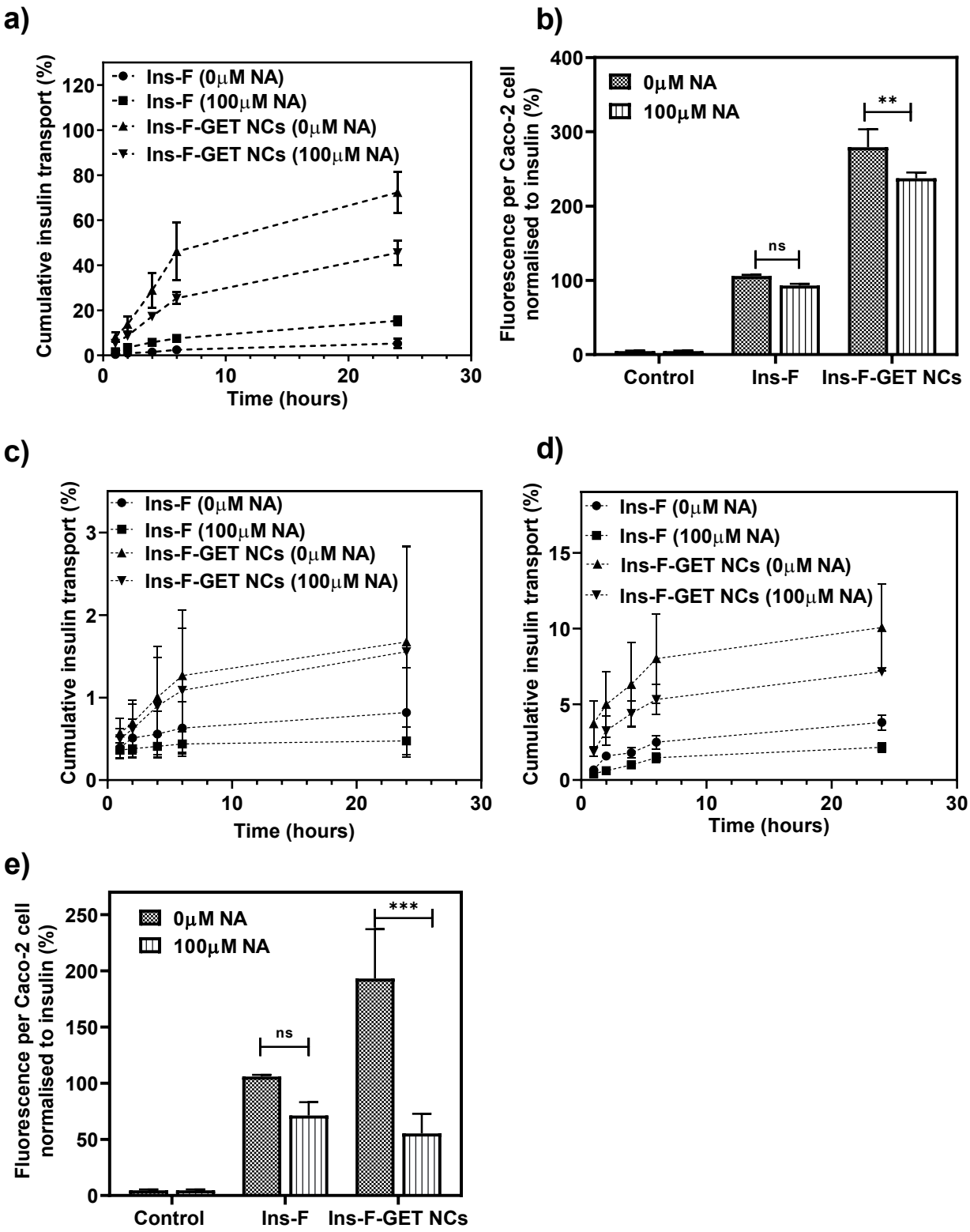

Figure 3. 9 Apical application of nor-adrenaline (NA) caused a reduction in GET-peptide mediated NHS-Fluorescein-insulin transport and cellular internalisation; a) Cumulative insulin transport with and without NA, b) Flow cytometric analysis of cellular internalisation showing reduced cellular uptake for both Ins-F and Ins-F-GET NCs in the presence of 100μM NA. Post-incubation cumulative release with and without 100μM NA from c) bottom, d) top well showing no significant effect

on insulin transport, and e) Flow analysis for cellular uptake post-transfection with and without NA showing reduced cellular uptake of both Ins-F and Ins-F-GET NCs in presence of NA. All values are presented as mean ± S.D, n=5, * = *p-value* <0.05, **= *p-value* <0.005, ***=*p-value* <0.0005, ****= *p-value* <0.0001, and *ns*= not significant. Mixed effect analysis with Ordinary One-way ANOVA and Two-way ANOVA with Tukey's test.

Different studies have reported use of various cell secretions regulators, specific progression inhibitors, and inhibitors of endocytosis for studying mechanism of cellular uptake or intracellular trafficking. Octa-arginine and its derivatives-based insulin NCs were studied for their cellular uptake using various specific endocytosis inhibitor such as; sodium azide (NaN_3), chlorpromazine (CPZ), methyl-β-cyclodextrin (MβCD), and 5-N-ethyl-isopropyl amiloride (EIPA). For both R6EW-F-insulin and R8-F-insulin, NaN_3 and EIPA caused decrease in fluorescent signals, MβCD lead to enhancement of fluorescent signal, and CPZ had no effect on cellular uptake, thus suggesting that cellular uptake of these NCs takes place via energy-dependent pathways, and that different modes of endocytosis are responsible for this uptake [125]. Different biochemical modulators were employed for studying mechanism of transalveolar absorption such as; NaN_3, 2-deoxyglucose, ammonium chloride (NH_4Cl), CPZ, nocodazole, and monensin. No significant decrease was seen in absorption of Ins-cR9 with monensin, CPZ, and NH_4Cl compared to control, while a 15% decreased and 40% increased absorption effect was seen with NaN_3, 2-deoxyglucose and nocodazole, respectively [132].

3.3.8.2. Effect of various cell secretion regulators on NCs cellular uptake and recycling

Intracellular progression is regarded as one of the essential components of transcellular transport. For investigating the mechanism of intracellular trafficking of carrier peptide-insulin complexes and their recycling, different cell secretion modulators were employed. Secretion of insulin is known to be regulated by various intracellular signals which are generated through neural or hormonal inputs and nutrients. Major intracellular signals of insulin secretion include ATP, Ca+2, phospholipid- derived structures i.e. inositol-triphosphate (IP3), and diacylglycerol, and cAMP [166]. Figure 3.10 shows the effects of cell secretion modulators on the

cumulative transport of Ins-F and Ins-F-GET NCs across the Caco-2 cell monolayers. For the Ins-F, FK (2 and 5 µM), BM, NAS, ATP, and YB (1 and 10 µM) exhibited an insignificant effect on cumulative transport from the Caco-2 monolayers (Figure 3.10a). Similarly, with Ins-F-GET NCs, the effects of these various cell secretion regulators were insignificant on cumulative transport of Ins-F-GET NCs. Additionally, cellular uptake and internalisation of Ins-F and Ins-F-GET NCs were quantified using the flow cytometer (Figure 3.10c). For Ins-F, all regulators except BM caused statistically significant increase in cellular uptake resulting in greater accumulation of insulin. For Ins-F-GET NCs, a statistically significant reduction in cellular internalisation was observed with ATP, and NAS, but YB caused significant increase in cellular uptake of NCs at low dose (1 µM), whereas a high dose of YB instigated a significant reduction in intracellular contents of Ins-F-GET NCs. Overall, there was increased intracellular accumulation of Ins-F and Ins-F-GET NCs in the presence of various cell secretion regulators compared to in their absence.

BM is cytosolic Ca^{+2} chelator, which causes blockade of insulin secretion by depleting cellular Ca^{+2}. BM has been reported to abolish the oleanolic acid-induced increased basal and stimulated insulin secretion from MIN-6 cells [167]. Pre-incubation with BM tends to abolish insulin release evoked by 1nM ryanodine, demonstrating that elevated cytosolic Ca^{+2} is responsible for insulin release rather than changes in luminal Ca^{+2} levels [168]. The results obtained with Ins-F-GET NCs in this study showed increased cellular contents comparative to control which was opposite to its intended action. On contrary, with free insulin decreased cellular contents were observed in presence of BM which is in agreement with the previously reported studies and its intended action. YB is a well-known potent inhibitor of α_2- receptors, and is known to markedly increase plasma levels of immuno-reactive insulin; and it may also inhibit adrenaline-induced hyperglycaemic response in mice [169]. Dose-dependent relationship of effect of YB on adrenaline induced blockage of insulin release has been reported, where YB at concentrations higher than 0.1 µM evidently antagonised the adrenaline inhibitory effect on insulin secretion [169]. Similar results were reported by Zhao *et al*., where YB hampered the NA-induced inhibition of both late and early phases of endocytosis [164]. These earlier studies co-relate well with the results obtained

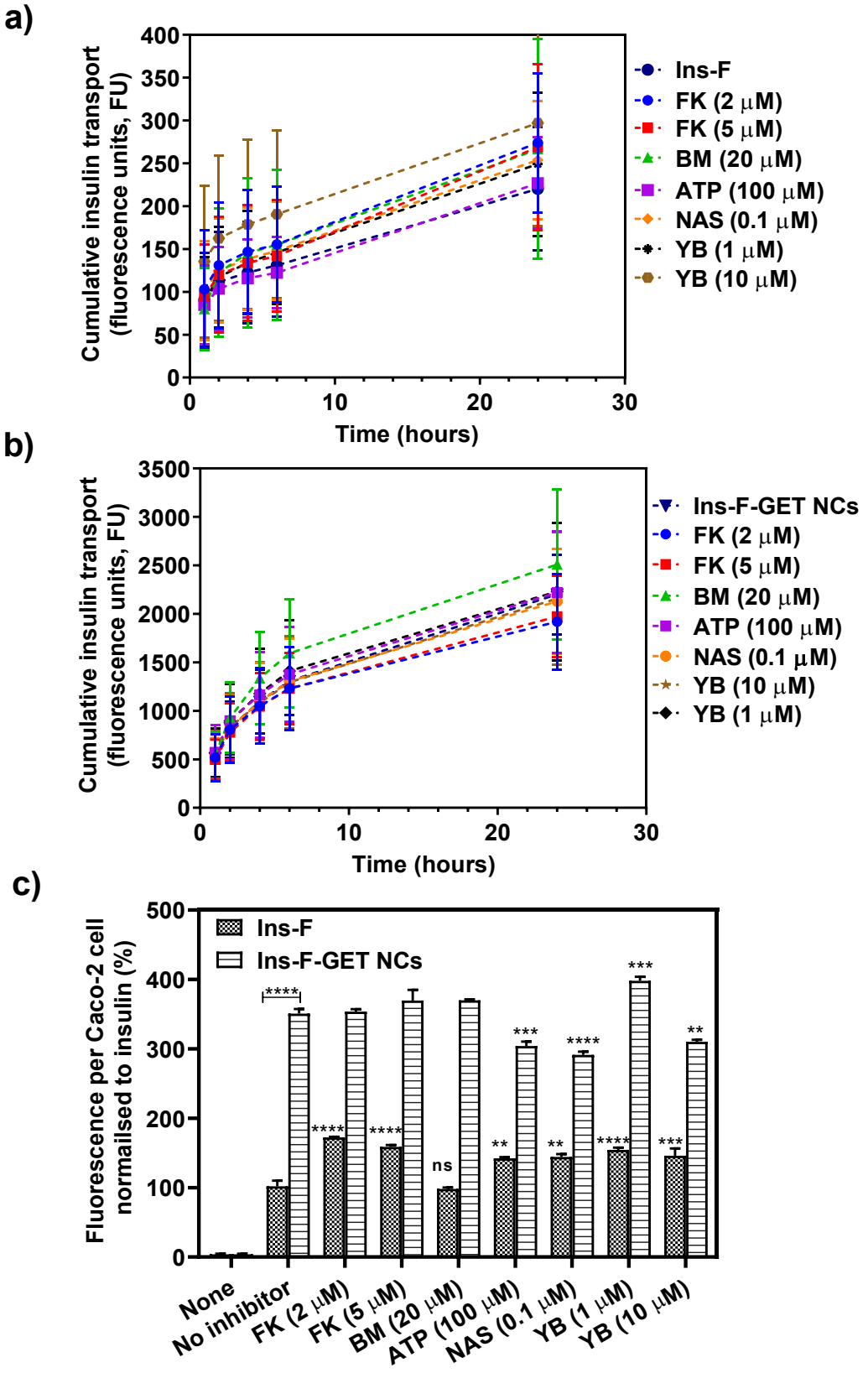

Figure 3. 10 Different cell secretion regulators were employed to determine the mechanism of NHS-Fluorescein-insulin uptake and its recycling across Caco-2 monolayers. a) Ins-F, and b) Ins-F-GET NCs showed statistically insignificant effect on secretion of pre-loaded insulin from monolayer. c) flow cytometer analysis

showed Ins-F accumulation in cells in presence of various regulators which was opposing to their intended roles, thus showing that these regulators do not affect insulin secretion from insulin reservoirs in cells, while for Ins-F-GET NCs only ATP, NAS, and high dose YB caused significant decrease in cellular insulin contents which is consistent with the conventional effect of these regulators. All values are presented as mean ± S.D, n=3, * = *p-value* <0.05, **= *p-value* <0.005, ***=*p-value* <0.0005, ****= *p-value* <0.0001, and *ns*= not significant. Two-way ANOVA with Tukey's test.

in this study, where low dose of YB caused increased cellular contents of NCs possibly due to above stated mechanism. While on increasing dose of YB to 10 µM, there was reduction in intracellular contents of NCs, whereas for free insulin all tested concentration resulted in increased cellular contents.

NAS is less hydrophobic analogue of naturally occurring ceramides and displays features of an active cell permeable surrogate. Inside cells, sphingosine is enzymatically converted to sphingosine-1-phosphate, which stimulates release of Ca^{+2} from different pools including 1,4,5-tris-phosphate-sensitive calcium pool. This leads to rapid and profound translocation of calcium from intracellular stores [170]. The results of this study reflected decreased cellular internalisation of NCs on incubating cells with NAS, which is in accordance with previously reported studies. FK is yet another example of cell secretion regulator, which stimulates the glucose induced insulin secretion by mimicking the actions of GLP-1 and PACAP to activate PKA [171]. Insulin release is augmented strongly by glucose in the presence of FK. Even under conditions of complete depletion of Ca^{+2}, FK tends to induce glucose stimulated insulin secretion [172]. FK can potentiate both phases of insulin secretion (early and late phase), but it has more significant effect on late phases of secretion [173]. In this study FK had no significant effect on uptake or secretion of NCs but for insulin a statistically significant increased cellular uptake was seen, which was opposite to its intended action.

3.3.9. Multifection for studying insulin recycling across Caco2-monolayers

3.3.9.1. Recycling assay with double delivery of NCs

As during preliminary experiments (Section 3.2.3) it was observed that insulin-GET NCs were released/ secreted following post-incubation from monolayers, this observation gave insight that accumulated insulin inside cells forms depots, which

undergoes recycling enabling cells to function as reservoir for sustained cells. Therefore, to understand this recycling phenomenon, this assay was designed where monolayers were exposed to multiple delivery (double/ triple) with NCs. Herein, post-incubation release of Ins-F and Ins-F-GET NCs (green or NHS-Fluorescein-labelled) was assessed from Caco-2 cells in the presence and absence of second delivery with red-labelled insulin (Ins-T, NHS-Rhodamine-labelled), schematic diagram is given in Figure 3.11a. Results of the study indicated that sequential inputs of insulin i.e. loading cells with more insulin (Ins-T or Ins-T-GET NCs) reduced the insulin output, whilst no delivery (SFM) drove more Ins-F-GET NCs out of the cells (Figure 3.11b and 3.11c). It can be seen from results (Figure 3.11b) that the Ins-F-GET NCs/No samples exhibited highest insulin transport, compared to those receiving second delivery with either Ins-T or Ins-T-GET NCs. Similarly, Ins-F/No samples showed more insulin transport compared to samples receiving second delivery. The results obtained were in agreement with flow cytometric results, where the Caco-2 cell monolayers receiving second delivery with the Ins-T or Ins-T-GET NCs showed accumulation of insulin within the cells as compared to the Caco-2 cells receiving no second delivery (Figure 3.11d and 3.11e). The cellular uptake for Ins-F-GET NCs/Ins-T-GET NCs was greatest comparative to all other possible combinations, possibly due to GET mediated enhanced cellular uptake and

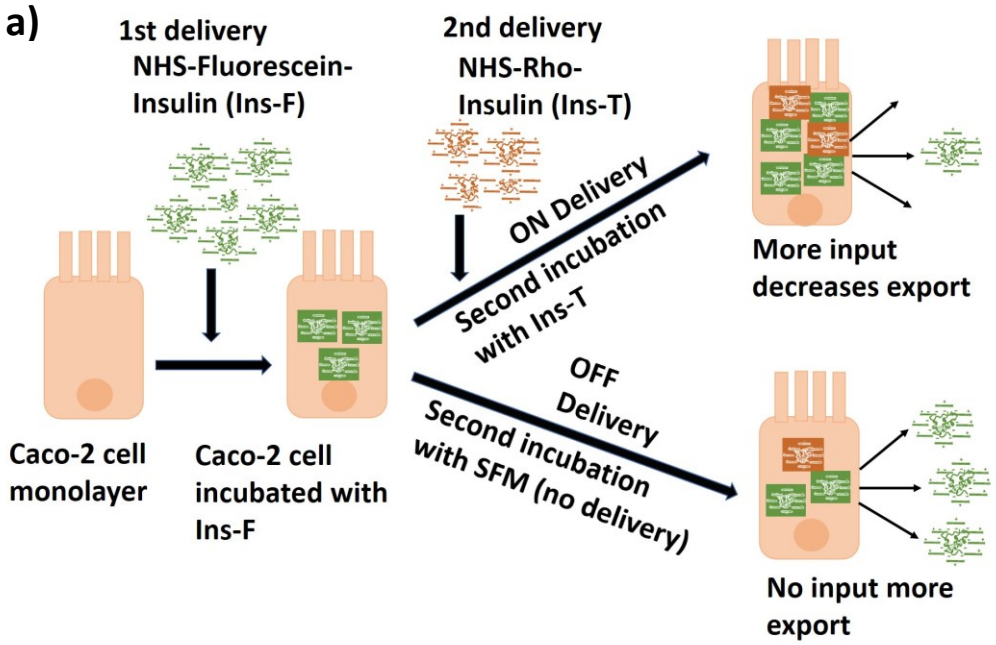

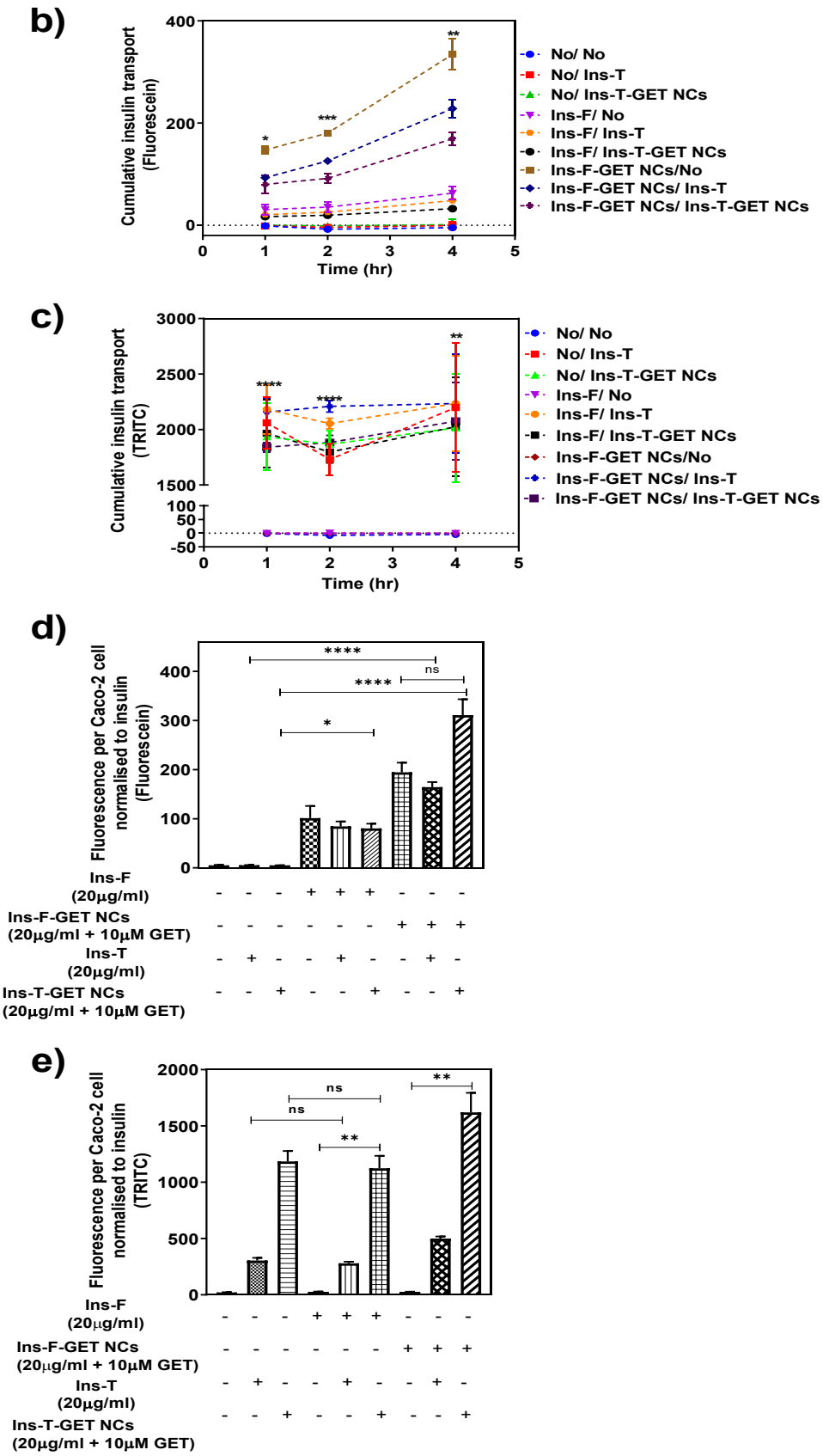

Figure 3. 11 a) Schematic illustration of Caco-2 cells receiving two deliveries with insulin showing that input with more insulin decreases the post-transfection

release of insulin-GET NCs leading to insulin accumulation in cells. Insulin recycling through Caco-2 cells was studied using green- (Ins-F) and red- (Ins-T) labelled insulin on its own or complexed with GET with subsequent two deliveries; Cumulative insulin transport in b) Fluorescein channel, and c) TRITC channel showing that multiple delivery tends to decrease the insulin transport, Flow cytometric analysis under d) Fluorescein channel and e) TRITC channel showing intracellular accumulation of insulin with multiple drug loading. All values are presented as mean ± S.D, n=5, * = *p-value* <0.05, **= *p-value* <0.005, ***=*p-value* <0.0005, ****= *p-value* <0.0001, and *ns*= not significant. One-way ANOVA with Dunn's and Tukey's test and Two-way ANOVA with Tukey's test.

multiple delivery. Thus, the input with more insulin decreases the post-incubation release of Ins-F-GET NCs, thereby leading to intracellular accumulation of insulin.

3.3.9.2. Recycling assay with triple delivery of NCs

This assay was performed to study whether the pre- (first delivery with non-labelled insulin, Ins i.e., N and N-GET) or post- (second delivery with NHS-Fluorescein-insulin, Ins-F i.e., F and F-GET) delivered insulin comes out first through the Caco-2 cells, by observing the post-incubation release of F and F-GET from these cells in presence of third delivery with NHS-Rhodamine- insulin (Ins-T i.e. T or T-GET) or just adding SFM (no delivery). A schematic of hypothesis is given below as flow chart, the results are given in Figure 3.12 along with schematic of observed results.

The results of the study revealed that the lastly delivered insulin comes out first, i.e. the cells receiving 1st delivery with No (just SFM) or non-labelled insulin followed by subsequent delivery of "F", showed more insulin release (F or F-GET) at all studied time points (1, 2 and 4hr) compared to the cells receiving 1st delivery with "F", and these results were statistically significant (Figure 3.12b-e). Here, the samples receiving "F" during 2nd delivery exhibited greater insulin transport compared to samples receiving 1st delivery with "F" (Figure 3.12b and 3.12d). Cellular uptake studies showed no difference in internalisation of free NHS-Fluorescein-labelled insulin whether receiving multiple transfections or just media (Appendix Figure 10.5). Similarly, N-GET /F-GET/No exhibited greatest cumulative insulin release, followed by N-GET/F-GET/T-GET as shown by fluorometric analysis (Figure 3.12c and 3.12e) which was further confirmed through flow cytometric

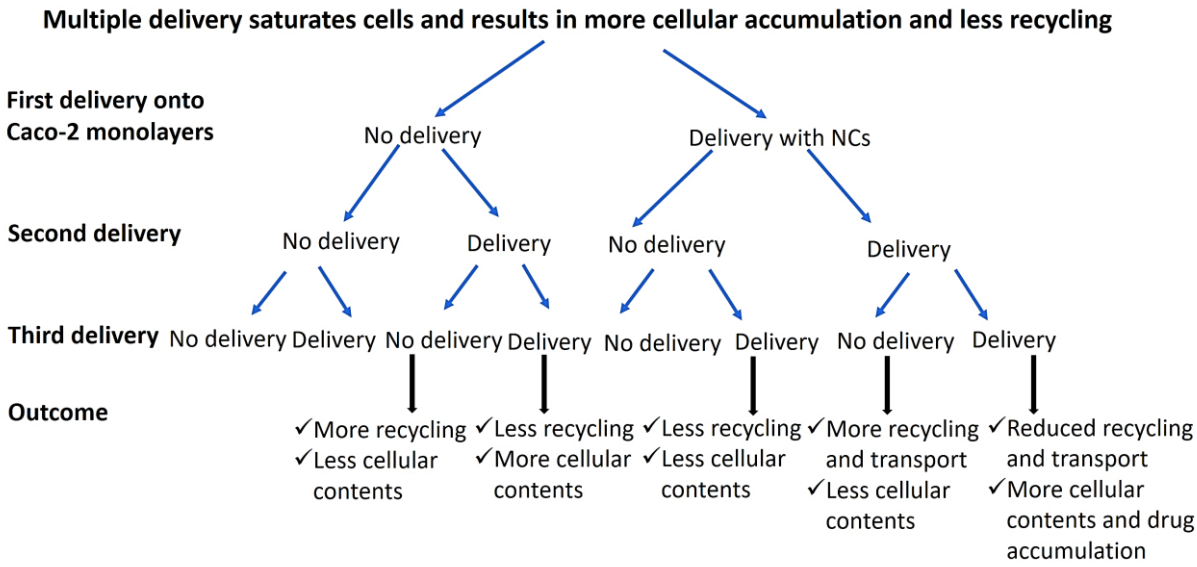

results showing greater insulin accumulation for the later sample (N-GET/F-GET/T-GET) (Figure 3.12g and 3.12i).

Additionally, cells receiving delivery combination of No/F-GET/T-GET and No/F-GET/No exhibited lesser post-incubation release than N-GET/F-GET/No and N-GET/F-GET/T-GET. This higher release for the 2nd set of samples could be due to pre-loading of cells with "N" which would have promoted greater release of 2nd delivered insulin (F). On the other hand, due to "No" 1st delivery (SFM) in the earlier sample set, more of the 2nd delivered insulin was accumulated in cells. This observation shows that 1st delivered insulin tends to accumulate in cells forming insulin depots inside cells, and becomes unavailable for recycling, while the lately delivered insulin being close to cell membrane gets recycled through the cells, whereas "No" 3rd delivery promoted greater insulin export. Therefore, the conclusion could be drawn that there is accumulation of 1st delivered insulin into cells and becomes unavailable for recycling, while the lately delivered insulin being close to cell membrane gets recycled through the cells. Therefore, when cells are loaded due to first delivery (as in N-GET/F-GET/No & N-GET/F-GET/T-GET), this preloading of cells leads to greater export and insulin recycling than when the cells receive no delivery. Interestingly, only F-GET exhibited this phenomenon of greater transport and cellular accumulation under multiple transfections, on the contrary the transport and internalisation of Ins-F was not significantly altered using multiple delivery (Appendix Figure 10.5), thus indicating that GET-peptide induced

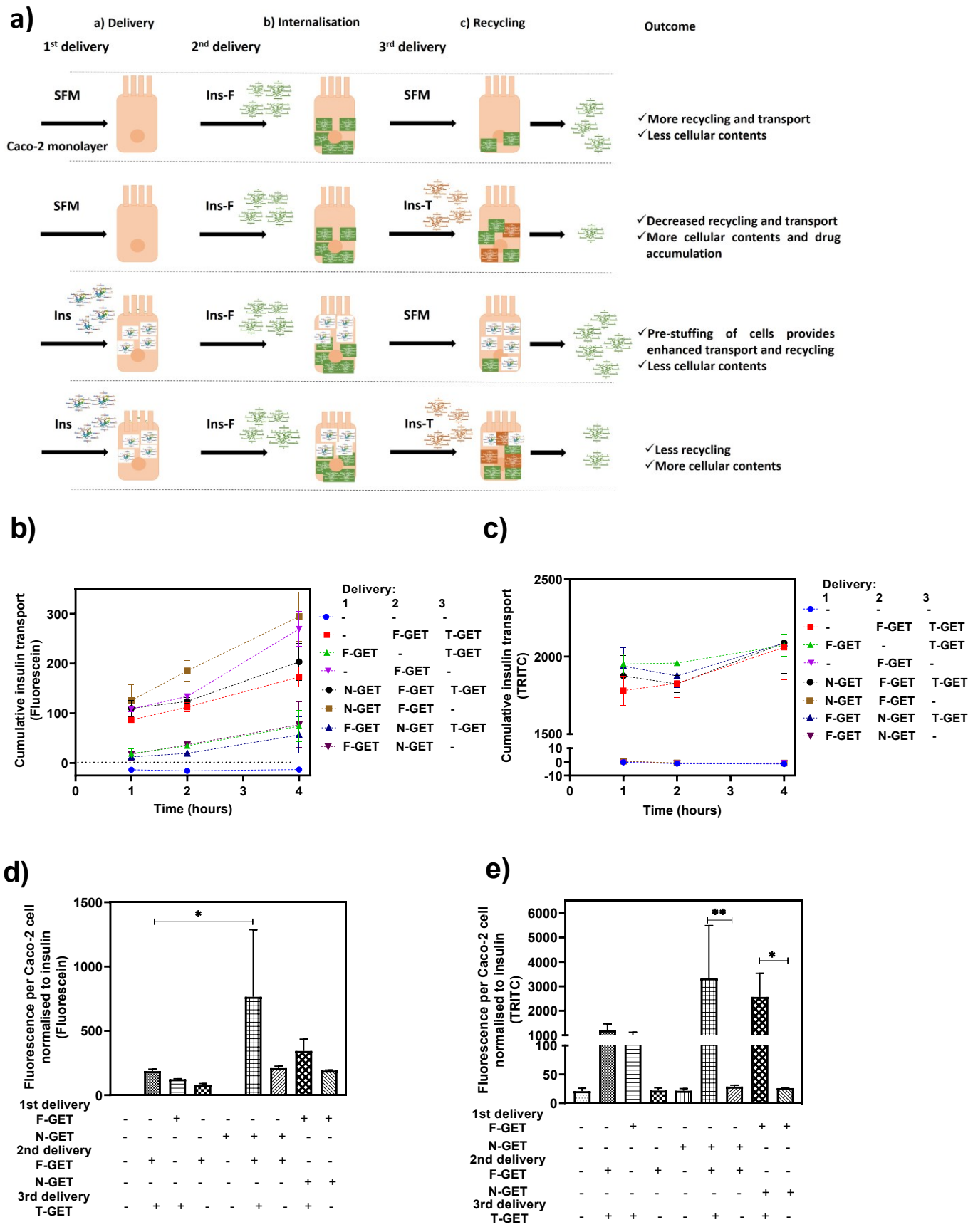

Figure 3. 12 a) A schematic for insulin recycling using three consecutive delivery i.e. two serial deliveries with non-labelled (N) and NHS-Fluorescein-labelled insulin (F),

respectively each for two hr, followed by analysis of post-incubation release in Ins-T or T. The graphs show cumulative transport of F-GET by, b) Fluorescein channel, and c) TRITC channel. The results indicated that cells with no first delivery (SFM) showed greater release than the cells getting first delivery with any type of insulin (N or F), additionally the later delivered insulin comes out first. Flow cytometry studies showing cellular accumulation following serial drug delivery d) Fluorescein channel and e) TRITC channel. The results revealed that insulin gets accumulated inside cells when receiving more than (>1) insulin delivery. All values are presented as mean ± S.D, n=5, * = *p-value* <0.05, **= *p-value* <0.005, ***=*p-value* <0.0005, ****= *p-value* <0.0001, and *ns*= not significant. One-way and Two-way ANOVA with Tukey's test.

enhanced recycling, transport, delivery, and internalisation of insulin.

Another interesting observation was that the release under the specific condition of no delivery (SFM) was greater compared to when cells were loaded with more insulin (3rd insulin delivery), showing that more input of insulin tends to hinder the output/recycling of insulin. F-GET/N-GET/T-GET had higher cellular uptake and internalisation then F-GET/N-GET/No, here again 3rd delivery led to higher cellular contents of insulin. Moreover, multiple delivery of NCs tends to inhibit insulin recycling, where greater input of insulin provided lesser output/export of insulin, resulting in intracellular accumulation of insulin and these results are consistent with those obtained with multiple (two) deliveries of NCs.

There have been reports in literature where different studies have employed various strategies to enhance the transduction/ transfection efficiency of carrier molecules together with the cargo of interest. The concept of multiple transfection protocol for achieving high gene transfer has been reported in earlier studies [174]. Multifection (multiple transfection) along with applied magnetic field (magneto-multi-fection) has been reported as a strategy for improving transfection efficiency of cargo molecules [175]. Multiple glycerol shock have been used as a strategy to improve the transfection of calcium phosphate across non-synchronised CHO DG44 cells. Where exposure to additional multiple osmotic shocks resulted in an increased expression of reported protein in cells which were not previously transfected with the initial treatment of cells [176].

3.3.9.3. Insulin recycling assay with alternative phases of On and Off delivery

The experiment was designed to assess effect of continuous and alternative On/Off delivery on the release of NCs from Caco-2 monolayers. The results suggested that with continuous delivery for 8 hr (On), more insulin comes out as compared to 1hr or 2hr or 4hr On/Off delivery, a schematic diagram is given in Figure 3.13a. Interestingly, with continuous 8hr delivery, the cumulative insulin release was two-fold greater than the alternative 4hr On/Off delivery, where the cells were incubated with NCs for a total duration of 4hr (Figure 3.13b). The order for cumulative insulin release was as follows; Continuous delivery > 2hr On/Off delivery > 1hr On/Off delivery > 4hr On/Off delivery. Although for all On/Off delivery samples, the total exposure time for NCs was collectively four hr, however cumulative transport for 4hr On/Off was 50% less than for continuous 8 hr, which was lesser compared to cumulative transport at 1 and 2 hr On/Off. This discrepancy in cumulative transport between different hours could be due to time independent effect of NCs exposure time to cell monolayers. Thus, showing that alternative phases of delivery have variable effect on insulin transport, and that continuous exposure drives greater insulin exocytosis where more cellular uptake leads to greater recycling. Flow cytometry results revealed more cellular uptake of NCs during continuous delivery, compared to cells receiving alternative On/Off delivery (Figure 3.13c). Here, again approximately two-fold greater cellular internalisation was observed for Caco-2 cells incubated with NCs for continuous 8hr compared to those receiving alternative 2- and 1- hr On/Off delivery.

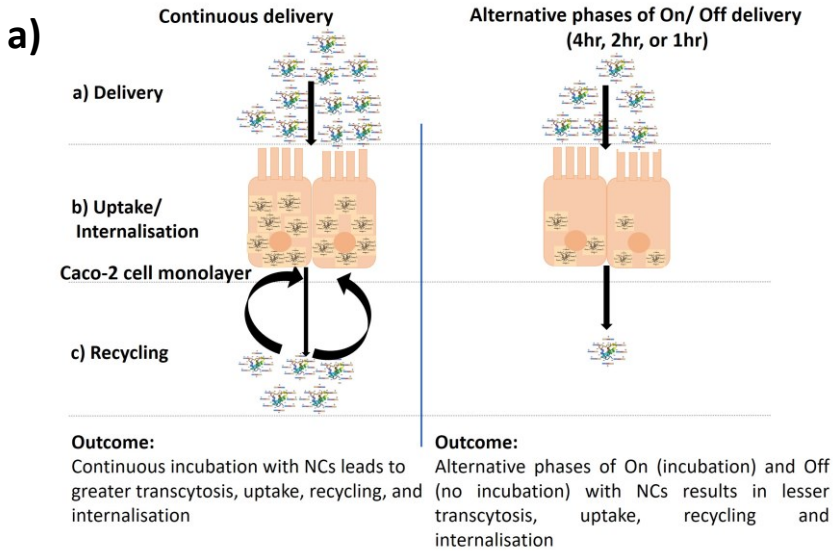

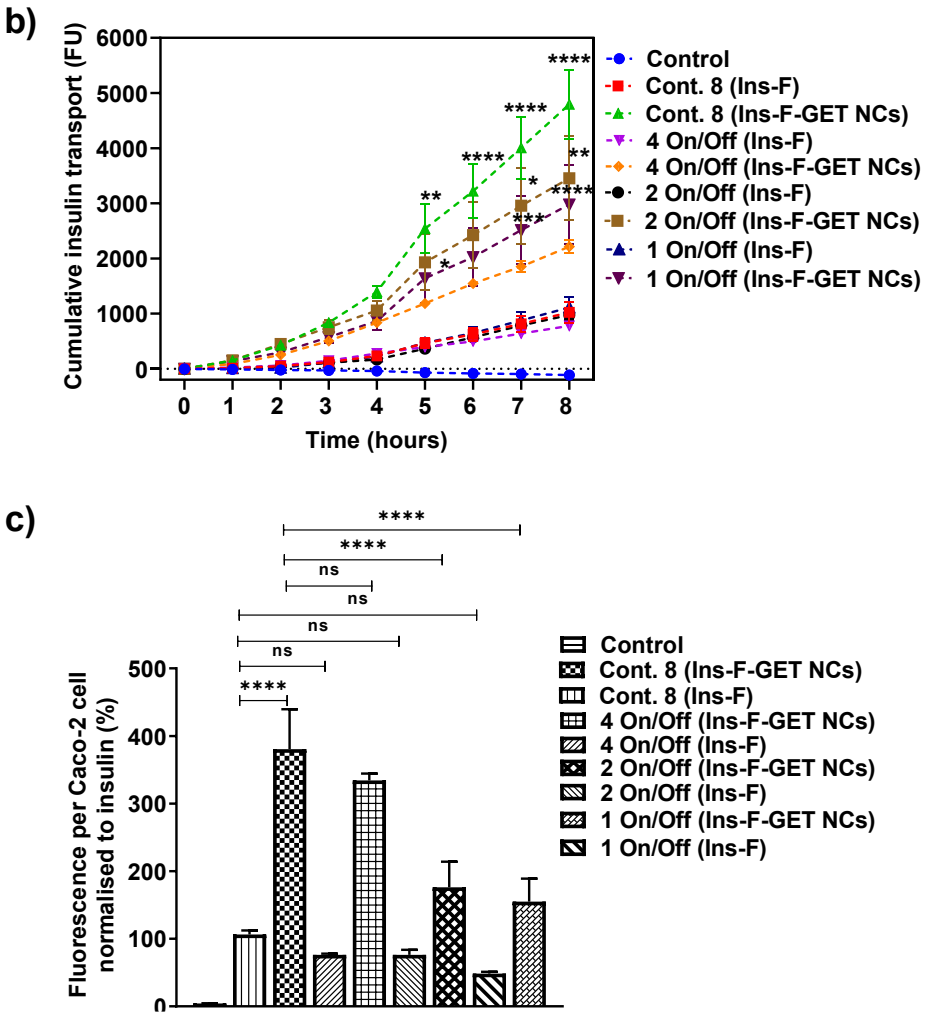

Figure 3. 13 A schematic of continuous and alternative phases of delivery and no delivery of Ins-F and Ins-F-GET NCs to Caco-2 cells for 8 hr using Transwell® inserts under standard experimental conditions is shown, b) continuous delivery leads to greater transcytosis of Ins-GET NCs across the Caco-2 monolayer on Transwell® inserts into basolateral chamber compared to the alternative phases of On/Off delivery, and c) Flow cytometry results revealed greater uptake by Caco-2 cells receiving continuous insulin delivery, these results were statistically significant. All values are presented as mean ± S.D, n=3, * = *p-value* <0.05, **= *p-value* <0.005, ***=*p-value* <0.0005, ****= *p-value* <0.0001, and *ns*= not significant. One-way and Two-way ANOVA with Tukey's test.

3.3.10. Fluorescence quenching of Ins-F* and Ins-F using different GET-peptides

Quenching of fluorescence for proprietary Ins-F* and in-house labelled Ins-F was evaluated by complexing both insulins with different concentrations of GET-peptide and its derivates, as shown in Figure 3.14. Fluorescence quenching was observed for Ins-F* on increasing the GET-peptide concentration, where 1µM concentration caused a marked decrease in fluorescence values, whereas 4µM

concentration of GET-peptides (L-PLR, D-PLR, FLR, PLR-Chol, PLR-C12, Chol-PLR, C12-PLR, PR, & PL) caused fluorescence values to reduce to zero for Ins-F* i.e. statistically significant as compared to control (Ins-F* with no modification). Different GET-peptides (L-PLR, D-PLR, PR, PL, and FLR) caused significant fluorescence quenching of Ins-F* by forming NCs with insulin through electrostatic binding of two molecules. Even the hydrophobically modified (using cholesterol or lauric acid) GET-peptides (PLR-Chol, PLR-C12, Chol-PLR, C12-PLR) showed statistically significant reduction of fluorescence values due to fluorescence quenching (Figure 3.14c). Whereas, with individual molecules which constitute GET-peptide (P, L, R, and LR), there was less than 50% reduction of fluorescence as shown in Figure 3.14a.

The trend of fluorescence quenching for Ins-F was similar to Ins-F*, but the fluorescent signals were not affected as greatly for the Ins-F, although still detectable on increasing the peptide concentration in similar ratio (Figure 3.14b). Likewise, the hydrophobically modified GET-peptide had a significant effect on fluorescent values of Ins-F but much less compared to Ins-F* (Figure 3.14d). Different GET-peptides caused fluorescence quenching to different extents, which was in the following order for Ins-F* i.e. FLR> L-PLR> PR> PL> D-PLR, while for Ins-F the order was different as follows; L-PLR >PR > PL > D-PLR > FLR. These results showed that the individual components that constitute GET-peptide system have a lesser effect on fluorescence values (quenching) of Sigma-FITC-insulin, but the combination of these constituent peptides reduced the fluorescence signals to considerable extent where no fluorescent signals were detectable. This provides evidence that the combination of constituent peptides acts synergistically in quenching the FITC-fluorescence for Ins-F*. While for NHS-Fluorescein-labelled insulin (Ins-F), fluorescence signals were not quenched completely with still >80% fluorescent signals were still detectable. This difference in fluorescence quenching of Ins-F (NHS-Fluorescein) and Ins-F* (Sigma-FTIC insulin) is due to the fact that NHS-Fluorescein (NHS-ester derivative) has higher specificity towards primary amine present in the side chain of lysine residues in the presence of other nucleophiles, thus it forms stable amide bond linkages following labelling

compared to FITC. Whereas FITC is reactive towards different nucleophiles including amine and sulfhydryl groups present in protein molecules.

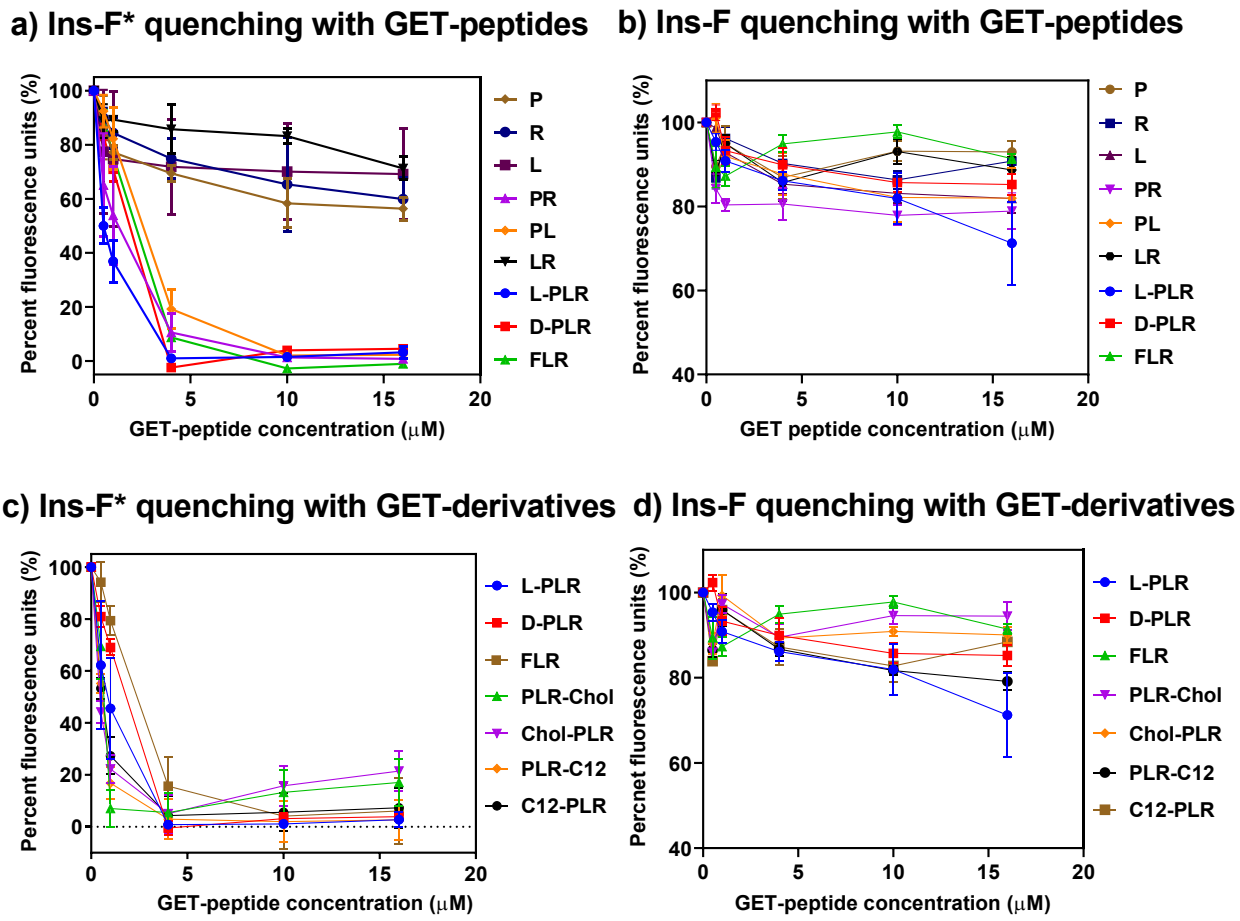

Figure 3. 14 a) Percent fluorescence quenching of Ins-F* with various GET-peptides at Ex= 420nm & Em= 520nm showing that L-PLR, D-PLR, FLR, PR, and PL peptides quench the fluorescence of Ins-F* completely (100%). Further Ins-F* was studied for its fluorescence quenching with individual constituents of GET, revealing that the individual constituents (P, R, L, PR & LR) cause less fluorescence quenching, while its the combination of these peptides that reduces the fluorescence values markedly (approaching zero), b) percent fluorescence quenching of Ins-F with GET and constituent peptides showing considerable fluorescent signals upon complexation, c) Ins-F* with various GET derivatives exhibited same pattern of 100% fluorescent quenching upon complexation, and d) Ins-F with different GET derivatives exhibited detectable fluorescent signals indicating lesser quenching. All values are presented as mean ± S.D, n=5, * = *p-value* <0.05, **= *p-value* <0.005, ***=*p-value* <0.0005, ****= *p-value* <0.0001, and *ns*= not significant. Two-way ANOVA with Tukey's test.

This assay was based on the principle of fluorescence quenching i.e. fluorescence of molecules gets quenched when several molecules are in close proximity either

due to self-association or oligomerisation [153]. This phenomenon of quenching may involve formation of dimers between proximate fluorophores, collisional quenching, energy transfer, transient excited state interaction, or may involve formation of non-fluorescent ground state species [154]. The FITC-fluorescence is slightly sensitive to the polarity of its environment, therefore it can be studied in solution. Additionally, the fluorescence of FITC gets quenched when there are several molecules in close proximity to FITC, therefore differences in fluorescence intensity between the untreated peptide and the proteolytic enzyme treated peptide gives a sign whether or not the peptide is complexed in the solution. Quenching of fibrinogen fluorescence was observed due to binding of multiple FITC-moieties to fibrinogen and their close proximity to each other. Additionally, greater quenching resulted due to thrombin induced polymerisation of FITC-fibrinogen, possibly due to greater interaction of neighbouring molecules in protofibrils aggregates. This thrombin based quenching was concentration dependent both at low and high ionic strength [177]. Quenching and dequenching based assay has also been used for studying RNA molecular interactions both *in-vitro* and *in-vivo*. Herein, FITC-labelled ribonucleotide was incorporated into RNA substrate, where the intramolecular quenching reduced the fluorescence quantum yield of intact RNA due to self-quenching phenomenon. These results indicated that fluorescence intensity of fluorophores is affected by adjacent molecules and interaction between identical fluorophores (self-quenching) [154]. Similarly, fluorescence intensity values for 3-fluorescein-labeled substrates were quenched on binding either to a hairpin ribozyme or its derived substrate binding strand. Herein, fluorescence quenching was used to determine cleavages, rate constant of substrate binding, and substrate dissociation. This study provided practical application of fluorescence quenching for various useful applications and thus can be regarded as useful *in-vitro* tool for various analysis based on fluorescence [178].

3.3.11. Fluorescence dequenching of Sigma-FITC-insulin with different proteases

To recover the fluorescence of Ins-F*, different proteolytic enzymes were used (Prot. K, Pepsin and Trypsin), as shown in Figure 3.15a. These enzymes were used in various working concentrations and different enzymes required different

amounts of time based on kinetics of reaction for recovering 100% fluorescence. This assay was based on the principle of fluorescence quenching resulting from either self-association or oligomerisation [153]. As a control, Ins-F* was treated with Prot. K (Figure 3.15b), trypsin (Figure 3.15c), and pepsin (3.15d) in same different concentrations (0.2 µg/µl, 0.1 µg/µl, and 0.05 µg/µl for Prot. K, 20 µg/µl, 10 µg/µl and 5 µg/µl for trypsin and 1 µg/µl for pepsin) as used for Ins-F*-GET NCs. The results showed that treating Ins-F* with these enzymes caused further increase in fluorescent intensity values, as these enzymes cleaved the insulin and separated the FITC molecules, resulting in an increase in fluorescent signals. As NHS-Fluorescein didn't exhibited quenching phenomenon where fluorescent signals were only marginally lowered on complexation with GET-peptide, therefore it wasn't tested for dequenching, rather free Ins-F* (fully fluorescent) was used as a control for comparison and was exposed to same enzymes.

Results showed that Prot. K caused rapid recovery of fluorescence of Ins-F*-GET NCs (dequenching of fluorescence), where within 40 min the fluorescence values were recovered to control values (non-complexed insulin) as shown in Figure 3.15e. With trypsin (Figure 3.15f), there was slower recovery of fluorescence as kinetics of reaction was slow, where in 180 min the values were recovered to the level of control (free insulin). With pepsin (in 10mM HCl) there was only 8-10-fold recovery of fluorescence over the entire time course (180 min) as shown in Figure 3.15g. These results suggested that Prot. K and trypsin can efficiently cleave the insulin--GET complex association to recover the fluorescence completely. Additionally, we observed that this dequenching phenomenon is time dependent not concentration dependent, while with pepsin the kinetics of reaction was slowest and only fraction of fluorescence could be recovered.

Many studies have employed the concept of dequenching as one of the convenient fluorescent based assays for various purposes. Dilution or segregation of probes results in "relief of quenching" also referred to as "dequenching", thus supplying a sensitive means of monitoring the process. One of the simplest ways to produce dequenching is to increase distance between fluorophores, or through biochemical reaction employing use of different enzyme systems. Fluorescence-based assay has been used for monitoring the activity of therapeutic enzymes *in-vivo* in real time i

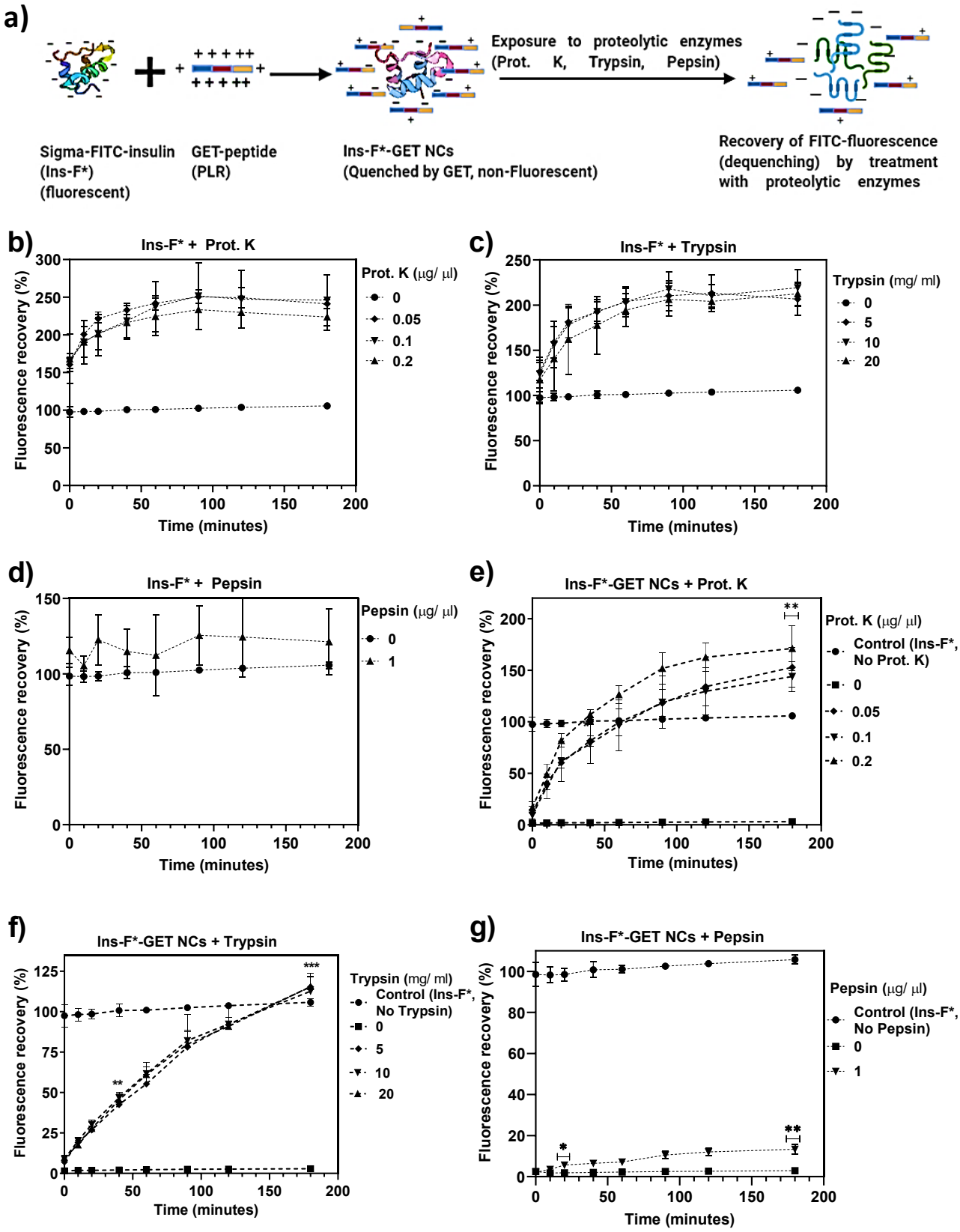

Figure 3. 15 a) Schematic illustration of dequenching of Sigma-FITC-insulin fluorescence using different proteolytic enzymes (Prot. K, trypsin, and pepsin); Ins-F* treatment with a) Prot. K, b) Trypsin, and c) Pepsin, all showing increase in fluorescent signal due to action of enzymes. Ins-F*-GET NCs treatment with d) Prot.

K complete fluorescence was recovered within 40 min, e) Trypsin dequenched the fluorescence completely in 180 min, and f) Pepsin recovered just fraction of fluorescence in 180 min, these all results were statistically significant in comparison to control. All values are presented as mean ± S.D, n=5, * = *p-value* <0.05, **= *p-value* <0.005, ***=*p-value* <0.0005, ****= *p-value* <0.0001, and *ns*= not significant. One-way and Two-way ANOVA with Tukey's test.

GIT. *In-vitro* incubation of intact peptide (Dabycl) with proline specific endopeptidases (PEPs) resulted in complete cleavage with 8-fold rise in fluorescence intensity. Thus, it can be concluded that fluorescence-based assays can be employed as better predictors and indicators of activity and stability of molecules [179]. Similarly, fluorescent ribonucleotide displayed fluorescence quenching following *in-vitro* transcription into RNA substrate, but the use of RNase A and RNase T1 showed considerable rates of dequenching and thus provided a convenient, sensitive, and quantitative assay for RNA degradation. This dequenching was concentration dependent and was inhibited by RNasin (ribonuclease inhibitor) [154]. Quenching and dequenching assay has been used to study fibrinogen polymerisation and fibrinolysis. Fluorescence quenching of fibrinogen was reduced by either addition of unlabelled fibrinogen or Gly-Pro-Arg-Pro to the reaction or through use of plasmin which resulted in cleavage of fibrinogen thus releasing FITC-fragments, showing that fluorescence quenching is a reversible phenomenon [177].

3.4. Conclusion

To conclude, GET-peptide displayed similar or even better cell penetration ability compared to conventional CPPs such as 8R, to enter the Caco-2 cell monolayers at low concentrations, thus improving cellular permeation and internalisation of insulin. This novel multidomain peptide sequence enhanced cumulative insulin transport by 8.7-fold, leading to improved transcytosis compared to non-modified insulin. Moreover, P_{app} values for GET-modified-insulin was significantly greater than for free insulin. GET-peptide and its derivatives all enhanced the transepithelial delivery of insulin to a considerable extent, leading to significantly improved insulin transport, transcytosis and intracellular uptake. GET-peptide had a transient and reversible effect on membrane integrity, as indicated by respective

TEER values and dextran assays. Dextran assay revealed that lowering of TEER by GET caused an enhancement in flux of low MW Dex (4.4KDa), which suggests that it might be problematic *in-vivo* due to its potential for cellular toxicity due to impaired integrity or membrane barrier which might led to absorption of pathogens such bacteria, viruses and lipopolysaccharides. There was significant effect of GET system on cellular viability of Caco-2 monolayers, as determined through AlamarBlue assay, but still >80% viability was observed. DMEM, serum free and phenol red free was found to be ideal medium for GET-peptide mediated insulin delivery onto Caco-2 monolayers, as it closely mimics *in-vivo* condition. Incubation with freeze dried NCs further enhanced the transfection efficiency, and thus stabilised these preparations.

Among studied cell secretion regulators only ATP, NAS and high dose of YB caused an increase in GET-peptide mediated insulin release, leading to reduced cellular contents of insulin. The phenomenon of insulin recycling showed an interesting effect where the use of multifection caused a decrease in insulin secretion or output, thus leading to cellular accumulation of NCs. These accumulated NCs may serve as an insulin reservoir which would provide post-incubation insulin release for longer time period, and thus giving insight for controlled release. GET-peptide formed NCs with insulin by coupling through electrostatic interactions, with binding leading to fluorescence quenching (reducing fluorescent signals) of Ins-F*, a phenomenon not seen with Ins-F. This difference in fluorescent behaviour of these two labelled insulin is attributed to fact that Ins-F being labelled with NHS-ester derivative of fluorescein has greater affinity and specificity towards primary amines in presence of other nucleophiles and moreover it forms stable amide bonds with proteins/ antibodies upon labelling in comparison to FITC which lack this specificity (binding to both primary and secondary amines) and thus forms unstable linkages. This quenching of fluorescence was reversible, and the fluorescence intensity values were recovered to normal values using different proteolytic enzymes. This quenching and dequenching of fluorescence led to the development of several assays for determining the stability of GET system and GET-peptide based NCs, and to demonstrate whether GET is still bound to insulin after being translocated inside cells. This all emphasises the importance of potential of GET system to enhance

transepithelial insulin delivery in order to promote the intracellular uptake of insulin *in-vitro,* and to further exploit stability and functional activity of NCs. Moreover, impaired barrier caused by GET should be kept in consideration and further studied *in-vivo* for indirect toxicity related to it.

Chapter 4: Characterisation, stability and functional activity assays for NCs

4.1. Introduction

To-date hundreds of CPPs have been known as potential delivery agents for bio-macromolecules. It has been reported that slight deviation could take place in CPP-mediated drug delivery due to differences in cell line or tissues for e.g. protein content or lipid composition of cell membrane, and rate of endocytosis [180]. For successful development of CPP based protein and peptide delivery systems, its necessary to enhance the efficacy, safety, and bioavailability together with the minimisation of toxic effects of CPP. As the plasma membrane is composed of an array of negatively charged moieties, therefore, to drive them inside cells, CPPs exploit their basic residues. The first logical interaction between negatively charged cell membrane and positively charged CPPs is electrostatic in nature, where lipids and polysaccharides of membrane will bind oppositely charged peptides before they find their way to internalisation in cells. Polyarginine (Rx) are regarded as efficient CPPs owing to presence of high degree of positive charges as imparted by guanidinium side-chains which facilitate its binding with negatively charged proteoglycan constituents embedded in cell membrane such as GAGs and sialic acid. The guanidinium side-chains in arginine forms bidentate H-bonds with negatively charged sulphate, phosphate and carboxylate groups on the surface of cell, while in case of lysine the ammonium cations can donate only one H-bond. All this results in the scavenging of counter anions which helps to attenuate the polarity of guanidinium group by forming a polar ion-pair complex which has ability to penetrate and diffuse into the biological membrane [112].

When using oligo/polymers, scavenging of counterions helps to attenuate charge repulsion among adjacent guanidinium entities, on the other hand for nearby ammonium ions reduction of pKa values provides attenuation of charge repulsion, thus resulting in more thermodynamically stable complexes between polyarginines compared to mono-arginine [181]. Role of positive charges in promoting uptake of macromolecules was demonstrated a long time ago by Rysen and Hancock, they

showed that uptake of albumin is improved considerably by tumour cells by mixing protein with high MW poly-L-lysine (PLL) [182].

This chapter aims to further explore insulin-GET peptide NCs, characterise them using different analytical and instrumental techniques, assessing stability of these NCs, and also to establish the functional activity of GET-modified insulin to prove that GET-peptide doesn't affect/alter the functional and pharmacological activity of native insulin. The difference in fluorescent behaviour of two insulins was further exploited to set up different assays based on quenching and dequenching of fluorescence intensities to establish the stability of both the GET system and the GET based NCs. This chapter will focus on following aspects of GET-system and GET based intracellular delivery as described below;

1. Characterising the Ins-F-GET NCs using different instrumental techniques.
2. Assessing the stability of GET-peptide system using Sigma-FITC insulin.
3. Determining the stability of GET-based insulin NCs using Sigma-FITC insulin.
4. Confocal and time-lapse microscopic imaging for determining localisation, intracellular distribution and cytotoxicity of Ins-F-GET NCs, respectively.
5. ImageStream analysis for quantifying the ratio of surface bond and internalised NCs using NHS-fluorescein insulin.
6. Testing functional activity of insulin-GET NCs using insulin-reporter iLite cells.

4.2. Experimental design

The focus of this chapter would be to characterise insulin and GET-based insulin NCs for their size and surface morphology, stability, and functional activity and also to image relative uptake using different instrumental techniques. Reference to each performed assay and respective detailed procedures can be located by referring to respective Sections as stated below. DLS zeta sizer was employed to determine size and surface charge of free and complexed insulin (Section 2.19), additionally TEM microscopy was used to further confirm size of these NCs and to determine their surface morphology (Section 2.20). CLSM (Section 2.21) and imageStream (Section 2.22) analysis was performed to visualise uptake of free and complexed insulin, and to establish ratio of surface bound and internalised NCs, respectively. Cytotoxicity assay was also performed to locate the safe concentration of GET-peptide, which would not compromise cellular viability

(Section 2.23). Different iso-forms of GET-peptide (L- and D-PLR) were tested for their proteolytic stability to uncover the stability potential of this non-viral vector (Section 2.24) for drug delivery. In addition to this, stability of GET-modified insulin (Ins-F*) was also determined using different assay by exposing to different pH conditions in presence of proteolytic enzymes (Section 2.25.1 and 2.25.2), and using differently labelled insulins (Section 2.25.3), moreover the stability of cell internalised NCs was also determined post-transcytosis (Section 2.25.4). After establishing stability of GET-based NCs, next step was to evaluate the functional activity of these NCs. Specialised suspension cells (iLite cells) with reporter transgene were employed to uncover the functional activity of insulin following complexation with GET-peptide and to determine GET concentration which causes maximum functional activity by activating cellular mechanism in these cells (Section 2.26). This assay was replicated for NCs following post-transcytosis across Transwell® inserts cultured with Caco-2 monolayer to determine the functional capability post-transcytosis (Section 2.27).

4.3. Results and Discussion

4.3.1. Characterisation of GET-based insulin nanocomplexes

4.3.1.1. DLS measurements for size and charge of Ins-GET NCs

Following initial cell-based translocation and transcytosis experiments, the next step was to identify the particle charge and size of both insulin and insulin-GET NCs. Samples were prepared using non-labelled insulin, and the reaction was carried out in deionised water to obtain NCs. Under these conditions (Figure 4.1), Ins with no modification showed three different sized population in range of 2.5-5 nm, 90-120 nm, and 600-1000 nm as shown in size distribution by intensity graph, while for the same sample, graphs based on size distribution by number showed that majority of Ins particles were in size range of 2.5-5nm. In case of Ins-GET NCs, the size distribution by intensity graph showed two different sized population between 200-450 nm and 700-950 nm, while size distribution by number graph showed NCs mainly in size range of 200-450nm and very few in range of 700-950nm. The charge measured for Ins and Ins-GET NCs was -14mV and +27mV, respectively.

To further refine results of size distribution, the freshly prepared samples were spun at low speed (200 ×g for 5min), and then analysed as shown in Figure 4.2. The results showed that Ins particles displayed a wide size distribution having average

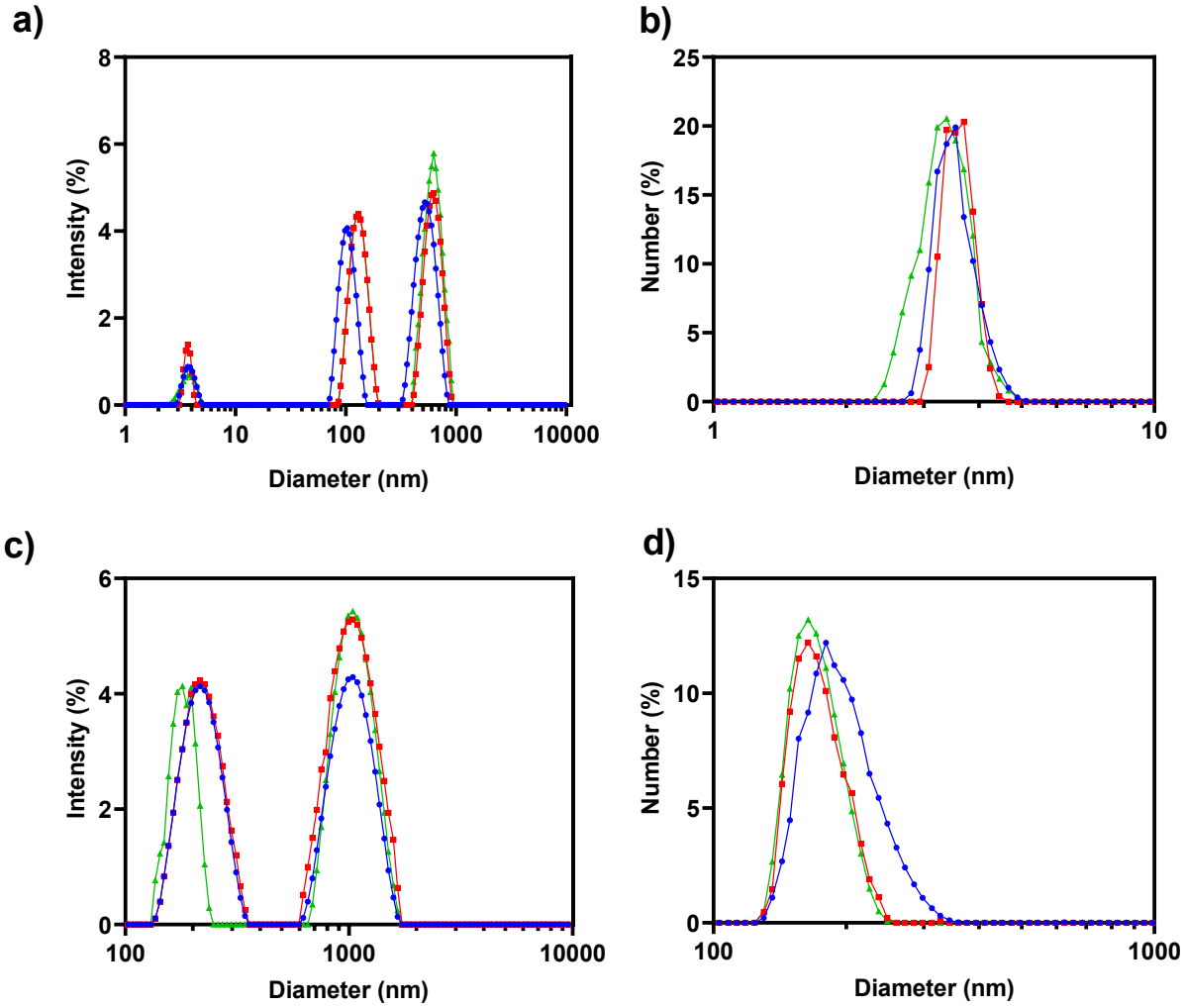

Figure 4. 1 Dynamic laser scattering measurement for size distribution of Ins (non-labelled) suspended in deionised water (pH 7) by a) intensity, b) number and Ins-GET NCs suspended in deionised water at neutral pH c) by intensity, and d) number. The results present a mean of 3 experiments and values are plotted as mean ± S.D.

diameter of 147nm as indicated by size distribution by intensity graph, and a surface potential of -14.1 mV as measured in dH_2O at neutral pH. For Ins-GET NCs, the average size distribution of NCs was 140nm as determined through intensity graphs, these NCs were highly positively charged having surface potential of +28.16mV. This change of particle charge from negatively charged insulin molecules to positively charged NCs shows that GET-peptide has bonded to insulin through electrostatic interaction, leading to formation of NCs with strong positive

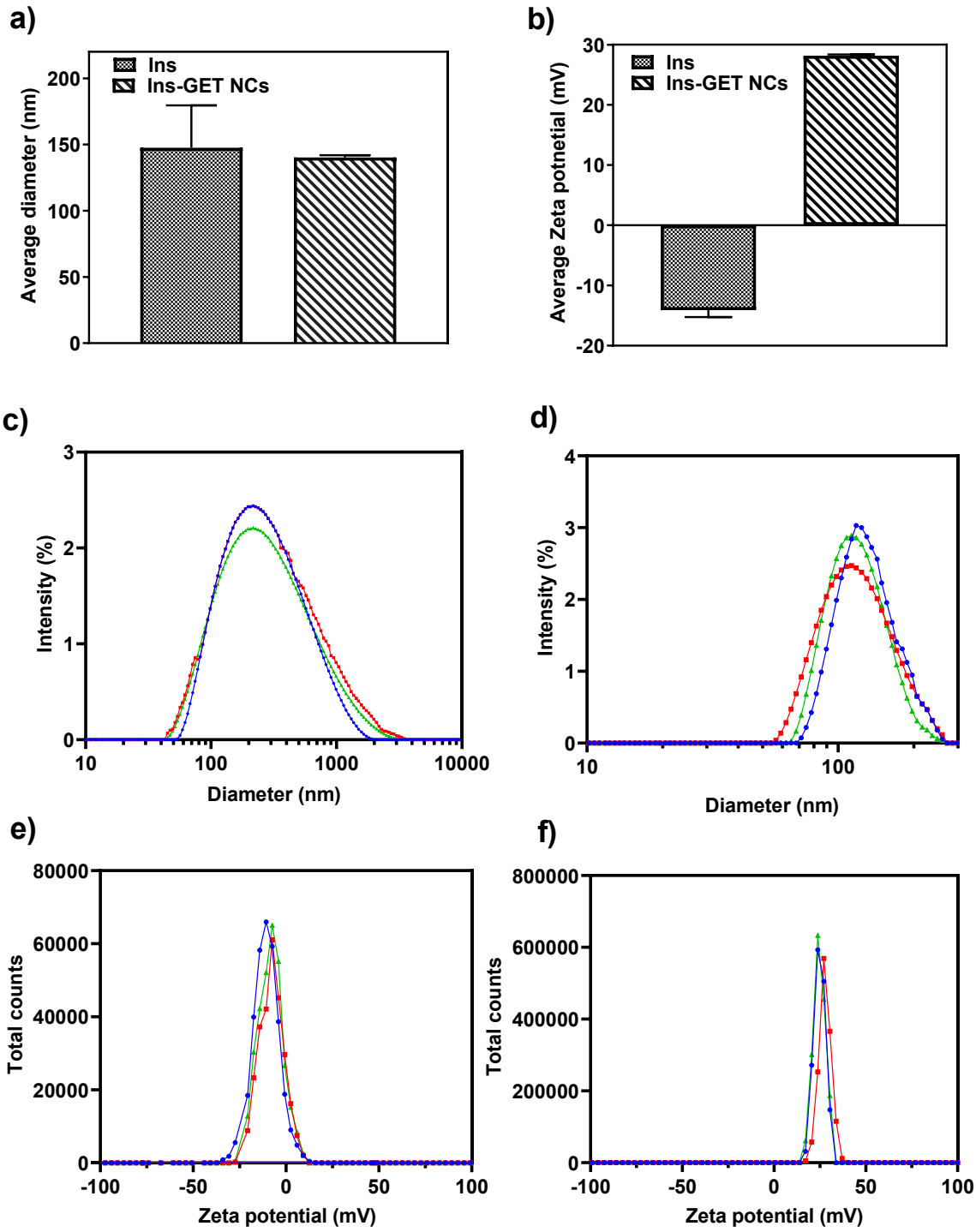

Figure 4. 2 Dyanmic laser scattering measurments of size distribution and surface charge of spun Ins and Ins-GET NCs suspended in deionised water at neutral pH. a) Comparative size distribution of Ins and Ins-GET NCs, b) Comparative surface charge of Ins and Ins-GET NCs, c) size distribution graph by intensity for Ins, d) size distribution graph for Ins-GET NCs, e) zeta potential graph for Ins, and f) Zeta potential graph for NCs. The results present mean of 3 measurments, and values are repesented as mean ± S.D.

charge. Shift of multiple peaks to single peak towards larger particle size (Figure 4.1), also confirmed the formation of NCs. These results indicated that positively charged GET-peptide can efficiently bind with negatively charged insulin through non-covalent/ electrostatic interactions thus forming NCs as depicted by charge reversal of insulin form negative to positive.

The average size of penetratin based-insulin carrier NCs [2:1 mix of insulin: penetratin to form polyelectrolyte complex (PEC)] was reported to be 148.3 nm. These CPP-rich NCs were highly positively charged displaying a surface charge potential of +20.9mV. These results indicated that CPP based NCs are strongly positively charged having size in nanometre range, which is in agreement with the results we obtained [144]. It has been reported that size of PEC depends on; carrier peptide, ratio of insulin to carrier-peptide/ CPP, and lastly the formulation pH. A group of researchers studied the effect of these variables i.e. pH and insulin-carrier peptide ratio (2:1, 4:1, 6:1, and 8:1) on the average size of NCs. Larger complexes were formed on increasing the carrier peptide-insulin molar ratio, additionally for each of these molar ratios there was a pH-dependent increase in complex sizes on increasing the pH from pH 5 to pH 7.4 [142].

The average size and surface potential of R8-insulin NCs, and hydrophobically modified-R8-insulin NCs both as enveloped in PEG-PGA coating and as non-enveloped complexes was determined. Results indicated that increasing molar ratio of R8: Insulin from 1:1 to 8:1 caused reversion of zeta potential values from -38mV to +0.1mV, while for non-coated C12-R8-insulin and Chol-R8-insulin NCs the values were reversed largely from -22mV to +10 and +20mV, respectively. For R8-insulin NCs, the particle size increased from 200nm to 2500nm on increasing molar ratio from 1:1 to 6:1, further increase to 8:1 resulted in reduction in particle size to 900nm [158].

4.3.1.2. Transmission electron microscopy (TEM)

TEM micrographs (Figure 4.3) were employed to confirm the size and morphology of Ins-F and Ins-F-GET NCs and were acquired using the FEI, TECNAI G2 12 Biotwin TEM instrument. TEM micrographs with no staining showed nanocomplexes in the size range of 5-20nm for Ins-F, and 50-90nm for Ins-F-GET NCs with an aggregated

network structure morphology. The protocol was repeated by staining of NCs loaded carbon coated copper grids with heavy metal stain. The acquired micrographs confirmed the size distribution of Ins-F and Ins-F-GET NCs, where each sample had different sized particles, similar to results obtained by DLS measurement. For Ins-F, the average size of particles was in two different ranges i.e. 3-25 nm, and for larger aggregates around 80-250nm, which was in agreement with Zetasizer results. For Ins-F-GET NCs, the average size of particles was larger compared to non-modified insulin, where the average diameter of NCs ranged between 100-350nm and 500-700nm for bigger aggregates. This shifting of size from small sized particles to larger ones and absence of smaller individual molecules indicated formation of GET-based NCs. It is evident from the images that morphology of Ins-F was in the form of small individual particles, in addition to this less developed network structures were also observed, due to the inherent property of insulin to form dimers and hexamers. The aggregated structure in TEM images for Ins-F revealed that insulin exists as a complex mixture of monomer, dimer, hexamer and larger aggregates in solution. On the other hand, for Ins-F-GET NCs the morphology of most NCs was denser with a large average diameter, additionally fewer looser network structures and small complexes were also observed. These results indicated that formation of PEC between insulin and GET-peptide leads to formation of large molecular complexes, and the absence of smaller molecules (2-5nm as observed in TEM image of Ins-F) further confirmed that both molecules have complexed together via electrostatic interaction.

Numerous studies have reported the property of insulin to self-aggregate in the form of dimers, hexamers and even larger aggregated denser structures. Insulin also forms fibrillar structures due to its inherent property of undergoing oligomerisation and aggregation. Insulin monomers misfold and tend to assemble into small MW oligomers such as dimers, trimers, and other small MW oligomers; when undergoing fibrillation, these low order oligomers aggregate to form bigger oligomers which further grow into linear fibrils [183, 184]. The results we found are in agreement with previously reported studies, where complexation of insulin with CPPs resulted in formation of complex aggregated structures. The morphology of penetratin- insulin NCs formulated in molar ratio of 4:1 at pH 5 and pH 7.4 was

imaged using TEM, where at pH 5 larger aggregated structures were observed which were denser compared to aggregates at pH 7.4 (looser network structures). Additionally, greater number of smaller complexes were observed at pH 5 [142]. Another study reported spherical non-aggregated morphology for CPP-insulin NCs at molar ratio of 2:1, with an average size of 148nm [144]. Further studies on CPP-insulin NCs for enhanced intestinal delivery of insulin have shown similar results, where TEM images revealed spherical structure for NCs, which were distributed evenly as separate entities [128].

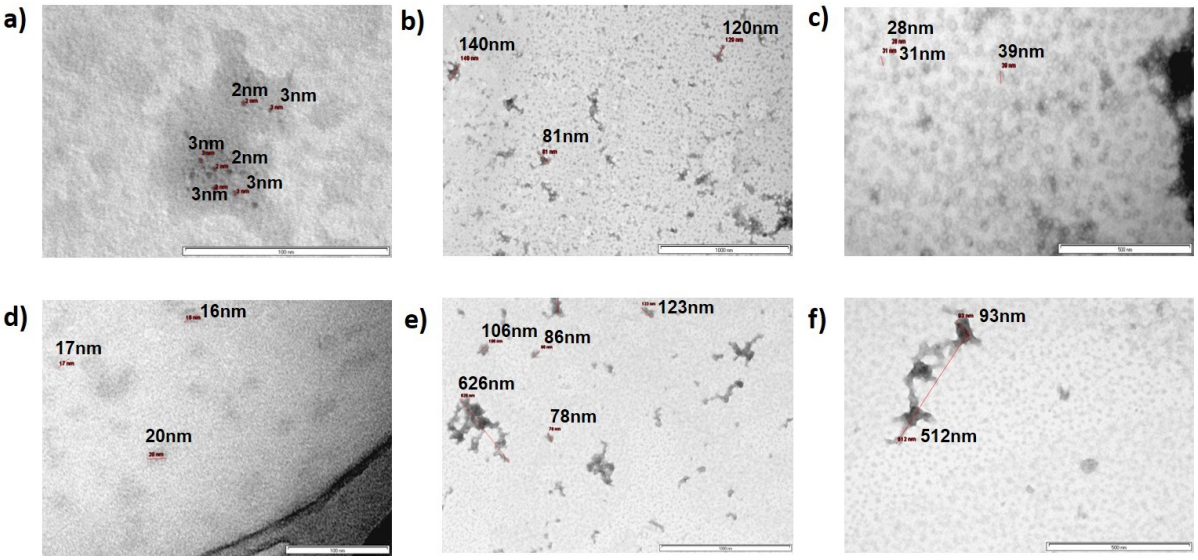

Figure 4. 3 Transmission electron micrographs of NHS-Fluorescein-insulin (Ins-F and Ins-F-GET NCs) at different magnifications. TEM images for Ins-F a) no stain at 160k magnification, and with heavy metal stain (HMS) at b) 20K, and c) at 43K magnification. TEM images acquired for Ins-GET NCs; d) no stain at 160k, and using HMS stain e) at 20K, and f) at 43K magnification. All measurements were taken in triplicate, white line represents scale bar of 100 (image 4.3a, and d), 500 (image 4.3c, and f) and 1000nm (image 4.3 b and e).

4.3.2. Imaging techniques for determination of intracellular localisation, its quantification, and cytotoxicity assessment

4.3.2.1. Confocal microscopy

Figure 4.4a, b, c and d show confocal micrographs of Caco-2 layers post-incubation with Ins-F and Ins-F-GET NCs in different cross-section views. More specifically, these figures depict cells labelled with cell cytoplasm tracker Red (Alexa-Fluor 647 Phalloidin), a non-specific whole cell cytoplasm label. The cellular nucleus was stained using Hoechst reagent in Blue, visible as closely packed cells covering the

whole image area, whereas Ins-F and NCs of Ins-F with GET in Green can be seen distributed throughout. Confocal images clearly showed the difference in relative uptake of insulin with and without GET-peptide, where GET-peptide greatly enhanced the cellular uptake and internalisation of insulin. Ins-F was not uptaken

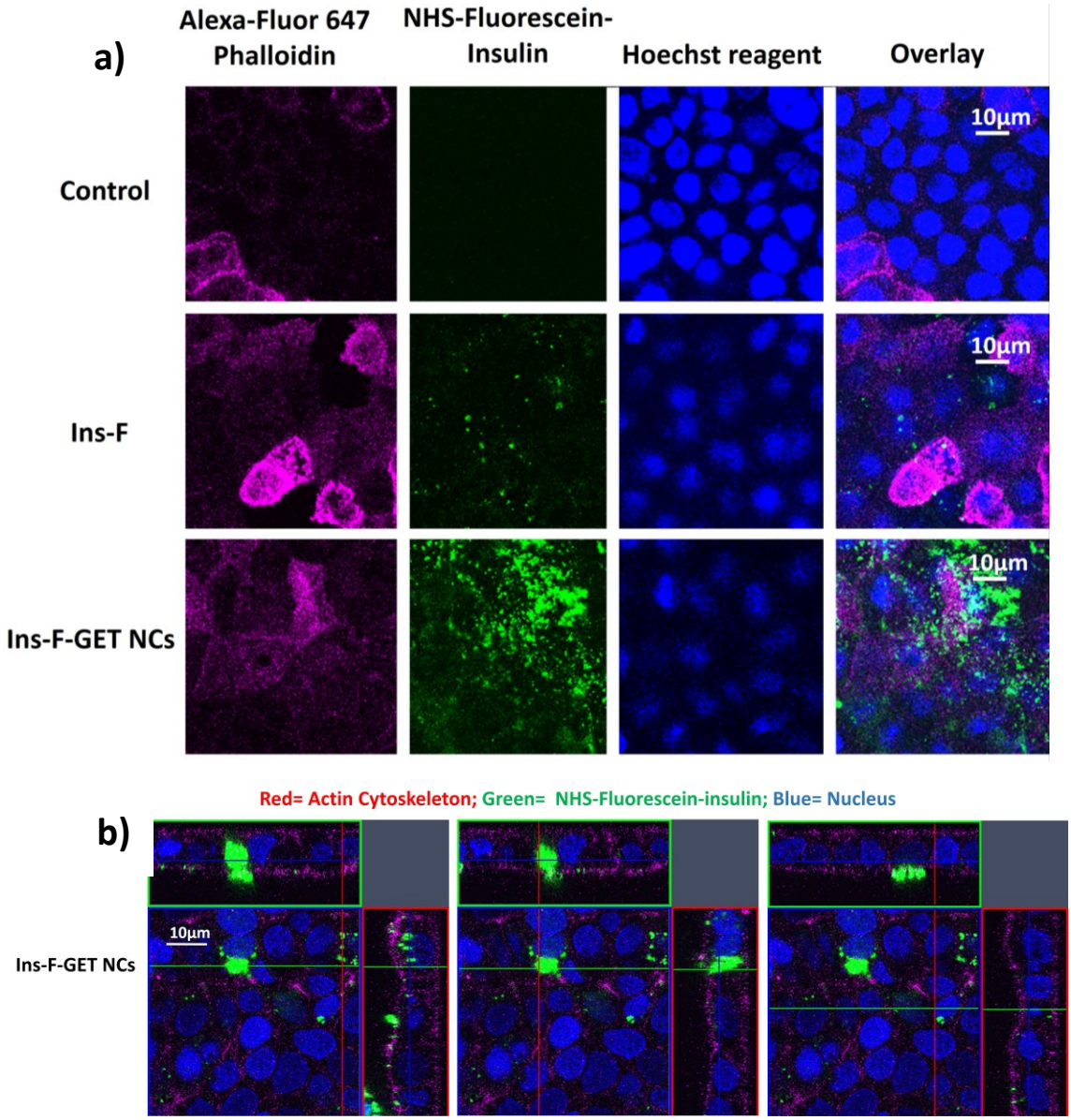

Figure 4. 4 Confocal laser scanning microscopy images for distribution of NHS-Fluorescein-insulin (Ins- F and Ins-F-GET NCs) on Caco-2 monolayer incubated for 5hr. Red, actin cytoskeleton; green, Ins-F or Ins-F-GET NCs; blue, nucleus. a) CLSM images of Caco-2 cells transfected with Ins-F and Ins-F-GET NCs upon staining with Alexa-fluoro-647 Phalloidin, and Hoechst reagent. It can be clearly seen from images that insulin cellular internalisation is significantly enhanced in the presence of GET peptide, leading to greater cellular accumulation. b) cross-section images showing NCs being widely distributed throughout the cytoplasm with some NCs adhered to the cellular surface as well. The scale bar presents 10 µm.

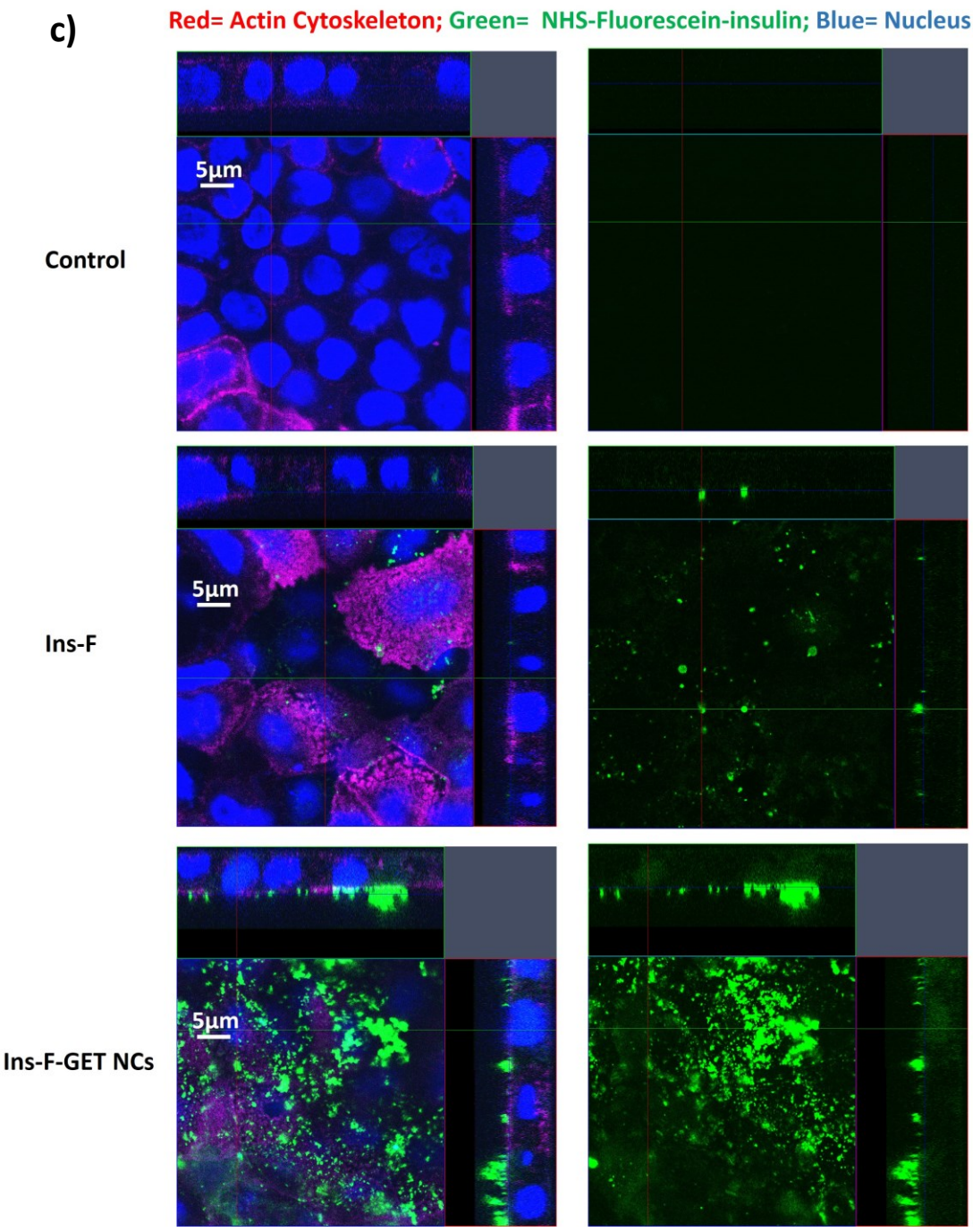

Figure 4.4c Confocal laser scanning microscopy images (y-z, x-y, and x-z sections, cross-sectional view) of Caco-2 cell membranes upon staining with different dyes. Ins-F-GET NCs are efficiently translocated across the Caco-2 cell monolayers compared to Ins-F alone, as evident by respective relative fluorescence of two molecules. Scale bar represents 5µm.

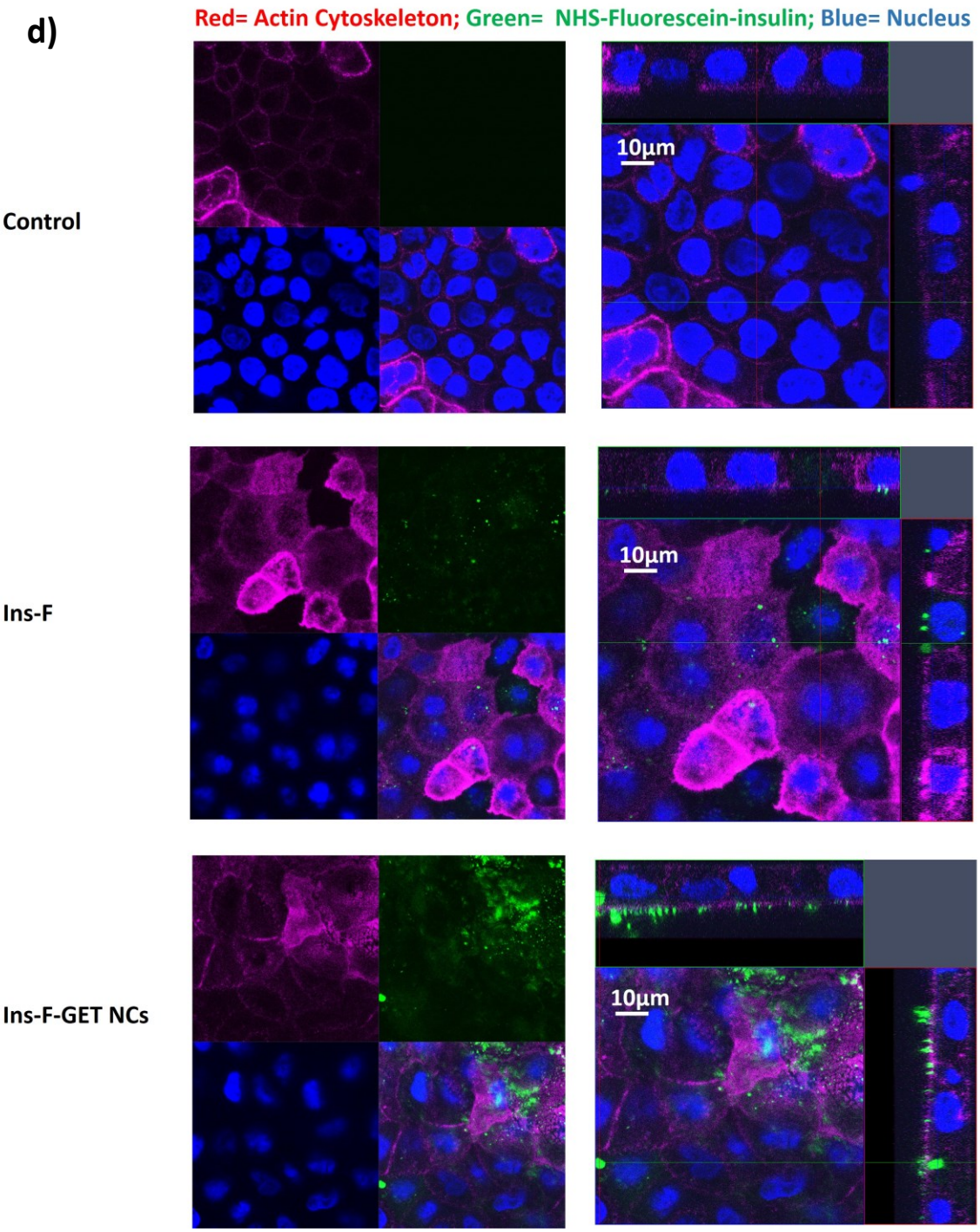

Figure 4.4d Confocal laser scanning microscopy images (y-z, x-y, and x-z sections, individual view and cross-sectional view) of Caco-2 cell monolayer incubated with Ins-F and Ins-F-GET NCs, following staining with Alexa-fluoro-647 and Hoechst reagent. Ins-F-GET NCs are efficiently translocated and internalised by Caco-2 cells leading to greater cellular accumulation compared to Ins-F with no modification, as evident by respective relative fluorescence of two molecules. Scale bar represents 10µm.

effectively, resulting in lower cellular accumulation, as indicated by less fluorescent signals seen in these acquired confocal images. Transverse, cross-section and split view showed less cellular permeation and accumulation for Ins-F compared to Ins-F-GET NCs. Figure 4.4b, cross-section image of samples treated with Ins-F-GET NCs showing intracellular distribution of NCs both in the cytoplasm of adjacent cells and on cellular surface as well. The samples treated with Ins-F-GET NCs displayed significantly more cellular uptake compared to free insulin, and these NCs were seen widely distributed throughout cell monolayers with localisation within different regions of cells including nuclear and cellular membranes. All possible views i.e. cross-section, transverse, and split view showed greater cellular absorption and internalisation for GET-based insulin NCs.

CPP-based insulin delivery studies have reported similar results, where CLSM images have shown stronger and greater fluorescent signals for samples receiving CPP-insulin NCs compared to insulin alone. The use of penetratin as a CPP for promoting insulin permeation through intestinal cells, has shown that PEN-insulin NCs exhibited much stronger fluorescent signals compared to free-insulin, where PEN-insulin NCs were seen diffused throughout the cytoplasm [128]. Another study demonstrated stability of CPP-insulin NCs, where CLSM images confirmed that most of the insulin was still associated with the CPP, as indicated by large areas of green (FITC-insulin) and red (TRITC-labelled penetratin) signals, which provided evidence that these NCs possessed the ability to efficiently permeate and get internalised by epithelium [144]. CLSM images have clearly indicated potential of IMT-P8 (novel CPP) in enhancing the cellular uptake and internalisation of model proteins (GFP and proapoptotic peptide (KLA)) compared to Tat -peptide. But in the absence of either type of CPP very poor fluorescent signals were observed for GFP [185]. Tat-CPP promoted cellular internalisation and transepithelial transport of enhanced Green fluorescent protein (eGFP) into cells extracted from midgut *Bombyx mori*. CLSM revealed that in absence of Tat-peptide, fluorescent signals were weak, while incubation with Tat-eGFP provided significantly enhanced fluorescent signal which was progressively increased with time and was seen uniformly diffused throughout the cytoplasm [186].

4.3.2.2. ImageStream analysis OR Dual imaging flow cytometry

ImageStream$^{®X}$ Mk-II Flow Cytometer was used for this assay, as this advanced instrument combines the features of flow cytometry (detailed imaging) with the microscopy (functional vision), therefore this technique provides the advantages of high sensitivity, speed, and phenotyping. This unique technique supplies a wide range of functional applications in the field of science which could not be attained when using either of the techniques alone. This instrument is considered ideal for studies related to determination of cellular internalisation, co-localisation, uptake, and ratio of internalised drug to total cell bound.

The relative cellular uptake and internalisation of Ins-F and Ins-F-GET NCs, and the ratio of internalised to surface bound Ins-F-GET NCs is shown in Figure 4.5 (acquired through IDEAS software). Figure 4.5a and 4.5b display internalisation of insulin in presence and absence of GET-peptide at two different time points i.e. 1 hr and 24 hr. These values were calculated using IDEAS software as described in Section 2.22, parameters were adjusted, and relative fluorescence was determined. There was significant difference in cellular uptake of Ins-F and Ins-F-GET NCs at both 1 and 24 hr. At 1 hr time point, there was no significant difference in internalised and surface bond Ins-F compared to Ins-F-GET NCs. At the 24-hr time point, there was significant difference in internalised and surface bound fraction of Ins-F and Ins-F-GET NCs, where NCs were greatly internalised and bond to surface, as compared to Ins-F. Figure 4.5c shows negative control where no fluorescent signals were detected for non-transfected cells serving as a control for cellular uptake. In Figure 4.5d and 4.5e the cellular uptake and ratio of internalised to surface bonded Ins-F at 1- and 24- hr is displayed in the form of graphs; results indicated that at 1 hr, there is poor cellular uptake while incubating cell monolayers for longer time leads to greater internalisation. Figure 4.5f and 4.5h show Ins-F-GET NCs images acquired at 1 and 24 hr, here again incubating cells with NCs for longer led to greater internalisation.

The ratio of internalised to surface bound NCs, revealed that more NCs were internalised into cells compared to surface bonded NCs, but overall the internalisation and accumulation was greatest for Ins-F-GET NCs at both time points compared to Ins-F. These results are in accordance with ones obtained

through *in-vitro* transcytosis assay and confocal microscopy, and thus provide strong evidence that GET significantly enhances the cellular uptake and accumulation of insulin. ImageStream analysis of Glu-Oct6-FITC-peptide showed better accumulation in nucleus of LNCaP and DU-145 cells compared to Glu-Ala-FITC; where approximately 50% of Glu-Oct6-FITC was localised in nucleus & 50% in cytoplasm. Whereas the extent of co-localisation of Glu-Oct6-PNA-FITC was nearly 20% cytoplasm and 70% in nucleus, as determined by IDEAS software [187]. Live cell imaging of R8-modified polymer dots (Pdots) indicated that cellular uptake of R8-Pdots by HeLa cells is instantaneous, where within 5 min fluorescent signals appear on cell membrane and intracellular signals were progressively increased over time, but unmodified Pdots showed negligible fluorescence. Different patterns of intracellular distribution for fluorescent signals was observed during the

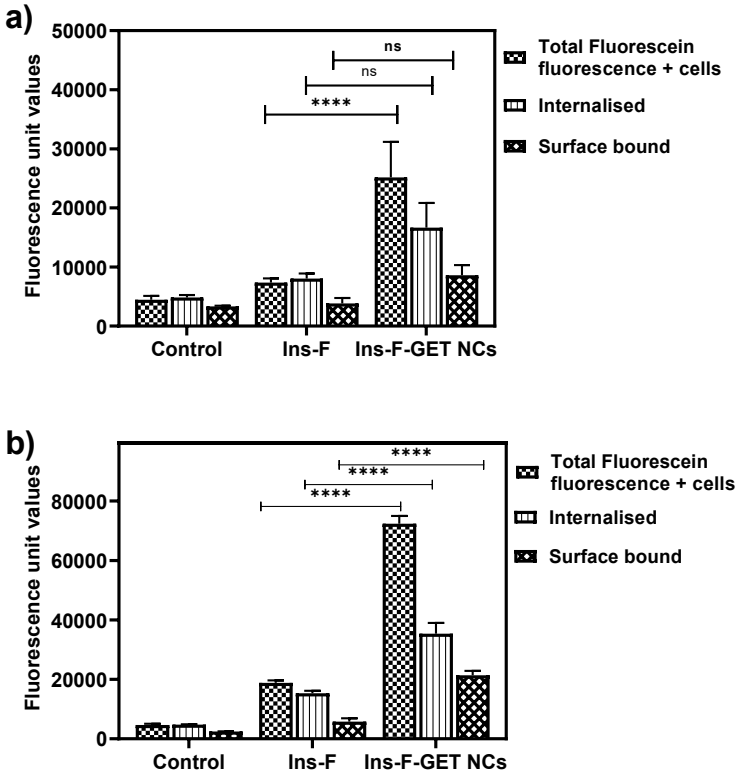

Figure 4. 5 ImageStream analysis showing comparative results for total fluorescence, Internalised and surface bonded NHS-Fluorescein-insulin (Ins-F and Ins-F-GET NCs) at a) 1- and b) 24 hr, respectively. The results indicated that Ins-F-GET NCs show greatest Total Fluorescein-fluorescence, internalisation and surface bonded NCs at both time points compared to Ins-F. All values are presented as mean ± S.D, n=2, where *= *p-value* <0.05, **= *p-value* <0.005, ***=*p-value* <0.0005, ****= *p-value* <0.0001, *ns*= not significant. Two-way ANOVA with Tukey's test.

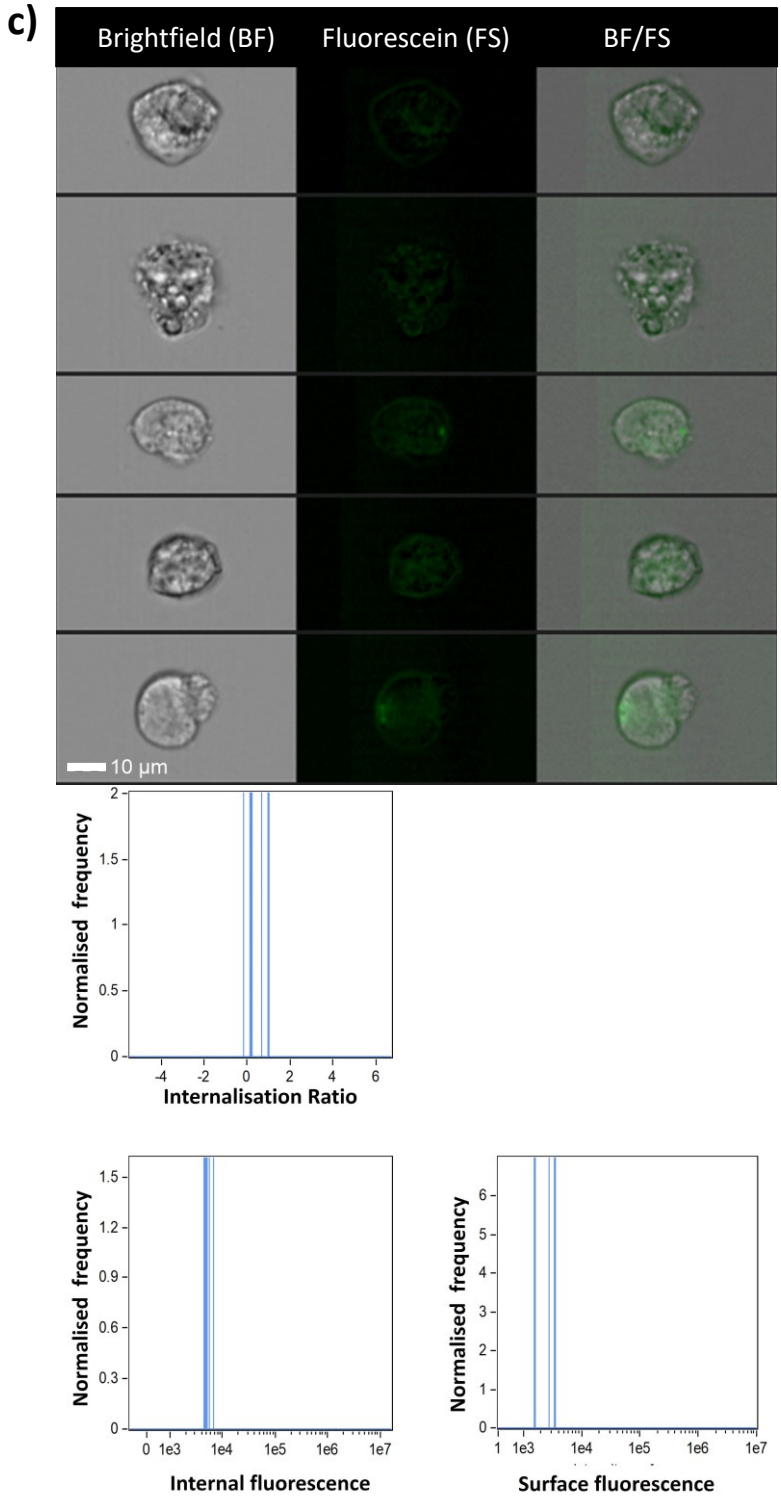

Figure 4.5c Image for Negative control (no transfection/ blank) showing cells with brightfield image, separate fluorescent images related to expression of NHS-Fluorescein labelled insulin with and without GET-peptide (Ins-F, green), and a composite image combining brightfield. Additionally, normalised frequency graphs for internalised ratio, internal and surface fluorescence were also obtained. No fluorescent signal was seen due to no transfection delivery. The scale bar indicates 10 µm.

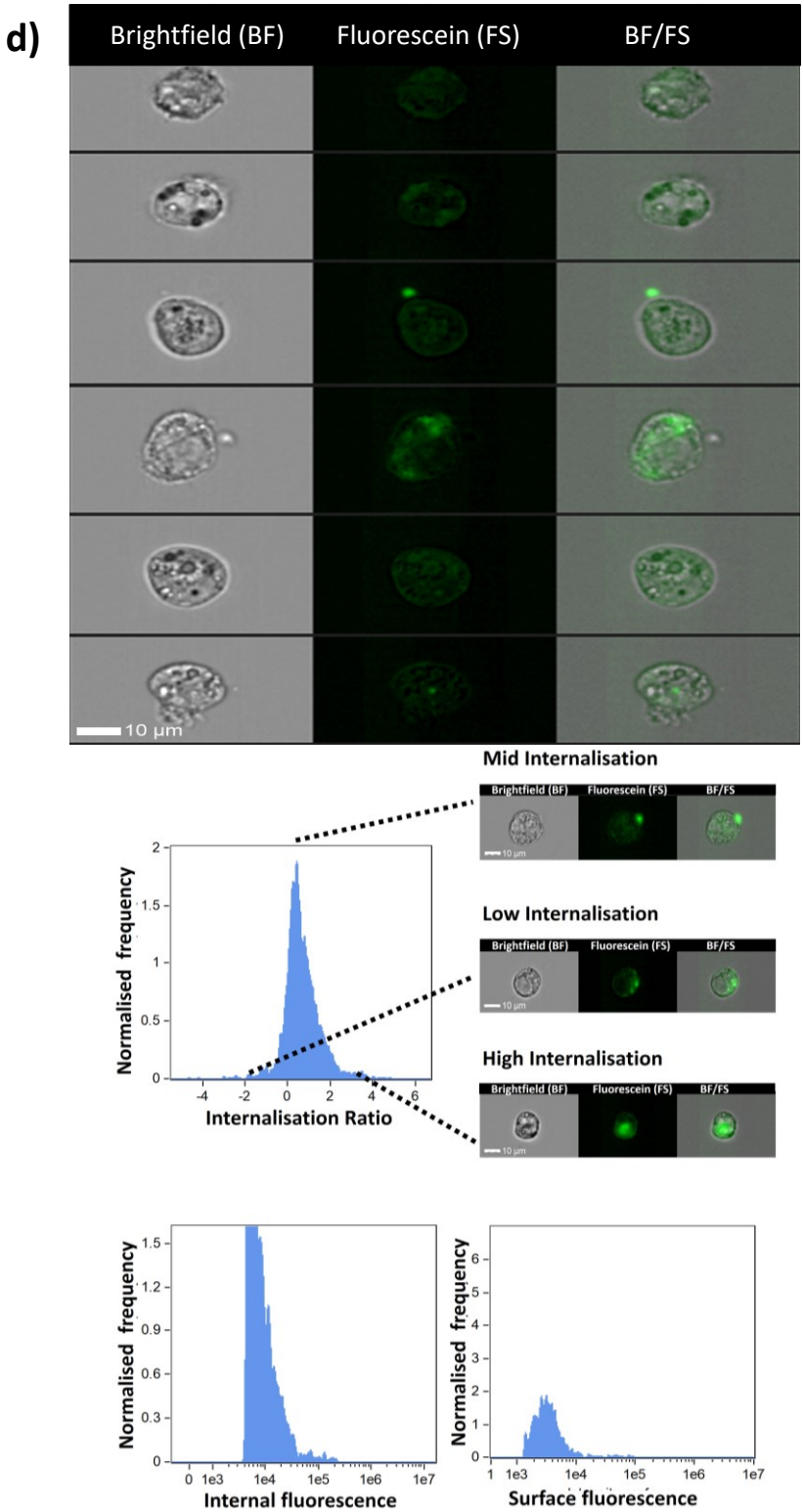

Figure 4.5d Image stream results for Ins-F (1hr incubation) showing cells with brightfield image, separate fluorescent images related to expression of NHS-Fluorescein-labelled insulin (Ins-F, green), and a composite image combining brightfield, showing uptake of Ins-F into cells. Additionally, normalised frequency graphs for internalised ratio, internal and surface fluorescence were also obtained, which indicated that majority of Ins-F is surface bonded. The scale bar indicates 10 µm.

e)

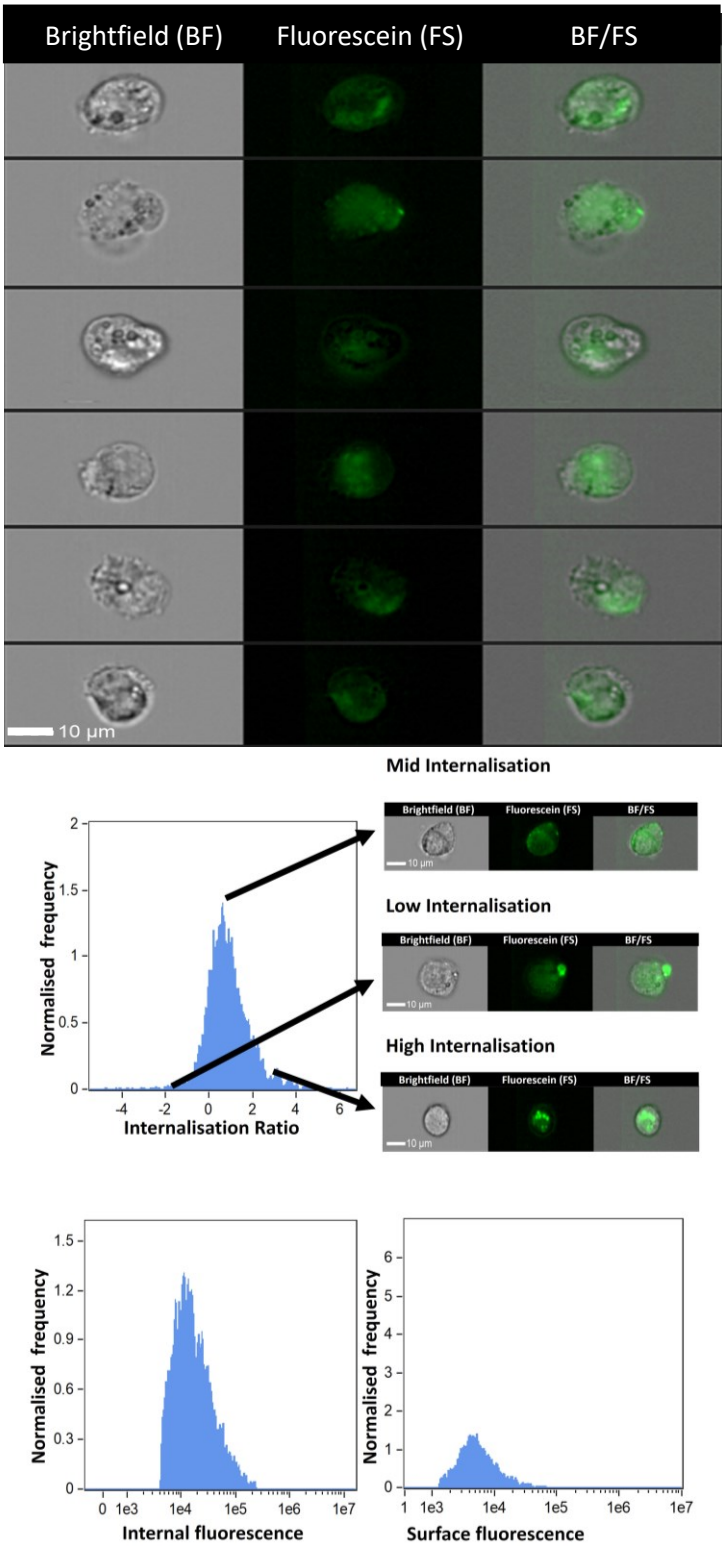

Figure 4.5e Image stream results for Ins-F (24hr incubation) showing cells with brightfield image, separate fluorescent images related to expression of NHS-Fluorescein-labelled insulin (Ins-F, green), and a composite image combining brightfield, showing significant uptake of Ins-F into cells. Additionally, normalised frequency graphs for internalised ratio, internal & surface fluorescence indicated equal amount of surface bound and internalised Ins-F. The scale bar indicates 10 µm.

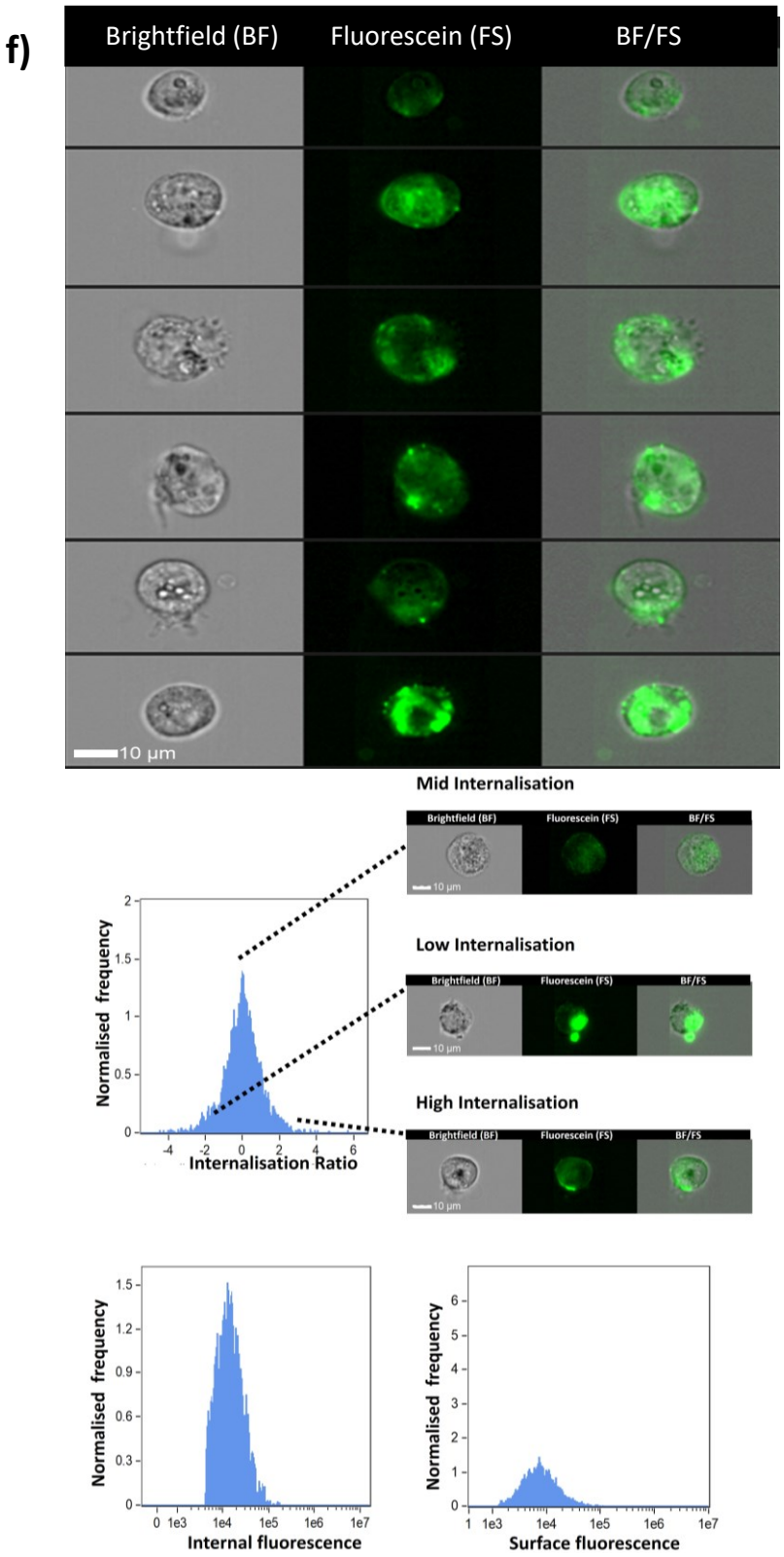

Figure 4.5f Image stream results for Ins-F-GET NCs (1hr incubation) showing cells with brightfield image, separate fluorescent images related to expression of NHS-Fluorescein labelled insulin (Ins-F, green), and a composite image combining brightfield, showing significant uptake of NCs into cells, as indicated by high fluorescent intensity. Additionally, normalised frequency graphs for internalised ratio, internal and surface fluorescence were also obtained, which indicated equal amount of internalised and surface bound NCs. The scale bar indicates 10 µm.

g)

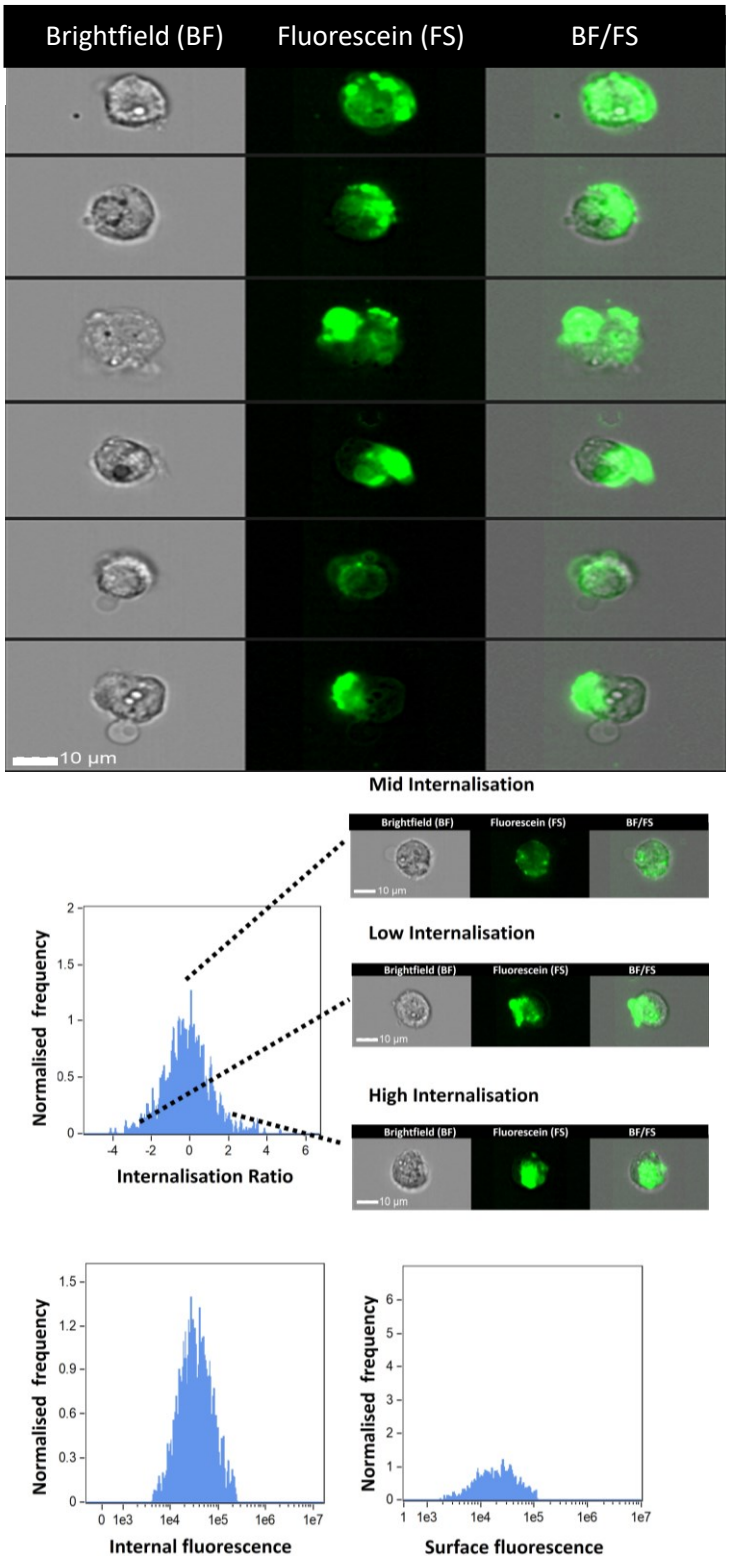

Figure 4.5g Image stream results for Ins-F-GET NCs (24hr incubation) showing cells with brightfield image, separate fluorescent images related to expression of NHS-Fluorescein labelled (Ins-F, green), and a composite image combining brightfield, showing brightest fluorescent signal indicating highest cellular internalisation and accumulation. Additionally, normalised frequency graphs for internalised ratio, internal and surface fluorescence showed more internalised NCs compared to surface bonded NCs. The scale bar indicates 10 µm.

early and late stages of cellular uptake, where majority of fluorescent intensity was located close to cellular membrane which gradually migrated towards perinuclear region around the nucleus in 48 hr [188].

4.3.2.3. Cytotoxicity assay

This assay uses Calcein AM and EthD-1 as fluorescent probes for live and dead cells, respectively. Calcein AM, a cell permeant non-fluorescent dye is instantly uptaken by live cells, which enzymatically through esterase activity gets converted to intensely fluorescent Calcein. This polyanionic Calcein dye is efficiently retained inside live cells and produces an intense green fluorescence. Live cells have intact plasma membrane, therefore EthD-1 (fluorescent DNA nucleic acid stain) is excluded from entering live cells, but it enters cells with damaged cellular membranes and gets bound to nucleic acid thus producing a bright red fluorescence in dead cells.

The effect of increasing concentrations of GET-peptide bond to insulin in the form of NCs (different NCs with correspondingly increasing concentration of GET) on cellular viability (Caco-2 monolayers) was analysed using cytotoxicity assay kit. Data showed that low amount of GET-peptide (1.25, 2.5, 5 and 10 μM) have insignificant cytotoxic effect on Caco-2 monolayers, as clearly seen in Figure 4.6, where few dead cells (red) were observed on incubating with NCs for a period of 24 hr. Almost all cells were viable as indicated by Calcein AM (green signal). These results indicated that amount of GET-peptide normally used in GET- based insulin NCs (10 μM) for translocation and transcytosis assays is safe and has no cytotoxic effect on Caco-2 monolayers. On doubling the GET-concentration from 10 μM to 20 μM, the ratio of dead cells increased, but still most cells were viable as indicated by stronger green signal by Calcein AM. Further increasing the concentration of GET-peptide to 40 μM, caused significantly more dead cells (red) (Figure 4.6), where the cells turned out to be highly responsive to EthD-1 due to more cell death, thus indicating this dose could be lethal for Caco-2 cells. These results indicated that concentration of GET-peptide (10 μM) used normally in NCs has no damaging effect on Caco-2 cells, maintains membrane integrity and is safe, but increasing the concentration around 40 μM causes considerable damaging effect and cellular death.

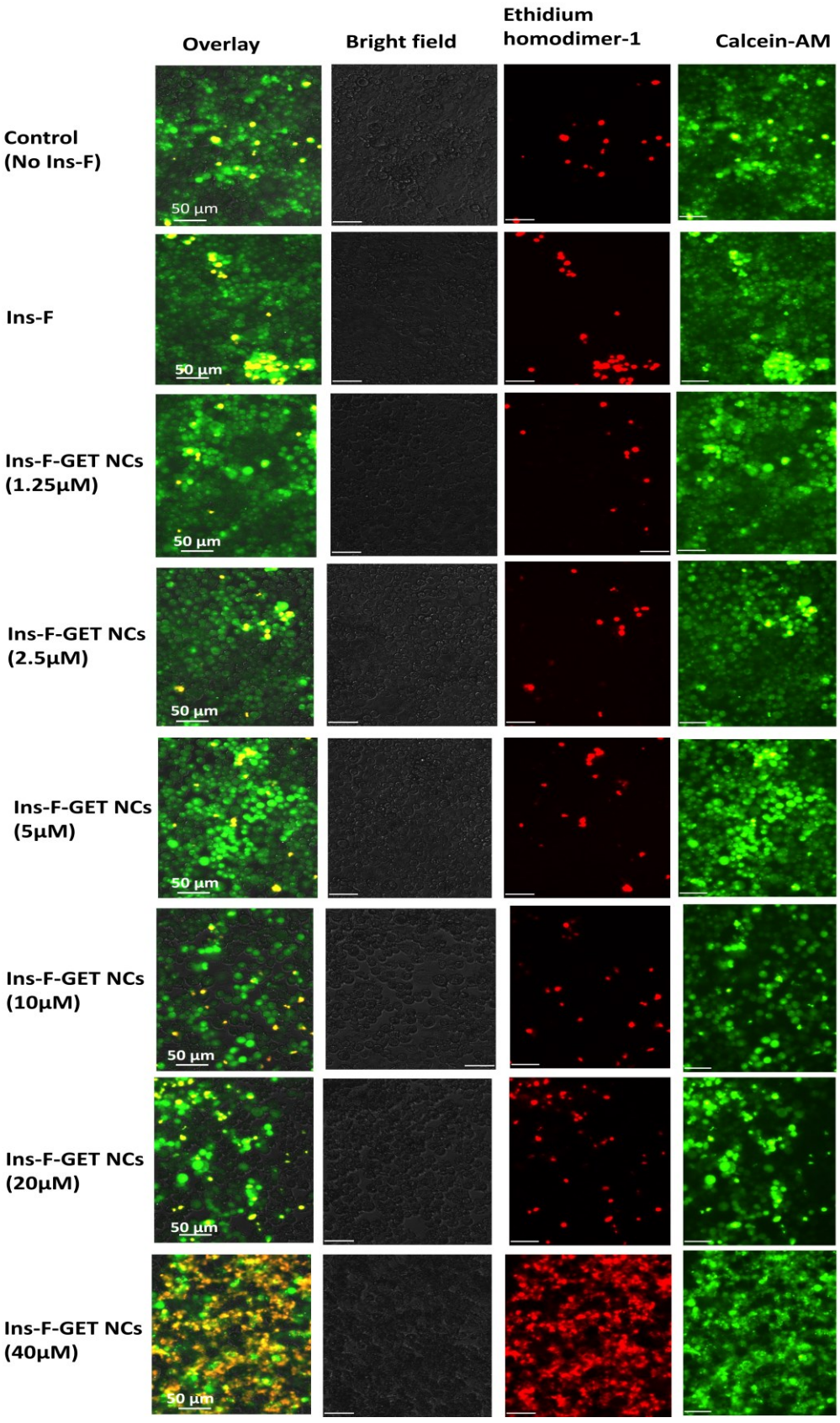

Figure 4. 6 Live (green)/dead (red) staining of Caco-2 monolayers after incubation with Ins-F-GET NCs formulated with progressively increasing concentration of GET-peptide. Images on the top two rows contain cells that were not exposed to GET,

the first as negative control (no transfection) and second incubated with free Ins-F; images on the lower rows were incubated with Ins-F-GET NCs having different molar ratio of GET-peptides for overnight. Results showed that increasing GET concentration near 40 μM causes considerable cytotoxic and damaging effect on Caco-2 cells and thus leads to cellular death. 20x lens was used. The scale bar represents 50μm, and n= 4.

The CPP-conjugated system utilising either oligoarginine (R7) or Streptolysin O (SLO)-were employed for delivery of model proteins (GFP and ESRRB protein), as both proteins regulate pluripotency-related genes for delivery in human testicular- (hTSCs) and human bone marrow- stromal cells (hBMSCs). The results of Live/Dead cytotoxicity assay revealed that viability of CPP-based system was 85.9% in hBMSCs and 90.0% in hTSCs compared to the control, on the other hand viability of SLO-mediated system was 76.4% in hBMSCs and 84.0% in hTSCs [189]. Live/Dead cytotoxicity assay indicated almost no red fluorescent signal in cells treated with R9-LK15, R9-LK15/miR-29b, and miR-29b NCs compared to control, but many dead cells were observed in cell samples treated with Lipo- and Lipo/miR-29b-based NCs revealing these systems to be severely cytotoxic [190].

4.3.3. Stability studies

4.3.3.1. Stability of GET-peptide system

For investigating the stability of GET-peptide system (termed as PLR), the L- and D-isoforms of GET-peptide (L-PLR and D-PLR) were pre-treated with Prot. K and just media i.e. SFM (No Prot. K) for a defined period of time in an incubator at 37 ^{o}C, followed by addition of FITC-insulin, a schematic diagram is given in Figure 4.7a. In the absence of enzyme both L-PLR and D-PLR were intact, stable, and quenched the fluorescence of Ins-F* (Figure 4.7b). Negative control consisted of heat inactivated Prot. K for comparison with samples, additional control consisted of Prot. K treated under similar conditions and finally exposed to Ins-F* (to give maximum fluorescence values by chopping FITC-molecules apart from insulin). Samples were compared to respective controls to give an indication of fluorescence quenching and dequenching depending upon stability condition of peptide (intact or cleaved) post-exposure to Prot. K. D-PLR was resistant to enzymatic degradation by Prot. K, as is evident from its fluorescence quenching action for Sigma-FITC-insulin

following exposure to this enzyme, as shown in Figure 4.7c. On the other hand, L-PLR was degraded by Prot. K as it lost its ability to quench Ins-F* fluorescence. Ins-F being labelled with NHS-ester derivative of fluorescein has greater affinity and specificity towards primary amines in presence of other nucleophiles and moreover it forms stable amide bonds with proteins/ antibodies upon labelling .In comparison Sigma-FITC insulin which is labelled with FITC, tends to bind both primary and secondary amines, this lack of specificity contributes to unstable linkages, whereas NHS-Fluorescein labelled insulin displays strong specificity towards primary amine groups and is thus more stable. These results suggested that the D-version of GET-peptide is more stable to degradation by proteolytic enzymes and can serve as a potential tool for oral delivery of insulin by protecting it from degradation in GI tract.

L-form of GET-peptide comprising of L-amino acids is more prone to metabolic instability in the intestinal lumen, compared to the corresponding peptide containing D-amino acids. These results indicated that D-amino acid version of GET system (D-PLR) was more stable than the corresponding L-form (L-PLR). This difference in sensitivities of L- and D- forms of peptides to degradation by enzymes also affects the ability of peptide to increase intestinal absorption of insulin. In addition to this proteolytic stability, the type of interaction between insulin and CPPs during complex formation (electrostatic and/or hydrophobic interaction) may also be a crucial factor in protecting insulin from enzymatic degradation [22, 191, 192]. Nielsen and co-workers have demonstrated similar findings where the D-form of penetratin was more resistant to enzymatic degradation *in-vivo* in rat intestinal fluid and effectively enhanced insulin absorption by alleviating enzymatic barrier compared to L-penetratin [141].

The results of this study co-relate with our results, where D-form of GET-peptide was found to be more stable to proteolytic degradation compared to L-GET-peptide. Relative stability of different isoforms of fluorescently labelled-octa-arginine derivatives (α-L-, α-D - and β-R8) was studied in human plasma by comparing the half-life time. The results were surprising as L-R8 derivative showed half-life of only 0.5 min in human plasma, while both the α-D - and β-R8 derivative were completely stable for a period of at least 7 days [193].

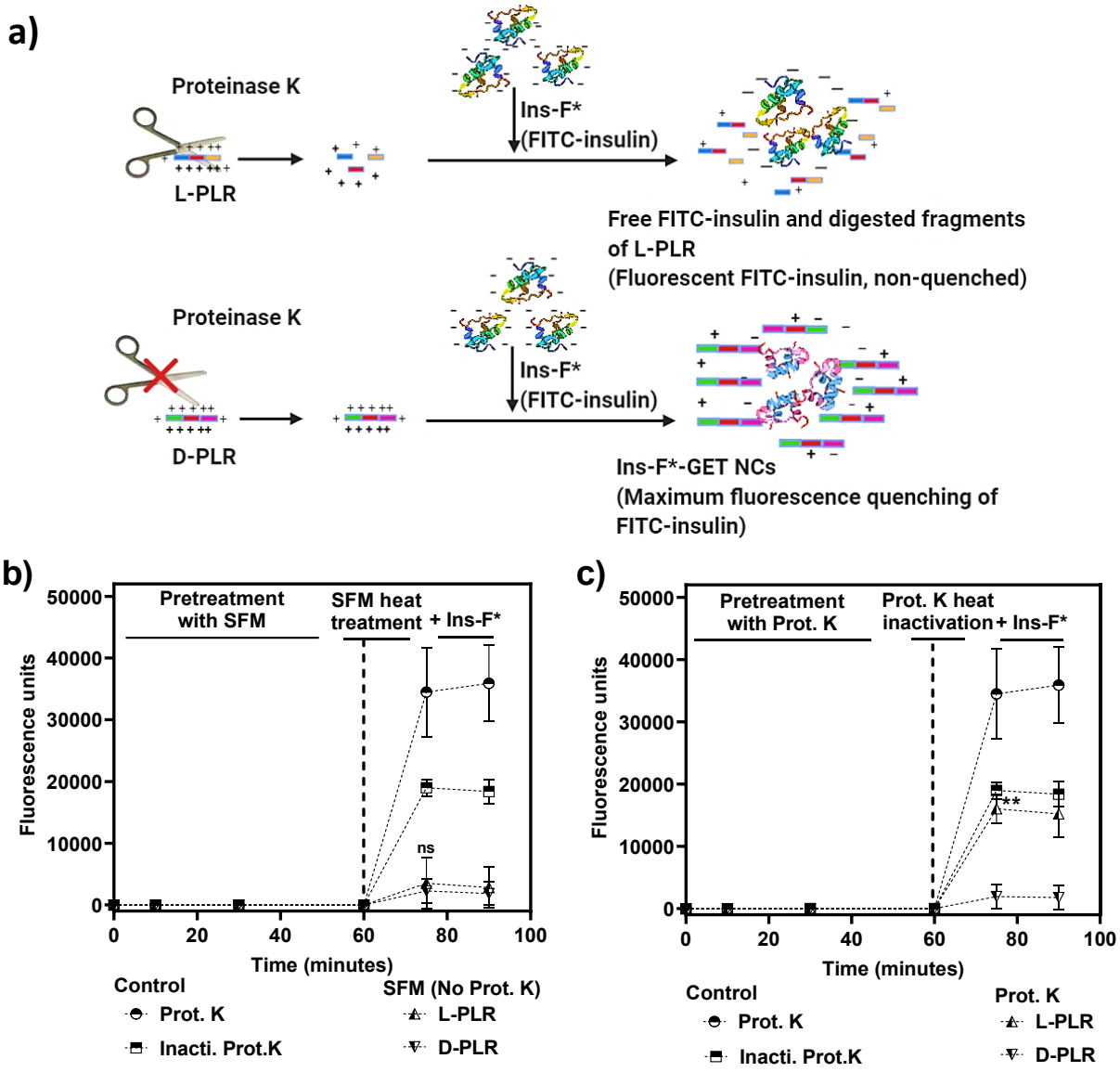

Figure 4. 7 a) Schematic illustration of stability assay of GET-peptide (L- and D-PLR) to digestion by Prot. K, b) GET-peptides digestion with SFM (no enzyme), and c) GET-peptide digestion with Prot. K showing that D-PLR is resistant to enzymatic degradation by Prot. K, as is evident from its fluorescence quenching action of Ins-F*. All values are presented as mean ± S.D, n=5, *= *p-value* <0.05, **= *p-value* <0.005, ***=*p-value* <0.0005, ****= *p-value* <0.0001, and *ns*= not significant. Two-way ANOVA with Tukey's test.

4.3.3.2. Stability of GET-based insulin nanocomplexes

4.3.3.2.1. Treatment with different pH conditions in presence of pepsin

A schematic presentation of this assay is given in Figure 4.8a. The stability of insulin-GET NCs was determined by exposing samples to pepsin enzyme at different pH conditions and subsequently analysing the fluorescent behaviour of Ins-F* and Ins-F*-GET NCs (Figure 4.8b and Figure 4.8c), respectively**.** As a control, Ins-F* and Ins-

F*-GET NCs were exposed to similar conditions in the absence of Pep, and the samples (treated with Pep) were compared for their fluorescent intensity to these controls. The insulin samples in neutral media condition (no exposure to HCl + Pep) showed maximum fluorescent intensity, while Ins-F*-GET NCs were least fluorescent due to quenching by GET. In acidic media (0.01M HCl containing Pep), Ins-F* fluorescence was reduced significantly as the FITC exhibits pH-dependent fluorescence behaviour and it loses its fluorescence property under acidic conditions, while for Ins-F*-GET NCs the fluorescent intensity was weakest firstly due to quenching and secondly due to loss of FITC-fluorescence in acidic environment. In third condition i.e. neutralising acidic samples by addition of 0.01N NaOH, the fluorescence recovery was observed, with Ins-F* the fluorescence was recovered (previously suppressed in acidic condition) and over time there was increase in fluorescence (due to action of Pep) and these results were statistically significant. Additionally, for Ins-F*-GET NCs (least fluorescent in acidic media), the addition of 0.01N NaOH caused fluorescence recovery (even more than the control at neutral, acidic and neutralisation after NaOH addition), showing that the Ins-F*-GET NCs are stable even under acidic conditions (Figure 4.8c). Moreover, Pep dequenched fluorescence of insulin-GET NCs by cleaving NCs, and its action was over the course of time. As discussed earlier in Section 3.3.11, different proteolytic enzymes could be employed for recovering the fluorescence of proteins.

There have been reports where *in-vitro* incubation of therapeutic peptide used in Celiac diseases with PEP caused complete cleavage of peptide with 8-fold increase in fluorescence intensity. Thus, concluding that fluorescence based assays can be used as better indicators of activity and stability of molecules [179]. Another example of overcoming fluorescence quenching of FITC-fibrinogen is either by the addition of unlabelled fibrinogen or Gly-Pro-Arg-Pro to the reaction or through the use of plasmin which cleaves fibrinogen [177]. Thus, fluorescence quenching is a reversible phenomenon which could be reversed by employing appropriate strategies, and the results of our study are in accordance with earlier studies, as the fluorescent signals for insulin were successfully recovered following exposure to proteolytic enzymes.

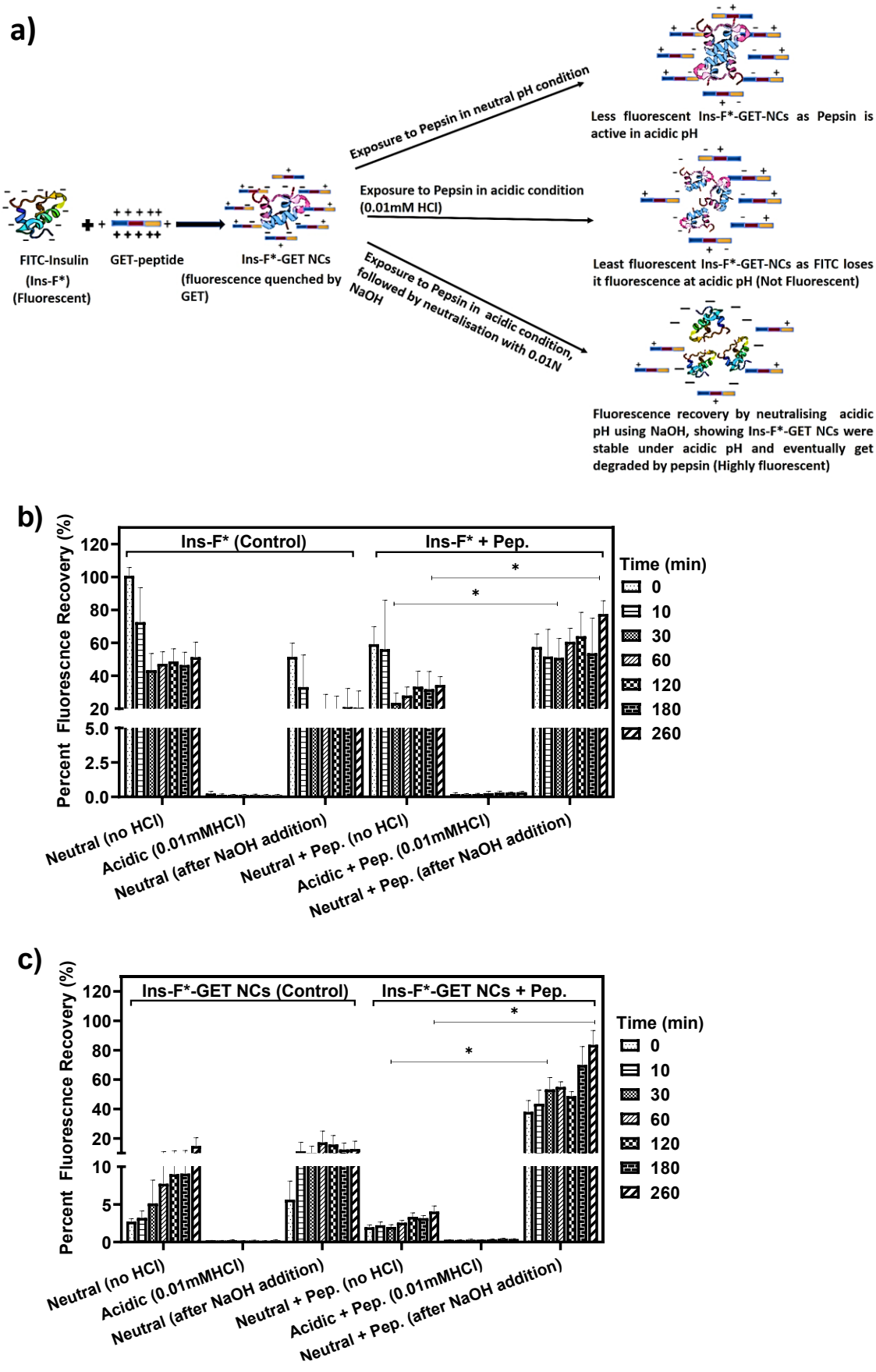

Figure 4. 8 a) Schematic illustration of Ins-F* stability with GET-peptide system and fluorescence behaviour in different pH condition in presence of Pep. b) Ins-F* was

least fluorescence at low pH, by addition of NaOH, the fluorescence was detectable, indicating that FITC loses it fluorescent behaviour under acidic conditions. c) Ins-F*-GET NCs in acidic media were least fluorescent, but on adding 0.01N NaOH (for neutralising pH) there is recovery of fluorescence showing that the insulin-GET NCs are even stable under acidic conditions, and additionally pepsin dequenches the fluorescence by disrupting these NCs. All values are presented as mean ± S.D, n=5, *= *p-value* <0.05, **= *p-value* <0.005, ***=*p-value* <0.0005, ****= *p-value* <0.0001, and *ns*= not significant. Two-way ANOVA with Tukey's test.

4.3.3.2.2. Treatment with commercial Biorelevant media simulating GI conditions

Figure 4.9a shows the behaviour of Ins-F* and Ins-F*-GET NCs in Biorelevant media mimicking the GI environment. This assay was based on the phenomenon of fluorescence quenching and dequenching, where the self-aggregation or close proximity of FITC-molecules resulted in quenching of fluorescence which was successfully reversed by employing different strategies such as dilution of systems or use of proteolytic enzymes. The fluorescent signals for Ins-F* (Figure 4.9b) remained constant in FaSSGF and FeSSIF over time, but in presence of proteolytic enzyme (Pep in FaSSGF and Pan in FaSSIF) the fluorescent intensity of samples was progressively increased with time compared to control (SFM). Additionally, FaSSIF without enzymes also caused an increase in fluorescent values for Ins-F* which could be due to components of buffer media causing FITC-molecules to be spaced out. Similarly, Ins-F*-GET NCs (fluorescence quenched) showed least fluorescent intensity in FaSSGF, FaSSIF, and FeSSIF, possibly due to self-aggregation of molecules in presence of GET (Figure 4.9c). These NCs in FaSSGF with Pep and FaSSIF with Pan showed phenomenon of fluorescence dequenching due to proteolytic action of enzymes, and this dequenching was time-dependent where the fluorescent values were increased over time. NCs displayed highest fluorescent values in FaSSIF containing Pan, which was even more than for Ins-F* indicating that the Pan enzyme has better chopping property than Pep, as it disrupted the complex within 10-30 min as evident by recovery of fluorescence values. These results revealed that presence of enzymes in media caused cleavage/ disruption of nanocomplexes by decomplexing GET from insulin, and resulted in an increase in fluorescence intensity, thus suggesting instability of NCs in Biorelevant media.

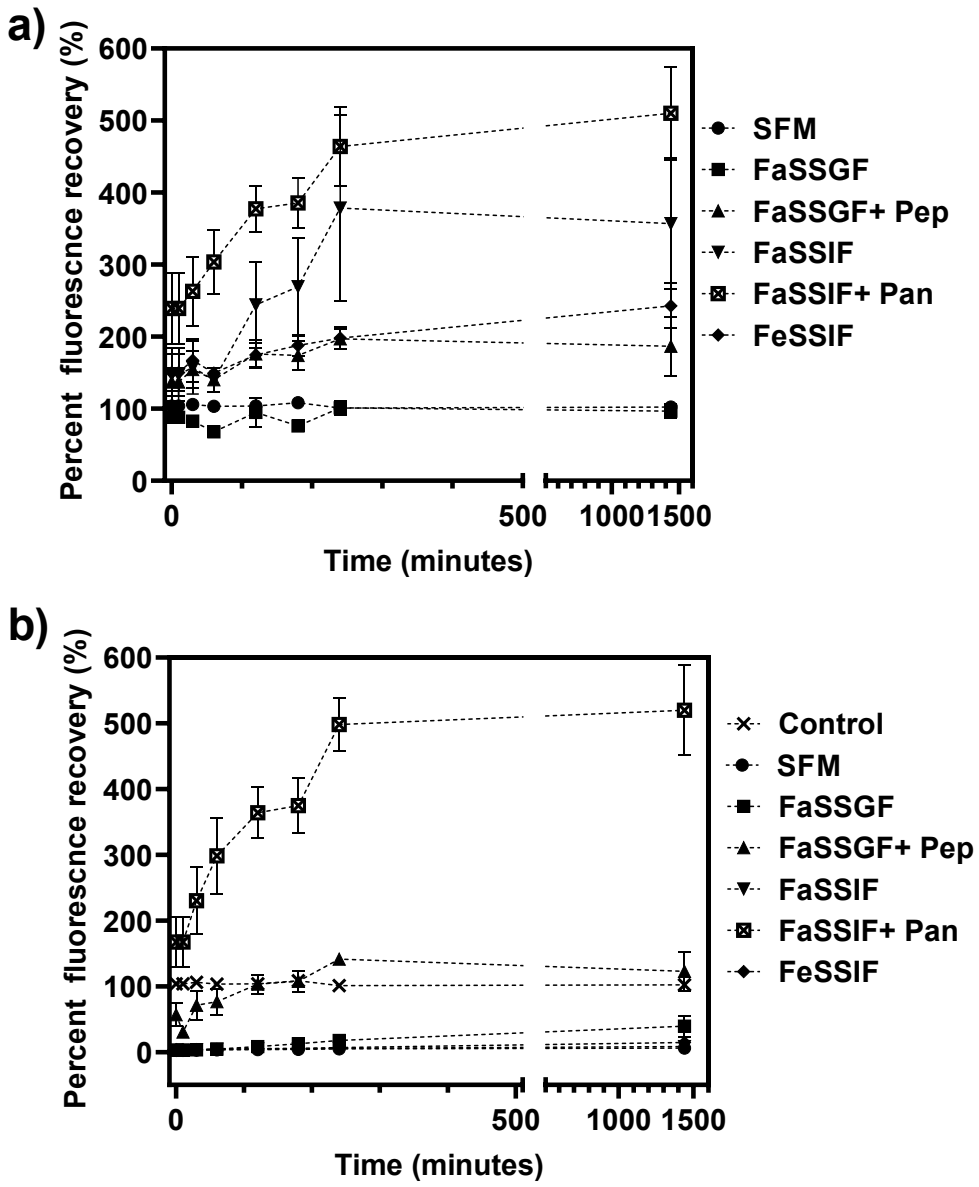

Figure 4. 9 Stability of Ins-F* and Ins-F* GET NCs in biorelevant media was assessed, where in presence of enzymes the NCs were degraded showing instability of NCs. a) Ins-F* stability and percent fluorescence recovery in different biorelevant media; FaSSGF, FaSSGF + Pep, FaSSIF, FaSSIF + Pan, and FeSSIF , control consisted of Ins-F* in SFM for comparison of fluorescent signals, and b) Ins-F*-GET NCs stability and fluorescence recovery in biorelevant media showing that presence of enzymes caused reversal of fluorescent intensity due to decoupling of GET from insulin depicting instability of NCs in presence of GI enzymes, control consisted of Ins-F* in SFM (100% or fully fluorescent) for comparison with NCs samples in different media. All values are presented as mean ± S.D, n=5, * = *p-value* <0.05, **= *p-value* <0.005, ***=*p-value* <0.0005, ****= *p-value* <0.0001, and *ns*= not significant. Two-way ANOVA with Tukey's test.

Therefore, these results provided insight that Ins-F*-GET NCs are unstable in the presence of conventional GI enzymes, as the NCs were chopped off by pepsin and pancreatin thus decoupling GET-peptide from insulin, which would limit the application of GET system for oral insulin delivery. As for achieving oral delivery, its necessary to have a stabilised system which is resistant to action of GI enzymes, or a carrier system is needed to further encapsulate and protect these NCs. This also implies that alternative approaches such as hydrophobically modified GET derivatives or covalent bonding of GET with insulin should be taken into consideration.

Biorelevant media has been used for studying the stability of PEG-PGA enveloped hydrophobically-modified-8R-peptide NCs. Branched or diblock PGA-PEG enveloped ENCPs displayed adequate colloidal stability in SIF for 4 hr, while in FaSSIF-V2 the branched PGA-PEG enveloped-ENCPs were largely aggregated but ENCPs with diblock coating were stable upto 6 hr [158]. One of the other studies used SGF and FaSSIF buffers for studying the *in-vitro* release from CPP-functionalised porous silicon NPs. The presence of bile salts in FaSSIF acted as wetting agent on the surface of NPs, which promoted insulin release, additionally burst release effect was only observed in FaSSIF (intestinal conditions) with no drug release in gastric conditions [194]. The results of these earlier studies contradict the results of our study, where GET-based NCs were found to be unstable in commercial biorelevant buffers simulating GI environment.

4.3.3.2.3. NCs stability using different labelled insulin

This assay was performed to assess the stability of insulin-GET NCs i.e. whether or not the GET-peptide detaches from the NCs to get bound to the available free added insulin. The results showed that upon addition of excess free insulin (Ins-F* or Ins-T) to the samples of insulin-GET complexes (Ins-F* or Ins-T with different GET contents), there was insignificant change in the fluorescent intensities of free insulin and insulin-GET NCs (Figure 4.10). Figure 4.10a shows a progressive decrease in fluorescence intensity of Ins-F* (FITC-channel) by adding increasing amounts of GET-peptide, leading to fluorescence quenching due to formation of Ins-F*-GET NCs. Analysis of same samples for TRITC-channel indicated that addition of Ins-T to Ins-F*-GET NCs caused a progressive increase in red fluorescence due to

increased contents of Ins-T (Figure 4.10b). Interestingly, for Ins-T-GET NCs with varying GET-peptide contents, the addition of free Ins-F* to these NCs showed constant green fluorescence values, but at higher GET concentration (2µM, 4µM, and 10µM) the green-fluorescent intensity was reduced. This suggested that there is some excess/ free peptide available to interact and complex with Ins-F*, as indicated by its fluorescence quenching (Figure 4.10c). Additionally, Ins-T-GET NCs exhibited comparable red fluorescence values to Ins-T (non-complexed insulin) showing constant fluorescence values (Figure 4.10d).

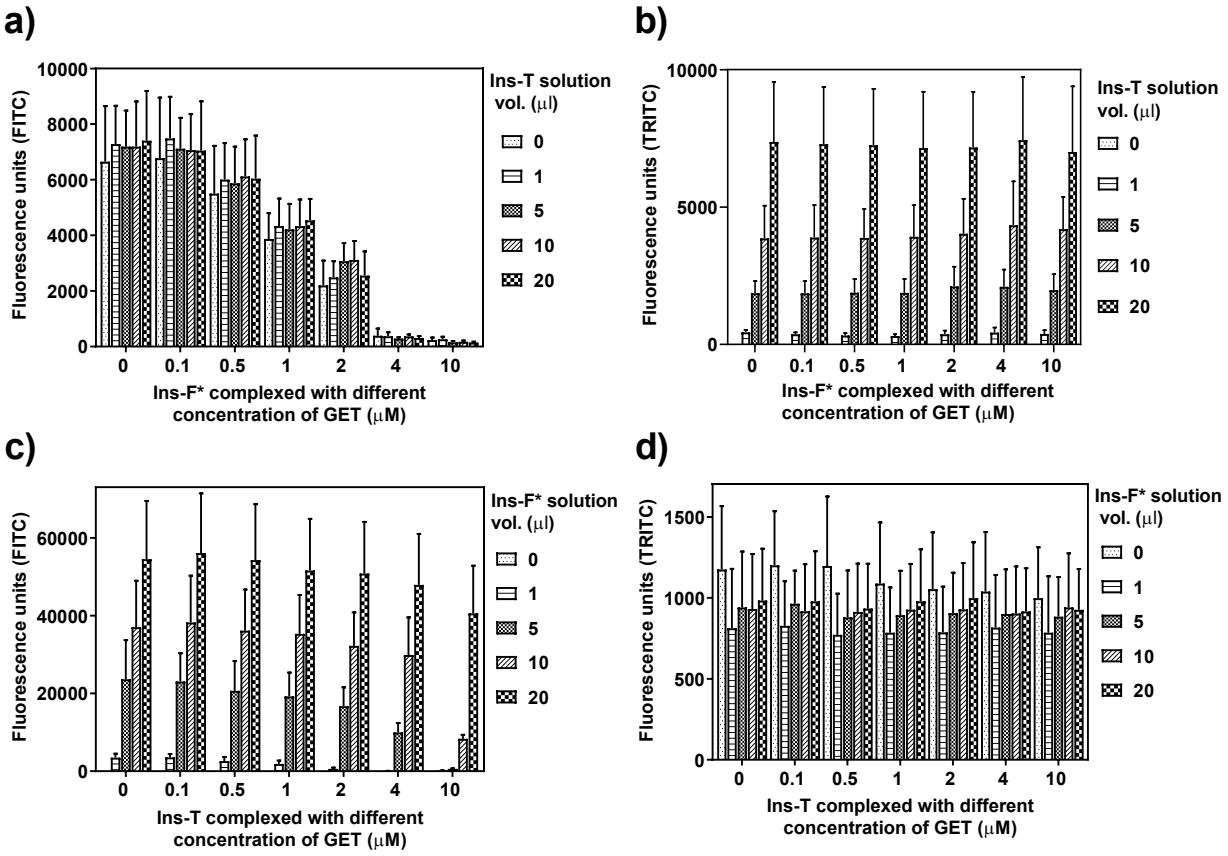

Figure 4. 10 Insulin-GET NCs (formed using FITC-insulin or Ins-T) were found to be stable as GET was not detached from NCs to get bound to free available insulin. a) Ins-F*-GET NCs with varying GET contents showing decrease in green fluorescence due to fluorescence quenching, b) Ins-F*-GET NCs on addition of Ins-T showed a progressive increase in red fluorescence, c) Ins-T-GET NCs with varying GET contents, on addition of Ins-F* showed variable effects where at higher concentration the FITC-fluorescence was decreased as excess peptide formed NCs with Ins-F* (quenching), and d) Ins-T-GET NCs showing constant fluorescence values. All values are presented as mean ± S.D, n=5, * = *p-value* <0.05, **= *p-value* <0.005, ***=*p-value* <0.0005, ****= *p-value* <0.0001, and *ns*= not significant. Two-way ANOVA with Tukey's test.

The insulin being negatively charged molecule forms complex with GET which is predominantly positively charged peptide via electrostatic interaction, and these interactions are relatively strong, thereby stabilising the insulin-GET NCs. Additionally, GET system tends to protect insulin from degradation, as demonstrated in previous section that insulin-GET NCs were fairly stable under acidic conditions (Section 4.3.3.2.1), but in the presence of GI enzymes the NCs get degraded (4.3.3.2.2) thus limiting applicability of this system. Thereby, the results of this assay predict that insulin-GET complexes are stabilised through the formation of electrostatic bonds between insulin and GET system, and that this peptide system does not dissociate from the insulin-GET NCs to get bound to the excess free insulin, except the excess of un-complexed GET-peptide (at higher concentration) which interacts with free insulin to form further new NCs.

4.3.3.2.4. Assay for analysing the stability of NCs collected post-transcytosis (both media from bottom transwell and cell internalised NCs)

Another important assay was developed using cell lysate i.e. Prot. K , to investigate the stability of insulin-GET-peptide NCs uptaken inside Caco-2 monolayers for assessing whether the GET-peptide stays complexed with insulin or gets detached after translocation inside Caco-2 cells. This assay was based on fluorescence quenching of Ins-F* upon complex formation with GET, which was reversed (dequenched) using cell lysate (Prot. K). Cell samples incubated O/N with drug-peptide NCs (previously less fluorescent due to fluorescence quenching by GET) upon treatment with Prot. K (20 µg /µl) displayed greater fluorescent signals. The control consisted of Ins-F*, collected post-transcytosis from bottom well with no exposure to Prot. K. The results indicated that this enzyme exerts its proteolytic action both on the cells and Ins-F*-GET NCs internalised in cells, resulting in fluorescence dequenching. The fluorescent intensity was increased progressively over time indicating that the action of enzyme is time dependent, while Ins-F*-GET NCs untreated with Prot. K (0 µg/µl) displayed poor fluorescent signals (Figure 4.11a). Additionally, exposing these samples to increased temperature of 56 ^{o}C (for maximum activity of Prot. K) for 10 min, showed a further increase in fluorescence values of samples, as the enzyme exerted its optimal effect to recover fluorescence.

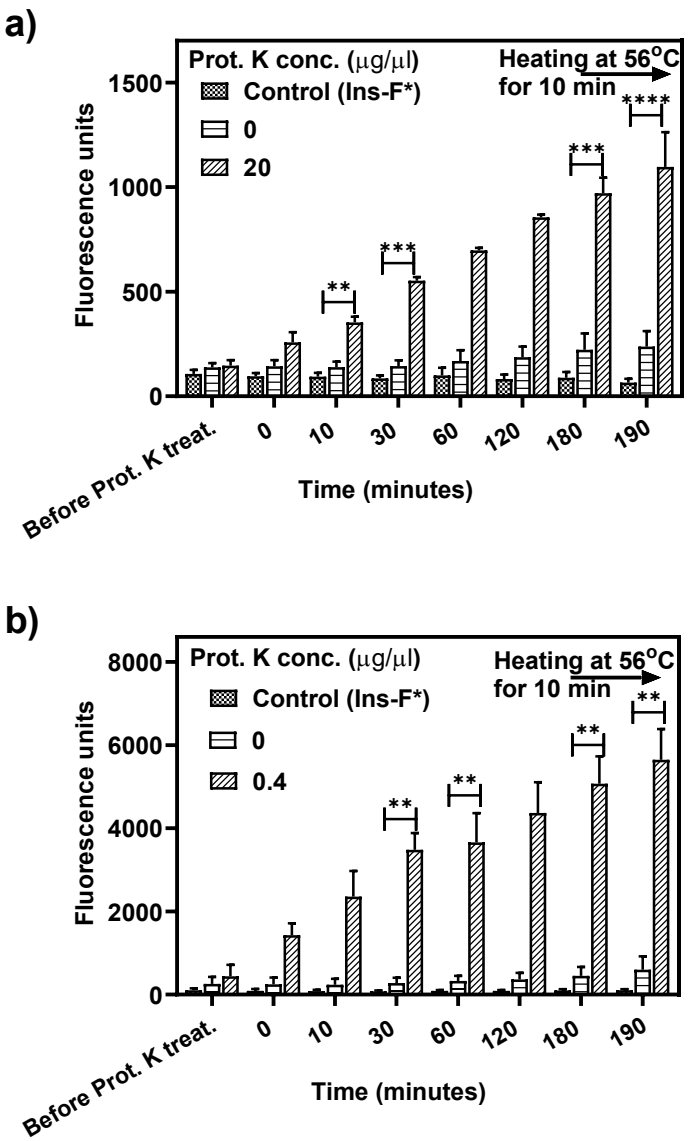

Figure 4. 11 Overnight incubation of Caco-2 cells with Ins-F* and Ins-F*-GET NCs (FITC-insulin), following treatment of incubated cell samples with Prot. K and just SFM (as control). a) The Ins-F*-GET NCs were sufficiently stable even after being translocated into cells, as the treatment of cell samples with Prot. K recovered the fluorescence, while cells encapsulating NCs untreated with Prot. K displayed quenched fluorescence, and b) media samples collected from bottom Transwell® following O/N incubation of cells with NCs also recovered fluorescence on exposure to Prot. K, while NCs untreated with Prot. K displayed quenched fluorescence. All values are presented as mean ± S.D, n=5, * = *p-value* <0.05, **= *p-value* <0.005, ***=*p-value* = <0.0005, ****= *p-value* <0.0001, and *ns*= not significant. Two-way ANOVA with Tukey's test.

Likewise, NCs-media samples were collected from bottom Transwell® (post-transcytosis) following O/N incubation with cells and treated in similar way with Prot. K, while Ins-F* collected post-incubation from bottom well served as a control

(Figure 4.11b). The results indicated that NCs are stable and still intact after O/N incubation with cells, as the quenched fluorescence of samples (NCs exposed to Prot. K i.e. 0.4µg/ µl) was recovered over time by the action of enzyme. While the NCs untreated with Prot. K (0 µg /µl) continued to display lower fluorescent signals. Therefore, it can be concluded that GET-peptide forms stable complexes with insulin via electrostatic interaction, as the GET-peptide remains bonded to insulin even after being translocated inside the cells as evident by quenched fluorescence of samples, which was dequenched using Prot. K.

4.3.4. Functional activity testing using *iLite*® Insulin assay reporter cells

These luciferase reporter cells are DT40 cells (avian) containing insulin-responsive reporter genes with transgene for receptor and are engineered genetically to be responsive to insulin. These cells are employed for quantification of insulin activity in human serum and anti-insulin neutralising antibodies. These cells display unique feature where detection of insulin activity in human serum has no interference from numerous factors present in serum (IGF-1 and IGF-2). Insulin gets bound to its high affinity heterodimeric receptors (CD220) to exerts its pharmacologic activity. It also possesses intrinsic activity for tyrosine kinase, where binding at α-chain of insulin receptor leads to dimerisation and auto-phosphorylation of receptor and results in signalling thorough IR-beta chain, which causes activation of insulin regulated Firefly luciferase reporter-gene construct. These insulin-reporter cells provide expression of Firefly luciferase, followed by cell count normalisation, and subsequently serum matrix effect is attained through a second reporter gene i.e. Renilla luciferase gene under the influence of a constitutive promotor. The Firefly luciferase signal is dependent on insulin concentration and thus directly reflects functional activity of insulin present in sample.

4.3.4.1. Determination of optimal GET-peptide concentration resulting in maximal functional activity

As our results indicated higher cellular uptake, internalisation and enhanced translocation efficiency for insulin using GET-peptide system, we sought to find out the GET-peptide concentration which induces maximal activity and to test whether insulin-GET NCs are still able to retain functional and biological activity of insulin. A

schematic presentation for reaction is given in Figure 4.12a. Consequently, the functional activity of Ins-GET NCs was compared against Ins (with no modification) as a positive control and GET-peptide (no Ins) as a negative control. Figure 4.12b shows that Ins (non-fluorescent; positive control) caused 4-fold induction of iLite cells, while progressively increasing concentration of GET tends to reduce the induction of these reporter cells. At the highest insulin concentration (200 μg/ml), the activity of these transgene reporter cells was suppressed, whereas at 20 μg/ml maximum induction of iLite cells was observed, while further lowering of insulin concentration caused reduction in induction but it was detectable. It is noteworthy that at optimum insulin concentration (20 μg/ml) normally used during translocation studies; a considerable induction of iLite cells was observed, thereby reflecting the functional activity of insulin. The reduction in functional activity of insulin on increasing the GET-peptide content was concentration independent, as the lowest concentration (0.0125 μM) produced nearly similar reduction in activity as the highest concentration of GET (50 μM). Thus, it would be reasonable to assume that relationship between functional activity and progressively increasing amount of GET is hard to contemplate. The optimal GET system concentration which results in maximal insulin functional activity was 10 μM, but overall with GET the cellular induction was reduced from 4-fold to 2-fold in contrast to control (insulin with no modification with GET-peptide). iLite cells were employed for clarification of molecular mechanism between different key signalling enzymes (Ras, Pl3K, and PLC-gamma). DT40-cells were also used to identify essential role of Zn^{+2} Transporter in regulating the activation of Erk and Akt in B-Cell signalling pathway [195]. Moreover, DT40 pre-B cells have been employed to study the role of annexin-5 in peroxide-induced Ca^{+2} signalling as a part of targeted gene disruption [196].

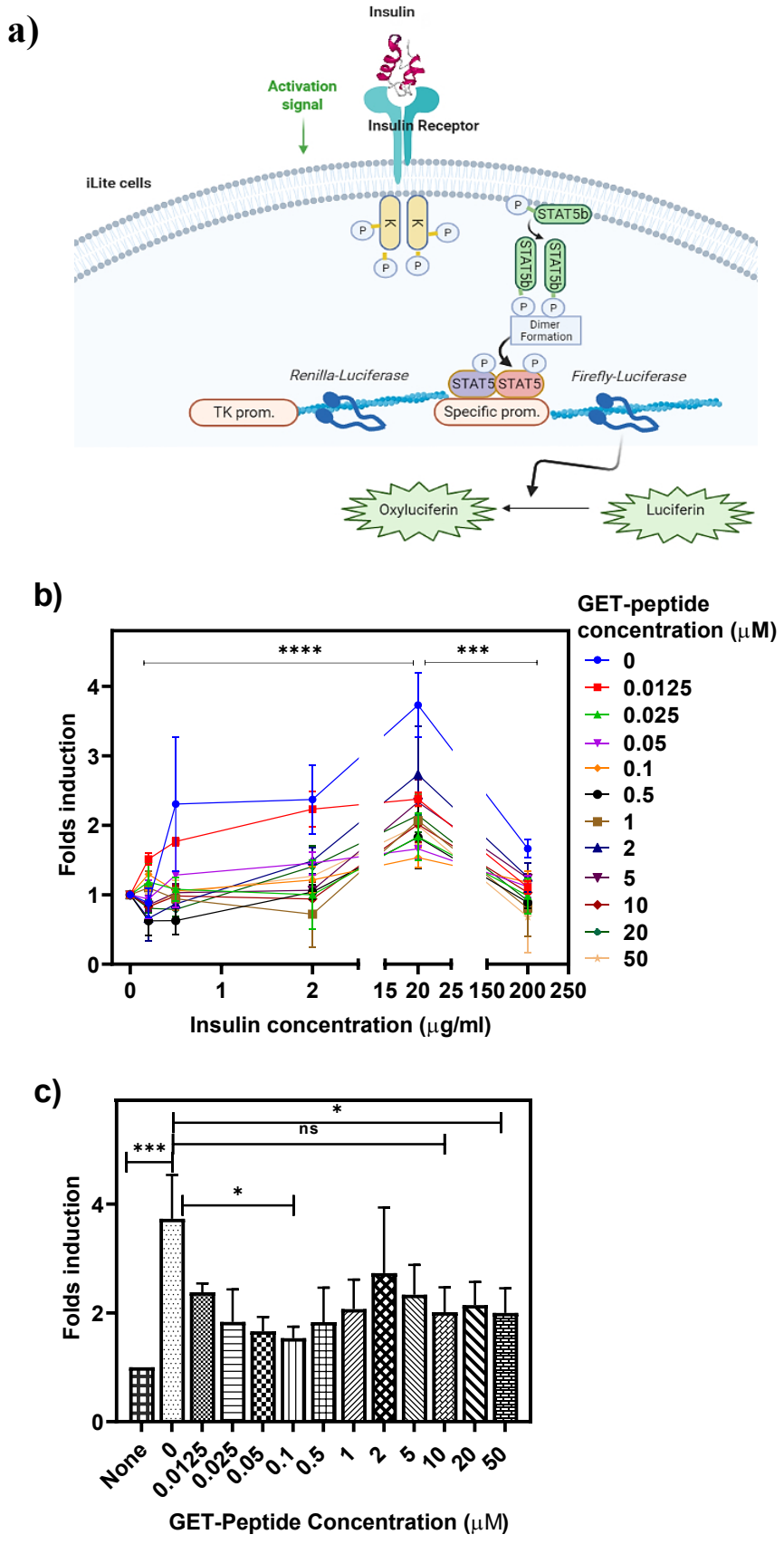

Figure 4. 12 a) A schematic illustration of functional activity of un-labelled insulin (Ins) using luciferase assay. The results showed b) insulin (positive control) caused 4-fold induction of iLite cells, while progressively increasing concentration of GET-

peptide caused reduction in this induction, c) at optimum insulin concentration of 20 µg/ml considerable induction of iLite cells upto 4-fold was observed, which was lessened on complexation with GET-peptide. All values are presented as mean ± S.D, n=3, * = *p-value* <0.05, **= *p-value* <0.005, ***=*p-value* <0.0005, ****= *p-value* <0.0001, and *ns*= not significant. Two-way ANOVA with Tukey's test.

4.3.4.2. Functional activity assay for post-transcytosis samples collected from Transwells®

The ability of insulin-GET NCs to retain functional activity of insulin was tested by analysing the activity of post-transcytosis released NCs from Transwells® onto these responsive transgenic iLite cells. Consequently, the functional activity of Ins-GET NCs was compared with the freshly prepared NCs and with the insulin as a positive control. Additionally, fluorescently labelled insulin (NHS-Fluorescein, Ins-F) alone and complexed with GET-peptide was analysed in similar way and compared against respective controls. The concentration of Ins was quantified in basolateral chamber in relation to Ins-F (free and complexed with GET-peptide) through fluorometric analysis using a microplate reader and final insulin concentration was tailored to constant concentration of 20µg/ml after appropriate dilution. Figure 4.13 showed that the post-transcytosis insulin samples with (Ins-GET NCs and Ins-F-GET NCs) and without GET-peptide (Ins and Ins-F) were only marginally lower in functional activity than the control, which indicated slight loss of functional activity (statistically insignificant). When comparing Ins and Ins-GET NCs, there is slightly more induction of iLite cells with Ins-GET complex compared to Ins. This anomaly in behaviour may be due to fact that Ins concentration was normalised in relation to NHS-Fluorescein insulin, so there could be more insulin concentration in samples collected from basal compartment then the anticipated which might have contributed to greater induction of iLite cells.

There was insignificant difference in the induction capability of control (freshly prepared NCs) and released samples collected post-incubation from Transwells®, thereby indicating that there is no loss of functional activity after translocation. Likewise, decreased induction of iLite cells by Ins-GET NCs compared to Ins was in agreement with the results in previous section 4.12, where insulin complexation with GET-peptide lowered its functional capability. Thus, it would be reasonable to

assume that translocated insulin and insulin-GET NCs are sufficiently stable and have efficiently retained their functional activity. This work provided evidence that complexes are likely to preserve their biological activity after uptake by a simulated gut epithelial walls of cells.

A group of researchers has reported the use of iLite insulin assay reporter cells (DT40 cells) for testing the biological activity of insulin pre-loaded in bi-polymer lipid hybrid nanocarrier (BLN). The results indicated slight decrease in biological activity for three of the four tested insulin concentrations, and the differences were insignificant. Thus, concluding that there was no remarkable difference in the biological activity of insulin entrapped in BLN compared to the fresh insulin samples, hence suggesting that the biological activity of insulin was preserved after entrapment in BLN [197].

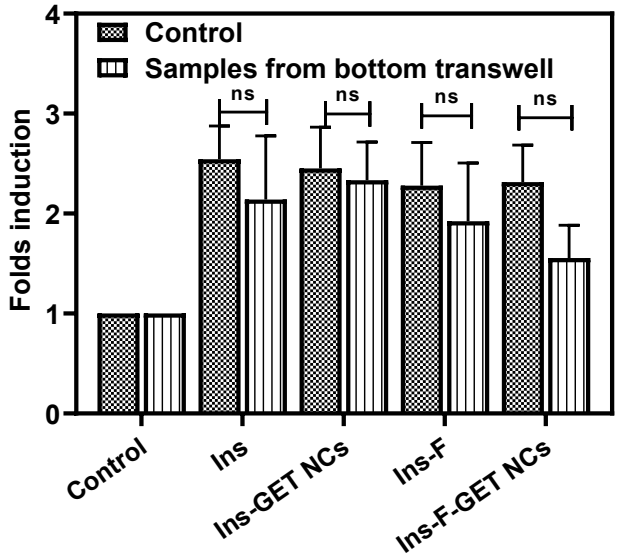

Figure 4. 13 Luciferase assay was performed using iLite cells (1:20 dilution) stimulated with the samples of non-fluorescent (Ins) and fluorescent insulin (Ins-F) alone or complexed with GET system (10µM). A statistically insignificant difference (*p-value* > 0.05) was observed between post-translocation samples collected from bottom well following overnight incubation with Caco-2 cells compared to freshly prepared control in inducing insulin-reporter cells. All values are presented as mean ± S.D, n=3, *= *p-value* <0.05, **= *p-value* <0.005, ***=*p-value* <0.0005, ****= *p-value* <0.0001, and *ns*= not significant. One-way ANOVA with Tukey's test.

4.4. Conclusion

In this chapter the average size, surface charge, stability and functional activity of GET-peptide based insulin NCs was determined. Formation of Ins-GET NCs resulted

in disappearance of small-molecule peaks in zeta sizing (peaks present in unmodified insulin graphs), additionally complexation with GET-peptide led to charge reversal from negative (charge of unmodified insulin) to strongly positively charged, both of which confirmed the formation of NCs by linking two molecules via electrostatic interactions. CLSM images supplied visual evidence of enhanced cellular internalisation of Ins-F-GET NCs compared to Ins-F, hence confirming that GET system promotes insulin internalisation. ImageStream analysis suggested that Ins-F-GET NCs exhibit greater intracellular concentration compared to Ins-F, and exposure for greater time resulted in increased internalisation. Live/Dead cytotoxicity assay revealed that increasing GET-peptide concentration to 40 µM results in considerable cytotoxic effect on cell monolayers, while lower doses had no damaging effect on cells. Therefore, the GET-peptide concentration of 10 µM normally used for transfection and transcytosis assay is safe and has no damaging effect on membrane integrity and cytotoxicity.

The D-isoform of GET-peptide was stable to enzymatic degradation by Prot. K, while L-isoform was degraded, revealing that D-PLR is resistant to proteolytic action of enzymes. Sigma-FITC insulin was employed for stability testing because of its unique feature of displaying fluorescence quenching upon complexation with GET-peptide. Sigma-FITC insulin is labelled with FITC, which binds to both primary and secondary amines, resulting in unstable linkages due to lack of specificity, whereas NHS-Fluorescein-insulin exhibits specificity towards primary amine groups and is thus more stable. Stability testing using Ins-F*-GET NCs revealed that formulated NCs are stabilised by electrostatic interaction, as GET stayed attached to insulin despite adding excess of insulin. GET-based insulin NCs were unstable in biorelevant media, as the presence of enzymes caused the cleavage/disruption of these NCs, thus indicating that they may have limited application *in-vivo*. This degradation in presence of GI enzymes necessitates formulation of carrier system, hydrophobic modification of GET or covalent binding of insulin with GET. Another assay analysed NCs in monolayers indicating that NCs stayed intact even after translocation inside the cells. iLite insulin assay-reporter cells were used for evaluating the functional activity of formulated NCs, results provided positive insight into application of GET-peptide in enhancing insulin permeability across gut

epithelial barrier, moreover insulin maintained and preserved its functional activity after formulation as NCs with GET system via electrostatic binding. These results suggested that insulin preserves its biological activity despite linking non-covalently to positively charged GET-peptide, enabling it to serve as an alternative approach to enhance insulin permeation as a step forward towards non-parenteral insulin delivery.

Chapter 5. Enteric polymer-based microparticles for Insulin-GET NCs and their characterisation

5.1. Introduction

As evident from previous studies, promising results of CPPs in enhancing transmucosal delivery of therapeutic proteins need further improvement in terms of designing formulation using functional excipients and/or employing advanced technologies for developing a suitable final dosage form. Eudragit™ is the commercial brand name for a wide range of polymethacrylate copolymers marketed by Evonik Industries, based on methacrylic-acid and methacrylic/ acrylic esters or their derivatives, and can be classified as anionic, cationic and neutral. These polymers are mostly used in designing controlled delivery systems, and Eudragit NPs have been regarded as efficient devices for drug delivery since last decade. Eudragit polymers are nontoxic, non-biodegradable, and non-absorbable. Eud-L-100, Eud-S-100, and Eud-FS-30D are anionic polymers, Eud-L-100 dissolves at pH > 6 and is commonly employed for enteric coatings, while Eud-S-100 is used for colon targeting as it is soluble at pH >7. Eud-FS-30D was introduced by increasing the proportion of esterified groups in Eud-L-100 from 50% to 100%, it dissolves at pH > 6.8 and is available as aqueous dispersion [198]. For targeting lysosomes calcium phosphate/Eudragit-E-100 NPs have been designed, similarly enteric NPs based on Eud-L-100-55 loaded with omeprazole were developed to circumvent the GIT acidic environment. Nanoparticles based on Eud-S-100 polymer have been formulated as intra-vaginal and colon-specific drug delivery systems due to their dissolution above pH 7. Oral drug bioavailability can be enhanced using Eud-L-100 NPs and these NPs are also used as pH-sensitive delivery system for dexamethasone dermal delivery [199].

8R-conjugated-carboxymethyl-β-cyclodextrin inclusion-complexes facilitated insulin uptake leading to significantly higher insulin internalisation across Caco-2 monolayers compared to insulin/CM-β-CD. Moreover, *in-vivo* studies in rats showed significant hypoglycaemic response, with enhanced insulin permeability, and no signs of toxicity [127]. Novel mucus-penetrating, biomimetic virus-like and charge reversible NPs (P-R8-Pho NPs) were formulated for overcoming barriers of

both mucus and epithelial membrane. Owing to neutrally charged surface, these NPs achieved rapid mucus penetration. Additionally, intestinal alkaline phosphatase mediated hydrolysis of surface-anchored anionic Pho resulted in charge reversal (+7.37 mV) leading to exposure of cationic moieties (8R) which efficiently induced CPP-mediated enhanced transport. *In-vivo* studies in rats showed significant hypoglycaemic effect and greater oral BA compared to single CPP-modified-P-8R NPs [200]. The cellular uptake and transport of insulin-Tat complex from Eud-S100 coated chitosan NPs was significantly greater than the NPs loaded with free insulin. *In-vivo* studies carried out on diabetic mice and normal minipigs showed higher pharmacodynamic BA for insulin-Tat loaded ES-coated chitosan-NPs compared to insulin loaded ES-coated chitosan-NPs [201].

The present work sets out to investigate the potential of Eud-L100 MPs formulated by pH-dependent precipitation method, in providing stability and protection to insulin-GET NCs and to further improve permeability of these NCs across the biological membrane through membrane modulation. Initial work consisted of optimising the preparation method, characterising enteric MPs and testing them for *in-vitro* release and transcytosis assay using Caco-2 monolayers. The interaction between polymer and Ins-F-GET NCs was explored further by employing different assays to investigate the reason of interaction. To rectify this interaction, concentrations showing significant interactions were inspected using different procedures. Furthermore, different anionic Eudragit polymers were also studied for their effect on decomplexation of GET-based insulin NCs.

5.2. Experimental design

In this Chapter, the particular focus was to formulate carrier system for GET-based insulin NCs in the form of enteric MPs and to characterise them using different analytical techniques. Reference to each performed assay and respective detailed procedures can be located by referring to respective Sections as stated below. MPs were formulated using pH-dependent precipitation method as described in Section 2.28, the process was optimised to get particles of uniform size. This was followed by characterisation of MPs for their size, charge (Section 2.29.1) and morphology (Section 2.29.2) using DLS Zeta sizer and SEM microscopy, respectively. Following

this drug loading contents and entrapment efficiency was determined (Section 2.29.3), and subsequently dissolution studies were performed in different buffer media mimicking GI microenvironment (Section 2.29.4). Cellular internalisation of these NCs loaded MPs was carried out using Transwell® (Section 2.29.5). The interaction between polymer and GET-peptide leading to decomplexation was studied using different assays, such as testing cellular internalisation of NCs under different polymer concentration (Section 2.30.1), employing different ratios of various anionic/ enteric Eudragit polymers (Section 2.30.2), and directly studying influence on decoupling using dequenching assay by measuring sample fluorescence following exposure to different concentration of these polymers (Section 2.30.3). Various approaches were adopted for overcoming this polymer-induced decomplexation including; employing poly-cationic reagents (Section 2.31.1), saturating NCs with excess of GET-peptide (Section 2.31.2), and by altering process of formulation (Section 2.31.3).

5.3. Results and Discussion

5.3.1. Eud-L-100 MPs characterisation

5.3.1.1. Average diameter and surface charge of MPs

The freshly prepared control (unloaded) Eud-L-100 MPs (prior to freeze drying) suspended as microsuspension in water and 2% trehalose had a mean particle size of 880 nm and 1110 nm with a negative potential of -16.50 and -8.0 mV, respectively as shown in Table 1. Similarly, for the insulin-loaded MPs suspended in water and 2% trehalose the size was 890 nm and 1310 nm, with a zeta potential of -19.20 and -9.50 mV, respectively. The mean size of the freeze-dried control, insulin, and insulin-GET loaded MPs (using 2% trehalose as cryo-protectant) resuspended in water was 1210 nm, 1230 nm, and 1310 nm with an average zeta potential of -8.80 mV, -7.50 mV, and -8.50 mV, respectively. These results indicated that average size for freeze dried MPs was greater compared to freshly prepared MPs for both unloaded and insulin-loaded MPs. Additionally, use of cryoprotectant also resulted in slightly bigger MPs compared to MPs in water.

Earlier studies have reported that NPs formulated using various pH sensitive polymers (L100-55, S-100, L-100: RL-100 (3:1), HP-55, HP-50, and CAP) exhibited

the same trend, where lyophilised NPs exhibited greater average diameter than the non-lyophilised NPs. Whereas, lyophilisation in the presence of a cryoprotectant (3% mannitol) caused an increase in size of NPs for all formulations comparative to non-lyophilised [199]. Freshly prepared thiolated Eud-L-100 NPs (Eud-Cys NPs) had a mean particle diameter of 324.4 nm with negative surface charge of -3.1mV, whereas mean size of lyophilised NPs resuspended in water was larger than freshly prepared NPs [202]. Freshly prepared insulin-loaded-Eud-L100-Cys/GSH NPs displayed an average diameter of 260.0 nm and surface charge of -3.1mV, whereas lyophilised NPs resuspended in water had a greater average size than non-lyophilised (292.3nm) with a surface potential of -3.6mV [146]. Thus, these results are in agreement with the results obtained in our study where the freeze-dried particles exhibited greater size with strongly negatively charged surface compared to freshly prepared MPs.

Table 5. 1. Characteristics of blank and insulin -loaded Eud-MPs (n=4).

MPs	**Freshly prepared MPs**		**Lyophilised MPs resuspended in water**	
	Particle size (nm)	**Zeta potential (mV)**	**Particle size (nm)**	**Zeta potential (mV)**
Control MPs	880	-16.50	1210	-8.80
Ins-F-MPs	890	-19.20	1230	-7.50
Ins-F-GET-MPs	-	-	1310	-8.50

5.3.1.2. Scanning electron microscopy

The lyophilised drug loaded, and unloaded MPs appeared as yellowish and whitish powder, respectively and were easily re-suspended in aqueous media. The SEM imaging of MPs (Figure 5.1) revealed that MPs were uniform and spherical in shape showing a smooth surface. The SEM imaging results for size are in accordance with the DLS measurement, wherein control and insulin-loaded MPs in water had smaller size compared to MPs resuspended in trehalose.

Previous studies have reported use of numerous cryoprotectants to protect the biological samples from damage related to freezing and to improve the stability of

formulated micro/nano-particulates. Cryoprotectants tend to from H-bonds with samples in place of water molecules when they are displaced during freezing stage, thus providing insulation to most ice crystals. Therefore, cryoprotectants tend to prevent aggregation of particulates during storage, thus imparting improved stability to formulation. Stability of insulin-loaded PLGA NPs was assessed in the presence of different cryoprotectants (10% w/v) i.e. trehalose, sucrose, glucose, sorbitol and fructose for period of 6 months following ICH guidelines. Herein, incorporation of cryoprotectants increased the stability of NPs upon storage and had variable effects on particles size compared to NPs without any cryoprotectant. An increase in average size was reported with addition of sucrose (559nm), fructose (712nm), and sorbitol (469nm) as a cryoprotectant, while with trehalose (396nm) and glucose (365nm) there was slight decrease in size compared to NPs with no added cryoprotectant (422nm). TEM images revealed smooth and spherical particles in presence of these cryoprotectants with larger size [203, 204].

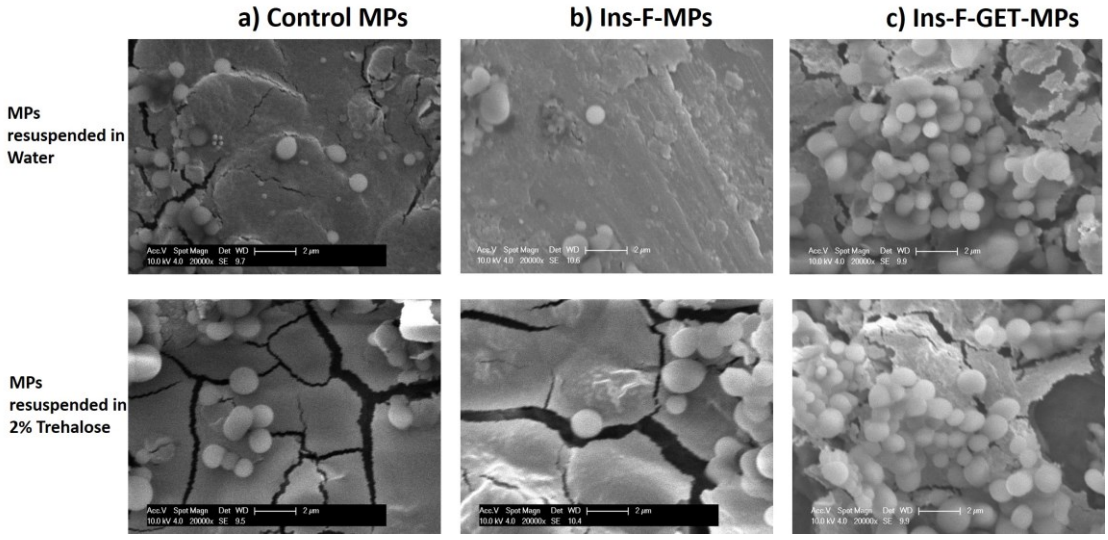

Figure 5. 1 Scanning electron micrographs of Eud-L100 MPs at 20K magnification prepared by precipitation method, where the freeze-dried MPs were resuspended either in pure DI water or 2% trehalose. (a) Control MPs, (b) Ins-F- loaded MPs, and (c) Ins-F-GET NCs loaded MPs. Cracks seen are from the platinum coating used for SEM visualisation. All numbers are in micrometers.

Doxorubicin-loaded polyethylene sebacate (PES) and pullulan NPs were developed using different cryoprotectants such as; trehalose, fructose and mannitol (2.5% - 15% w/v). An increase in mean particle size was observed on freeze drying in the presence of cryoprotectants compared to NPs freeze dried in the absence of these

agents. Interestingly, increased concentration of cryoprotectants resulted in a decrease in size of NPs, where 15% w/v cryoprotectants provided NPs with size almost equal to size of NPs without cryoprotectant, thus enabling control in size growth [205]. All of these earlier studies are in accordance with results of our study, where lyophilised MPs exhibited greater diameter compared to freshly prepared non-lyophilised MPs, additionally incorporation of cryoprotectant (Trehalose in this case) also contributed to larger particle size with smooth spherical shape.

5.3.1.3. Entrapment efficiency and Drug Loaded contents

The drug entrapment efficiency (%EE) was determined using both indirect and direct method and is listed in Table 2. Percent EE determined via direct method is more accurate and reliable, as in this case specific quantity of drug loaded MPs were re-dispersed/ dissolved in defined volume of PBS and amount entrapped was quantified by measuring the respective samples fluorescence as compared to indirect method where fluorescence/ absorbance of supernatant was measured following MPs preparation. The % EE determined for Ins-F-loaded MPs by indirect and direct method was found to be 77.21 % and 29.75 %, respectively while for Ins-F-GET-loaded MPs %EE by direct and indirect method was reported to be 23.36 % and 71.78 %, respectively. The percent drug loaded content for the MPs was only 2.24% w/w, whereas theoretical drug loading for these MPs was 7.5% w/w. These drug content values were too low and thus disadvantageous as they imply a very high drug wastage during the preparation and that large quantity of polymer/ carrier would be needed to encapsulate required dose of drug and to attain sufficient amount of drug at the site of action. This low incorporation efficiency of drug would be attribute to water soluble nature of insulin, which undergoes rapid partitioning into aqueous phase and thus leads to reduced entrapment into MPs during polymer precipitation/ deposition.

Eud-cys NPs exhibited higher loading efficiency (LE) and loading content (LC) of 96.4% and 19.4%, respectively, where oral administration of these NPs provided a prolonged hypoglycaemic effect with a relatively higher bioavailability [202]. Similarly lyophilised Eud-Cys/GSH NPs displayed lower % loading efficiency and % loading contents compared to freshly prepared NPs [146]. Insulin-loaded Chitosan

NPs had % EE of 82.5% with % drug loading of 17.2%, while Eud-S-100 coated insulin and insulin-Tat loaded NPs had %EE of 81.2% and 80.6%, respectively, with % LC of 15.2% and 13.4%, respectively [201]. Comparable results were observed in our study where insulin and insulin-GET loaded Eud-L-100 MPs exhibited higher percent entrapment efficiency (>70%). Whereas, Low drug incorporation of water-soluble drugs such as 5-fluorouracil and procaine HCL has been reported in PLGA NPs prepared by nanoprecipitation method [206, 207].

Table 5. 2. Percent entrapment efficiency measurements using direct and indirect method (n=4)

MPs	% Entrapment efficiency (Indirect method)	% Entrapment efficiency (Direct method)
Ins-F-MPs	77.21%	29.75%
Ins-F-GET-MPs	71.78%	23.36%

Dosing of insulin based on percent drug loaded contents in formulated enteric MPs was calculated as follows;

Potency of Human recombinant insulin: ≥27.5 units per mg

Theoretical Loaded Insulin = 500mcg/6.7 mg of Formulation = 7.5% w/w

Actual Loaded Insulin = 2.24 % w/w (150mcg drug/6.7mg formulation)

Means each mg of formulation has 22.38 mcg (0.02238 mg) of Insulin

Unit Conversions: 1 mg Insulin = 27.5 IU

0.0223 mg Insulin= 0.615 IU

Without severe insulin resistance, insulin dose lies between 0.5 and 1 unit/kg/day, while in prepubertal children it usually varies from 0.7 to 1 unit/kg/day. Assuming average adult body weight to be 72kg, dose per day would be calculated as;

0.5 x 72kg = 36 IU or

1 x 72kg = 72 IU

Thus, taking e.g. 60% 'for safety' 36- 72 units x 60% = 22- 44 IU / day

0.615 IU present in 1 mg of Formulation; so this dose of 22-44 IU will be present in 36-72 mg of formulation.

5.3.1.4. *In-vitro* release studies

The insulin release was evaluated by the centrifugation method under simulated GI conditions. As shown in Figure 5.2, the insulin was retained by the MPs at low gastric pH of 1.2, while a faster release was observed on changing the medium to nearly neutral/alkaline pH of intestine (either pH 6.8 or 7.4). About 20% and 40% of Ins-F and Ins-F-GET NCs were released from these MPs at pH 6.8 PBS within 0.5hr and 50% and 70% of Ins-F and Ins-GET NCs were released within 2 hr. Furthermore, insulin was found to have greater release from MPs in pH 7.4 buffer compared to in pH 6.8 buffer. At pH 7.4 medium, about 91% and 114% of Ins-F and Ins-F-GET NCs was released within 1 hr, and in 4 hr approximately 98% of Ins-F and 121% of Ins-F-GET NCs was released from MPs, and the release profile attained plateau after 2 hr, indicating that all of the loaded drug has been released. This suggested that MPs undergo more complete dissolution and release at pH 7.4 than at lower alkaline pH.

Insulin is a peptide with a PI of 5.3, at higher pH particularly above 6.0 it gets negatively charged, thereby maintaining a distance from the polyanion complex due to electrostatic repulsion. Insulin attains neutral charge when its PI is reached, resulting in diffusion of insulin into the polyanionic complex core via network structure onto the surface. Additionally, Ins-F-GET NCs are strongly positively charged (imparted by basic arginine residues of GET), which may further facilitate the diffusion of insulin into polyanionic core of MPs. As pH varies below the PI, the insulin is positively charged; leading to formation of MPs following the self-assembly of oppositely charged polyanionic microspheres (Eud-L-100) and thus encapsulating the drug (insulin). At pH 7.4, carboxyl groups of Eud-L-100 get ionised bearing a negative charge, the resultant electrostatic repulsion between polymer and insulin provides a major driving force for the release of insulin, as a result of their similar charge at neutral pH a competitive release takes place through the pores of polymeric material. The results of our study are in agreement with the previously reported studies where greater insulin release was reported from Eul-cys/GSH NPs at pH 7.4 than at pH 1.2 [146]. Poly-caprolactone/Eudragit NPs displayed initial burst release in PBS at pH 7.4 and 37^{o}C, where almost 43% drug was released within 30 min and approximately 69% of insulin was released in

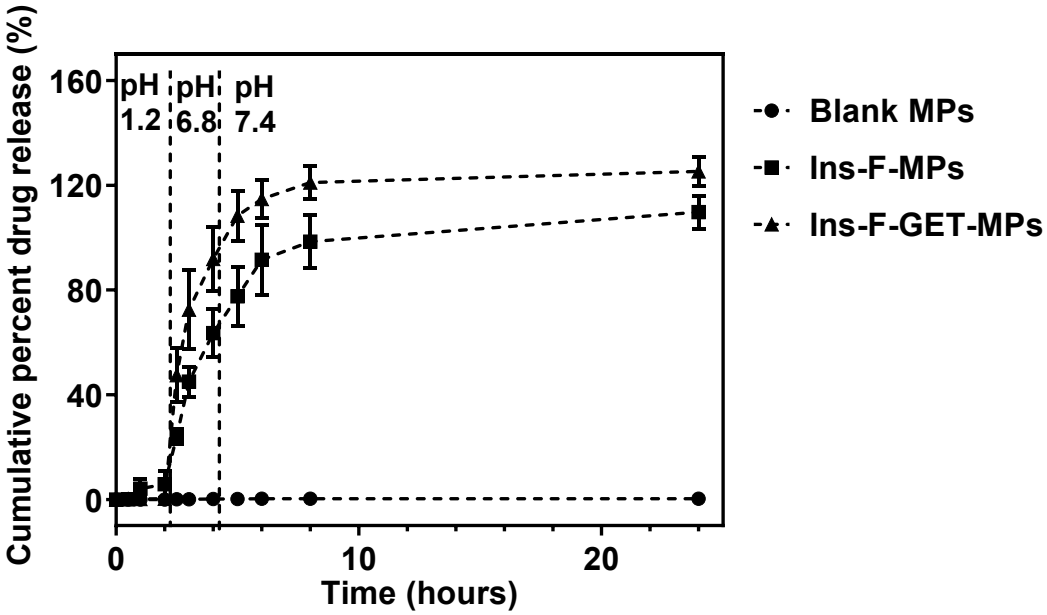

Figure 5. 2 *In-vitro* release profile of NHS-Fluorescein-insulin from freeze-dried Eud-L100 MPs at pH 1.2, 6.8, and 7.4. Cumulative release profile of blank MPs, Ins-F-MPs, and Ins-F-GET MPs at pH 1.2, 6.8, and 7.4 as a function of time, showing more insulin release at pH 7.4 compared to pH 6.8, and Ins-F-GET NCs exhibited greater release compared to Ins-F at all studied pH. Indicated values are mean ± S.D (n=5).

24 hr [208]. Similarly, another study reported pH-dependent release of insulin and insulin-Tat from the Eud-S-100 coated chitosan NPs, where less than 10% insulin was released from ES-Tat-cNPs during 4hr at pH 1.2, with 40% insulin release at pH 6.8 in 1 hr, while at pH 7.4 relatively fast and complete insulin release was attained within 6 hr [201]. All of these studies co-relate well with the results of our study, where the formulated Eud-L100 MPs provided pH-dependent release of insulin from MPs while protecting insulin from degradation at low acidic pH.

5.3.1.5. *In-vitro* cellular uptake across Caco-2 monolayers

Figure 5.3 shows the *in-vitro* cellular transport of insulin loaded Eud-L-100 MPs. Incubation of Ins-F-GET NCs loaded MPs with Caco-2 monolayers indicated no significant difference from the Ins-F-MPs. There was insignificant difference in cellular uptake of Ins-F-MPs and Ins-F-GET NCs MPs compared to Ins-F (control). This suggest that insulin released from these MPs is sufficiently stable and active to penetrate across the formed monolayer, while Ins-F-GET loaded MPs didn't promoted the insulin transport significantly, here GET mediated enhanced insulin

transport was not observed, this could be possibly due to interaction between polymer and GET-peptide.

Eud-L-100 is polyanionic polymer, the ratio of carboxylic groups to ester groups in Eud-L-100 is 1:1 with MW of 125,000g/mol, on the other hand insulin has MW of only 5805g/mol, being 22-times smaller in size compared to polymer. This high degree of anionic character imparted by carboxylic groups in Eud-L-100 together with its large MW contributes to competition between polymer and insulin for binding to GET-peptide. This competition between insulin and polymer for binding with positively charged GET may result in decoupling of GET from insulin-GET NCs and its binding to polymer, thus nullifying GET-peptide mediated enhanced insulin transport across the Caco-2 monolayers. Thus, indicating that GET-peptide decouples from Ins-F-GET NCs during formulation of MPs due to competition and interaction between polymer and insulin which might have resulted in poor transport of insulin across monolayers.

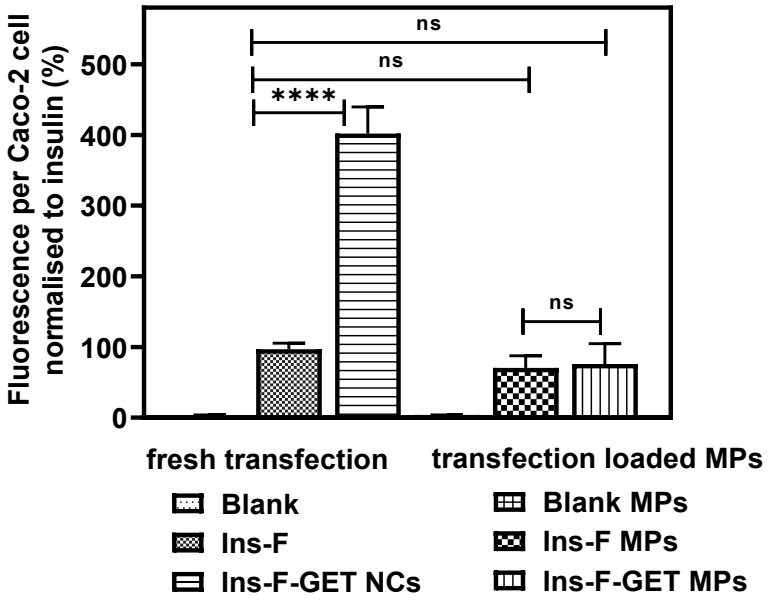

Figure 5. 3 Cellular uptake profile of Eud-L100 MPs across Caco-2 monolayers. Incubation of Caco-2 monolayers with Ins-F and Ins-F-GET loaded Eud-L100 MPs indicated that there is no significant improvement in cellular uptake of insulin upon encapsulation in MPs compared to the control where non-enveloped fresh Ins-F-GET NCs exhibited 4-fold greater cellular internalisation of insulin. All values are presented as mean ± S.D, n=5, * = *p-value* <0.05, **= *p-value* <0.005, ***=*p-value* <0.0005, ****= *p-value* <0.0001, and *ns*= not significant. One-way ANOVA with Tukey's test.

PEG-PGA enveloped 8R-insulin NCs exhibited very low insulin internalisation across Caco-2 monolayers in contrast with NCPs and PGA-PEG ENCPs where considerably high insulin internalisation of 79% and 48% was obtained, respectively. As the NCPs were not stable in intestinal fluids and unable to diffuse through the mucus barrier, therefore this high internalisation capacity of NCPs was not translated into the *in-vivo* situation [158].

5.3.2. Demonstrating interaction between polymer and peptide

5.3.2.1. Insulin internalisation assay in presence of Eud-L100

Figure 5.4 shows the effect of Eud-L100 solution on cellular internalisation of Ins-F and Ins-F-GET NCs upon incubation with Caco-2 monolayers under standard conditions. The intensity of fluorescent signals measured through flow cytometry was used as an indicator of quantification of cellular internalisation of insulin. Application of Eud-L-100 solution concentration equivalent to concentration in MPs suspension (0.8mg/ml), showed a significant reduction in cellular uptake of Ins-F-GET NCs compared to Ins (control, no added polymer or 0mg/ml) and Ins-F-

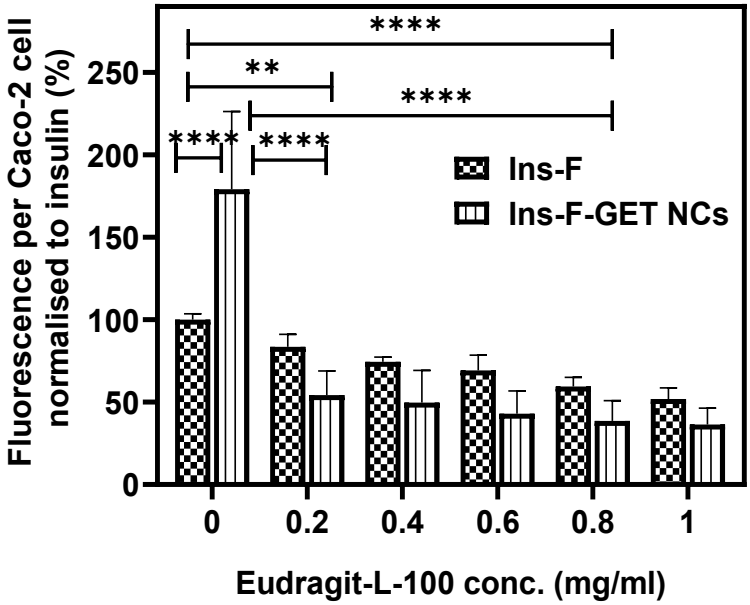

Figure 5. 4 Effect of Eud-L100 on cellular uptake and internalisation of NHS-Fluorescein-insulin (Ins-F and Ins-F-GET NCs) following 24 hr incubation with Caco-2 monolayers. Results are expressed as percent fluorescence per Caco-2 cell normalised to insulin, where all studied polymer concentration caused a significant reduction in cellular uptake of Ins-F and Ins-F-GET NCs. All values are presented as mean ± S.D, n=5, * = *p-value* <0.05, **= *p-value* <0.005, ***=*p-value* <0.0005, ****= *p-value* <0.0001, and *ns*= not significant. Two-way ANOVA with Tukey's test.

GET NCs (positive control, no added polymer). These results indicated that applying even lowest concentrations of polymer significantly affects the cellular uptake and internalisation of GET-based insulin NCs. These results clearly show interaction between polymer and GET-peptide, thereby suggesting that insulin may compete with polymer to bind with GET-peptide, as a result GET might decouple from NCs to get bonded to polymer, and thus nullifies the GET-peptide mediated enhanced cellular uptake of insulin.

5.3.2.2. Insulin internalisation assay in presence of other Eudragit polymers

The effect of Eud-S-100 and Eud-FS-30D on the cellular uptake of Ins-F and Ins-F-GET NCs across Caco-2 monolayers was studied and is presented in Figure 5.5a and 5.5b, respectively. Both profiles exhibited typical pattern of a concentration dependent steep decline in cellular internalisation of Ins-F and Ins-F-GET NCs across Caco-2 cells in presence of these polymers. Even lowest concentration of Eud-S-100 polymer (0.2mg/ml) caused a significant reduction in cellular uptake of both Ins-F and Ins-F-GET NCs compared to control (Ins-F and Ins-F-GET NCs with no polymer). Interestingly Eud-FS-30D exhibited variable effect on cellular internalisation of NCs where the low concentrations of Eud-FS-30D polymer (0.2 and 0.4mg/ml) caused a significant improvement of GET-peptide mediated transport of NCs compared to positive control (NCs with no polymer), while this low polymer contents had no effect on transport of un-modified insulin. This suggests that low concentration of Eud-FS-30D acts synergistically with GET-peptide to promote the cellular transport of Ins-F-GET NCs. However, increasing Eud-FS-30D concentration above 0.4mg/ml resulted in a considerable reduction in internalisation of NCs into cells.

These results indicated that anionic Eudragit polymers tend to prevent/ decrease the absorption, uptake and internalisation of both insulin and GET-based insulin NCs at concentration (0.8mg/ml) proposed to be used during preparation of Eudragit based MPs. This reduction in cellular uptake was observed even at lowest concentration of polymers (0.2mg/ml) for both Eud-L-100 and Eud-S-100. These results clearly indicated that strongly anionic Eudragit polymers (Eud-L100 with 1:1 of carboxylic to ester groups and Eud-S100 with 1:2 carboxylic to ester groups) interfere and interact with GET, thus preventing the GET-peptide mediated

enhanced insulin transport across the cells. On the other hand, reducing degree of anionic character by selecting polymers with less free anionic groups such as -COOH group in this case, may prevent this interaction between polymer and GET and thus might avoid decreased cellular uptake of NCs in presence of polymer. Therefore, it could be concluded that an appropriate polymer or blend of polymers needs to be selected with less anionic character (free -COOH groups). This should maintain pH-dependent release at alkaline pH and prevent drug release under acidic conditions to protect insulin from harsh GI conditions. Alternatively, a biomimetic delivery system could be formulated for Ins-F-GET NCs. This system would hold densely charged surface consisting of both cationic and anionic groups but yet overall neutrally charged, which would envelop cationic insulin-GET NCs. Upon enzymatic cleavage, this system will reveal cationic surface which in turn will facilitate cellular uptake. With these novel biomimetic systems, it would be possible to attain desired feature of protection, pH-dependent release, no decomplexation of NCs, yet maintaining the CPP-mediated enhanced cellular internalisation of insulin.

Oral delivery of micro- or nano-particulates must overcome two barriers, firstly the mucus layer which is secreted continuously and fully covers the intestinal epithelium and secondly the intestinal epithelial cells. Intestinal mucus is regarded robust barrier which has tendency to immobilise and remove bacteria, pathogens and even exotic particles such as delivery system possessing hydrophobic and cationic properties [209, 210]. For overcoming this mucosal barrier, small mucus-penetrating particles with hydrophilic and neutral charge (PEGylation/ mucus insert effect) were developed, due to their inherent ability to diffuse unhindered across the mucus. But this mucus insert surface generates issues related to less affinity towards lipophilic and negatively charged cellular membrane which might result in an inefficient cellular uptake [211]. It's important to note that delivery systems designed to overcome these two barriers need unique or even extraordinary surface properties such as; neutrally charged and hydrophilic surface for bypassing mucosal barrier, and cationic and hydrophobic surface for crossing epithelial barrier thus rendering them intractable in a single delivery system [212]. Viruses display distinctive surface properties i.e. densely charged with both cationic and

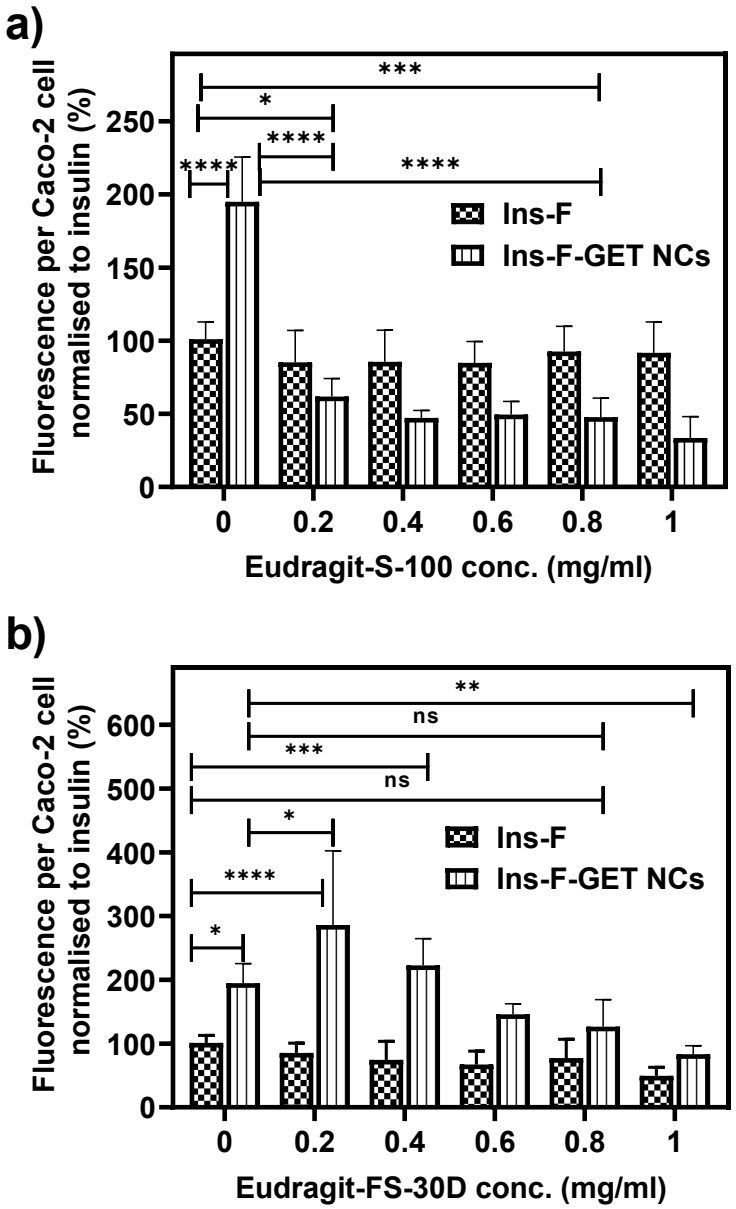

Figure 5. 5 Effect of Eudragit polymers on cellular uptake and internalisation of NHS-Fluorescein-insulin (Ins-F and Ins-F-GET NCs) following 24 hr incubation with Caco-2 monolayers; a) Eud-S-100 all used concentrations resulted in marked reduction in internalisation of both Ins-F and Ins-F-GET NCs, and b) Eud-FS-30D where low polymer contents synergistically improved GET mediated insulin uptake but higher concentration decreased the cellular uptake. All values are presented as mean ± S.D, n=5, * = *p-value* <0.05, **= *p-value* <0.005, ***=*p-value* <0.0005, ****= *p-value* <0.0001, and *ns*= not significant. Two-way ANOVA with Tukey's test.

anionic groups but yet possessing overall neutral surface. Therefore, its possible to introduce anionic groups into cationic-CPP based delivery systems (micro/nano-particles), i.e. biomimetic systems which would rapidly diffuse across mucus and will subsequently undergo direct translocation across the epithelium [209, 213].

Protein corona liposomes (PcCLs) displaying diametrically opposite surface properties have been developed, where hydrophilic and neutrally charged surface of PcCLs facilitated the mucus penetration. Gradual enzymatic degradation of protein corona exposed CLs, where charge reversal from negative to positive promoted the transepithelial transport of insulin [214]. Simple dilauroyl phosphatidylcholine (DLPC) and poly-lactic acid (PLA) NPs are densely coated with zwitterions, with excellent mucus penetration ability that contributed towards high affinity for epithelial cells and strong interaction with cell surface transporter PEPT1. Thus, leading to significant improvement of (4.5-fold) cellular uptake of DLPC NPs in comparison to PEGylated NPs and displayed greater oral BA compared to free insulin [215].

5.3.2.3. Dequenching using different Eudragit polymers

The dequenching assay was conducted using Sigma-FITC insulin or Ins-F* to further confirm the interaction and interference of Eudragit polymers with Ins-F*-GET NCs which caused reduced cellular uptake of NC-loaded Eud-MPs. Here, again Ins-F*-GET NCs were incubated with progressively increasing concentrations of different anionic Eudragit polymer and fluorescent intensities of samples were measured as function of time using a microplate reader (Figure 5.6). Thus, degree of dequenching or recovery of sample fluorescence was used as an indicator of decoupling of GET-peptide from insulin and therefore to predict the stability of these NCs in the presence of polymers. As a control for comparison, the effect of various concentrations of different Eudragit polymers (Eud-L100, Eud-S100, Eud-FS-30D) was studied on free Ins-F* as shown in Figure 5.6a-5.6c, while positive control consisted of Ins-F* and Ins-F*-GET with no added polymer. The results showed an increase in fluorescence of Ins-F* with all studied concentration of Eudragit-polymers, which could be attributed to dilution of samples and moving insulin-molecules apart which altogether contributed towards increased fluorescent signals.

Figure 5.6d, shows instantaneous and complete dequenching of fluorescent intensity of Ins-F*-GET NCs (statistically significant) within 10-30min with lowest concentration (0.1mg/ml) of Eud-L100, and this effect was consistent with all the

studied concentrations of polymer. These results indicated that Eud-L100 (1:1 ratio of free -COOH to ester group) is strongly negatively charged where even lowest amounts of polymer (0.1mg/ml) also exhibited high affinity for GET-peptide resulting in immediate decoupling of GET from NCs as reflected by fluorescence recovery of NCs, thus confirming the interaction between polymer and GET-peptide. With Eud-S100, dequenching was not immediate, where 80-90% sample fluorescence was recovered in 4 hr (240 min), and complete fluorescence recovery was attained in 24 hr (Figure 5.6e). This slower dequenching by Eud-S100 (1:2 ratio of free -COOH to ester group) could be attributed to lesser anionic/ carboxylic groups in this polymer compared to Eud-L100, which might take longer to decouple GET from NCs, with complete fluorescence recovery in 24hr. This suggests that reduced anionicity of polymer tends to delay the process of decomplexation of GET-peptide.

Interestingly with Eud-FS-30D (1:10 ratio of free -COOH to ester group, MW 280000g/mol), the dequenching of fluorescence was much delayed, moreover complete fluorescence recovery was not observed for studied concentrations (Figure 5.6f). A time and concentration dependent effect was observed on dequenching, where the sample fluorescence values were increased slowly over time and this effect was also dependent on amount of added polymer in reaction mixture. The low concentrations (0.1 and 0.2mg/ml) of Eud-FS-30D provided 55-60% fluorescence recovery in 4 hr and not more then 60-70% recovery of fluorescent signals in 24 hr. Even with the highest amount (0.8 and 1mg/ml) of Eud-FS-30D, no complete fluorescence recovery was seen over the course of 24 hr. Therefore, it can be concluded that controlling the degree of anionicity and number of free carboxylic groups in polymer or by choosing polymer with reduced anionic character, this polymer mediated decoupling/ decomplexation of GET from NCs could be prevented preferentially.

These results are in agreement with the results obtained in Section 5.3.2.2 where both Eud-L100 and Eud-S100 caused significant reduction in cellular uptake of Ins-F-GET NCs even with the lowest amounts of polymers (0.2mg/ml), while with Eud-FS-30D low doses of polymer acted synergistically with GET-peptide to improve

cellular uptake of insulin but there was reduction in uptake on higher doses. These results also explain the failure of Eud-L100 MPs in promoting the *in- vitro* transport

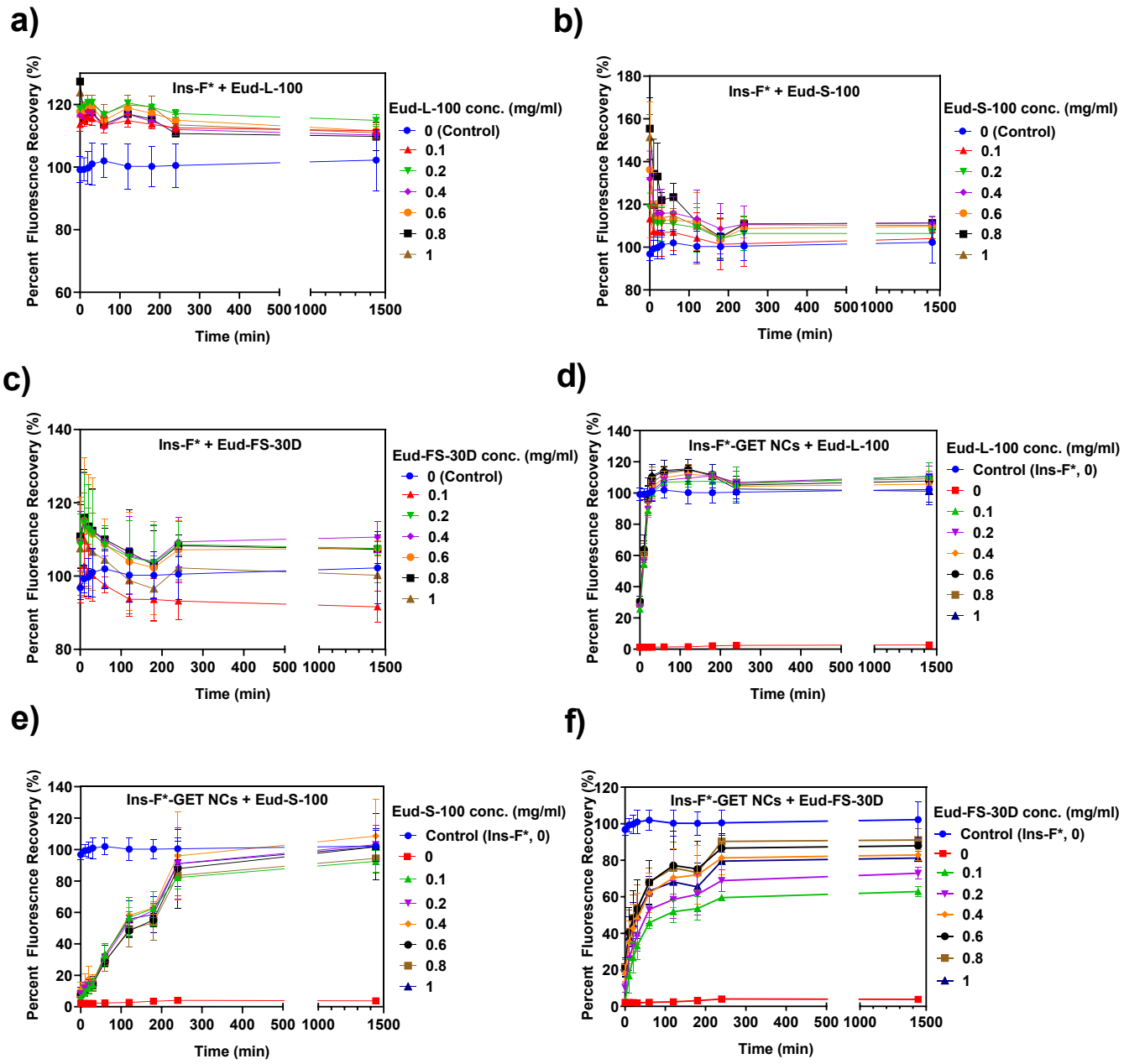

Figure 5. 6 Eudragit polymers decomplexes GET-peptide from Ins-F* (Sigma-FITC-insulin) resulting in recovery of fluorescence. Ins-F* dequenching with a) Eud-L-100, b) Eud-S-100, c) Eud-FS-30D showing increase in sample fluorescence on exposure to these polymeric solutions possibly due to dilution effect. Ins-F*-GET NCs fluorescence dequenching with d) Eud-L-100 showing instantaneous complete fluorescence recovery within 30min, e) Eud-S-100 caused full recovery of fluorescence in 24 hr, and f) with Eud-FS-30D full fluorescence recovery was not observed. All values are presented as mean ± S.D, n=5, * = *p-value* <0.05, **= *p-value* <0.005, ***=*p-value* <0.0005, ****= *p-value* <0.0001, and *ns*= not significant. Two-way ANOVA with Tukey's test.

across Caco-2-monolayers (section 5.3.1.5), as during MPs preparation there was greater likelihood for GET getting decoupled from Ins-F-GET NCs and to irreversibly bound to polymer and thus abolishing the GET-mediated enhanced insulin uptake and internalisation across Caco-2 monolayers.

5.3.3. Strategies for overcoming interaction between polymer and GET

5.3.3.1. Using different poly-cationic amino acids

The introduction of poly-cationic species may prevent the disruption of electrostatic interaction between GET-peptide and insulin in the presence of polymer, or may serve as an approach to counteract the negative charges or to interact with groups imparting anionic character in an attempt to stabilise the complex in the presence of enteric polymers. Figure 5.7. shows the effect of different poly-cationic species (L-histidine and PLL) on cellular internalisation of Ins-F and Ins-F-GET NCs. Control consisted of Ins-F and Ins-F-GET NCs with no added polymer (1mg/ml) and no poly-cations, and sample fluorescence (cellular internalisation) was compared with these controls. Addition of 1mg/ml L-histidine showed no significant enhancement in cellular uptake of NCs compared to Ins-F, while simultaneous addition of higher concentration of L-histidine showed variable effects. Overall, addition of L-histidine resulted in further reduction in internalisation compared to samples containing NCs with polymer and no L-histidine. At 10mM L-histidine, the cellular uptake of NCs was significantly decreased compared to control, additionally increasing amounts of L-histidine (40 and 80mM) also had negative effects on cellular uptake of NCs. For Ins-F, addition of L-histidine at all concentration had no significant effect in improving insulin internalisation.

Similarly, effect of PLL on cellular internalisation of Ins-F and NCs is shown in Figure 5.7b. The results clearly indicated that GET-peptide mediated enhanced cellular uptake of NCs (control, values compared with Ins-F) was significantly decreased in presence of 1mg/ml polymer (Eud-L100). PLL had no beneficial effect in overcoming the effect of polymer and there was no improvement in cellular internalisation of Ins-F and Ins-F-GET NCs on increasing the concentration of PLL from 0 to 80mM.

This could be possibly due to fact that low MW PLL (4KDa) was not efficient enough to counteract the negative charges of polymer.

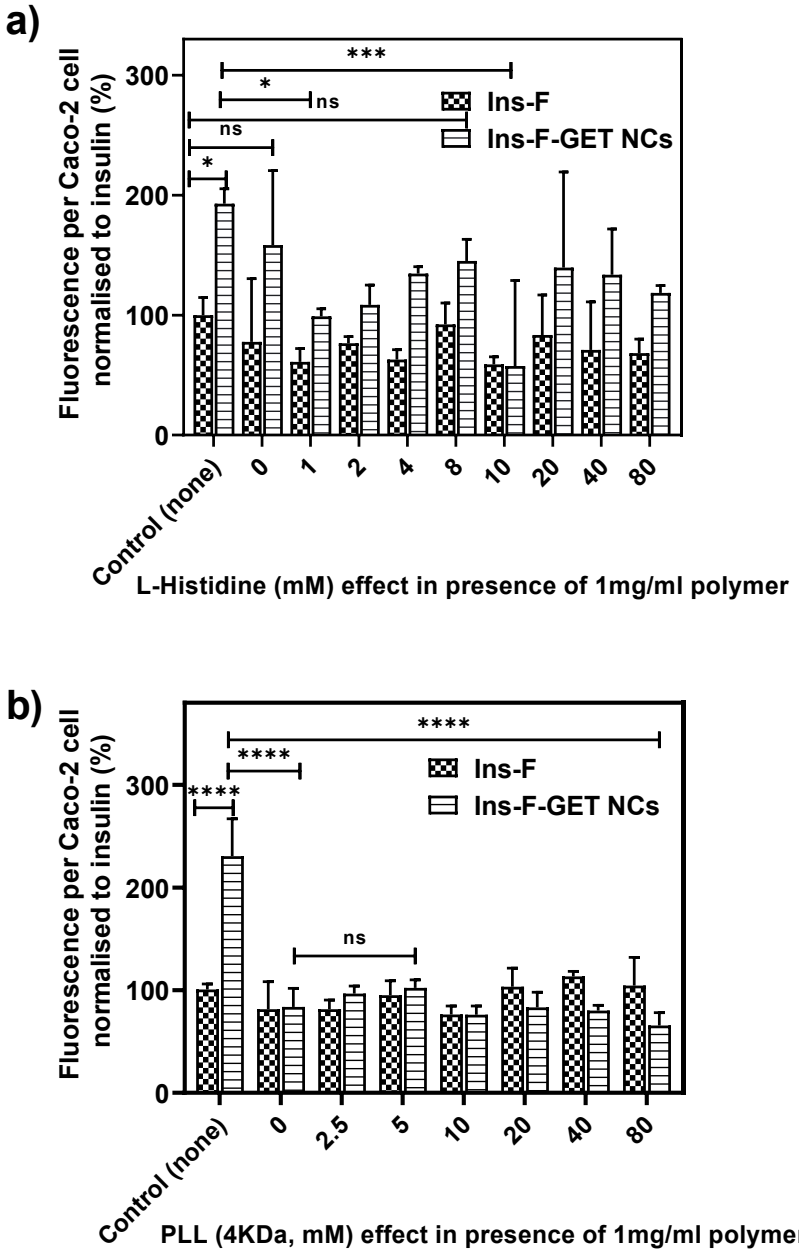

Figure 5. 7 Effect of poly-cationic amino acids on cellular internalisation of NHS-Fluorescein insulin (Ins-F and Ins-F-GET NCs). a) L-histidine exhibited variable effect on internalisation of NCs, there was no significant enhancement in internalisation of NCs in presence of polymer, control consisted of Ins-F and Ins-F-GET NCs in SFM with no polymer and no L-histidine, and b) poly-L-lysine due to its low MW showed no effect on uptake of both Ins-F and Ins-F-GET NCs in presence of polymer, control consisted of Ins-F and Ins-F-GET NCs in SFM with no polymer and no PLL. All values are presented as mean ± S.D, n=5, * = *p-value* <0.05, **= *p-value* <0.005, ***=*p-value* <0.0005, ****= *p-value* <0.0001, and *ns*= not significant. Two-way ANOVA with Tukey's test.

The second part of this approach was based on employing dequenching and quenching assay to analyse the effect of high MW PLL to recover the fluorescence of Ins-F*-GET NCs. PLL (70-150KDa, 0.01%) was added in different concentration to NCs, results were expressed as percent fluorescence recovery compared to control i.e. Ins-F* (fully fluorescent, no polymer serving as positive control) and Ins-F*-GET NCs (negative control with 100% quenching) with no added polymer (Figure 5.8a). Complete dequenching was achieved within 30-60 min following polymer addition (1mg/ml, Eud-L-100), adding PLL in low doses (0.0015, 0.0031, and 0.00625 mg/ml) had no effect on sample fluorescence. On increasing PLL concentration to 0.0125mg/ml, 50% dequenching of samples was attained, thus indicating that high doses of PLL could possibly prevent the decoupling of GET-peptide from NCs, hence stabilising the NCs partially.

To further explore effect of high MW PLL on stabilising NCs, different concentrations of PLL were incubated with Ins-F*GET-NCs in presence of two different levels of polymer (1mg/ml and 0.5mg/ml). Results were expressed as % fluorescence recovery as given in Figure 5.8b and c, respectively. At 1mg/ml polymer concentration, addition of 0.02mg/ml PLL (70-150KDa) caused 80% fluorescence recovery in 4hr, while increasing PLL concentration to 0.04mg/ml resulted only in 20% dequenching of fluorescence in specified time, indicating that high concentration of high MW PLL prevents decoupling of GET form NCs and stabilises NCs from getting degraded. While in presence of 0.5mg/ml polymer, only 50% sample fluorescence was recovered with 0.02mg/ml of PLL in 4hr, while at 0.04mg/ml PLL, only 15-20% sample fluorescence was dequenched in stated time, thus indicating that reducing polymer contents from 1mg/ml to 0.5mg/ml tends to enhance the protecting effect of PLL on NCs. These results suggested that tailoring the polymer concentration and using right type and concentration of poly-cations may result in protection and stabilisation of NCs which in turn could prevent polymer mediated decoupling of GET from NCs.

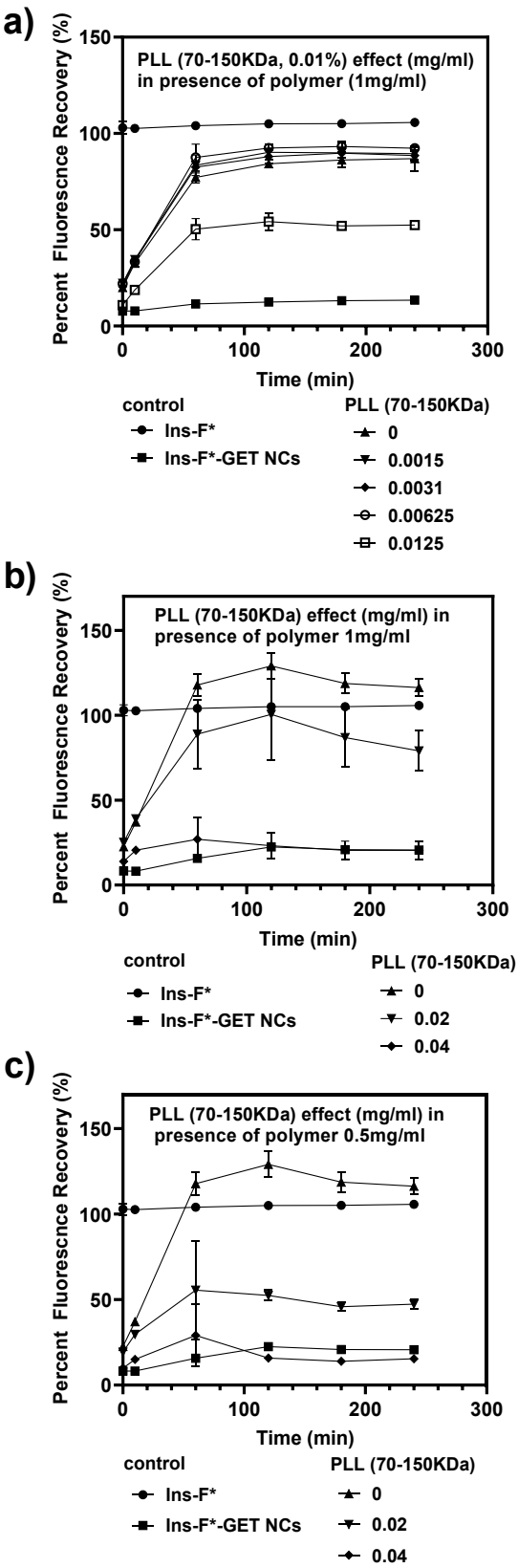

Figure 5. 8 Effect of high molecular weight poly-L-lysine was studied on quenching and dequenching of Ins-F*-GET NCs (Sigma-FITC-insulin based NCs) in the presence of polymer in an attempt to prevent polymer-induced decoupling of GET from NCs, control consisted of Ins-F* and Ins-F*-GET NCs untreated with polymer and with no addition of PLL. a) PLL in low doses had no significant effect on fluorescent values,

b) PLL effect in presence of 1mg/ml polymer indicated that high dose (0.04mg/ml) of PLL prevents the decoupling of GET from NCs vs 0.02mg/ml PLL compared to Ins-F*-GET NCs (control), and c) PLL effect in presence of 0.5mg/ml polymer showed that reducing polymer concentration tends to prevent the decoupling of GET at both studied concentrations of PLL (0.02mg/ml and 0.04mg/ml). All values are presented as mean ± S.D, n=5, * = *p-value* <0.05, **= *p-value* <0.005, ***=*p-value* <0.0005, ****= *p-value* <0.0001, and *ns*= not significant. Two-way ANOVA with Tukey's test.

5.3.3.2. Saturation with GET-peptide

Figure 5.9 shows another approach for stabilising Ins-F*-GET NCs in presence of 1mg/ml polymer (Eud-L-100) by adding excess of GET-peptide to reverse the dequenching, results were expressed as media relative fluorescence units. Control consisted of Ins-F* (fully fluorescent) and Ins-F*-GET NCs (100% quenched due to complexation with GET peptide, indicator of stable and intact NCs). The results indicated that addition of excess of GET caused no reversal of fluorescence quenching of insulin, suggesting that GET binds irreversibly to highly negatively charged polymer. Adding excess of GET until 24x concentration had no effect on fluorescence values, while further addition of 34x, 44x and 54x caused a significant reduction in fluorescent intensity of Ins-F* but still there was no 100% fluorescence quenching, moreover the reaction mixture turned turbid.

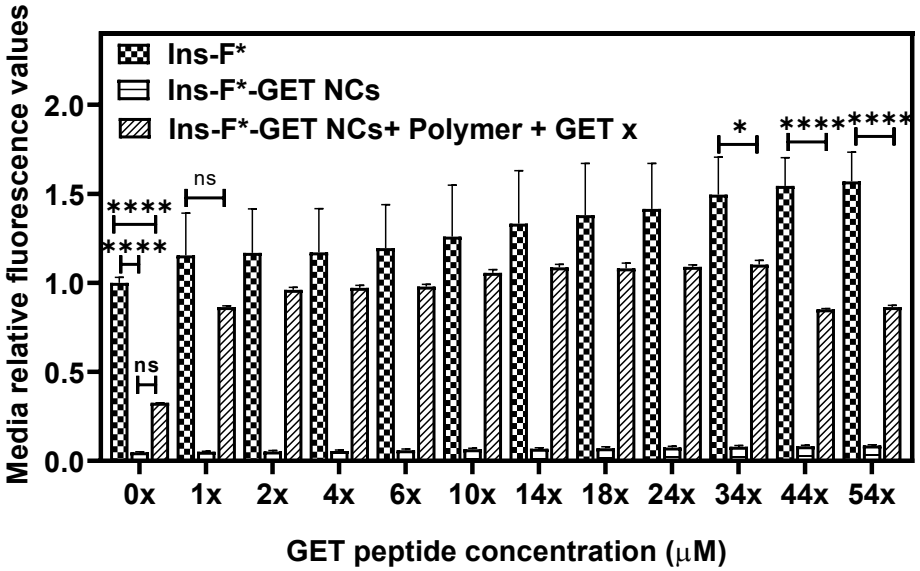

Figure 5. 9 Effect of addition of excess GET-peptide on fluorescence quenching and dequenching of Ins-F*-GET NCs (Sigma-FITC insulin based NCs). Dequenched fluorescence of NCs caused by polymer was not completely reversed on addition of excess GET, adding 34x-54x concentration of GET peptide only caused partial

fluorescence quenching indicating that added GET tends to bound with polymer. All values are presented as mean ± S.D, n=3, * = *p-value* <0.05, **= *p-value* <0.005, ***=*p-value* <0.0005, ****= *p-value* <0.0001, and *ns*= not significant. One-way ANOVA with Tukey's test.

Owing to high MW of polymer and being densely negatively charged compared to insulin, both factors contributed to irreversible decomplexation of GET from NCs, where even addition of excess GET upto 54-fold didn't reversed back the quenching completely. Therefore, it can be concluded that addition of excess GET or saturation with GET does not reverses dequenching, it can be speculated that even excess of GET gets bound to polymer due to high degree of free -COOH groups in polymer, and as a result complete quenching of insulin was not achievable.

5.3.3.3. Order of addition testing for formulation variables

Another approach for overcoming polymer induced decomplexation of Ins-F-GET NCs during formulation of Eud-L100 MPs, was to alter the order of mixing and to use excess of GET (10µM, 20µM, and 30µM) in NCs during MPs preparation, as shown in Figure 5.10. The results indicated that altering order of mixing had no

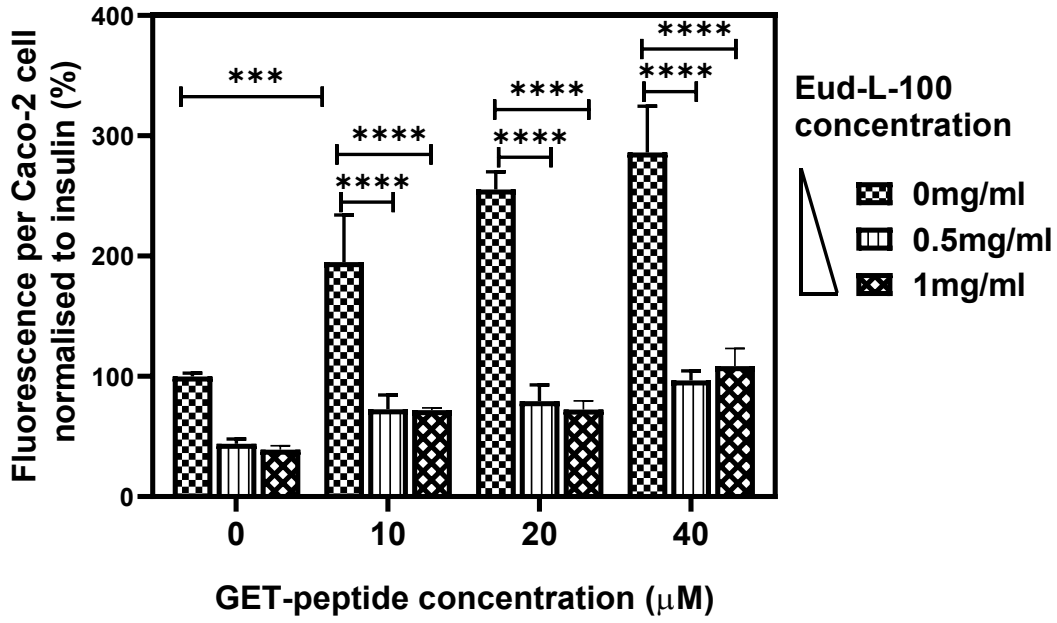

Figure 5. 10 Effect of altering order of mixing during formulation of MPs was evaluated on cellular internalisation of NHS-Fluorescein-insulin (Ins-F and Ins-F-GET NCs) formed with different concentration of GET-peptide in the presence of different concentration of polymer. These was no significant effect on cellular internalisation of Ins-F-GET NCs (with different GET) on changing the order of mixing for MPs formulation. All values are presented as mean ± S.D, n=2, * = *p-*

value <0.05, **= *p-value* <0.005, ***=*p-value* <0.0005, ****= *p-value* <0.0001, and *ns*= not significant. Two-way ANOVA with Tukey's test.

significant effect on improving the cellular internalisation for all NCs formulated with different GET contents. Additionally, lowering polymer concentration to half during MPs preparation, also showed insignificant effect on cellular internalisation of MPs. These results suggested that despite changing order of mixing, reducing polymer content to half, and even increasing GET contents to twice or thrice times of normally used concentration for NCs, had no protective effect on polymer induced decoupling of GET from NCs and did not imparted stabilisation to NCs, with no beneficial effect of this approach on improving cellular internalisation of Ins-F-GET NCs.

5.4. Conclusion

This chapter demonstrates use of pH-sensitive polymer (Eud-L-100) to fabricate microparticulates to serves as an enteric coated carrier system for Ins-F-GET NCs. Eud-L-100 MPs were synthesised using pH-dependent microprecipitation method, these MPs exhibited an average particle size of 1100-1300 nm and negative zeta potential (-8 to -7 mV). These particles had low drug loaded contents (2.24% w/w), which is disadvantageous as there is loss of more than 50% of drug, reflecting increased cost to achieve desired dosage. Thus, its necessary to adopt alternative methods which would provide increased drug loading. The insulin release from Eud-L100 MPs showed that these MPs prevent insulin release under simulated gastric media while maximum drug release was observed in PBS (pH 7.4). The *in-vitro* cellular uptake studies revealed that these MPs displayed no improvement in cellular internalisation, where GET-peptide mediated enhanced insulin transport and internalisation was abolished when formulated as MPs. This abolishing effect was further evaluated using different assay to demonstrate the possible interaction between the polymer and GET-peptide, which resulted in decoupling of GET from the NCs during preparation of MPs (step of mixing polymer with either Ins-F or Ins-F-GET NCs, and then lowering pH to form MPs).

To further confirm this decoupling and interaction of polymer and GET-peptide, the effect of different Eudragit polymers was directly assessed on internalisation of

both Ins-F and Ins-F-GET NCs and dequenching assays were also performed. Results indicated that Eud-L-100 and Eud-S-100 significantly reduced the cellular internalisation of NCs, while with Eud-FS-30D lower doses acted synergistically to improve the GET-mediated insulin transport but higher doses caused decreased cellular internalisation. Eud-L-100 and Eud-S-100 completely recovered the fluorescence (dequenching) of NCs, while with Eud-FS-30D only 50-60% dequenching was observed with the highest dose, thus suggesting that reduced degree of anionic character may prevent this polymer mediated decomplexation. Different strategies were employed to overcome this polymer mediated decomplexation of GET from NCs such as; using different poly-cations, saturation with GET, and changing the order of mixing during MPs preparation. Based on results obtained it can be concluded that this polymer mediated decomplexation /destabilisation of NCs can be prevented by reducing the degree of anionicity of polymer or tailoring the polymers and employing appropriate combination of polymers which would provide pH-dependent release at alkaline pH, will prevent drug release at acidic pH and protect NCs from degradation in harsh GI conditions. Alternatively, such delivery systems could be designed which are overall neutrally charged but carry both anionic and cationic species, here the hydrophilic neutral surface would promote passage through mucosal barriers while the hydrophobic and cationic surface would enhance cell-surface interaction which will enable efficient internalisation. Additionally, formulating polymeric delivery systems densely coated with zwitterion would also serve as an efficient carrier for overcoming both mucosal and epithelial barriers to achieve efficient drug delivery with improved bioavailability for therapeutic proteins.

Chapter 6. Enteric coated minicapsules loaded with freeze-dried NCs

6.1. Introduction

Capsules are considered one of the convenient drug delivery system (DDS), as these can control the release and stability of drugs in GIT and are being employed to deliver wide range of drugs orally. Factors which influence formulation's performance are; rate of capsule swelling and disintegration, water penetration in formulation, and release of drug contents in GIT, all of which ultimately influence the bioavailability of drugs. In pharmaceutical industry, enteric coatings are being used extensively and have been widely experimented in an attempt for oral insulin delivery. It has been proposed that it's possible to achieve greater insulin BA by designing "site-specific" insulin release in locations further down in the GIT. One of the earliest applications for oral insulin delivery consisted of different formulations based on insulin loaded polyacrylic-coated gelatin capsules, which exhibited pH-dependent release kinetics. Results indicated that Eud-RS1 and -RS2 based systems containing insulin, provided significant reductions in blood glucose levels when delivered orally with significant pharmacological bio-availabilities [216]. In another study, capsules were coated using different Eudragit polymers (Eud-L100 and -S100), where Eud-S100 capsules showed slower release at pH 7 in comparison to Eud-L100 capsules. *In-vivo* studies indicated that Eud-L100 capsules released most of the insulin in stomach, duodenum and jejunum regions, while Eud-S100 coated capsules provided insulin release in ileal segments of small intestine [217].

Freeze drying is regarded as one of the most useful methods for handling and stabilising the micro- and nanoparticulate systems. During freeze drying process the removal of water from protein loaded micro-/ nanoparticulates may be fundamental step to promote the stability of loaded protein and to avoid the hydrolytic degradation of these particle matrix in aqueous suspension [218, 219]. Many sugars or polyols are employed as nonspecific protein stabilisers in solution during freeze-drying and freeze-thawing thus serving both as effective lyoprotectants and cryoprotectants, examples include glucose, fructose, trehalose, sucrose, and sorbitol. Cryoprotectants tend to minimise instability of NPs during freeze -drying process, protecting them against mechanical stress of ice crystals,

prevents their aggregation, and additionally preserves the proteins native structure after freeze drying. The glass transition temperature of polymeric matrixes could be affected by cryoprotectants, which is crucial factor in obtaining cake with a stable amorphous form, good redispersibility, appropriate residual water contents, and most importantly excellent protein stabilisation upon storage [218, 220-222].

L-asparaginase was protected from dissociation during freeze drying by using 2% glucose or lactose, while 2% mannitol didn't provided this protection possibly due to loss of close interaction with protein and its crystallisation [223]. The formation of dimers in TNF was inhibited during storage at 37 °C by both trehalose and sucrose [224]. Similarly, glycine alone or in combination with mannitol reduced the aggregation of lyophilised antibody-vinca-conjugate upon storage at 25°C [225]. Mannitol has been reported to protect LDH during freeze-thawing at range of 0.5–1 M [226]. Glycine and mannitol are most frequently used bulking agents, where glycine offers several advantages such as high solubility, non-toxicity, and high eutectic temperature [227].

For many proteins conversion of α-helix to β-sheet has been observed during lyophilisation in water such as human recombinant albumin, bovine pancreatic trypsin inhibitor, chymotrypsinogen, and porcine insulin [219]. Insulin is far more stable in its freeze-dried amorphous state compared to its crystalline state against dimer formation and deamidation at water concentrations up to 15% [228]. Protein–protein aggregation and interaction can be prevented by physical dilution and separation of protein molecules, same mechanism has been proposed for stabilisation of certain proteins including insulin in presence of trehalose by inhibition of covalent dimerisation at 35°C [229]. Similarly, dextrose has been employed to significantly inhibit the moisture-induced aggregation of bovine insulin at 1:1 ratio of protein to excipient, on the other hand trehalose had no significant effect in stabilising the protein [230].

In this chapter, enteric-coated M-Caps loaded with freeze-dried Ins-F and Ins-F-GET NCs were developed for the oral insulin delivery. This study was based on basic concept that enteric-coated M-Caps would stay intact under the acidic conditions of stomach but will undergo rapid dissolution in basic environment of small intestine. Thus, these enteric M-Caps could prevent release and disintegration of

freeze dried NCs in the stomach and will subsequently increase the amount of intact NCs being delivered to the proximal segment of small intestine, which in turn may contribute to increased insulin bioavailability.

6.2. Experimental design

Last chapter of this draft outlines process to freeze-dry insulin and GET-based insulin NCs employing bulking agents, testing them *in-vitro* on Caco-2 monolayers and formulating enteric polymer coated mini-capsules. Reference to each performed assay and respective detailed procedures can be located by referring to respective Sections as stated below. Firstly, cellular internalisation of free and GET-modified insulin was tested in presence of different bulking agents and their combination (Section 2.23.1), this was followed by freeze drying of NCs along with added proportion of cryoprotectants (Section 2.23.2). These NCs freeze-dried with bulking agents were then studied for their cellular uptake across grown monolayers (Section 2.23.3). Next step was to establish protocol for coating mini-capsules with aqueous enteric polymer solution using manual dipping (Section 2.23.4). Lastly, these capsules were tested for *in-vitro* release in Biorelevant media both in presence and absence of GI enzymes (Section 2.23.5).

6.3. Results and discussion

6.3.1. Cellular internalisation in presence of different bulking agents

Figure 6.1 shows the cellular internalisation of Ins-F and Ins-F-GET NCs across Caco-2 monolayers upon co-incubation with various bulking agents. D-mannitol was tested in concentration ranging from 0-40mg/ml (Figure 6.1a). Although the cellular internalisation of NCs was reduced insignificantly in presence of D-mannitol but still there was significant cellular uptake of NCs in presence of all tested concentration of D-mannitol compared to control (Ins-F). Likewise, in presence of different amount of sucrose the cellular internalisation of both Ins-F and Ins-F-GET NCs was affected insignificantly, where all concentrations exhibited negligible effect on cellular uptake of NCs. Additionally, cellular uptake and internalisation of NCs was yet significantly greater than Ins-F in presence of sucrose as a bulking agent (Figure 6.1b).

With Glycine, no effect was observed on cellular internalisation of both Ins-F and Ins-F-GET NCs, and NCs had significantly greater internalisation compared to Ins-F at all studied concentrations (Figure 6.1c). Additionally, the effect of combination or multiple bulking agents at different working concentrations was analysed on the cellular uptake of Ins-F and Ins-F-GET NCs. The combination of D-mannitol and sucrose exhibited similar trend of cellular uptake for NCs as for each of these bulking agents alone (Figure 6.1d), as combination with concentration of 40mg/ml D-mannitol and 10mg/ml sucrose exhibited greatest cellular internalisation of NCs compared to all tested concentrations of individual and combinatorial bulking agents. Similarly, the effect of combination of D-mannitol and glycine at two different concentration was assessed on cellular uptake of NCs (Figure 6.1d). At highest dose, each of these bulking agents showed remarkably greater cellular uptake of Ins-F-GET NCs, thus indicating that bulking agents do not interfere with GET-mediated enhanced permeation and internalisation of insulin across Caco-2 monolayers. To conclude, all studied concentrations of these bulking agents and even their combination had insignificant effect on cellular uptake process and hence are safe to be employed as a bulking agent for the freeze drying of both insulin and NCs.

For solid protein formulations, crystallising bulking agent would be required to impart one of the following features: to improve product elegance, provide sufficient mechanical support to final cake, to improve dissolution of formulation, and lastly to prevent collapse and blowing out of the product. Therefore, a suitable bulking agent should have following properties; protein compatibility, minimal or no toxicity, good solubility, and high eutectic temperature, all of which would contribute to efficient freeze drying. Various bulking agents may influence the stability of solid protein to different extents, hence there's a need for careful selection of an appropriate bulking agent and its relative amount [219]. Additionally, for obtaining a product with acceptable shelf life, good stability and better quality, the principles of physical, chemical, and engineering needs to be taken into consideration. The cryoprotectants tend to minimise instability of NPs during freeze-drying process, protecting them against mechanical stress, preventing aggregation, and preserving the proteins native structure following

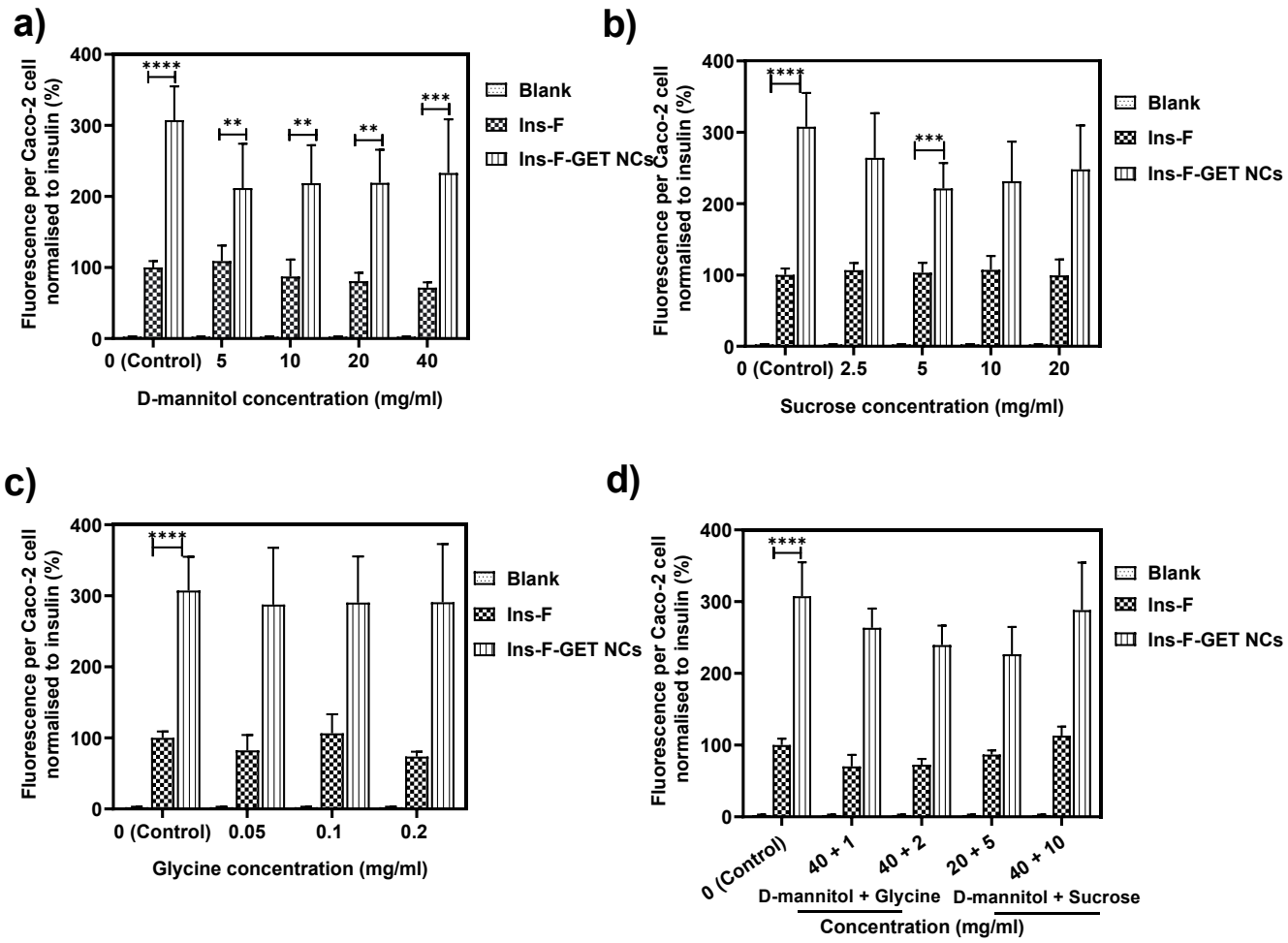

Figure 6. 1 Various bulking agents showing differences in cellular uptake of NHS-Fluorescein-insulin in presence and absence of GET system, where high concentration of bulking agents significantly improved cellular uptake. a) D-mannitol, b) Sucrose, c) Glycine, and d) mix of D-mannitol with glycine and sucrose, respectively. All values are presented as mean ± S.D, n=5, * = *p-value* <0.05, **= *p-value* <0.005, ***= *p-value* <0.0005, ****= *p-value* <0.0001, and *ns*= not significant. Two-way ANOVA with Tukey's test.

freeze drying [218, 220-222]. Insulin loaded PLGA NPs were dehydrated employing a standard freeze-dried cycle using cryoprotectants; trehalose, sucrose, fructose, glucose and sorbitol at concentration of 10% (w/v). Over time there was change in shape of NPs surface, and sorbitol provided the best morphological stability under all storage conditions [203].

6.3.2. Cellular internalisation of NCs freeze dried with bulking agents

The cellular internalisation of Ins-F and Ins-F-GET NCs freeze dried with various working concentration of bulking agents was assessed across Caco-2 monolayers

as shown in Figure 6.2. NCs freeze dried with various concentration of D-mannitol exhibited improved cellular internalisation compared to control (both freshly prepared Ins-F, NCs and freeze-dried Ins-F with bulking agent). D-mannitol at 20 and 40mg/ml induced higher cellular internalisation of freeze dried NCs compared to freshly prepared NCs, thus suggesting that freeze dried NCs preserved the GET-mediated enhanced cellular permeation and uptake of insulin (Figure 6.2a). Similarly, freeze-dried NCs and insulin with sucrose exhibited greater cellular uptake compared to respective controls prepared freshly and both of the tested concentrations acted to improve the GET-mediated enhanced insulin internalisation (Figure 6.2b).

Similarly, Glycine based freeze-dried NCs displayed higher cellular uptake and internalisation compared to control (Ins-F) at all tested concentrations as shown in Figure 6.2c. In case of NCs freeze-dried with combination of bulking agents i.e. D-mannitol + sucrose at two different concentrations (40mg/ml +10mg/ml or 20mg/ml + 5mg/ml), an improvement in cellular internalisation of NCs was observed. These results indicated that combination of D-mannitol and sucrose may serve as an appropriate combination of bulking agents for freeze drying NCs by not interfering with GET-mediated insulin transport, stabilising NCs, and additionally further improving permeation and internalisation in comparison to fresh NCs. On the other hand, NCs freeze dried with combination of D-mannitol and glycine exhibited peculiar behaviour, where both tested concentration of these combinatory bulking agents (D-mannitol + glycine, 40mg/ml + 1mg/ml and 40mg/ml + 2mg/ml) resulted in reduction in cellular internalisation of NCs compared to control (fresh Ins-F-GET NCs), but yet the internalisation of these freeze-dried NCs was significantly higher than Ins-F (control) (Figure 6.2d).

Overall, it could be concluded that each of these bulking agents when freeze dried with NCs tends to improve the cellular uptake of NCs, while in case of multiple bulking agent the combination of D-mannitol and sucrose freeze-dried with NCs displayed greatest uptake and internalisation. These results indicated that D-mannitol and sucrose would be an optimal bulking agent mix for freeze drying GET-based insulin NCs without interfering with their permeation and by imparting stability to these NCs. But use of this combination would be limited due to its

administration in diabetic patients which already have high serum glucose levels. Therefore, alternatively the combination of D-mannitol and glycine was employed for further use in M-Caps, where freeze-dried NCs were filled in M-Caps and subsequently coated with enteric polymer.

Numerous studies have reported increased stability and improved activity for delivery systems/ formulations in presence of different bulking agents, which co-relates well with the results of our study. Doxorubicin-loaded polyethylene sebacate NPs underwent aggregation upon freeze drying (no cryoprotectants), where in presence of trehalose an amorphous powder was formed upon freeze drying, while with mannitol, fructose or dextrose softened and collapsed frozen matrix was obtained [205]. CPP (PepFect 14) based siRNA NCs with mannitol (bulking agent) have shown to exhibit greater stability in simulated gastric-

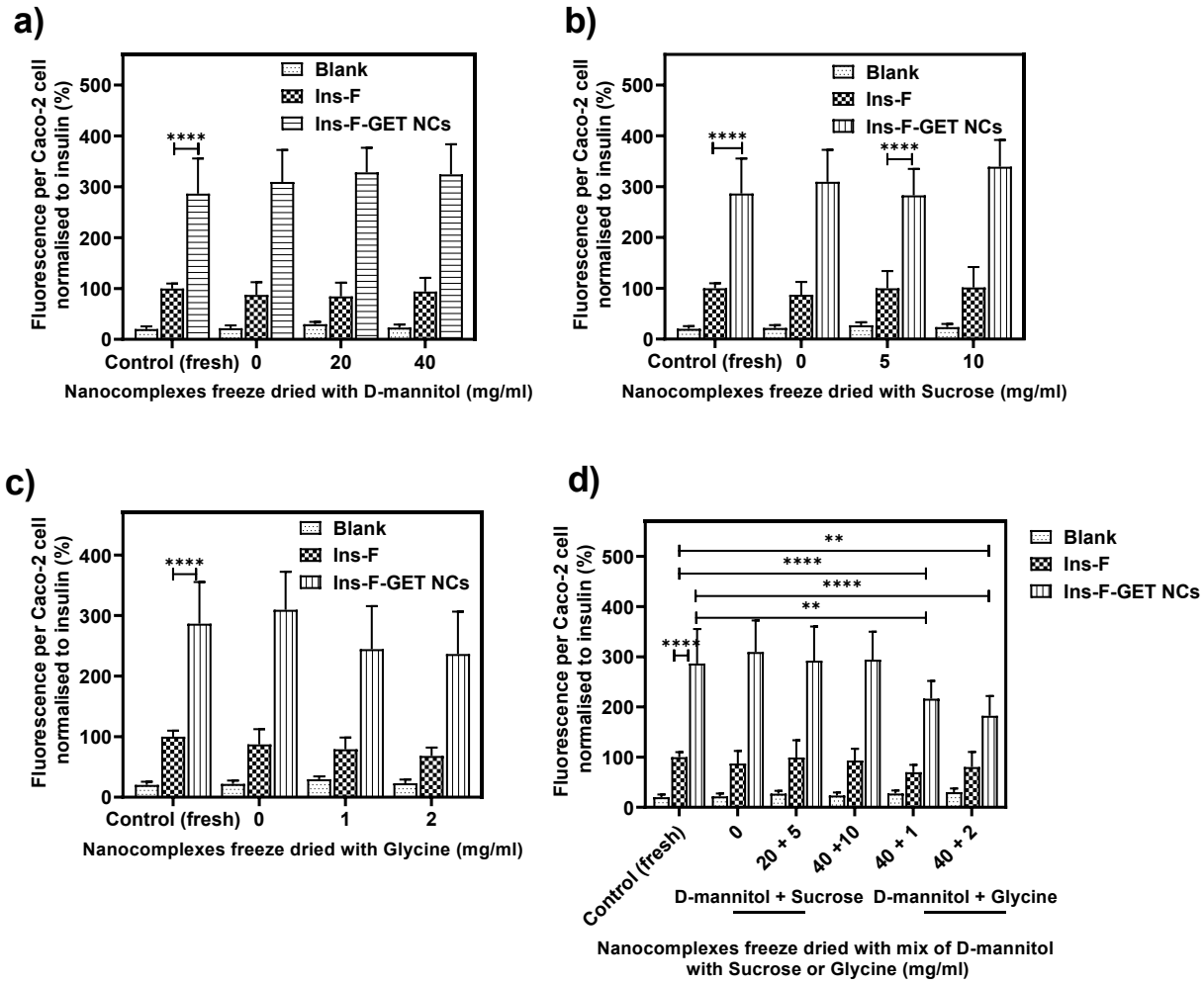

Figure 6. 2 Cellular internalisation of freeze-dried of NHS-Fluorescein-insulin (Ins-F and Ins-F-GET NCs) in presence of different bulking agent showing improved

internalisation. a) D-mannitol, b) Sucrose, c) Glycine, and d) mix of D-mannitol with Glycine and Sucrose, respectively. All values are presented as mean ± S.D, n=5, * = *p-value* <0.05, **= *p-value* <0.005, ***=*p-value* <0.0005, ****= *p-value* <0.0001, and *ns*= not significant. Two-way ANOVA with Tukey's test.

condition containing Pep. Moreover, these NCs were able to elicit efficient RNA interference response (RNAi) in different cell lines, and freeze-dried NCs were as active as freshly prepared NCs in mediating RNAi response even in SGF [231]. Freeze-dried PLGA NPs exhibited increased (by 18%) insulin release in first two hr possibly due to formation of pores and provided sustained release for upto 48 hr, where presence of trehalose further increased insulin release. But release of insulin was reduced in presence of glucose, fructose, sucrose and mannitol compared to PLGA NPs freeze dried with no added cryoprotectants [204].

6.3.3. *In-vitro* dissolution testing of M-Caps in commercial Biorelevant media

Enteric coated M-Caps (filled with NCs freeze dried with D-mannitol & glycine) were tested for *in-vitro* drug release in biorelevant media both in presence and absence of enzymes simulating the GI conditions, to study dissolution profile of enteric coating, and subsequent drug release following disruption of coating and capsules, a schematic is given in Figure 6.3a. The dissolution and drug release profile of NHS-Fluorescein-insulin (Ins-F and Ins-F-GET NCs) loaded enteric M-Caps in biorelevant media with no added enzymes showed no drug release in FaSSGF (pH 1.6) simulating the acidic environment of stomach, increasing the pH to slightly alkaline by placing these M-Caps in FeSSIF (pH 5) resulted in dissolution of capsule coating and drug release (Figure 6.3b). Maximum drug release was observed in FaSSIF (pH 6.5) simulating the intestinal conditions, here the enteric coating was completely dissolved, and drug was released gradually from capsules by diffusion through pores formed in swelled capsules until the capsules were dissolved completely (9 hr) and complete drug release was attained. The release in FaSSIF was two times greater than in FeSSIF, these results indicated that higher pH leads to more complete dissolution of enteric coating and hence greater drug release.

On the other hand, in the presence of enzymes in biorelevant media, abrupt drug release was observed from M-Caps (Figure 6.3c). This abrupt release could be attributed to non-uniform coating or cracks in coating, moreover presence of Pep

in FaSSGF might have caused slight degradation of M-Caps coating resulting in burst drug release, where a fraction of drug was released from capsules within first two hr. Additionally, placing M-Caps in FeSSIF provided further release of drug due to dissolution of enteric coating, and subsequent placement in FaSSIF containing Pan enzyme provided much greater drug release possibly due to complete dissolution of enteric coated capsules. The capsules were completely dissolved within 9 hr in commercially available buffer media with no leftover traces of capsules shells or coating, as indicated by visual inspection and also by plateau of drug release following 9 hr, where constant drug levels were maintained until 24 hr.

The best validated and most used small animal model are rats, which are being extensively used for studying the basic pharmacokinetics, pharmacodynamics, and bioavailability. Therefore, different studies have reported the use of freeze-dried drug loaded gastro-resistant capsules which have been adapted for rats [232, 233]. These capsules offer several advantages including; increased rates of intact molecules delivery to specific regions of intestine leading to increased bioavailability, and that capsules coating is independent of the capsule contents [234]. PCcaps size 9 capsules (Capsugel) coated with Eud-L100-55 (using a ready-to-use enteric formula i.e. Acryl-Eze), were dissolved less than 10% in 2hr in SGF, while not less than 80% was dissolved in SIF in 45 min. *In-vivo* study in rats, revealed that enteric M-Caps were resistant in stomach with no apparent leaks on capsules and were disintegrated within 1-1.5 hr in early duodenum [235]. Eud-S100 coated gelatin M-Caps filled with barium sulphate have been employed for studying the tracking of non-disintegrating solid dosage form i.e.GI transit and gastric emptying using x-ray imaging, here short length capsules (3.5 and 4.8mm) were emptied from the stomach while the commercial length capsules (7.8mm) were retained [232]. PEG-PGA enveloped-R8 NCs when tested *in-vivo* by orally administering insulin-loaded ENCPs encapsulated in enteric (Eud-L100) coated M-Caps, results revealed mild systemic drug effects possibly due to retention of ENCPs in intestinal epithelium which served as a reservoir providing slower drug release [158].

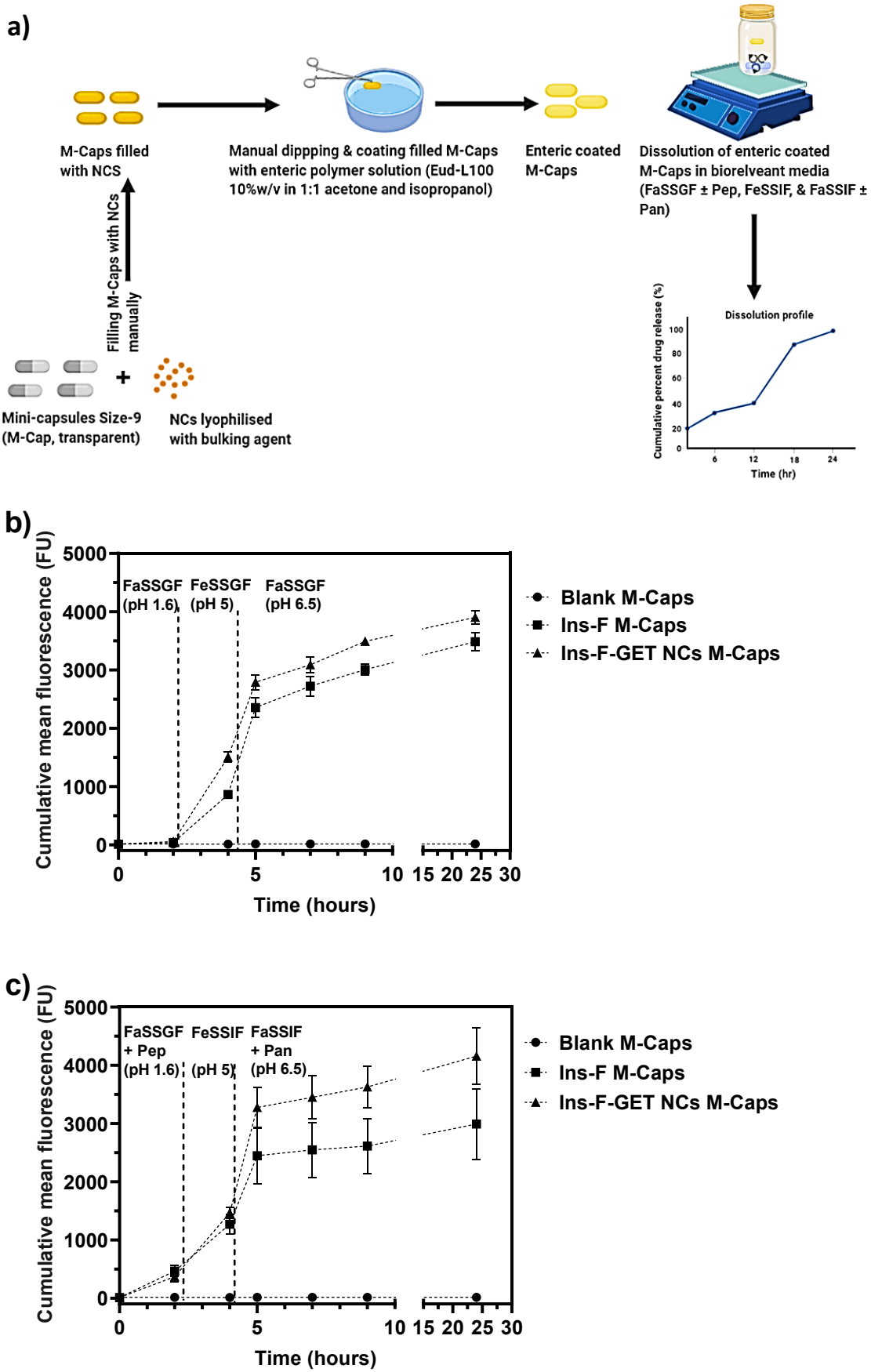

Figure 6. 3 *In-vitro* dissolution profile of enteric coated mini-Capsules filled with freeze-dried NHS-Fluorescein-insulin based nanocomplexes (with bulking agent; D-

mannitol + glycine). a) Schematic for filling and coating of M-Caps (Size-9) with NCs freeze dried with bulking agent and subsequent testing of dissolution profile in Biorelevant media, b) Dissolution profile in biorelevant media with no added enzymes showing no or minimal drug release at low pH in FaSSGF, increasing the pH to alkaline as in FeSSIF (pH 5) and FaSSIF (pH 6.5) provided maximum and complete drug release due to dissolution of coating and subsequently the capsules shells, and c) Biorelevant media in presence of enzymes showed slight abrupt drug release during initial hr, while at higher pH with enzymes more complete drug release was obtained. All values are presented as mean ± S.D, n=3.

Thermostable spray-dried virus-like particle (VLP) vaccine was filled in size-9 gelatin M-Caps followed by manual coating with enteric polymer (Eud-L30-D55). The results indicated greatly elicited low antibody titers following oral administration, and this response was lower compared to the response generated by intramuscular administration of VLPs [236]. These earlier studies provide insight that enteric coated M-Caps provide an alternative strategy for oral administration of drug entities while preventing drug release in acidic environment, which is in concordance with our results where NCs release was prevented in FaSSGF, thereby protecting and preserving NCs.

6.4. Conclusion

This work demonstrated that use of different bulking agents and their combinations (D-mannitol, sucrose and glycine) had negligible effect on cellular internalisation of Ins-F and Ins-F-GET NCs, and internalisation of NCs was significantly greater compared to un-modified Ins-F. Results indicated that using bulking agents is safer and does not interfere with GET-mediated enhanced insulin permeation, transport, and internalisation while maintaining the NCs integrity and stability. Furthermore, NCs freeze-dried with bulking agent displayed greater internalisation and uptake compared to freshly prepared control (with no freeze drying and no bulking agents). Enteric coated M-Caps preserved the coating and prevented drug release at low acidic pH in FaSSGF simulating the conditions of stomach, on progression to alkaline pH of intestine as in FeSSIF and FaSSIF with pH 5 and pH 6.5, respectively the enteric coating on capsule was dissolved, followed by swelling of capsules and resulting in drug release by diffusion, while in the presence of enzymes, faster drug release was observed. These gelatine capsules

were dissolved completely within 9hr. This work therefore showed that GET based NCs can be freeze-dried in presence of different bulking agents without interfering with GET-mediated enhanced cellular uptake of insulin and these enteric based M-Caps provided protection to NCs. The proposed approach potentially could provide benefits for oral insulin delivery; however the concepts must be tested i*n-vivo* in animal models as preliminary studies.

Chapter 7. General Discussion

Emergence of CPPs as powerful trans-epithelial delivery vectors for efficient intracellular drug delivery has revolutionised the field of therapeutics. CPPs have been reported to form complexes with insulin either through covalent or non-covalent linkages, these NCs in turn mediate enhanced intracellular delivery into cells together with improvement of transfection efficiency [12, 21, 22, 191, 237]. In this study, potential of GET-peptide (following complexation with insulin as NCs) in enhancing trans-epithelial delivery and transcytosis efficiency of insulin was evaluated. Polyarginines are positively charged peptides, which owing to their higher degree of positivity are regarded as most efficient CPPs, as the cationic residues or guanidinium side-chains on polyarginine facilitate bidentate binding with negatively charged cell surface proteoglycans. For efficient translocation of polyarginines into the cells an optimal length of peptide sequence is essentially required [120]. Numerous studies have reported the use of 8R as promoter of intracellular drug delivery orally, nasally and even to deliver drugs across the blood brain barrier into the brain [22, 122, 125, 130, 238]. P21 derived from HB-EGF is regarded as heparin-binding domain due to its strong binding affinity for heparin. The amphipathic peptide LK15 in the GET-system acts as a linker molecule between CPP and GAG-binding motif, it exhibits optimal size for maximum lytic activity together with membrane activity and DNA condensation ability.

GET system was able to significantly improve the intracellular permeation and transcytosis of insulin by greater than > 8.7 -fold compared to control i.e. insulin (Chapter 3). This efficient intracellular uptake and transcytosis was due to distinct regions that constitute GET system, where P21 a heparin-sulphate binding domain enabled efficient coupling with cell surface GAGs, and 8R promoted CPP-mediated endocytosis into the cells. Therefore, inclusion of P21 and 8R in this novel multidomain fusion peptide tends to act synergistically to enhance the cellular uptake of insulin across Caco-2 cell monolayers. GET-peptide modulates membrane permeability and integrity as indicated by lowering of TEER values, indicating that both trans- and paracellular route are involved in uptake of GET-based insulin NCs. This opening of natural barriers i.e. TJs tends to serve as a double-edged sword.

Regardless of pharmaceutical advantages; this opening of TJs together with APIs intake may result in irreversible uptake of pathogens i.e. viruses, bacteria and lipopolysaccharides from the membrane barriers e.g. inner gut where they resided permanently or opportunistically. Reports from previous studies have revealed that this increased intestinal permeability is associated with higher incidence of autoimmune diseases and infections, of which inflammatory bowel disease is a common example [239]. Moreover, this enhanced intestinal permeability could contribute to various other diseases including Type-I diabetes [240, 241], HIV/AIDS [242], graft-versus-host disease propagation (GVHD) [243] and etc. Biomaterials mediated opening of TJs might be short-lived and reversible following few hours or days, however its not known that whether this periodic repeated opening of TJs could compromise body's natural immune defence in term of repairing capacity and would it led to autoimmune conditions or allergies [244]. A noteworthy example of TJ opener is GIPET technology containing sodium caprate which was developed by Novo Nordisk for oral insulin delivery and reached Phase 2 trials, but despite the success in clinical outcome; unfortunately the company had to suspend the trial as the product was not commercially viable because of low oral absorption efficacy [245].

Despite the fact that CPPs are highly efficient in enhancing *in-vitro* cellular uptake of therapeutic moieties across most cell-lines but yet there are limitations for their *in-vivo* applications. Limitations of CPPs for *in-vivo* use include complete lack of cell specificity, as CPPs-cargo complexes are distributed throughout the body independently of the way of administration which also underlines the CPP's potential as a therapeutic approach [105, 115]. Studies have also revealed that coupling of CPPs to cell-specific antibodies tends to improve their *in-vitro* cellular internalisation, but *in-vivo* significantly reduced selectivity was observed as the non-targeted sites/ tissues uptake the chimeric constructs via non-specific internalisation [246]. Thus, this issue is one of the major drawbacks associated with the use of CPPs for *in-vivo* delivery, therefore there is need for alternative strategies which promote cell-specificity. Development of activatable CPPs (ACPPs) is regarded as ground-breaking advancement and has evolved recently to impart specificity to CPPs, which comprise CPPs and a covalently attached inhibitory

domain which undergo cleavage by tissue specific proteases to enable ACPP entry into cells [247]. Other challenges posed while using CPPs include their high instability and susceptibility to degradation when exposed to biological fluids e.g. gastric or intestinal fluids, blood, intracellular or extracellular fluids containing proteolytic enzymes. Likewise, in this study GET-based insulin NCs were unstable and were degraded in biorelevant media (mimicking GI environment) containing GI enzymes (Chapter 4). To overcome these stability issues associated with CPPs, different approaches are being adopted such as changing stereochemistry, backbone modification, modifying amino acid residues, and stablising CPPs. One of the other concerns is toxicity associated with highly cationic nature of CPPs as associated with other cationic polymers such as poly-l-lysine and poly-ethylene imine [247]. Many studies have provided evidence that CPPs don't display this toxicity such as Toro *et al.*, confirmed that Tat was non-toxic to lymphocytes at concentrations upto 300µM [248]. Similarly, Tat, Rev, VP22 and Antp displayed no toxicity in Hela or Jurkat cells at 20-30µM doses [249]. Incubation of Tat peptide with primary or immortalised keratinocytes also displayed no evidence of toxicity at concentrations between 200-400µM. It is notable that in these toxicity assays the CPPs concentration was very large which is far above the concentrations typically being used to delivery drug molecules into cells (ranging from 1-10µM) [250].

The recommended insulin dosage for most Type-I diabetic patients is 0.5- 1.0 IU per kg/ day [251]. As average adult body weight is 72 kg; therefore, per day insulin requirement for a diabetic patient with type-I diabetes would be 2.14×10^{-4} to 4.25×10^{-4} mmol per day.

Daily insulin requirement for Type-I Diabetes = 0.5 – 1 IU/ kg/ day

Where 1 IU is equivalent to = 0.0349 mg or 3.49×10^{-5} g

1mg of Human recombinant insulin contains = 27.5 IU

Daily insulin requirement for Type-I Diabetes = 1.745×10^{-5} to 3.49×10^{-5} g/ kg/ day

For adult of 72Kg, daily insulin requirement would be = 0.124×10^{-2} to 0.247×10^{-2} g/ day or 1.24mg- 2.4mg/ day or 1240-2470µg/ day or 2.14×10^{-4} to 4.25×10^{-4} mmols per day

In terms of IU insulin dose would be = 34.1 IU – 66IU

Here, concentrations used for *in-vitro* studies i.e. amount of insulin per well was 5µg which in terms of IU is equal to 0.14 IU (Chapter 3). As according to functional activity assay; upon complexation with GET-peptide, insulin was still biologically active (>70%), therefore it would be practically feasible to delivery daily insulin requirement for an adult with average weight (72 kg) using this carrier system. Commercially marketed insulin preparation contain 100-200 IU/ ml in 10ml vial, which is 3.7mg/ ml, as insulin-GET NCs (20µg/ml) are prepared in solution so its possible to formulate concentrated solution of NCs for oral administration to provide bolus-insulin dose. While for basal -doses, long-acting insulin analogues could be used for complexation with GET or alternatively hydrophobically-modified-GET derivative could be complexed with insulin to test for sustained insulin effects. Therefore, it would be possible to deliver both bolus and basal doses following insulin modification with GET-peptide.

To encapsulate sensitive therapeutic drugs such as proteins, pH-sensitive polymer could be used which will protect these drugs from degradation. The delivery systems based on these polymers can be engineered to stay stable at low acidic pH of stomach but providing drug release at higher pH of the intestine. Here, two major issues were encountered with enteric polymer-based MPs, firstly the polymer induced decoupling of GET from insulin (instability) and secondly low percent drug loading (chapter 5). Preparation methods which provide high drug-loading contents for water soluble drugs should be adopted. As method used to formulate MPs in this study provided much lower loaded contents, which will lead to increased wastage and at the same time more cost for the pharmaceutical firm and ultimately for the consumer itself. Using systems densely populated with cationic and anionic groups but overall neutrally charged and possessing charge reversal properties should be explored for oral delivery of protein drugs, as it would minimise polymer induced decomplexation of GET from insulin. Biomimetic virus-like and charge reversible NPs (P-R8-Pho- NPs) displayed dual features of overcoming the barriers of mucus and epithelium for oral delivery of insulin [200]. Chitosan based micelles (phosphorylated chitosan-stearic acid conjugates, CSSAP) have also been reported to display zeta potential changing property on exposure to intestinal alkaline phosphatases, resulting in shift of charge from negative to

neutral which ultimately promoted the mucosal drug delivery [252]. Freeze drying is considered most useful method for handling and stabilising micro- and nanoparticulate systems, thus circumventing unwanted changes upon storage. In this study NCs were successfully freeze-dried using bulking agents and these freeze-dried NCs were more efficient in undergoing enhanced uptake across Caco-2 monolayers compared to free insulin and fresh NCs (Chapter 6). During freeze drying process the removal of water from protein loaded micro-/ nano-particulates may be fundamental step for preserving stability and avoiding hydrolytic degradation of loaded protein in aqueous suspension [218, 219].

Our study complements other researches aiming at engineering functional insulin complexes with improved intracellular translocation and efficient transcytosis. However, the method employed for this study was unique, as it utilised novel fusion peptide coupling CPPs with heparin binding domain to act synergistically for enhancement of intracellular delivery which was attained simply. This is in comparison to studies using chemical cross-linking for coupling CPPs with insulin, such as Liang and co-workers used chemical conjugation to link insulin with TAT-peptide in the presence of cross-linker involving covalent bonds [21], which is far more complex and is based on chemical cross-linking. Furthermore, introduction of highly efficient GET system tends to overcome the limitations associated with conventional methods, and their efficiency in promoting intracellular delivery.

Many pharmaceutical firms have initiated clinical development of CPPs for systemic and local administration, currently over 25 clinical trials involving CPPs are under investigation, with few in Phase-3. Despite extensive work has been conducted on the use of CPPs as drug-delivery vectors, but still their mechanism for cell penetration is debatable. Moreover, their use is limited due to lack of thorough knowledge, such as whether translocation of CPPs is increased when TJs are compromised e.g under inflammatory conditions. Thus, further understanding of CPPs will result in more advances in the application of CPPs as safe, efficient, and functional vectors. Development of robust *in-vitro* models which give adequate idea about *in-vivo* conditions and establishment of reliable *in-vivo* models to attain consistent results which could be co-related are highly desirable. Similarly, analytical methods with high sensitivity and reliability should be developed in order

to detect both unmodified and modified CPPs, together with CPPs which reached their site of action. Moreover, there is a need to explore and develop advanced target-specific delivery systems based on CPPs which would display minimal adverse effects, escape endosomal entrapment, and have optimal plasma half-life for resolving issues which hinder the clinical applicability of CPPs.

Chapter 8. Conclusion and future work

8.1. Conclusion

CPPs have received considerable importance as an attractive delivery vehicle due to their inherent ability to cross the biological membrane and mediate the cellular uptake of cargoes. CPPs are capable of traversing across different intact biological membranes such as; intestinal epithelium barriers, nasal epithelium, transalveolar epithelium, and blood brain barrier. This study demonstrates complexation of GET-peptide with insulin to form NCs through electrostatic interaction, which in turn tends to improve the absorption, permeation, transcytosis, and internalisation of insulin across *in-vitro* Caco-2 cell monolayers, which mimic physical barrier function of intestine but don't offer any mucosal barrier. Lowering of TEER values is a major concern, as it might limit application of GET system for oral insulin delivery. Additionally, stability assays have revealed that D-isoform of GET peptide system is stable to degradation by proteolytic enzymes and that the insulin-GET NCs are sufficiently stable and stay intact even after translocation inside cells. These GET-based insulin NCs retained functional activity as depicted by luciferase assay performed using Insulin assay reporter cells, thus suggesting that non-covalent modification of insulin with GET does not affects the pharmacological activity of insulin. Complexation of insulin with GET-peptide generated slightly bigger NCs and the surface charge changed from negatively charged insulin to strong positively charged insulin-GET NCs. Microscopic techniques i.e. CLSM and ImageStream analysis provided evidence that insulin-GET NCs were internalised in significantly greater amounts compared to unmodified insulin, and that these NCs are distributed evenly throughout the cytoplasm. Cell viability i.e. AlamarBlue assay and Live/Dead cytotoxicity assay indicated that amount of GET-peptide in NCs doesn't affects the viability of Caco-2 monolayers. NCs were freeze dried in presence of different bulking agent for efficient handling and enhancing stability. NCs freeze dried with bulking agent exhibited greater cellular internalisation. Enteric coated M-Caps (size 9) filled with NCs freeze dried with bulking agents were developed as a step forward toward *in-vivo* testing. These enteric coated M-Caps protected and prevented release of NCs under acidic conditions, while at higher pH

the coating was dissolved thus providing drug release. GET-peptide based systems are efficient tools for overcoming low permeability of cargoes particularly protein drugs; but still it needs extensive work to establish efficacy of this system *in-vivo* for enhancing insulin bioavailability. Keeping in mind potential indirect toxicity associated with GET-peptide in terms of modulating barrier function (as indicated by lowered TEER values), which might limit applicability of this system. Therefore, its necessary to conduct trials on small animals both healthy and with GI inflammatory disease to understand potential of toxicity before moving towards further development.

8.2. Future work

Based on the findings in this study the proposed recommendations for future studies include; designing different GET derivatives with modified sequence such as; incorporation of another CPP instead of 8R, hydrophobically modifying GET by linking with hydrophobic moieties such as lauric acid, cholesterol to form covalent linkages with insulin, and incorporating cleavable linkages in this multidomain sequence which will lead to cleavage or degradation of GET in systemic circulation by interstitial or serum proteases thus ensuring release of free and biologically active monomeric insulin, and further testing these derivatives for enhancing the permeability and internalisation of insulin in form of NCs, characterising them and testing them both in *in-vitro* and *in-vivo*. In order to meet the requirement of bolus-basal dosing regimen, there's a need to conduct trial on long-and intermediate acting insulin using GET system to test their translocation efficiency, stability and functional activity following modification with GET and to determine whether it is possible to attain basal dosing. This should be followed by testing in small animal models to study whether basal-bolus dosing is attained and maintained using Long- and short-acting insulin derivatives, respectively co-modified with GET.

It would be beneficial to explore the permeability of insulin-GET NCs with co-culture of Caco-2 and HT-29 MTX cells (preconditioned with methotrexate) to provide added benefit of expressing mucins in culture, where the mucus layer would provide additional physical barriers to transport of NCs. Alternatively, these Caco-2 cells could be cultured, and mucus secretions extracted from pig or rat

intestine could be used to study the behaviour, stability, permeability and internalisation of NCs.

The mechanism of cellular uptake needs further exploration, which could be achieved by using specific inhibitors of active and passive transport. Sodium azide depletes energy and can be used as active transport inhibitor, whereas filipin, chlorpromazine, and amiloride can be used as specific inhibitors of endocytosis for caveloae-mediated endocytosis, clathrin-mediated endocytosis, and macropinocytosis, respectively. Temperature dependent uptake studies for insulin-GET NCs would be conducted at 37, 16, and 4 ^{o}C to further verify the cellular uptake mechanism, where energy dependent endocytosis would be inhibited at 16 ^{o}C due to interference with intracellular vesicular fusion events, on the other hand energy-independent direct translocation would not be affected by temperature modulation. Moreover, it would be useful to conduct *in-vivo* studies in animal models to investigate the bioavailability and potential toxicity of the proposed approach and whether enteric coated M-Caps would maintain sustained hypoglycaemic effects either encapsulated alone or in combination with bulking agent. The parameters monitored during *in-vivo* studies would include; measuring blood glucose levels (hypoglycaemic response over time), quantification of insulin levels in serum/plasma, determination of relative bio-availabilities, toxicity, and biodistribution of NCs in different organs. The onset of actions, AUC, bioavailability, inter/intra subject variability in absorption and delay between administration of enteric capsules should be compared. The effect of food and fasting on the onset of action and bioavailability could also be compared.

Future work on these GET-based insulin NCs could also be directed towards more controlled, neutrally charged or charge reversible nano-carrier system for oral insulin delivery. Drug delivery systems displaying zeta potential changing property could be designed to contain cationic groups shielded by anionic moieties in the form of phosphate esters, which upon exposure to alkaline phosphatase enzyme (ALP) in body are cleaved off resulting in change of zeta potential from negative to neutral or positive. Additionally, employing this GET system for the oral delivery of other anti-diabetic peptides (GLP-1, GIP, Peptide YY) should also be taken into consideration.

Chapter 9. References

1. Rehmani, S. and J.E. Dixon, *Oral delivery of anti-diabetes therapeutics using cell penetrating and transcytosing peptide strategies.* Peptides, 2018. **100**: p. 24-35.

2. Chin, J., et al., *Insight of current technologies for oral delivery of proteins and peptides.* Drug Discovery Today: Technologies, 2012. **9**(2): p. e105-e112.

3. Park, K., I.C. Kwon, and K. Park, *Oral protein delivery: Current status and future prospect.* Reactive and Functional Polymers, 2011. **71**(3): p. 280-287.

4. Fasano, A., *Innovative strategies for the oral delivery of drugs and peptides.* Trends in biotechnology, 1998. **16**(4): p. 152-157.

5. Craik, D.J., et al., *The future of peptide-based drugs.* Chemical biology & drug design, 2013. **81**(1): p. 136-147.

6. Fosgerau, K. and T. Hoffmann, *Peptide therapeutics: current status and future directions.* Drug discovery today, 2015. **20**(1): p. 122-128.

7. Choonara, B.F., et al., *A review of advanced oral drug delivery technologies facilitating the protection and absorption of protein and peptide molecules.* Biotechnology advances, 2014. **32**(7): p. 1269-1282.

8. Muheem, A., et al., *A review on the strategies for oral delivery of proteins and peptides and their clinical perspectives.* Saudi Pharmaceutical Journal, 2016. **24**(4): p. 413-428.

9. Shaji, J. and V. Patole, *Protein and peptide drug delivery: oral approaches.* Indian journal of pharmaceutical sciences, 2008. **70**(3): p. 269.

10. Dissanayake, S., et al., *Recent developments in anticancer drug delivery using cell penetrating and tumor targeting peptides.* Journal of Controlled Release, 2017.

11. Gupta, S., et al., *Oral delivery of therapeutic proteins and peptides: a review on recent developments.* Drug delivery, 2013. **20**(6): p. 237-246.

12. Kamei, N., et al., *Noninvasive insulin delivery: the great potential of cell-penetrating peptides.* Therapeutic delivery, 2013. **4**(3): p. 315-326.

13. Farkhani, S.M., et al., *Cell penetrating peptides: efficient vectors for delivery of nanoparticles, nanocarriers, therapeutic and diagnostic molecules.* Peptides, 2014. **57**: p. 78-94.

14. Figueiredo, I.R., et al., *Cell-penetrating peptides: A tool for effective delivery in gene-targeted therapies.* IUBMB life, 2014. **66**(3): p. 182-194.

15. Koren, E. and V.P. Torchilin, *Cell-penetrating peptides: breaking through to the other side.* Trends in molecular medicine, 2012. **18**(7): p. 385-393.

16. Milletti, F., *Cell-penetrating peptides: classes, origin, and current landscape.* Drug discovery today, 2012. **17**(15): p. 850-860.

17. Khafagy, E.-S. and M. Morishita, *Oral biodrug delivery using cell-penetrating peptide.* Advanced drug delivery reviews, 2012. **64**(6): p. 531-539.

18. Svensen, N., J.G. Walton, and M. Bradley, *Peptides for cell-selective drug delivery.* Trends in pharmacological sciences, 2012. **33**(4): p. 186-192.

19. Khalil, I.A., et al., *High density of octaarginine stimulates macropinocytosis leading to efficient intracellular trafficking for gene expression.* Journal of Biological Chemistry, 2006. **281**(6): p. 3544-3551.

20. Nakase, I., et al., *Cellular uptake of arginine-rich peptides: roles for macropinocytosis and actin rearrangement.* Molecular therapy, 2004. **10**(6): p. 1011-1022.

21. Liang, J.F. and V.C. Yang, *Insulin-cell penetrating peptide hybrids with improved intestinal absorption efficiency.* Biochemical and biophysical research communications, 2005. **335**(3): p. 734-738.

22. Kamei, N., et al., *Usefulness of cell-penetrating peptides to improve intestinal insulin absorption.* Journal of Controlled Release, 2008. **132**(1): p. 21-25.

23. Verdurmen, W.P., et al., *Preferential uptake of L-versus D-amino acid cell-penetrating peptides in a cell type-dependent manner.* Chemistry & biology, 2011. **18**(8): p. 1000-1010.

24. Dixon, J.E., et al., *Highly efficient delivery of functional cargoes by the synergistic effect of GAG binding motifs and cell-penetrating peptides.* Proceedings of the National Academy of Sciences, 2016. **113**(3): p. E291-E299.

25. Jacob, D., et al., *Synthesis and identification of FITC-insulin conjugates produced using human insulin and insulin analogues for biomedical applications.* Journal of fluorescence, 2016. **26**(2): p. 617-629.

26. Association, A.D., *Diagnosis and classification of diabetes mellitus.* Diabetes care, 2014. **37**(Supplement 1): p. S81-S90.

27. Carino, G.P. and E. Mathiowitz, *Oral insulin delivery.* Advanced drug delivery reviews, 1999. **35**(2): p. 249-257.

28. Bell, G.I. and K.S. Polonsky, *Diabetes mellitus and genetically programmed defects in β-cell function.* Nature, 2001. **414**(6865): p. 788-791.

29. National Diabetes Data Group, *Classification and diagnosis of diabetes mellitus and other categories of glucose intolerance.* Diabetes, 1979. **28**(12): p. 1039-1057.

30. Atkinson, M.A., G.S. Eisenbarth, and A.W. Michels, *Type 1 diabetes.* The Lancet, 2014. **383**(9911): p. 69-82.

31. Graves, P.M. and G.S. Eisenbarth, *Pathogenesis, prediction and trials for the prevention of insulin-dependent (type 1) diabetes mellitus.* Advanced drug delivery reviews, 1999. **35**(2): p. 143-156.

32. Association, A.D., *Diagnosis and classification of diabetes mellitus.* Diabetes care, 2013. **36**(Supplement 1): p. S67-S74.

33. Bell, G.I. and K.S. Polonsky, *Diabetes mellitus and genetically programmed defects in β-cell function.* Nature, 2001. **414**(6865): p. 788.

34. Lernmark, Å., *Type 1 Diabetes.* Clinical Chemistry, 1999. **45**(8): p. 1331-1338.

35. Brange, J. and A. Vølund, *Insulin analogs with improved pharmacokinetic profiles.* Advanced drug delivery reviews, 1999. **35**(2-3): p. 307-335.

36. Hirsch, I.B., *Insulin delivery devices—pumps and pens.* Diabetes technology & therapeutics, 2010. **12**(S1): p. S-115-S-116.

37. Owens, D.R., *New horizons—alternative routes for insulin therapy.* Nature Reviews Drug Discovery, 2002. **1**(7): p. 529-540.

38. Rorsman, P., et al., *The cell physiology of biphasic insulin secretion.* Physiology, 2000. **15**(2): p. 72-77.

39. Seino, S., T. Shibasaki, and K. Minami, *Dynamics of insulin secretion and the clinical implications for obesity and diabetes.* The Journal of clinical investigation, 2011. **121**(6): p. 2118-2125.

40. Duckworth, W.C., R.G. Bennett, and F.G. Hamel, *Insulin degradation: progress and potential.* Endocrine reviews, 1998. **19**(5): p. 608-624.

41. Daly, M., *Sugars, insulin sensitivity, and the postprandial state.* The American journal of clinical nutrition, 2003. **78**(4): p. 865S-872S.

42. Atlas, I.D. *IDF Diabetes Atlas*. 2019 [cited 2019 13-11-19]; 9th:[Available from: https://www.diabetesatlas.org/en/.

43. Wong, T.W., *Design of oral insulin delivery systems.* Journal of drug targeting, 2010. **18**(2): p. 79-92.

44. Cnop, M., et al., *Mechanisms of pancreatic β-cell death in type 1 and type 2 diabetes: many differences, few similarities.* Diabetes, 2005. **54**(suppl 2): p. S97-S107.

45. Ogurtsova, K., et al., *IDF Diabetes Atlas: Global estimates for the prevalence of diabetes for 2015 and 2040.* Diabetes Research and Clinical Practice, 2017.

46. Eisenbarth, G.S., *Update in type 1 diabetes.* The Journal of Clinical Endocrinology & Metabolism, 2007. **92**(7): p. 2403-2407.

47. Gianani, R., et al., *Dimorphic histopathology of long-standing childhood-onset diabetes.* Diabetologia, 2010. **53**(4): p. 690-698.

48. Akerblom, H., et al., *Primary prevention of type 1 diabetes by nutritional intervention: description of a pilot study.* Autoimmunity, 1993. **15**: p. 58.

49. Elliott, R.B., et al., *A population based strategy to prevent insulin-dependent diabetes using nicotinamide.* Journal of Pediatric Endocrinology and Metabolism, 1996. **9**: p. 501-510.

50. Pociot, F., J. Reimers, and H. Andersen, *Nicotinamide—biological actions and therapeutic potential in diabetes prevention.* Diabetologia, 1993. **36**(6): p. 574-576.

51. Carel, J.-C., et al., *Cyclosporine delays but does not prevent clinical onset in glucose intolerant pre-type 1 diabetic children.* Journal of autoimmunity, 1996. **9**(6): p. 739-745.

52. Belchetz, P.E. and P.J. Hammond, *Mosby's color atlas and text of diabetes and endocrinology*. 2003: Elsevier Health Sciences.

53. Adams, G., N. Wang, and Y. Cui, *Future alternative therapies in a quest to halt aberrations in diabetes mellitus.* Biomedicine & pharmacotherapy, 2005. **59**(6): p. 296-301.

54. Flood, T., *Advances in insulin delivery systems and devices: beyond the vial and syringe.* Insulin, 2006. **1**(3): p. 99-108.

55. Peppas, N.A. and N.J. Kavimandan, *Nanoscale analysis of protein and peptide absorption: insulin absorption using complexation and pH-sensitive hydrogels as delivery vehicles.* european journal of pharmaceutical sciences, 2006. **29**(3): p. 183-197.

56. Butler, A.E., et al., *β-cell deficit and increased β-cell apoptosis in humans with type 2 diabetes.* Diabetes, 2003. **52**(1): p. 102-110.

57. Stumvoll, M., B.J. Goldstein, and T.W. van Haeften, *Type 2 diabetes: principles of pathogenesis and therapy.* The Lancet, 2005. **365**(9467): p. 1333-1346.

58. Chausmer, A.B., *Zinc, insulin and diabetes.* Journal of the American College of Nutrition, 1998. **17**(2): p. 109-115.

59. Burke, J.P., et al., *Rapid rise in the incidence of type 2 diabetes from 1987 to 1996: results from the San Antonio Heart Study.* Archives of Internal Medicine, 1999. **159**(13): p. 1450-1456.

60. Owens, D.R., B. Zinman, and G.B. Bolli, *Insulins today and beyond.* The lancet, 2001. **358**(9283): p. 739-746.

61. Brange, J. and L. Langkjœr, *Insulin structure and stability*, in *Stability and Characterization of Protein and Peptide Drugs*. 1993, Springer. p. 315-350.

62. Rekha, M. and C.P. Sharma, *Oral delivery of therapeutic protein/peptide for diabetes–future perspectives.* International journal of pharmaceutics, 2013. **440**(1): p. 48-62.

63. Blundell, T., et al., *Insulin: The Structure in the Crystal and its Reflection in Chemistry and Biology by.* Advances in protein chemistry, 1972. **26**: p. 279-402.

64. Mo, R., et al., *Emerging micro-and nanotechnology based synthetic approaches for insulin delivery.* Chemical Society Reviews, 2014. **43**(10): p. 3595-3629.

65. Derewenda, U., et al., *Molecular structure of insulin: the insulin monomer and its assembly.* British Medical Bulletin, 1989. **45**(1): p. 4-18.

66. Kaarsholm, N.C., H.C. Ko, and M.F. Dunn, *Comparison of solution structural flexibility and zinc binding domains for insulin, proinsulin, and miniproinsulin.* Biochemistry, 1989. **28**(10): p. 4427-4435.

67. Yip, C.C. and P. Ottensmeyer, *Three-dimensional structural interactions of insulin and its receptor.* Journal of Biological Chemistry, 2003. **278**(30): p. 27329-27332.

68. Czech, M.P., *The nature and regulation of the insulin receptor: structure and function.* Annual Review of Physiology, 1985. **47**(1): p. 357-381.

69. Kahn, C., *The molecular mechanism of insulin action.* Annual review of medicine, 1985. **36**(1): p. 429-451.

70. Kahn, C.R. and M. White, *The insulin receptor and the molecular mechanism of insulin action.* The Journal of clinical investigation, 1988. **82**(4): p. 1151-1156.

71. Pessin, J.E. and A.R. Saltiel, *Signaling pathways in insulin action: molecular targets of insulin resistance.* The Journal of clinical investigation, 2000. **106**(2): p. 165-169.

72. Shulman, G.I., *Cellular mechanisms of insulin resistance.* The Journal of clinical investigation, 2000. **106**(2): p. 171-176.

73. Renukuntla, J., et al., *Approaches for enhancing oral bioavailability of peptides and proteins.* International journal of pharmaceutics, 2013. **447**(1): p. 75-93.

74. Bruno, B.J., G.D. Miller, and C.S. Lim, *Basics and recent advances in peptide and protein drug delivery.* Therapeutic delivery, 2013. **4**(11): p. 1443-1467.

75. Hamman, J.H., G.M. Enslin, and A.F. Kotzé, *Oral delivery of peptide drugs.* BioDrugs, 2005. **19**(3): p. 165-177.

76. Torchilin, V.P. and A.N. Lukyanov, *Peptide and protein drug delivery to and into tumors: challenges and solutions.* Drug discovery today, 2003. **8**(6): p. 259-266.

77. Kompella, U.B. and V.H. Lee, *Delivery systems for penetration enhancement of peptide and protein drugs: design considerations.* Advanced drug delivery reviews, 2001. **46**(1): p. 211-245.

78. Ramesan, R.M. and C.P. Sharma, *Challenges and advances in nanoparticle-based oral insulin delivery.* Expert review of medical devices, 2009. **6**(6): p. 665-676.

79. Pauletti, G.M., et al., *Structural requirements for intestinal absorption of peptide drugs.* Journal of controlled release, 1996. **41**(1-2): p. 3-17.

80. Rautio, J., et al., *Prodrugs: design and clinical applications.* Nature Reviews Drug Discovery, 2008. **7**(3): p. 255-270.

81. Dressman, J.B., K. Thelen, and E. Jantratid, *Towards quantitative prediction of oral drug absorption.* Clinical pharmacokinetics, 2008. **47**(10): p. 655-667.

82. Andrews, C.W., L. Bennett, and X.Y. Lawrence, *Predicting human oral bioavailability of a compound: development of a novel quantitative structure-bioavailability relationship.* Pharmaceutical Research, 2000. **17**(6): p. 639-644.

83. Goldberg, M. and I. Gomez-Orellana, *Challenges for the oral delivery of macromolecules.* Nature reviews Drug discovery, 2003. **2**(4): p. 289.

84. Ménard, S., et al., *Paracellular versus transcellular intestinal permeability to gliadin peptides in active celiac disease.* The American journal of pathology, 2012. **180**(2): p. 608-615.

85. Antunes, F., et al., *Models to predict intestinal absorption of therapeutic peptides and proteins.* Current drug metabolism, 2013. **14**(1): p. 4-20.

86. Catnach, S., P. Fairclough, and S. Hammond, *Intestinal absorption of peptide drugs: advances in our understanding and clinical implications.* Gut, 1994. **35**(4): p. 441.

87. Bai, J.P. and G.L. Amidon, *Structural specificity of mucosal-cell transport and metabolism of peptide drugs: implication for oral peptide drug delivery.* Pharmaceutical research, 1992. **9**(8): p. 969-978.

88. Zhu, L., et al., *Oral absorption basics: pathways and physicochemical and biological factors affecting absorption*, in *Developing solid oral dosage forms*. 2017, Elsevier. p. 297-329.

89. Liu, Z., S. Wang, and M. Hu, *Oral absorption basics: pathways, physico-chemical and biological factors affecting absorption.* Developing solid oral dosage forms: Pharmaceutical theory and practice. Elsevier, MA, USA, 2009: p. 265-266.

90. Salamat-Miller, N. and T.P. Johnston, *Current strategies used to enhance the paracellular transport of therapeutic polypeptides across the intestinal epithelium.* International Journal of Pharmaceutics, 2005. **294**(1-2): p. 201-216.

91. Stella, V.J., *Prodrug approaches to enhancing the oral delivery of poorly permeable drugs*, in *Prodrugs*. 2007, Springer. p. 37-82.

92. Tomita, M., et al., *Enhancement of colonic drug absorption by the paracellular permeation route.* Pharmaceutical research, 1988. **5**(6): p. 341-346.

93. Frankel, A.D. and C.O. Pabo, *Cellular uptake of the tat protein from human immunodeficiency virus.* Cell, 1988. **55**(6): p. 1189-1193.

94. Green, M. and P.M. Loewenstein, *Autonomous functional domains of chemically synthesized human immunodeficiency virus tat trans-activator protein.* Cell, 1988. **55**(6): p. 1179-1188.

95. Joliot, A., et al., *Antennapedia homeobox peptide regulates neural morphogenesis.* Proceedings of the National Academy of Sciences, 1991. **88**(5): p. 1864-1868.

96. Theodore, L., et al., *Intraneuronal delivery of protein kinase C pseudosubstrate leads to growth cone collapse.* Journal of Neuroscience, 1995. **15**(11): p. 7158-7167.

97. Fawell, S., et al., *Tat-mediated delivery of heterologous proteins into cells.* Proceedings of the National Academy of Sciences, 1994. **91**(2): p. 664-668.

98. Futaki, S., et al., *Arginine-rich peptides An abundant source of membrane-permeable peptides having potential as carriers for intracellular protein delivery.* Journal of Biological Chemistry, 2001. **276**(8): p. 5836-5840.

99. Wender, P.A., et al., *The design, synthesis, and evaluation of molecules that enable or enhance cellular uptake: peptoid molecular transporters.* Proceedings of the National Academy of Sciences, 2000. **97**(24): p. 13003-13008.

100. Copolovici, D.M., et al., *Cell-penetrating peptides: design, synthesis, and applications.* ACS nano, 2014. **8**(3): p. 1972-1994.

101. Fonseca, S.B., M.P. Pereira, and S.O. Kelley, *Recent advances in the use of cell-penetrating peptides for medical and biological applications.* Advanced drug delivery reviews, 2009. **61**(11): p. 953-964.

102. Kristensen, M. and H.M. Nielsen, *Cell-penetrating peptides as tools to enhance non-injectable delivery of biopharmaceuticals.* Tissue Barriers, 2016. **4**(2): p. e1178369.

103. Heitz, F., M.C. Morris, and G. Divita, *Twenty years of cell-penetrating peptides: from molecular mechanisms to therapeutics.* British journal of pharmacology, 2009. **157**(2): p. 195-206.

104. Bechara, C. and S. Sagan, *Cell-penetrating peptides: 20years later, where do we stand?* FEBS letters, 2013. **587**(12): p. 1693-1702.

105. Vivès, E., J. Schmidt, and A. Pèlegrin, *Cell-penetrating and cell-targeting peptides in drug delivery.* Biochimica et Biophysica Acta (BBA)-Reviews on Cancer, 2008. **1786**(2): p. 126-138.

106. Brooks, H., B. Lebleu, and E. Vivès, *Tat peptide-mediated cellular delivery: back to basics.* Advanced drug delivery reviews, 2005. **57**(4): p. 559-577.

107. Chugh, A. and F. Eudes, *Cellular uptake of cell-penetrating peptides pVEC and transportan in plants.* Journal of Peptide Science, 2008. **14**(4): p. 477-481.

108. Jones, A.T., *Macropinocytosis: searching for an endocytic identity and role in the uptake of cell penetrating peptides.* Journal of cellular and molecular medicine, 2007. **11**(4): p. 670-684.

109. Fittipaldi, A., et al., *Cell membrane lipid rafts mediate caveolar endocytosis of HIV-1 Tat fusion proteins.* Journal of Biological Chemistry, 2003. **278**(36): p. 34141-34149.

110. Alves, I.D., et al., *Membrane interaction and perturbation mechanisms induced by two cationic cell penetrating peptides with distinct charge distribution.* Biochimica et Biophysica Acta (BBA)-General Subjects, 2008. **1780**(7): p. 948-959.

111. Joanne, P., et al., *Lipid reorganization induced by membrane-active peptides probed using differential scanning calorimetry.* Biochimica et Biophysica Acta (BBA)-Biomembranes, 2009. **1788**(9): p. 1772-1781.

112. Rothbard, J.B., et al., *Role of membrane potential and hydrogen bonding in the mechanism of translocation of guanidinium-rich peptides into cells.* Journal of the American Chemical Society, 2004. **126**(31): p. 9506-9507.

113. Wender, P.A., et al., *The design of guanidinium-rich transporters and their internalization mechanisms.* Advanced drug delivery reviews, 2008. **60**(4): p. 452-472.

114. Nagahara, H., et al., *Transduction of full-length TAT fusion proteins into mammalian cells: TAT-p27Kip1 induces cell migration.* Nature medicine, 1998. **4**(12): p. 1449-1452.

115. Schwarze, S.R., et al., *In vivo protein transduction: delivery of a biologically active protein into the mouse.* Science, 1999. **285**(5433): p. 1569-1572.

116. Elmquist, A. and Ü. Langel, *In vitro uptake and stability study of pVEC and its all-D analog.* Biological chemistry, 2003. **384**(3): p. 387-393.

117. Palm, C., et al., *Peptide degradation is a critical determinant for cell-penetrating peptide uptake.* Biochimica et Biophysica Acta (BBA)-Biomembranes, 2007. **1768**(7): p. 1769-1776.

118. Najjar, K., et al., *An l-to d-amino acid conversion in an endosomolytic analog of the cell-penetrating peptide TAT influences proteolytic stability, endocytic uptake, and endosomal escape.* Journal of biological chemistry, 2017. **292**(3): p. 847-861.

119. Mitchell, D.J., et al., *Polyarginine enters cells more efficiently than other polycationic homopolymers.* The Journal of Peptide Research, 2000. **56**(5): p. 318-325.

120. Morishita, M., et al., *A novel approach using functional peptides for efficient intestinal absorption of insulin.* Journal of controlled release, 2007. **118**(2): p. 177-184.

121. Nakase, I., et al., *Accumulation of arginine-rich cell-penetrating peptides in tumors and the potential for anticancer drug delivery in vivo.* Journal of controlled release, 2012. **159**(2): p. 181-188.

122. Kamei, N., M. Morishita, and K. Takayama, *Importance of intermolecular interaction on the improvement of intestinal therapeutic peptide/protein absorption using cell-penetrating peptides.* Journal of Controlled Release, 2009. **136**(3): p. 179-186.

123. Kamei, N., et al., *Exploration of the key factors for optimizing the in vivo oral delivery of insulin by using a noncovalent strategy with cell-penetrating peptides.* Biological and Pharmaceutical Bulletin, 2018. **41**(2): p. 239-246.

124. Kamei, N., et al., *Determination of the optimal cell-penetrating peptide sequence for intestinal insulin delivery based on molecular orbital analysis with self-organizing maps.* Journal of pharmaceutical sciences, 2013. **102**(2): p. 469-479.

125. Zhang, Y., et al., *Amphiphilic lipopeptide-mediated transport of insulin and cell membrane penetration mechanism.* Molecules, 2015. **20**(12): p. 21569-21583.

126. Zhang, L., et al., *Improving intestinal insulin absorption efficiency through coadministration of cell-penetrating peptide and hydroxypropyl-β-cyclodextrin.* Carbohydrate polymers, 2012. **87**(2): p. 1822-1827.

127. Yang, L., et al., *A cell-penetrating peptide conjugated carboxymethyl-β-cyclodextrin to improve intestinal absorption of insulin.* International journal of biological macromolecules, 2018. **111**: p. 685-695.

128. Zhu, X., et al., *Penetratin derivative-based nanocomplexes for enhanced intestinal insulin delivery.* Molecular pharmaceutics, 2013. **11**(1): p. 317-328.

129. Rudolph, C., et al., *Oligomers of the arginine-rich motif of the HIV-1 TAT protein are capable of transferring plasmid DNA into cells.* Journal of Biological Chemistry, 2003. **278**(13): p. 11411-11418.

130. Khafagy, E.-S., et al., *Effect of cell-penetrating peptides on the nasal absorption of insulin.* Journal of Controlled Release, 2009. **133**(2): p. 103-108.

131. Khafagy, E.-S., et al., *Structural requirements of penetratin absorption enhancement efficiency for insulin delivery.* Journal of Controlled Release, 2010. **143**(3): p. 302-310.

132. Patel, L.N., et al., *Conjugation with cationic cell-penetrating peptide increases pulmonary absorption of insulin.* Molecular pharmaceutics, 2009. **6**(2): p. 492-503.

133. Kamei, N. and M. Takeda-Morishita, *Brain delivery of insulin boosted by intranasal coadministration with cell-penetrating peptides.* Journal of Controlled Release, 2015. **197**: p. 105-110.

134. Eltaher, H.M., et al., *Highly efficient intracellular transduction in three-dimensional gradients for programming cell fate.* Acta biomaterialia, 2016. **41**: p. 181-192.

135. Thiagarajan, L., H.A.D.M. Abu-Awwad, and J.E. Dixon, *Osteogenic programming of human mesenchymal stem cells with highly efficient intracellular delivery of RUNX2.* Stem cells translational medicine, 2017. **6**(12): p. 2146-2159.

136. Abu-Awwad, H.A.-D.M., L. Thiagarajan, and J.E. Dixon, *Controlled release of GAG-binding enhanced transduction (GET) peptides for sustained and highly efficient intracellular delivery.* Acta biomaterialia, 2017. **57**: p. 225-237.

137. Lee, J.Y., et al., *Characterization of the surface immobilized synthetic heparin binding domain derived from human fibroblast growth factor-2 and its effect on osteoblast differentiation.* Journal of Biomedical Materials Research Part A: An Official Journal of The Society for Biomaterials, The Japanese Society for Biomaterials, and The Australian Society for Biomaterials and the Korean Society for Biomaterials, 2007. **83**(4): p. 970-979.

138. Osman, G., et al., *PEGylated enhanced cell penetrating peptide nanoparticles for lung gene therapy.* Journal of controlled release, 2018. **285**: p. 35-45.

139. Markides, H., et al., *Ex vivo MRI cell tracking of autologous mesenchymal stromal cells in an ovine osteochondral defect model.* Stem cell research & therapy, 2019. **10**(1): p. 25.

140. Raftery, R.M., et al., *Highly Versatile Cell-Penetrating Peptide Loaded Scaffold For Efficient and Localized Gene Delivery To Multiple Cell Types: From Development to Application in Tissue Engineering.* Biomaterials, 2019: p. 119277.

141. Nielsen, E.J.B., et al., *In vivo proof of concept of oral insulin delivery based on a co-administration strategy with the cell-penetrating peptide penetratin.* Journal of Controlled Release, 2014. **189**: p. 19-24.

142. Kristensen, M., et al., *Penetratin-mediated transepithelial insulin permeation: Importance of cationic residues and pH for complexation and permeation.* The AAPS journal, 2015. **17**(5): p. 1200-1209.

143. Daimon, Y., et al., *Dependence of intestinal absorption profile of insulin on carrier morphology composed of β-cyclodextrin-grafted chitosan.* Molecular Pharmaceutics, 2016.

144. Shan, W., et al., *Overcoming the diffusion barrier of mucus and absorption barrier of epithelium by self-assembled nanoparticles for oral delivery of insulin.* ACS nano, 2015. **9**(3): p. 2345-2356.

145. Zhu, S., et al., *Enhanced oral bioavailability of insulin using PLGA nanoparticles co-modified with cell-penetrating peptides and Engrailed secretion peptide (Sec).* Drug delivery, 2016. **23**(6): p. 1980-1991.

146. Zhang, Y., et al., *Thiolated Eudragit-based Nanoparticles for Oral Insulin Delivery: Preparation, Characterization, and Evaluation Using Intestinal Epithelial Cells In Vitro.* Macromolecular bioscience, 2014. **14**(6): p. 842-852.

147. Moroz, E., S. Matoori, and J.-C. Leroux, *Oral delivery of macromolecular drugs: Where we are after almost 100 years of attempts.* Advanced drug delivery reviews, 2016. **101**: p. 108-121.

148. Lundbæk, J.A., *Regulation of membrane protein function by lipid bilayer elasticity—a single molecule technology to measure the bilayer properties*

experienced by an embedded protein. Journal of physics: Condensed matter, 2006. **18**(28): p. S1305.

149. Higashiyama, S., J.A. Abraham, and M. Klagsbrun, *Heparin-binding EGF-like growth factor stimulation of smooth muscle cell migration: dependence on interactions with cell surface heparan sulfate.* The journal of cell Biology, 1993. **122**(4): p. 933-940.

150. Sakuma, T., et al., *CD9 antigen interacts with heparin-binding EGF-like growth factor through its heparin-binding domain.* The Journal of Biochemistry, 1997. **122**(2): p. 474-480.

151. Nimesh, S., et al., *Enhanced gene delivery mediated by low molecular weight chitosan/DNA complexes: effect of pH and serum.* Molecular biotechnology, 2010. **46**(2): p. 182-196.

152. Lee, H., J.H. Jeong, and T.G. Park, *PEG grafted polylysine with fusogenic peptide for gene delivery: high transfection efficiency with low cytotoxicity.* Journal of Controlled Release, 2002. **79**(1-3): p. 283-291.

153. Oren, Z., et al., *Structure and organization of the human antimicrobial peptide LL-37 in phospholipid membranes: relevance to the molecular basis for its non-cell-selective activity.* Biochemical Journal, 1999. **341**(Pt 3): p. 501.

154. Kwon, S. and J.H. Carson, *Fluorescence Quenching and Dequenching Analysis of RNA Interactionsin Vitroandin Vivo.* Analytical biochemistry, 1998. **264**(2): p. 133-140.

155. Kamei, N., et al., *Mechanistic study of the uptake/permeation of cell-penetrating peptides across a caco-2 monolayer and their stimulatory effect on epithelial insulin transport.* Journal of pharmaceutical sciences, 2013. **102**(11): p. 3998-4008.

156. Bechara, C., et al., *Tryptophan within basic peptide sequences triggers glycosaminoglycan-dependent endocytosis.* The FASEB Journal, 2013. **27**(2): p. 738-749.

157. Kristensen, M., et al., *Conjugation of cell-penetrating peptides to parathyroid hormone affects its structure, potency, and transepithelial permeation.* Bioconjugate chemistry, 2015. **26**(3): p. 477-488.

158. Niu, Z., et al., *PEG-PGA enveloped octaarginine-peptide nanocomplexes: an oral peptide delivery strategy.* Journal of controlled release, 2018. **276**: p. 125-139.

159. Pappalardo, J.S., et al., *Improved transfection of spleen-derived antigen-presenting cells in culture using TATp-liposomes.* Journal of controlled release, 2009. **134**(1): p. 41-46.

160. Li, W., et al., *Cell penetrating peptide-based polyplexes shelled with polysaccharide to improve stability and gene transfection.* Nanoscale, 2015. **7**(18): p. 8476-8484.

161. Taverner, A., et al., *Enhanced paracellular transport of insulin can be achieved via transient induction of myosin light chain phosphorylation.* Journal of Controlled Release, 2015. **210**: p. 189-197.

162. Cho, C.-F., et al., *Blood-brain-barrier spheroids as an in vitro screening platform for brain-penetrating agents.* Nature communications, 2017. **8**: p. 15623.

163. Kamei, N., et al., *Hydrophobic amino acid tryptophan shows promise as a potential absorption enhancer for oral delivery of biopharmaceuticals.* Pharmaceutics, 2018. **10**(4): p. 182.

164. Zhao, Y., et al., *Hormonal inhibition of endocytosis: novel roles for noradrenaline and G protein Gz.* The Journal of physiology, 2010. **588**(18): p. 3499-3509.

165. Zhao, Y., et al., *Noradrenaline inhibits exocytosis via the G protein βγ subunit and refilling of the readily releasable granule pool via the αi1/2 subunit.* The Journal of physiology, 2010. **588**(18): p. 3485-3498.

166. Seino, S., *Cell signalling in insulin secretion: the molecular targets of ATP, cAMP and sulfonylurea.* Diabetologia, 2012. **55**(8): p. 2096-2108.

167. Kumar, D.P., et al., *Activation of transmembrane bile acid receptor TGR5 stimulates insulin secretion in pancreatic β cells.* Biochemical and biophysical research communications, 2012. **427**(3): p. 600-605.

168. Johnson, J.D., et al., *Ryanodine receptors in human pancreatic β cells: localization and effects on insulin secretion.* The FASEB journal, 2004. **18**(7): p. 878-880.

169. Nakaki, T., T. Nakadate, and R. Kato, *α 2-Adrenoceptors modulating insulin release from isolated pancreatic islets.* Naunyn-Schmiedeberg's archives of pharmacology, 1980. **313**(2): p. 151-153.

170. Ghosh, T.K., J. Bian, and D.L. Gill, *Intracellular calcium release mediated by sphingosine derivatives generated in cells.* Science, 1990. **248**(4963): p. 1653-1656.

171. Wiedenkeller, D.E. and G.W. Sharp, *EFFECTS OF FORSKOUN ON INSULIN RELEASE AND CYCLIC AMP CONTENT IN RAT PANCREATIC ISLETS.* Endocrinology, 1983. **113**(6): p. 2311-2313.

172. Komatsu, M., et al., *Augmentation of insulin release by glucose in the absence of extracellular Ca2+: new insights into stimulus-secretion coupling.* Diabetes, 1997. **46**(12): p. 1928-1938.

173. Li, J., et al., *Novel regulation by Rac1 of glucose-and forskolin-induced insulin secretion in INS-1 β-cells.* American Journal of Physiology-Endocrinology and Metabolism, 2004. **286**(5): p. E818-E827.

174. Yamamoto, M., et al., *High efficiency gene transfer by multiple transfection protocol.* The Histochemical Journal, 1999. **31**(4): p. 241-243.

175. Pickard, M.R., P. Barraud, and D.M. Chari, *The transfection of multipotent neural precursor/stem cell transplant populations with magnetic nanoparticles.* Biomaterials, 2011. **32**(9): p. 2274-2284.

176. Grosjean, F., et al., *Multiple glycerol shocks increase the calcium phosphate transfection of non-synchronized CHO cells.* Biotechnology letters, 2006. **28**(22): p. 1827-1833.

177. Wu, J.-H. and S.L. Diamond, *A fluorescence quench and dequench assay of fibrinogen polymerization, fibrinogenolysis, or fibrinolysis.* Analytical biochemistry, 1995. **224**(1): p. 83-91.

178. Walter, N.G. and J.M. Burke, *Real-time monitoring of hairpin ribozyme kinetics through base-specific quenching of fluorescein-labeled substrates.* Rna, 1997. **3**(4): p. 392-404.

179. Fuhrmann, G. and J.-C. Leroux, *In vivo fluorescence imaging of exogenous enzyme activity in the gastrointestinal tract.* Proceedings of the National Academy of Sciences, 2011. **108**(22): p. 9032-9037.

180. Räägel, H., P. Säälik, and M. Pooga, *Peptide-mediated protein delivery—Which pathways are penetrable?* Biochimica et Biophysica Acta (BBA)-Biomembranes, 2010. **1798**(12): p. 2240-2248.

181. Sakai, N. and S. Matile, *Anion-mediated transfer of polyarginine across liquid and bilayer membranes.* Journal of the American Chemical Society, 2003. **125**(47): p. 14348-14356.

182. Ryser, H.J.-P. and R. Hancock, *Histones and basic polyamino acids stimulate the uptake of albumin by tumor cells in culture.* Science, 1965. **150**(3695): p. 501-503.

183. Grudzielanek, S., et al., *Cytotoxicity of insulin within its self-assembly and amyloidogenic pathways.* Journal of molecular biology, 2007. **370**(2): p. 372-384.

184. Kelly, J.W., *Alternative conformations of amyloidogenic proteins govern their behavior.* Current opinion in structural biology, 1996. **6**(1): p. 11-17.

185. Gautam, A., et al., *Topical delivery of protein and peptide using novel cell penetrating peptide IMT-P8.* Scientific reports, 2016. **6**: p. 26278.

186. Cermenati, G., et al., *The CPP Tat enhances eGFP cell internalization and transepithelial transport by the larval midgut of Bombyx mori (Lepidoptera, Bombycidae).* Journal of insect physiology, 2011. **57**(12): p. 1689-1697.

187. Lewis, H.D., et al., *Creation of a novel peptide with enhanced nuclear localization in prostate and pancreatic cancer cell lines.* BMC biotechnology, 2010. **10**(1): p. 79.

188. Luo, Y., et al., *Live-cell imaging of octaarginine-modified polymer dots via single particle tracking.* Cell proliferation, 2019. **52**(2): p. e12556.

189. Jo, J., et al., *Cell-penetrating peptide (CPP)-conjugated proteins is an efficient tool for manipulation of human mesenchymal stromal cells.* Scientific reports, 2014. **4**: p. 4378.

190. Liu, Q., et al., *Delivery of miRNA-29b Using R9-LK15, a Novel Cell-Penetrating Peptide, Promotes Osteogenic Differentiation of Bone Mesenchymal Stem Cells.* BioMed research international, 2019. **2019**.

191. Khafagy, E.-S., et al., *Efficiency of cell-penetrating peptides on the nasal and intestinal absorption of therapeutic peptides and proteins.* International journal of pharmaceutics, 2009. **381**(1): p. 49-55.

192. Pappenheimer, J.R., et al., *Intestinal absorption and excretion of octapeptides composed of D amino acids.* Proceedings of the National Academy of Sciences, 1994. **91**(5): p. 1942-1945.

193. Purkayastha, N., et al., *Enantiomeric and Diastereoisomeric (Mixed) L/D-Octaarginine Derivatives–A Simple Way of Modulating the Properties of Cell-Penetrating Peptides.* Chemistry & biodiversity, 2013. **10**(7): p. 1165-1184.

194. Shrestha, N., et al., *Thiolation and Cell-Penetrating Peptide Surface Functionalization of Porous Silicon Nanoparticles for Oral Delivery of Insulin.* Advanced Functional Materials, 2016. **26**(20): p. 3405-3416.

195. Taniguchi, M., et al., *Essential role of the zinc transporter ZIP9/SLC39A9 in regulating the activations of Akt and Erk in B-cell receptor signaling pathway in DT40 cells.* PloS one, 2013. **8**(3): p. e58022.

196. Kubista, H., et al., *Annexin 5 mediates a peroxide-induced Ca2+ influx in B cells.* Current Biology, 1999. **9**(23): p. 1403-1408.

197. Boushra, M., et al., *Development of bi-polymer lipid hybrid nanocarrier (BLN) to improve the entrapment and stability of insulin for efficient oral delivery.* Journal of Drug Delivery Science and Technology, 2019. **49**: p. 632-641.

198. Thakral, S., N.K. Thakral, and D.K. Majumdar, *Eudragit®: a technology evaluation.* Expert opinion on drug delivery, 2013. **10**(1): p. 131-149.

199. Sahle, F.F., et al., *Formulation and comparative in vitro evaluation of various dexamethasone-loaded pH-sensitive polymeric nanoparticles intended for dermal applications.* International journal of pharmaceutics, 2017. **516**(1-2): p. 21-31.

200. Wu, J., et al., *Biomimetic viruslike and charge reversible nanoparticles to sequentially overcome mucus and epithelial barriers for oral insulin delivery.* ACS applied materials & interfaces, 2018. **10**(12): p. 9916-9928.

201. Chen, S., et al., *Eudragit S100-coated chitosan nanoparticles co-loading tat for enhanced oral colon absorption of insulin.* AAPS PharmSciTech, 2017. **18**(4): p. 1277-1287.

202. Zhang, Y., et al., *Thiolated Eudragit nanoparticles for oral insulin delivery: preparation, characterization and in vivo evaluation.* International journal of pharmaceutics, 2012. **436**(1-2): p. 341-350.

203. Fonte, P., et al., *Stability study perspective of the effect of freeze-drying using cryoprotectants on the structure of insulin loaded into PLGA nanoparticles.* Biomacromolecules, 2014. **15**(10): p. 3753-3765.

204. Fonte, P., et al., *Effect of cryoprotectants on the porosity and stability of insulin-loaded PLGA nanoparticles after freeze-drying.* Biomatter, 2012. **2**(4): p. 329-339.

205. Guhagarkar, S.A., et al., *Polyethylene sebacate–doxorubicin nanoparticles for hepatic targeting.* International journal of pharmaceutics, 2010. **401**(1-2): p. 113-122.

206. Govender, T., et al., *PLGA nanoparticles prepared by nanoprecipitation: drug loading and release studies of a water soluble drug.* Journal of Controlled Release, 1999. **57**(2): p. 171-185.

207. Niwa, T., et al., *Preparations of biodegradable nanospheres of water-soluble and insoluble drugs with D, L-lactide/glycolide copolymer by a novel spontaneous emulsification solvent diffusion method, and the drug release behavior.* Journal of Controlled Release, 1993. **25**(1-2): p. 89-98.

208. Damgé, C., et al., *Poly (ε-caprolactone)/eudragit nanoparticles for oral delivery of aspart-insulin in the treatment of diabetes.* Journal of pharmaceutical sciences, 2010. **99**(2): p. 879-889.

209. Cone, R.A., *Barrier properties of mucus.* Advanced drug delivery reviews, 2009. **61**(2): p. 75-85.

210. Liu, M., et al., *Developments of mucus penetrating nanoparticles.* asian journal of pharmaceutical sciences, 2015. **10**(4): p. 275-282.

211. Ensign, L.M., et al., *Mucus penetrating nanoparticles: biophysical tool and method of drug and gene delivery.* Advanced Materials, 2012. **24**(28): p. 3887-3894.

212. Ensign, L.M., R. Cone, and J. Hanes, *Oral drug delivery with polymeric nanoparticles: the gastrointestinal mucus barriers.* Advanced drug delivery reviews, 2012. **64**(6): p. 557-570.

213. Lai, S.K., Y.-Y. Wang, and J. Hanes, *Mucus-penetrating nanoparticles for drug and gene delivery to mucosal tissues.* Advanced drug delivery reviews, 2009. **61**(2): p. 158-171.

214. Wang, A., et al., *Protein corona liposomes achieve efficient oral insulin delivery by overcoming mucus and epithelial barriers.* Advanced healthcare materials, 2019. **8**(12): p. 1801123.

215. Shan, W., et al., *Enhanced oral delivery of protein drugs using zwitterion-functionalized nanoparticles to overcome both the diffusion and absorption barriers.* ACS applied materials & interfaces, 2016. **8**(38): p. 25444-25453.

216. Touitou, E. and A. Rubinstein, *Targeted enteral delivery of insulin to rats.* International journal of pharmaceutics, 1986. **30**(2-3): p. 95-99.

217. MORISHITA, M., et al., *Site-dependent effect of aprotinin, sodium caprate, Na2EDTA and sodium glycocholate on intestinal absorption of insulin.* Biological and Pharmaceutical Bulletin, 1993. **16**(1): p. 68-72.

218. Holzer, M., et al., *Physico-chemical characterisation of PLGA nanoparticles after freeze-drying and storage.* European Journal of Pharmaceutics and Biopharmaceutics, 2009. **72**(2): p. 428-437.

219. Wang, W., *Lyophilization and development of solid protein pharmaceuticals.* International journal of pharmaceutics, 2000. **203**(1-2): p. 1-60.

220. Heller, M.C., J.F. Carpenter, and T.W. Randolph, *Protein formulation and lyophilization cycle design: Prevention of damage due to freeze-concentration induced phase separation.* Biotechnology and bioengineering, 1999. **63**(2): p. 166-174.

221. Izutsu, K.-I., et al., *Effect of counterions on the physical properties of l-arginine in frozen solutions and freeze-dried solids.* International journal of pharmaceutics, 2005. **301**(1-2): p. 161-169.

222. Kadoya, S., et al., *Freeze-drying of proteins with glass-forming oligosaccharide-derived sugar alcohols.* International journal of pharmaceutics, 2010. **389**(1-2): p. 107-113.

223. Adams, G.D. and J.R. Ramsay, *Optimizing the lyophilization cycle and the consequences of collapse on the pharmaceutical acceptability of erwiniaL-Asparaginase.* Journal of pharmaceutical sciences, 1996. **85**(12): p. 1301-1305.

224. Hora, M.S., R.K. Rana, and F.W. Smith, *Lyophilized formulations of recombinant tumor necrosis factor.* Pharmaceutical research, 1992. **9**(1): p. 33-36.

225. Roy, M., et al., *The effects of formulation and moisture on the stability of a freeze-dried monoclonal antibody-vinca conjugate: a test of the WLF glass transition theory.* Developments in biological standardization, 1992. **74**: p. 323-39; discussion 340.

226. Carpenter, J.F., J.H. Crowe, and T. Arakawa, *Comparison of solute-induced protein stabilization in aqueous solution and in the frozen and dried states.* Journal of Dairy Science, 1990. **73**(12): p. 3627-3636.

227. Akers, M.J., et al., *Glycine crystallization during freezing: the effects of salt form, pH, and ionic strength.* Pharmaceutical research, 1995. **12**(10): p. 1457-1461.

228. Pikal, M.J. and D.R. Rigsbee, *The stability of insulin in crystalline and amorphous solids: observation of greater stability for the amorphous form.* Pharmaceutical research, 1997. **14**(10): p. 1379-1387.

229. Strickley, R.G. and B.D. Anderson, *Solid-state stability of human insulin II. Effect of water on reactive intermediate partitioning in lyophiles from pH 2–5 solutions: Stabilization against covalent dimer formation.* Journal of pharmaceutical sciences, 1997. **86**(6): p. 645-653.

230. Katakam, M. and A.K. Banga, *Aggregation of insulin and its prevention by carbohydrate excipients.* PDA journal of pharmaceutical science and technology, 1995. **49**(4): p. 160-165.

231. Ezzat, K., et al., *Solid formulation of cell-penetrating peptide nanocomplexes with siRNA and their stability in simulated gastric conditions.* Journal of controlled release, 2012. **162**(1): p. 1-8.

232. Saphier, S., et al., *Gastro intestinal tracking and gastric emptying of solid dosage forms in rats using X-ray imagining.* International journal of pharmaceutics, 2010. **388**(1-2): p. 190-195.

233. Sonaje, K., et al., *Enteric-coated capsules filled with freeze-dried chitosan/poly (γ-glutamic acid) nanoparticles for oral insulin delivery.* Biomaterials, 2010. **31**(12): p. 3384-3394.

234. Cole, E.T., et al., *Enteric coated HPMC capsules designed to achieve intestinal targeting.* International journal of pharmaceutics, 2002. **231**(1): p. 83-95.

235. Reix, N., et al., *Duodenum-specific drug delivery: in vivo assessment of a pharmaceutically developed enteric-coated capsule for a broad applicability in rat studies.* International journal of pharmaceutics, 2012. **422**(1-2): p. 338-340.

236. Saboo, S., et al., *Optimized formulation of a thermostable spray-dried virus-like particle vaccine against human papillomavirus.* Molecular pharmaceutics, 2016. **13**(5): p. 1646-1655.

237. Kamei, N., et al., *Permeation characteristics of oligoarginine through intestinal epithelium and its usefulness for intestinal peptide drug delivery.* Journal of Controlled Release, 2008. **131**(2): p. 94-99.

238. Sakuma, S., et al., *Oligoarginine-linked polymers as a new class of penetration enhancers.* Journal of Controlled Release, 2010. **148**(2): p. 187-196.

239. Landy, J., et al., *Tight junctions in inflammatory bowel diseases and inflammatory bowel disease associated colorectal cancer.* World journal of gastroenterology, 2016. **22**(11): p. 3117.

240. Hawkins, B., et al., *Increased blood–brain barrier permeability and altered tight junctions in experimental diabetes in the rat: contribution of hyperglycaemia and matrix metalloproteinases.* Diabetologia, 2007. **50**(1): p. 202-211.

241. Bosi, E., et al., *Increased intestinal permeability precedes clinical onset of type 1 diabetes.* Diabetologia, 2006. **49**(12): p. 2824-2827.

242. Marchetti, G., C. Tincati, and G. Silvestri, *Microbial translocation in the pathogenesis of HIV infection and AIDS.* Clinical microbiology reviews, 2013. **26**(1): p. 2-18.

243. Nalle, S.C., et al., *Graft-versus-host disease propagation depends on increased intestinal epithelial tight junction permeability.* The Journal of clinical investigation, 2019. **129**(2): p. 902-914.

244. Yeh, T.-H., et al., *Mechanism and consequence of chitosan-mediated reversible epithelial tight junction opening.* Biomaterials, 2011. **32**(26): p. 6164-6173.

245. Walsh, E.G., et al., *Oral delivery of macromolecules: rationale underpinning Gastrointestinal Permeation Enhancement Technology (GIPET®).* Therapeutic delivery, 2011. **2**(12): p. 1595-1610.

246. Anderson, D., et al., *Tumor cell retention of antibody Fab fragments is enhanced by an attached HIV TAT protein-derived peptide.* Biochemical and biophysical research communications, 1993. **194**(2): p. 876-884.

247. Reissmann, S., *Cell penetration: scope and limitations by the application of cell-penetrating peptides.* Journal of Peptide Science, 2014. **20**(10): p. 760-784.

248. Toro, A., et al., *Intracellular delivery of purine nucleoside phosphorylase (PNP) fused to protein transduction domain corrects PNP deficiency in vitro.* Cellular immunology, 2006. **240**(2): p. 107-115.

249. Sugita, T., et al., *Comparative study on transduction and toxicity of protein transduction domains.* British journal of pharmacology, 2008. **153**(6): p. 1143-1152.

250. Akkarawongsa, R., et al., *Corneal toxicity of cell-penetrating peptides that inhibit herpes simplex virus entry.* Journal of Ocular Pharmacology & Therapeutics, 2006. **22**(4): p. 279-289.

251. Hirsch, I.B., *Type 1 diabetes mellitus and the use of flexible insulin regimens.* American family physician, 1999. **60**(8): p. 2343.

252. Le-Vinh, B., et al., *Chitosan based micelle with zeta potential changing property for effective mucosal drug delivery.* International journal of biological macromolecules, 2019. **133**: p. 647-655.

Chapter 10. Appendix

10.1. Published review article

Peptides

journal homepage: www.elsevier.com/locate/peptides

Oral delivery of anti-diabetes therapeutics using cell penetrating and transcytosing peptide strategies

Sahrish Rehmani, James E. Dixon*

Wolfson Centre for Stem Cells, Tissue Engineering, and Modelling (STEM), Centre of Biomolecular Sciences, School of Pharmacy, University of Nottingham, Nottingham, NG7 2RD, UK

ARTICLE INFO

Keywords:
Oral drug delivery
Peptide drugs
Nanoparticles
Cell penetrating peptides
Peptide permeability
Bioavailability
Human intestinal tissue
Transcytosis
Transepithelial transport

ABSTRACT

Oral delivery of insulin and other anti-diabetic peptides is inhibited by low intestinal absorption caused by the poor permeability across cellular membranes and the susceptibility to enzymatic degradation in the gastrointestinal tract. Cell-penetrating peptides (CPPs) have been investigated for a number of years as oral absorption enhancers for hydrophilic macromolecules by electrostatic or covalent conjugation on in conjunction with nanotechnology. Endogenous cellular uptake mechanisms present in the intestine can be exploited by engineering peptide conjugates that transcytose; entering cells by endocytosis and leaving by exocytosis. Efficiently delivering hydrophilic and sensitive peptide drugs to safely transverse the digestive barrier with no effect on gut physiology using remains a key driver for formulation research. Here we review the use of CPP and transcytosis peptide approaches, their modification and use in delivering anti-diabetic peptides (with the primary example of Insulin and engineered homologues) by direct oral administration to treat diabetes and associated metabolic disorders.

1. Introduction

Recent advances in biotechnology and molecular engineering have led to the development and manufacture of an increasing number of new therapeutic proteins/peptides, especially those modifying natural variants of hormones that control glucose homeostasis. Formidable obstacles exist to achieve effective oral delivery of proteinaceous molecules; including low stability, poor absorption, and lack of lipophilicity resulting in low permeation through intestinal and interstitial tissues (Fig. 1). Along with rapid inactivation/degradation by gastrointestinal (GI) enzymes the bioavailability and therapeutic efficacy of such therapeutics is severely compromised (Fig. 2) [1,2].

The prerequisite steps needed for oral absorption of peptides, digestive transit (in stomach, GI fluids, and residence time in absorption window), the crossing biological intestinal barriers (by diffusion, paracellular or transcellular transport) and ultimately the routing (portal route or systemic exposure) of the therapeutic to the site of action are all important in engineering such therapies (Fig. 3). Each of these steps is associated with a particular type of barrier (chemical, biochemical or physical) that restricts peptide drug entry into the systemic circulation. It is therefore a major focus of this field to promote the permeation of such barriers without affecting their important role as barriers against toxins and pathogens exiting the digestive system.

In recent years several novel peptide delivery strategies have emerged for overcoming the problems of biopharmaceutical instability associated with proteins/peptide, thereby improving productivity and reducing metabolism of peptide drugs along with alternative routes of administration. For oral delivery penetration enhancers such as cell penetrating peptides [CPPs], protease inhibitors, polymeric or mucoadhesive carriers, and chemical modification are beginning to increase the bioactivity of these therapeutics to functional levels. Other routes including mucosal (through nasal spray, sublingual or pulmonary delivery), transdermal (patches) and improved controlled release parenteral routes (s.c., i.m. or i.v) will all be important in future efforts especially in the antidiabetic peptide field.

This review will focus on various CPP and transcytosing peptides based technologies that have been applied for improving the delivery and bioavailability of anti-diabetic peptides by the oral route. These approaches could however be readily adapted to other administration routes as there also require the ability to effectively transverse biological barriers (Fig. 4).

10.2. Calibration curve for NHS-Fluorescein-insulin

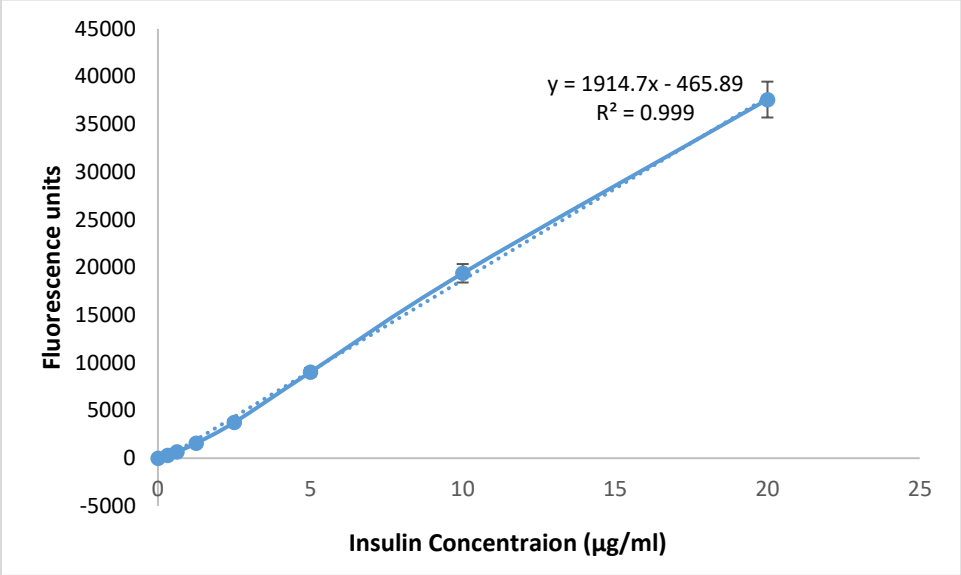

Figure 10.1. Standard curve for Ins-F.

10.3. Fluorescence Quenching of Ins-F* and Ins-F with various GET peptides at Ex= 490nm and Em= 500-580nm with 5nm intervals

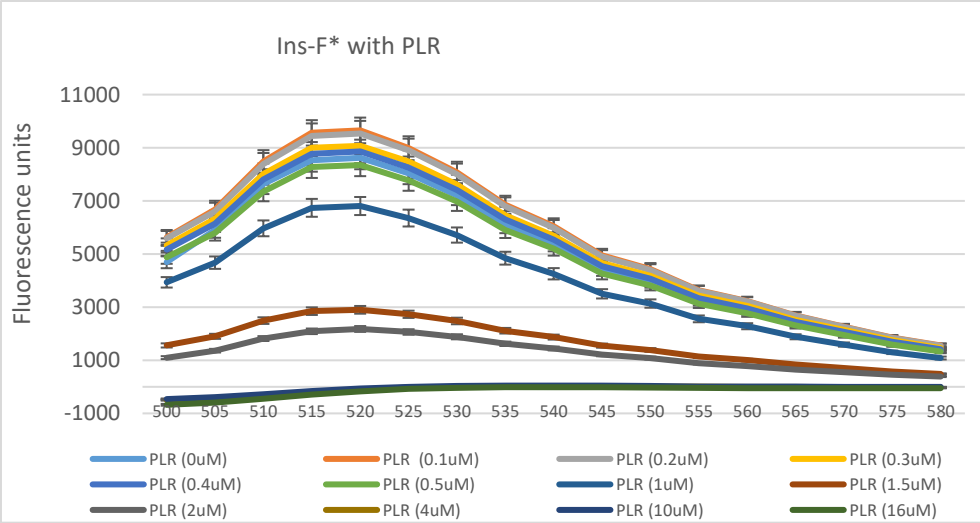

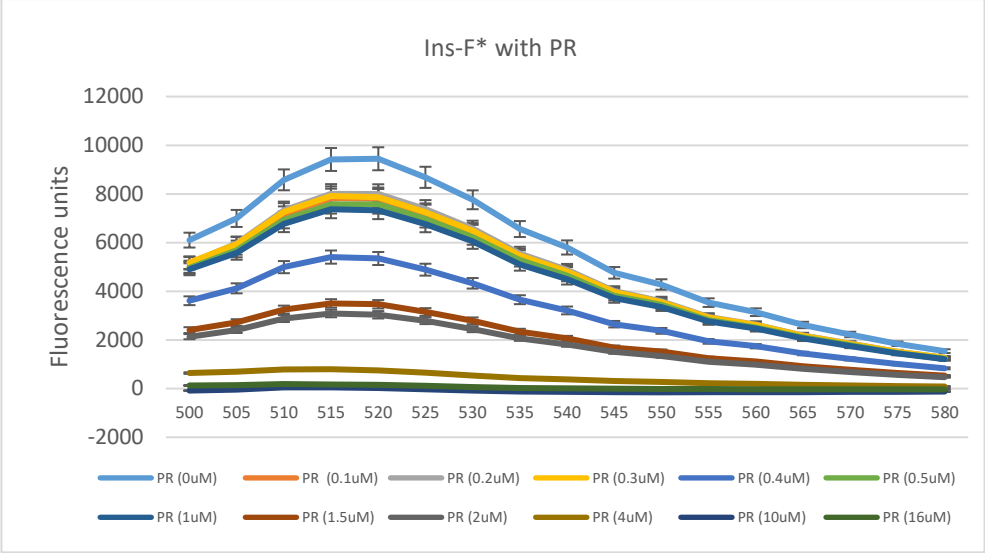

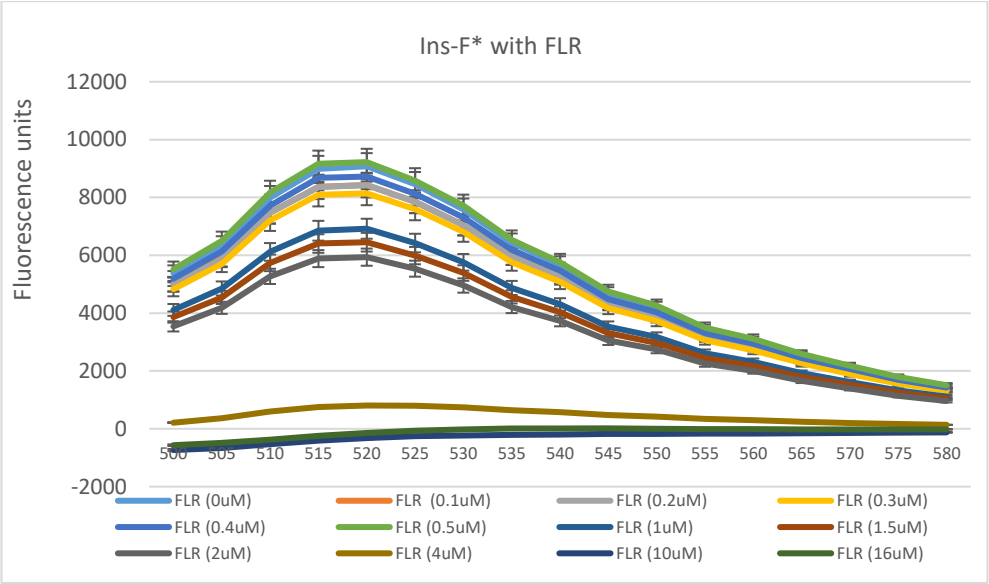

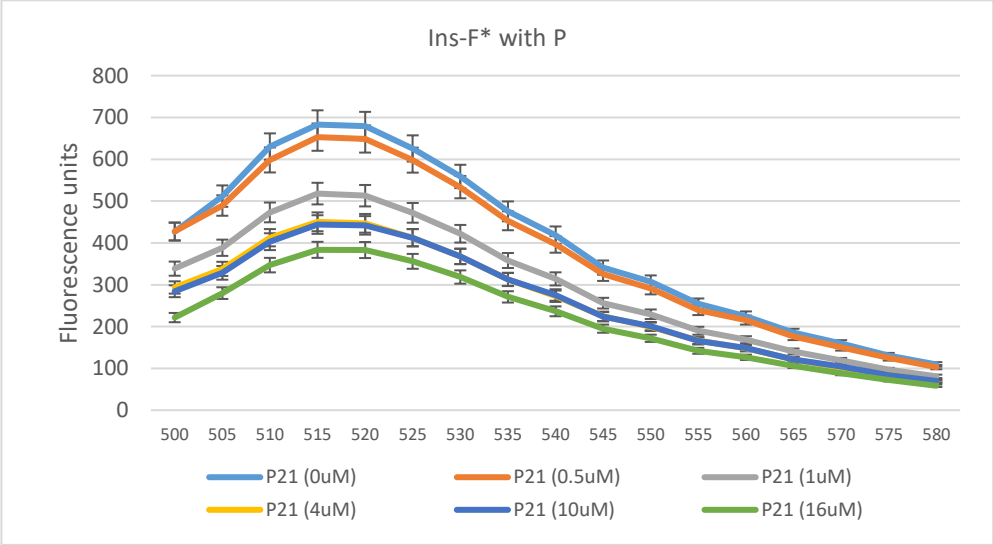

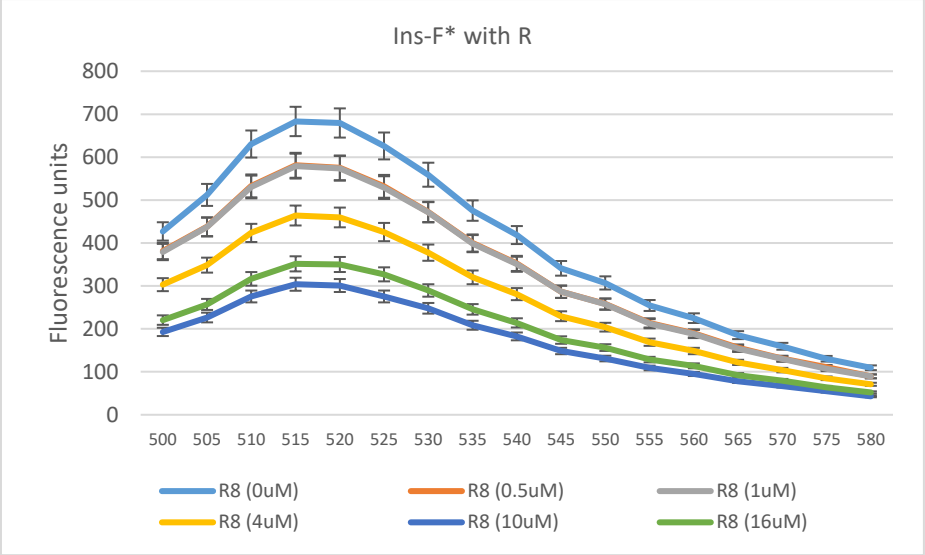

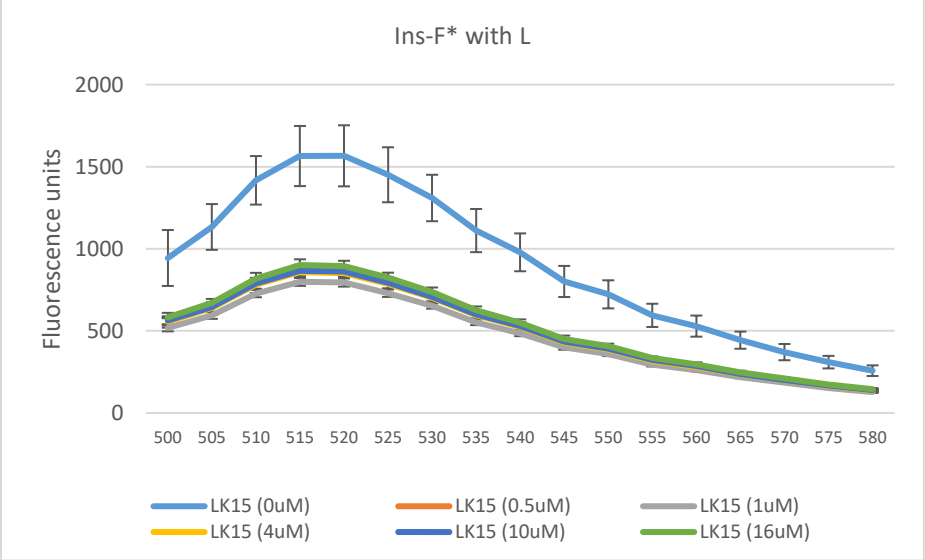

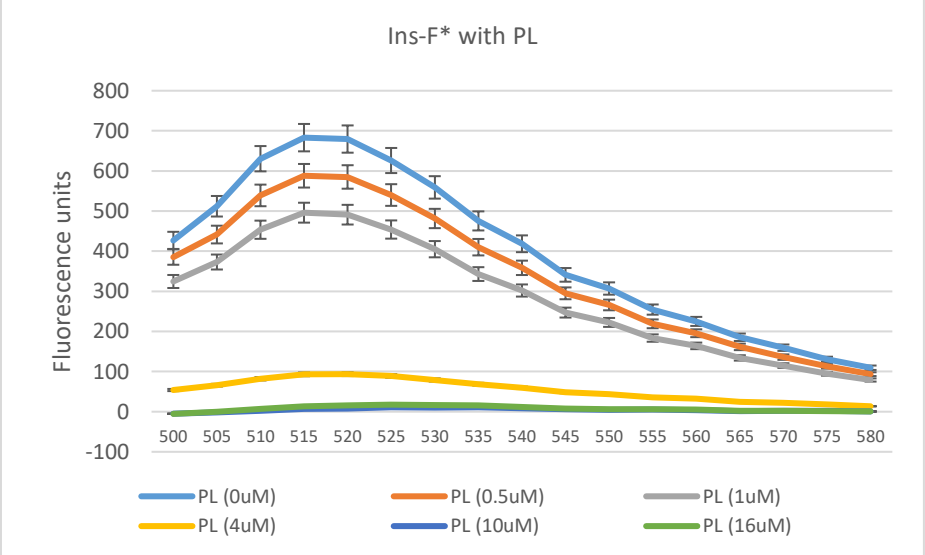

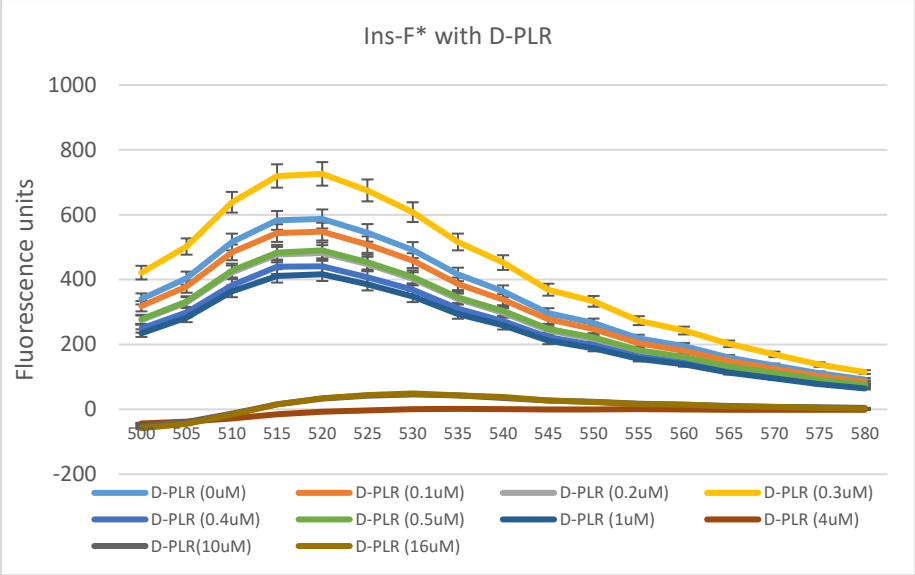

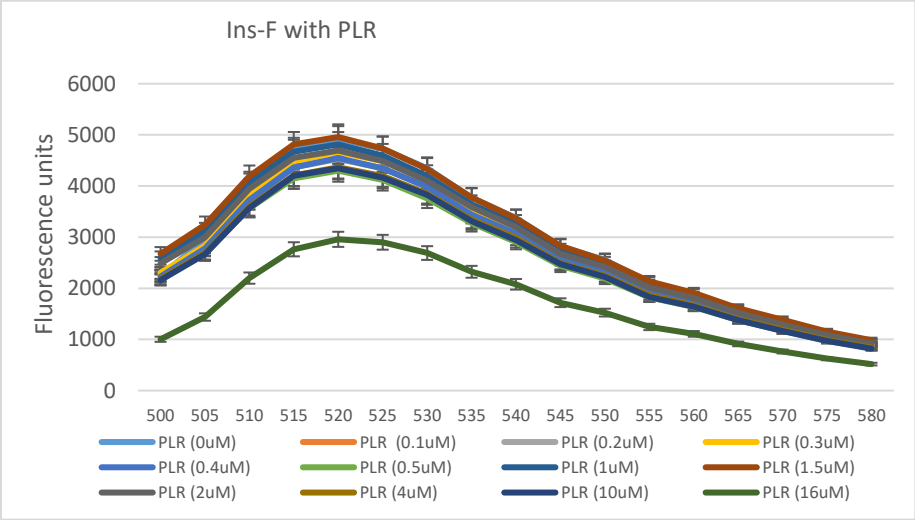

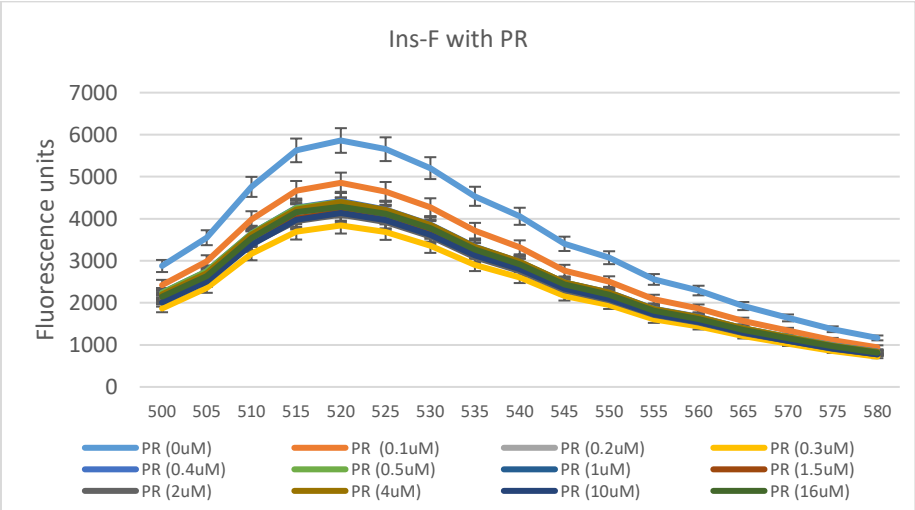

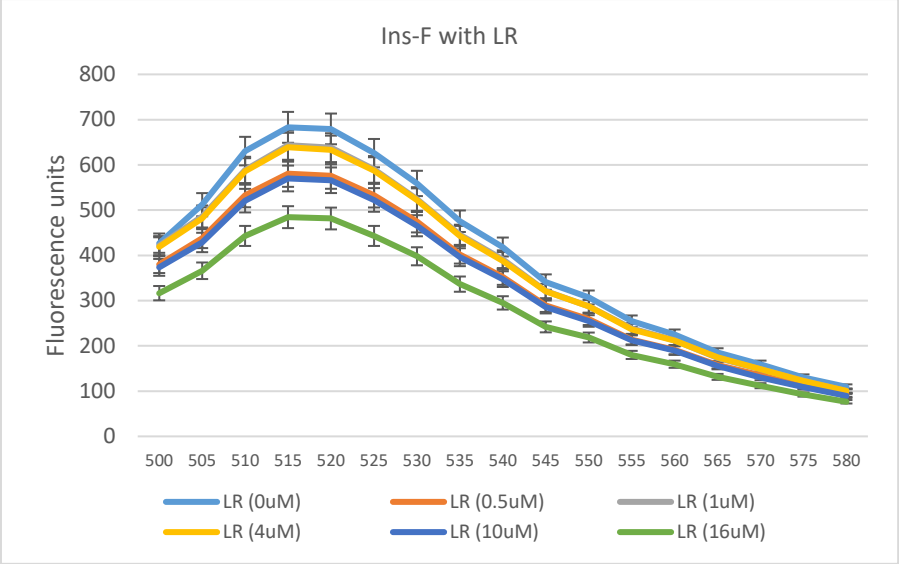

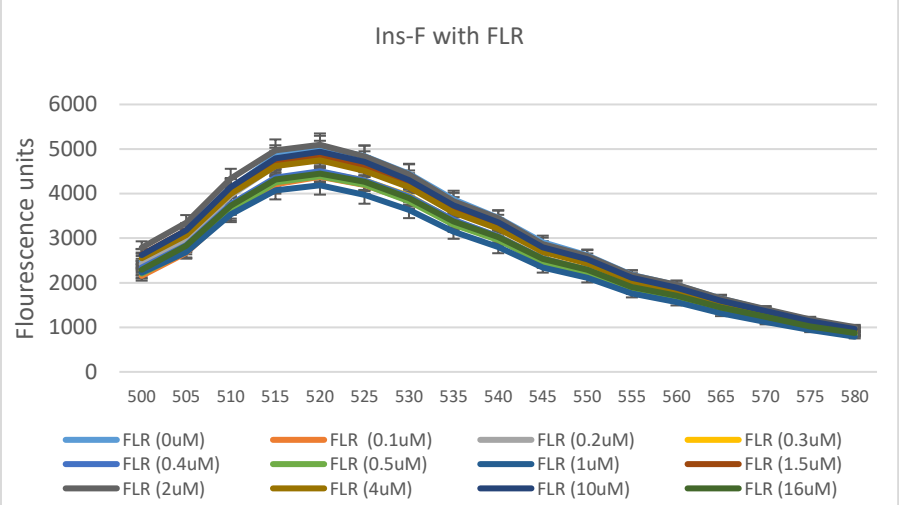

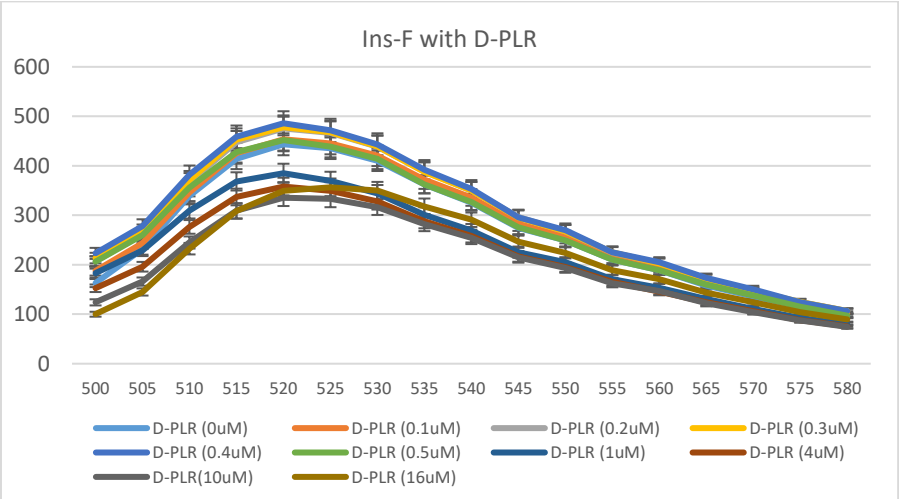

Figure 10.2 Fluorescence quenching of Ins-F (NHS-Fluorescein insulin) and Ins-F* (Sigma-FITC insulin) with GET-peptide and derivatives.

10.4. Calibration curve for NHS-Fluorescein- (Ins-F) and NHS-Rhodamine- insulin (Ins-T) for multiple drug delivery

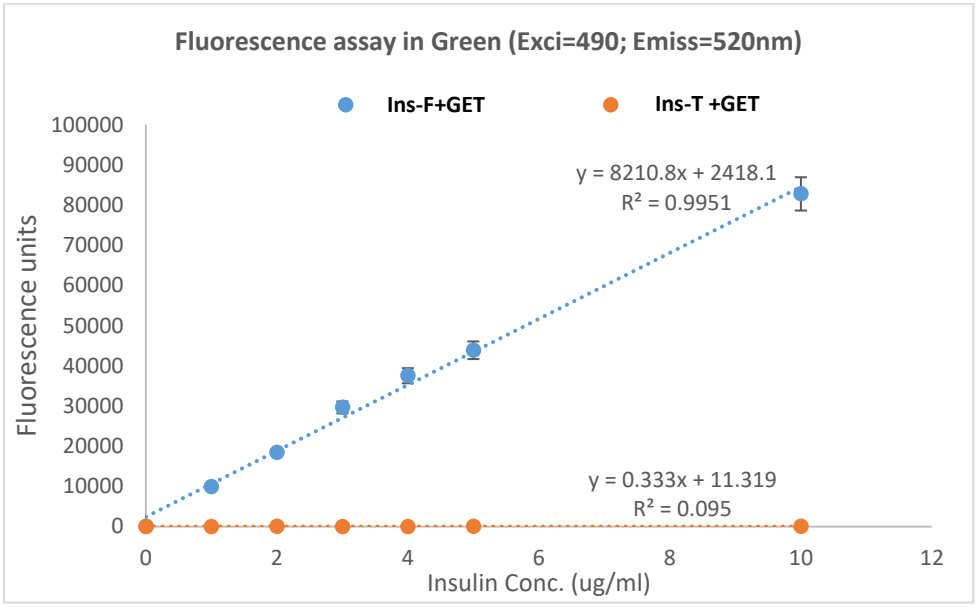

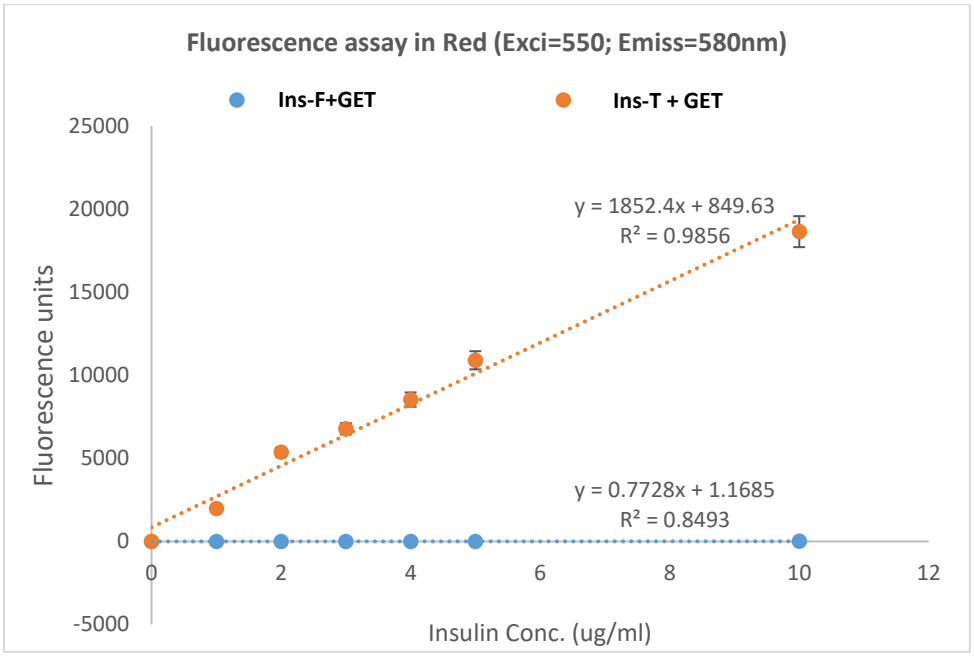

Figure 10.3 Calibration curve for Ins-F and Ins-T complexed with GET-peptide.

10.5. Cellular uptake of NHS-Rhodamine-labelled insulin (Ins-T) with GET-peptide

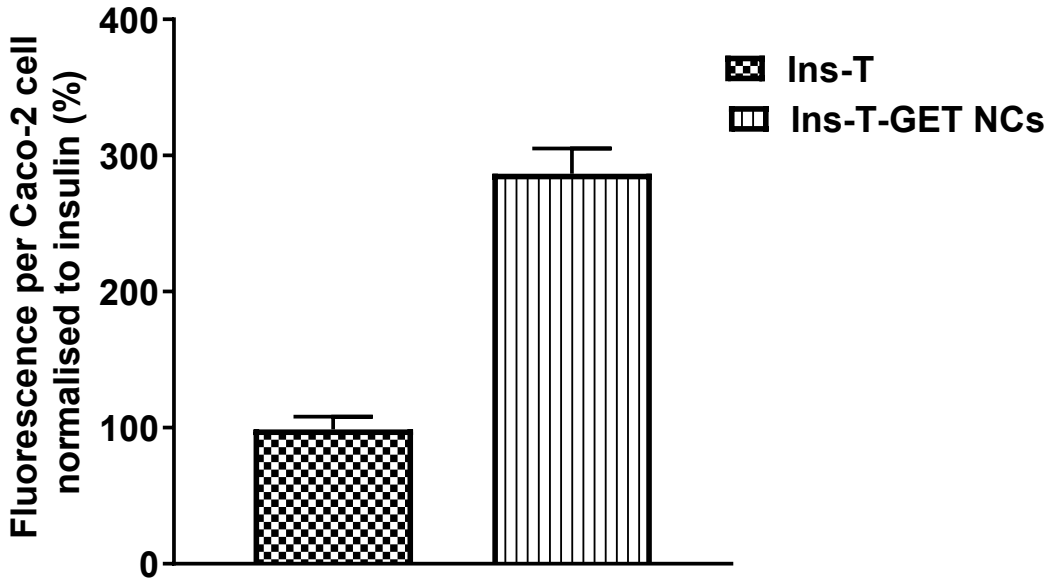

Figure 10.4 Cellular internalisation of Ins-T with GET peptide.

10.6. Heparin dequenching of Sigma-FITC insulin based NCs (Ins-F*-GET NCs)

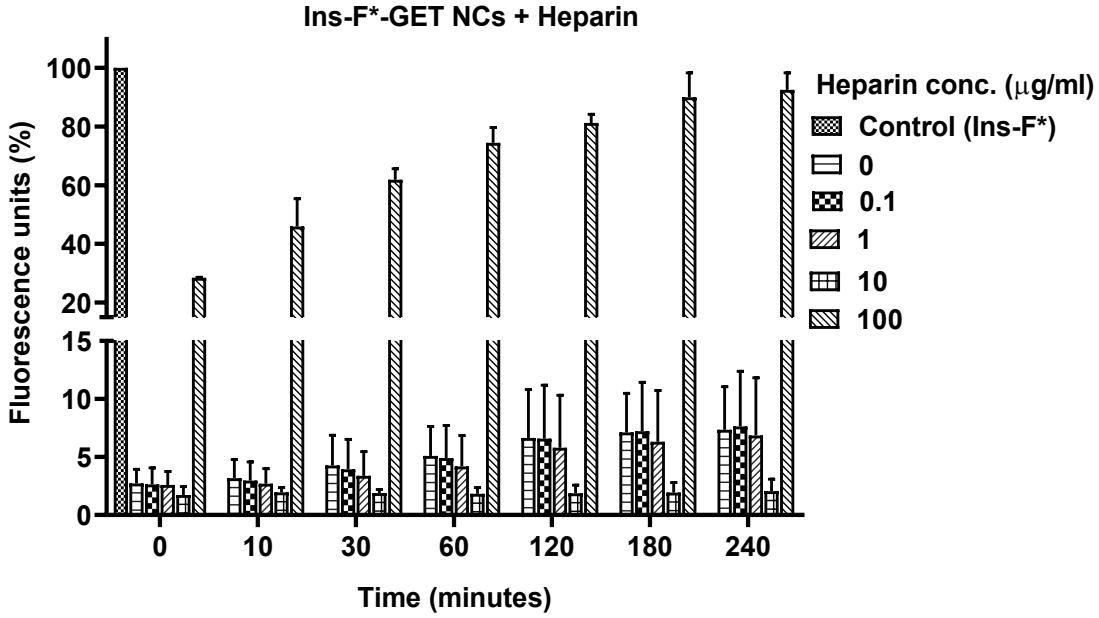

Figure 10.5 Fluorescence recovery of Ins-F*-GET NCs using heparin in different doses.

10.7. Multifection with triple delivery of NCs

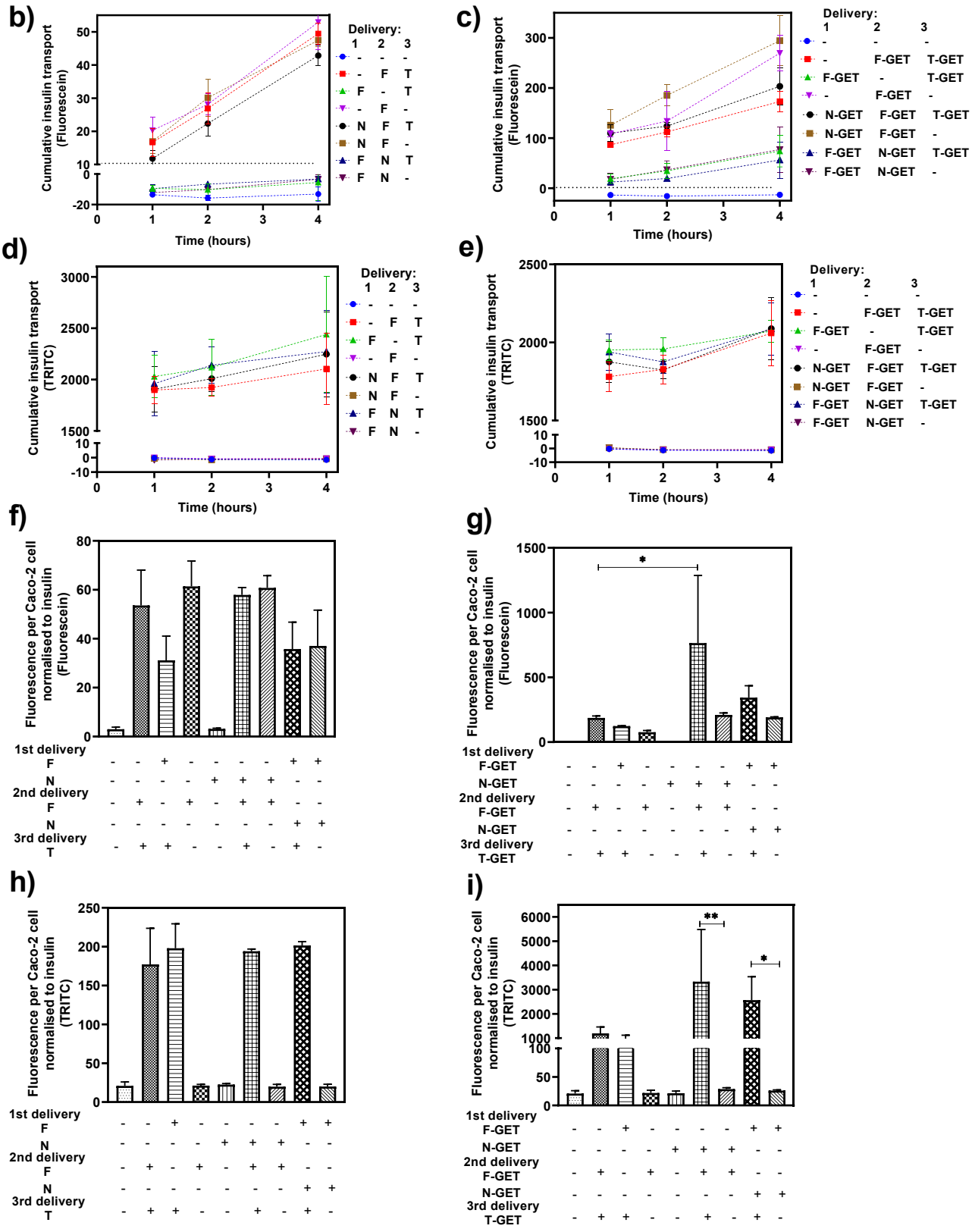

Figure 10.6 Insulin recycling using three consecutive delivery i.e. two serial deliveries with non-labelled (N) and NHS-Fluorescein-labelled insulin (F), respectively each for two hr, followed by analysis of post-transfection release in Ins-T or T.